



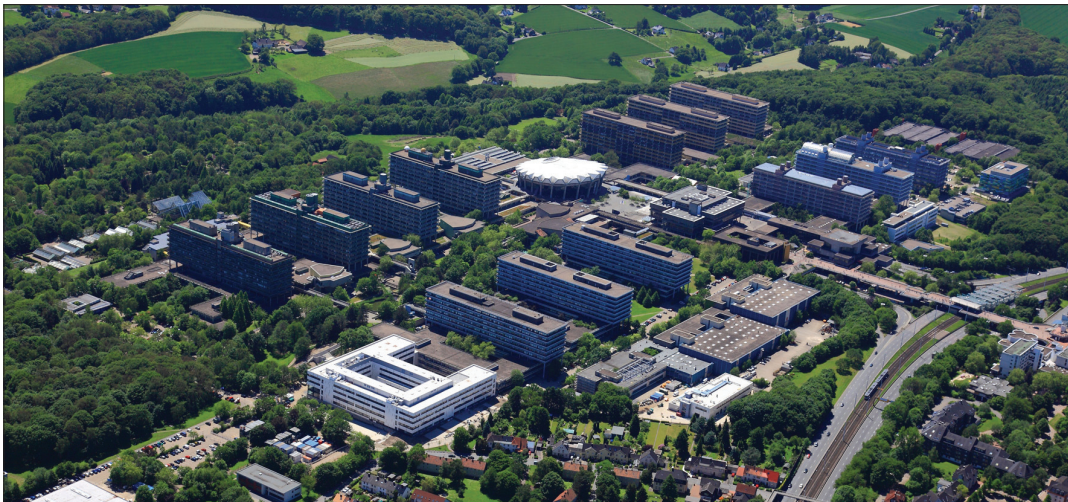
IODP
INTERNATIONAL OCEAN
DISCOVERY PROGRAM



IODP/ICDP Kolloquium 2018

Ruhr-Universität Bochum

14. – 16. März 2018

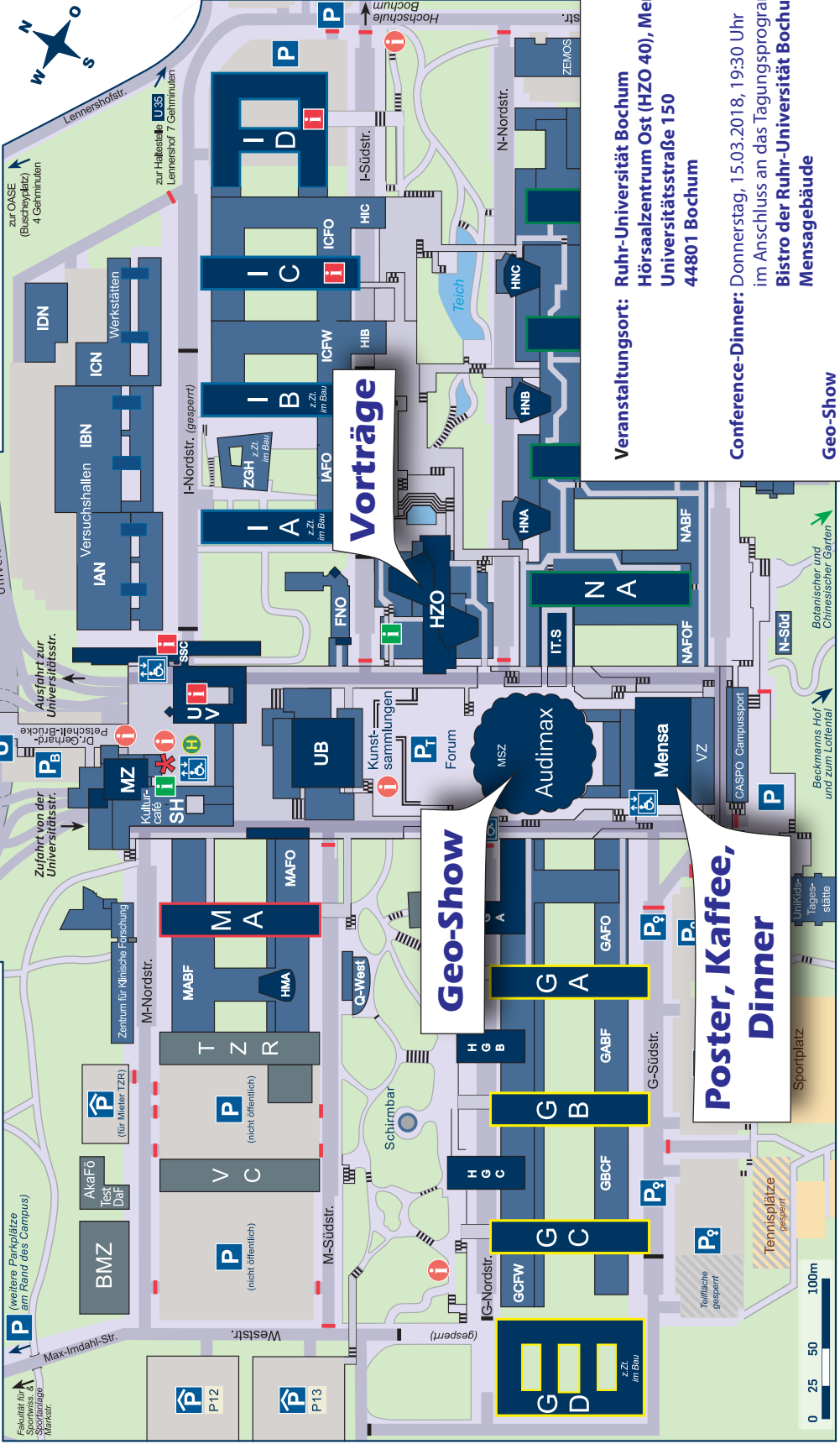


DFG Deutsche
Forschungsgemeinschaft

**RUHR
UNIVERSITÄT
BOCHUM**

RUB

CAMPUSPLAN



© 2017 Copyright/Bearbeitung: AG Geomatik - Geographisches Institut der RUB (M. Geißner, S. Steinert, W. Herzog), Aktualisierung: Dez. 2011 (A. Langosch)

Veranstaltungsort: Ruhr-Universität Bochum
Hörsaalzentrum Ost (HZO 40), Mensafoyer
Universitätsstraße 150
44801 Bochum

Conference-Dinner: Donnerstag, 15.03.2018, 19:30 Uhr
im Anschluss an das Tagungsprogramm
Bistro der Ruhr-Universität Bochum,
Mensagebäude

**Geo-Show
„Unterirdisch“:**
Donnerstag, 15.03.2018, 10:30 – 12:00 Uhr
Audimax Ruhr-Universität Bochum
Universitätsstraße 150
44801 Bochum

- SH Studierende
- SSC Studierende
- TZR Technologie
- UB Universität
- UV Universitäts
- VC Vita Campus
- VZ Veranstaltung
- ZGH Zentrum für
- ZN Zentrums für

- U U-Bahn-Haltestelle
- BMZ Biomedizin-Zentrum Bochum
- CASPO Campus-Sportanlage
- CC Campus-Center
- FNO Forum Nord-Ost
- HZO Hörsaalzentrum Ost
- MSZ Multimedia-Support-Zentrum
- MZ Musikisches Zentrum
- IT.S IT-SERVICES

- P Parkhaus
- P Parkplatz
- P♀ Frauenparkplatz
- P♂ Besucherparkplatz
- P♂ Zentrales Parkhaus (Teilgarage unter Campus)
- P♂ Tennisplätze gesperrt
- P♂ Teilfläche gesperrt

- I Information
- I interne Information
- I Info-Tafel
- I Außenaufzug
- I Bushaltestelle
- I Schranke (Zufahrt eingeschränkt)
- I Zufahrt gesperrt

Einige Zusatzinformationen:

Mittagessen:

Die Mensa ist von 11.00 - 14.30 Uhr geöffnet. Es kann zwischen mehreren Gerichten ausgewählt werden. Nach Zusammenstellung des Essens kann eine Barzahlung an den meisten Kassen (Hinweisschilder beachten) erfolgen.

Das Bistro, ebenfalls im Mensagebäude, ist von 11.00 - 16.00 Uhr geöffnet. Hier kann ebenfalls bar bezahlt werden.

Conference Dinner:

Das Conference Dinner findet am 15.3.2018 ab 19.30 Uhr im Bistro des Mensagebäudes statt. Getränke sind nicht in dem Dinner enthalten, müssen also individuell bezahlt werden.

Für die 1- 1.5 Stunden zwischen dem letzten Vortrag am 15.3. und dem Beginn des Conference Dinners gibt es eine Reihe von Cafés und Gaststätten im Umfeld der RUB (5 Minuten Fußweg).

Q-West :

200 m westlich der Mensa, Campusgelände südlich von Gebäude MA.

Kulturcafé:

100 m nordwestlich des Hörsaalgebäudes im Zugangsbereich zur Uni.

Summa Cum Laude:

500 m nördlich der Mensa, über Fußgängerbrücke in den Eingangsbereich des Unicenters.

Le Clochard:

Über Fußgängerbrücke im östlichen Teil des Unicenters.

Dienstag, 13. März 2018

Im Vorlauf zum IODP/ICDP Kolloquium:

11:00

GESEP School 2018: “Geoscientific and Environmental Drilling, Sampling and Analysis”

Key topics:

1. Drilling & sampling of rock, sediment and ice
2. Geophysical downhole, environmental and mud logging
3. On-site core, cutting & fluid analyses
4. Visit of active drill site and borehole logging

Ende: Mittwoch, 14. März 2018, 13:00 Uhr

Mittwoch, 14. März 2018

10:00

13:00

Registrierung

13:00

13:30

Begrüßung

Neues aus den Programmen

13:30

13:50

S. Krastel
ICDP Rückblick auf 2017 - Wie geht es weiter?

13:50

14:10

J. Erbacher / A. Bornemann
ICDP Rückblick auf 2017 - Wie geht es weiter?

50 Jahre Ocean Drilling I

14:10

14:55

B. Ildefonse
50 years of ocean drilling in the ocean crust: Some milestones

14:55

16:30

Posterpräsentationen & Snacks

IODP & ICDP Themen

16:30

16:50

S. Müller
A crystallization-temperature profile through paleo-oceanic crust (Wadi Gideah transect, Oman ophiolite): Application of the ree-in-plagioclase-clinopyroxene partitioning thermometer & implications for a refined crustal accretion model

16:50

17:10

R. Kühn
Texture and modelled elastic anisotropy of oceanic crust formed at the slow-spreading mid-Atlantic ridge at Atlantis Massif, sampled during IODP Expedition 357 – First results

17:10

17:30

A. Türke
Subsurface Observatory at Surtsey, SUSTAIN Drilling Project

17:30

17:50

U. Riller
Target-rock fluidization during peak-ring formation of the Chicxulub impact crater inferred from Expedition 364 drill core

17:50

18:10

F. Schulte
Impact melt dynamics during peak-ring formation of the Chicxulub crater, Mexico

Donnerstag, 15. März 2018

IODP & ICDP Themen

8:30	8:50	<i>K. Adler</i> Impact of geogenic CO₂ on deep microbial ecosystems in the Hartoušov mofette system, NW Bohemia
8:50	9:10	<i>F. Schubert</i> Exploring microbial sulphate reduction under high temperature and pressure – Results of a pilot study on samples from IODP Exp. 370
9:10	9:30	<i>M. Stranghörner</i> Microbially mediated alteration and Fe mobilization from basaltic rocks of the HSDP2 drill core, Hilo, Hawaii
9:30	9:50	<i>A. Friese</i> Methanogenesis predominated microbial organic matter mineralization in the ferruginous sediments of Earth's early oceans
9:50	10:10	<i>T. Bauersachs</i> Cyanobacterial blooms and their role in the formation of bottom water hypoxia in the Baltic Sea
10:10	10:30	<i>H. Simon</i> Pre-stack depth migration in an anisotropic crystalline environment at the COSC-1 borehole, central Sweden
10:30	13:00	Posterpräsentationen & Kaffee-/Mittagspause
		parallel stattfindend:
10:30	12:00	Geo-Show „unterirdisch“ (Audimax an der RUB, Universitätsstr. 150)
13:00	13:20	<i>C. Dinske</i> Rupture Processes and Magnitude Statistics of the 2014 M5.5 Earthquake Sequence Below a Gold Mine in Orkney, South Africa
13:20	13:40	<i>L. Steinmann</i> 3D deep seismic imaging of the magmatic-hydrothermal system and architecture of the Campi Flegrei caldera to complement an amphibian ICDP/IODP drilling effort
13:40	14:00	<i>U. Weckmann</i> Regional two-dimensional magnetotelluric profile in West Bohemia/Vogtland reveals deep conductive channel into the earthquake swarm region
14:00	14:20	<i>F. Bergmann</i> Channel-levee evolution and stratigraphy at the middle Bengal Fan – Integrating multichannel-seismic data and IODP Expedition 354 results
14:20	14:40	<i>S. Prader</i> Floristic and climatic characterization of the New Jersey hinterland during the Oligocene-Miocene transition in relation to major glaciation events
14:40	15:00	<i>A. Wittke</i> Ca isotope geochemistry in marine deep sea sediments of the Eastern Pacific
15:00	16:30	Posterpräsentationen & Kaffeepause
<i>IODP Fahrtberichte</i>		
16:30	16:45	<i>W. Menapace</i> IODP Expedition 366 Report: “Mariana convergent margin & South Chamorro seamount”

16:45	17:00	<i>F. van der Zwan</i> IODP Expeditions 367/368 Report: “South China Sea Rifted Margin”
17:00	17:15	<i>H.-J. Brumsack</i> IODP Expedition 369 Report “Australia Cretaceous Climate and Tectonics”
17:15	17:30	<i>M. Brunet</i> IODP Expedition 372 Cruise Report: “Creeping Gas Hydrate Slides and LWD for Hikurangi Subduction Margin”
17:30	17:45	<i>E. Dallanave</i> IODP Expedition 371 “Tasman Frontier Subduction Initiation and Paleogene Climate”
<i>IODP & ICDP Themen</i>		
17:45	18:00	<i>T. Haberzettl</i> Towards an ICDP drilling at Lake Nam Co (Tibet)
18:00	18:15	<i>M. Weber</i> IODP Expedition 382 – Iceberg Alley Paleooceanography & South Falkland Slope Drift
ab 19:30	Gemeinsames Abendessen (Bistro an der RUB, Mensagebäude)	
Freitag, 16. März 2018		
<i>50 Jahre Ocean Drilling II</i>		
09:00	09:45	<i>P. Wilson</i> Coupling of ocean and terrestrial climate: Testing the origins of the Sahara Desert after fifty years of ocean drilling
<i>IODP & ICDP Themen</i>		
09:45	10:05	<i>S. Steinig</i> Early Cretaceous South Atlantic opening - modelling the effects of geography, bathymetry and radiative forcing
10:05	10:25	<i>B. Petrick</i> Heat exchange through the Indonesian Throughflow during the Middle Pleistocene Transition
10:25	11:10	Posterpräsentationen & Kaffeepause
11:10	11:30	<i>J. Grützner</i> A new seismic stratigraphy for the Agulhas Plateau resembles major paleo-oceanographic changes in the Indian-Atlantic Ocean gateway since the late Miocene
11:30	11:50	<i>I. Kousis</i> Centennial-scale vegetation dynamics and climate variability in SE Europe during Marine Isotope Stage 11 based on a pollen record from Lake Ohrid
11:50	12:10	<i>A. Prokopenko</i> North American Plio-Pleistocene sedimentary record from the extinct paleo-Lake Idaho, USA – a progress report
12:10	13:00	Posterprämierung und Schlussworte

TEILNEHMERLISTE

<u>Name</u>	<u>Vorname</u>	<u>Institution und Ort</u>
Adhikari	Rishi Ram	MARUM - Zentrum für Marine Umweltwissenschaften, Universität Bremen
Adler	Karsten	GFZ, Helmholtz-Zentrum Potsdam, Deutsches GeoForschungsZentrum, Potsdam
Albers	Elmar	Fachbereich Geowissenschaften, Universität Bremen
Allstädt	Frederik	Institut für Geowissenschaften, Universität Heidelberg
Almееv	Renat	Institut für Mineralogie, Universität Hannover
Amorim Catunda	Maria Carolina	Institut für Geowissenschaften, Universität Heidelberg
Anagnostou	Eleni	GEOMAR, Helmholtz-Zentrum für Ozeanforschung, Kiel
Andreev	Andrej	Institut für Geologie und Mineralogie, Universität Köln
Bahr	André	Institut für Geowissenschaften, Universität Heidelberg
Bauersachs	Thorsten	Institut für Geowissenschaften, Universität Kiel
Behling	Hermann	Albrecht-von-Haller Institut für Pflanzenwissenschaften, Universität Göttingen
Behrmann	Jan	GEOMAR, Helmholtz-Zentrum für Ozeanforschung, Kiel
Bergmann	Fenna	Fachbereich Geowissenschaften, Universität Bremen
Bickert	Torsten	MARUM - Zentrum für Marine Umweltwissenschaften, Universität Bremen
Blaser	Patrick	Institut für Geowissenschaften, Universität Heidelberg
Bornemann	André	IODP, Bundesanstalt für Geowissenschaften und Rohstoffe, Hannover
Böttcher	Michael	Sektion Marine Geologie, Leibniz-Institut für Ostseeforschung, Warnemünde
Brandl	Philipp	GEOMAR, Helmholtz-Zentrum für Ozeanforschung, Kiel
Bretschneider	Lisa	GEOMAR, Helmholtz-Zentrum für Ozeanforschung, Kiel
Brumsack	Hans-Jürgen	ICBM, Institut für Chemie und Biologie des Meeres, Universität Oldenburg
Brunet	Morgane	MARUM - Zentrum für Marine Umweltwissenschaften, Universität Bremen
Brzelinski	Swaantje	Institut für Geowissenschaften, Universität Heidelberg
Burmeister	Christian	Institut für Geographie und Geologie, Universität Greifswald
Burschil	Thomas	LIAG, Leibniz-Institut für Angewandte Geophysik, Geozentrum Hannover
Cáceres	Francisco	Institut für Geo- und Umweltwissenschaften, Universität München
Conze	Ronald	GFZ, Helmholtz-Zentrum Potsdam, Deutsches GeoForschungsZentrum, Potsdam
Cvetkoska	Aleksandra	Department of Animal Ecology and Systematics, Universität Giessen
Dallanave	Edoardo	Department für Geo- und Umweltwissenschaften, Universität München
Davis	Tim	GFZ, Helmholtz-Zentrum Potsdam, Deutsches GeoForschungsZentrum, Potsdam
De Vleeschouwer	David	MARUM - Zentrum für Marine Umweltwissenschaften, Universität Bremen
Deik	Hanaa	Geologisches Institut, RWTH Aachen
Dersch-Hansmann	Michaela	Hessische Staatskanzlei, Abteilung Europa und Internationale Angelegenheiten, Wiesbaden
Dinske	Carsten	Fachrichtung Geophysik, Freie Universität Berlin
Drinkorn	Catherine	GFZ, Helmholtz-Zentrum Potsdam, Deutsches GeoForschungsZentrum, Potsdam
Dultz	Stefan	Institut für Bodenkunde, Leibniz Universität Hannover
Dummann	Wolf	Institut für Geologie und Mineralogie, Universität Köln
Dupont	Lydie	MARUM - Zentrum für Marine Umweltwissenschaften, Universität Bremen
Düsing	Walter	Institut für Erd- und Umweltwissenschaften, Universität Potsdam
Egger	Lisa	IODP, Bundesanstalt für Geowissenschaften und Rohstoffe, Hannover
Elger	Judith	GEOMAR, Helmholtz-Zentrum für Ozeanforschung, Kiel
Elsner	Danny	Institut für Geowissenschaften, Universität, Kiel
Erbacher	Jochen	IODP, Bundesanstalt für Geowissenschaften und Rohstoffe, Hannover
Erzinger	Jörg	GFZ, Helmholtz-Zentrum Potsdam, Deutsches GeoForschungsZentrum, Potsdam
Faak	Kathrin	Institut für Geologie, Mineralogie und Geophysik, Universität Bochum
Flehsig	Christina	Institut für Geophysik und Geologie, Universität Leipzig
Flögel	Sascha	GEOMAR, Helmholtz-Zentrum für Ozeanforschung, Kiel
Foerster	Verena	Institut für Geologie und Mineralogie, Universität Köln
Frank	Martin	GEOMAR, Helmholtz-Zentrum für Ozeanforschung, Kiel

<u>Name</u>	<u>Vorname</u>	<u>Institution und Ort</u>
Friedrich	Oliver	Institut für Geowissenschaften, Universität Heidelberg
Friese	André	GFZ, Helmholtz-Zentrum Potsdam, Deutsches GeoForschungsZentrum, Potsdam
Gabriel	Gerald	LIAG, Leibniz-Institut für Angewandte Geophysik, Hannover
Geissler	Wolfram	AWI, Helmholtz-Zentrum für Polar- und Meeresforschung, Bremerhaven
Geprägs	Patrizia	MARUM - Zentrum für Marine Umweltwissenschaften, Universität Bremen
Gischler	Eberhard	Institut für Geowissenschaften, Goethe-Universität, Frankfurt
Gohl	Karsten	AWI, Helmholtz-Zentrum für Polar- und Meeresforschung, Bremerhaven
Groeneveld	Jeroen	MARUM - Zentrum für Marine Umweltwissenschaften, Universität Bremen
Grunert	Patrick	Institut für Geologie und Mineralogie, Universität Köln
Grützner	Jens	AWI, Helmholtz-Zentrum für Polar- und Meeresforschung, Bremerhaven
Gu	Fang	Albrecht-von-Haller Institut für Pflanzenwissenschaften, Universität Göttingen
Gussone	Nikolaus	Institut für Mineralogie, Universität Münster
Haberzettl	Torsten	Institut für Geographie, Universität Jena
Hallenberger	Max	Energy & Mineral Resources Group, RWTH Aachen
Hasberg	Ascelina	Institut für Geologie und Mineralogie, Universität Köln
Hathorne	Edmund	GEOMAR, Helmholtz-Zentrum für Ozeanforschung, Kiel
Heeschen	Katja	GFZ, Helmholtz-Zentrum Potsdam, Deutsches GeoForschungsZentrum, Potsdam
Henrich	Barbara	Institut für Geowissenschaften, Universität Heidelberg
Herrle	Jens	Institut für Geowissenschaften, Universität Frankfurt
Hess	Kai-Uwe	Department für Geo- und Umweltwissenschaften, Universität München
Hesse	Katja	Institut für Mineralogie, Universität Hannover
Heubeck	Christoph	Institut für Geowissenschaften, Universität Jena
Hochmuth	Katharina	AWI, Helmholtz-Zentrum für Polar- und Meeresforschung, Bremerhaven
Hofmann	Peter	Institut für Geologie und Mineralogie, Universität Köln
Holbourn	Ann	Institut für Geowissenschaften, Universität Kiel
Hörner	Tanja	GFZ, Helmholtz-Zentrum Potsdam, Deutsches GeoForschungsZentrum, Potsdam
Hübscher	Christian	Fachbereich Geowissenschaften, Universität Hamburg
Ildefonse	Benoit	Géosciences Montpellier, Universität Montpellier
Jakob	Kim	Institut für Geowissenschaften, Universität Heidelberg
Janssen	Christoph	GFZ, Helmholtz-Zentrum Potsdam, Deutsches GeoForschungsZentrum, Potsdam
Jöhnck	Janika	Institut für Geowissenschaften, Universität, Kiel
Kaboth	Stefanie	Department of Geosciences, National Taiwan University
Kallmeyer	Jens	GFZ, Helmholtz-Zentrum Potsdam, Deutsches GeoForschungsZentrum, Potsdam
Kasper	Thomas	Institut für Geographie, Universität Jena
Kästner	Felix	GFZ, Helmholtz-Zentrum Potsdam, Deutsches GeoForschungsZentrum, Potsdam
Köster	Male	AWI, Helmholtz-Zentrum für Polar- und Meeresforschung, Bremerhaven
Kotov	Sergey	MARUM - Zentrum für Marine Umweltwissenschaften, Universität Bremen
Kotthoff	Ulrich	Center for Natural History, Universität Hamburg
Kousis	Ilias	Institut für Geowissenschaften, Universität Heidelberg
Koutsodendris	Andreas	Institut für Geowissenschaften, Universität Heidelberg
Kowatsch	Alexander	Institute for Applied Geophysics and Geothermal Energy, RWTH Aachen
Krastel	Sebastian	Institut für Geowissenschaften, Universität, Kiel
Krause	Mathias	Institut für Geowissenschaften, Universität Kiel
Kriegerowski	Marius	Institut für Erd- und Umweltwissenschaften, Universität Potsdam
Krüger	Johanna	Institut für Biochemie und Biologie, Universität Potsdam
	Hermann-	
Kudraß	Rudolf	MARUM - Zentrum für Marine Umweltwissenschaften, Universität Bremen
Kühn	Rebecca	GEOMAR, Helmholtz-Zentrum für Ozeanforschung, Kiel
Kuhnt	Wolfgang	Institut für Geowissenschaften, Universität Kiel
Kurzawski	Robert	GEOMAR, Helmholtz-Zentrum für Ozeanforschung, Kiel
Kutovaya	Anna	Institute for Geology and Geochemistry of Petroleum and Coal, RWTH Aachen
Lamy	Frank	AWI, Helmholtz-Zentrum für Polar- und Meeresforschung, Bremerhaven
Lauterbach	Stefan	Leibniz Laboratory for Radiometric Dating and Stable Isotope Research, Universität, Kiel

<u>Name</u>	<u>Vorname</u>	<u>Institution und Ort</u>
Lay	Vera	TU Bergakademie Freiberg, Institute of Geophysics and Geoinformatics
Lehnert	Oliver	Geozentrum Nordbayern, Universität Erlangen-Nürnberg
Leicher	Niklas	Institut für Geologie und Mineralogie, Universität Köln
Lindhorst	Katja	Institut für Geowissenschaften, Universität, Kiel
Link	Jasmin	Institut für Umweltphysik, Universität Heidelberg
Linsler	Stefan	Institut für Mineralogie, Universität Hannover
Lippold	Jörg	Institut für Geowissenschaften, Universität Heidelberg
Lübbers	Julia	Institut für Geowissenschaften, Universität, Kiel
Lückge	Andreas	Bundesanstalt für Geowissenschaften und Rohstoffe, Hannover
Lüniger	Guido	DFG Deutsche Forschungsgemeinschaft, Bonn
Mangelsdorf	Kai	GFZ, Helmholtz-Zentrum Potsdam, Deutsches GeoForschungsZentrum, Potsdam
Matthiessen	Jens	AWI, Helmholtz-Zentrum für Polar- und Meeresforschung, Bremerhaven
McCormack	Jeremy	Institut für Geologie, Mineralogie und Geophysik, Universität Bochum
Menapace	Walter	Fachbereich Geowissenschaften, Universität Bremen
Meschede	Martin	Institut für Geographie und Geologie, Universität Greifswald
Mock	Dominik	Institut für Mineralogie, Universität Hannover
Möller	Carla	Università degli Studi di Milano
Müller	Marcel	Fachrichtung Geophysik, Freie Universität Berlin
Müller	Samuel	Institut für Geowissenschaften, Universität Kiel
Mutterlose	Jörg	Institut für Geologie, Universität Bochum
Najdahmadi	Bitia	GFZ, Helmholtz-Zentrum Potsdam, Deutsches GeoForschungsZentrum, Potsdam
Neave	David	Institut für Mineralogie, Universität Hannover
Nickschick	Tobias	Institut für Geophysik und Geologie, Universität Leipzig
Nowaczyk	Norbert	GFZ, Helmholtz-Zentrum Potsdam, Deutsches GeoForschungsZentrum, Potsdam
Pälike	Heiko	MARUM - Zentrum für Marine Umweltwissenschaften, Universität
Panagiotopoulos	Kostas	Institut für Geologie und Mineralogie, Universität Köln
Petrick	Benjamin	Max-Planck-Institut für Chemie, Mainz
Pierdominici	Simona	GFZ, Helmholtz-Zentrum Potsdam, Deutsches GeoForschungsZentrum, Potsdam
Piller	Werner	Institut für Erdwissenschaften, Universität Graz
Pöppelmeier	Frerk	Institut für Geowissenschaften, Universität Heidelberg
Prader	Sabine	Center for Natural History, Universität Hamburg
Prokopenko	Alexander	Institut für Geologie und Mineralogie, Universität Köln
Pross	Jörg	Institut für Geowissenschaften, Universität Heidelberg
Reiche	Sönke	Institute for Applied Geophysics and Geothermal Energy, RWTH Aachen
Reifenröther	Ramon	Institut für Geologie und Mineralogie, Universität Köln
Reuning	Lars	EMR, Geologisches Institut, RWTH Aachen
Reusch	Anna	Fachbereich Geowissenschaften Universität Bremen
Riller	Ulrich	Institut für Geowissenschaften, Universität Hamburg
Röhl	Ulla	MARUM - Zentrum für Marine Umweltwissenschaften, Universität Bremen
Sarnthein	Michael	Institut für Geowissenschaften, Universität Kiel
Scheu	Bettina	Institut für Geo- und Umweltwissenschaften, Universität München
Schiebel	Ralf	Max-Planck-Institut für Chemie, Mainz
Schindlbeck	Julie	Institut für Geowissenschaften, Universität Heidelberg
Schleicher	Anja Maria	GFZ, Helmholtz-Zentrum Potsdam, Deutsches GeoForschungsZentrum, Potsdam
Schneider	Ralph	Institut für Geowissenschaften, Kiel
Schubert	Florian	GFZ, Helmholtz-Zentrum Potsdam, Deutsches GeoForschungsZentrum, Potsdam
Schuck	Bernhard	GFZ, Helmholtz-Zentrum Potsdam, Deutsches GeoForschungsZentrum, Potsdam
Schulte	Felix	Institut für Geologie, Universität Hamburg
Schulze	Nora	Fachbereich Geowissenschaften, Universität Bremen
Schwab	Markus	GFZ, Helmholtz-Zentrum Potsdam, Deutsches GeoForschungsZentrum, Potsdam
Schwalb	Antje	Institute of Geosystems und Bioindication, Technische Universität Braunschweig
Schwark	Lorenz	Institut für Geowissenschaften, Universität Kiel

<u>Name</u>	<u>Vorname</u>	<u>Institution und Ort</u>
Schwenk	Tilmann	Fachbereich Geowissenschaften, Universität Bremen
Simon	Helge	Institut für Geophysik und Geoinformatik, TU Bergakademie Freiberg
Sonntag	Iris	DFG Deutsche Forschungsgemeinschaft, Bonn
Spieß	Volkhard	Universität Bremen
Stanislawski	Katja	MARUM - Zentrum für Marine Umweltwissenschaften, Universität Bremen
Stein	Rüdiger	AWI, Helmholtz-Zentrum für Polar- und Meeresforschung, Bremerhaven
Steinig	Sebastian	GEOMAR, Helmholtz-Zentrum für Ozeanforschung, Kiel
Steinmann	Lena	Fachbereich Geowissenschaften, Universität Bremen
Strack	Dieter	International Oil & Gas Consultant, Ratingen
Stranghörner	Marius	Institut für Mineralogie, Leibniz Universität Hannover
Strehlow	Karen	GEOMAR, Helmholtz-Zentrum für Ozeanforschung, Kiel
Stuch	Beatrix	DFG Deutsche Forschungsgemeinschaft, Bonn
Süfke	Finn	Institut für Geowissenschaften, Universität Heidelberg
Tanganan	Deborah	MARUM - Zentrum für Marine Umweltwissenschaften, Universität Bremen
Thomas	Ariel	Institute for Applied Geophysics and Geothermal Energy, RWTH Aachen
Tjallingii	Rik	GFZ, Helmholtz-Zentrum Potsdam, Deutsches GeoForschungsZentrum, Potsdam
Türke	Andreas	Universität Bremen
Uenzelmann-Neben	Gabriele	AWI, Helmholtz-Zentrum für Polar- und Meeresforschung, Bremerhaven
Ulfers	Arne	LIAG, Leibniz-Institut für Angewandte Geophysik, Hannover
Umlauf	Josefine	Institut für Geophysik und Geologie, Universität Leipzig
Unterfeld	Christel	ICDP, Institut für Geowissenschaften, Universität, Kiel
Uzar	Edith	IODP, Bundesanstalt für Geowissenschaften und Rohstoffe, Hannover
van der Zwan	Foukje	GEOMAR, Helmholtz-Zentrum für Ozeanforschung, Kiel
Vogt	Christoph	Fachbereich Geowissenschaften, Universität Bremen
Voigt	Maximilian	Fachrichtung Geophysik, Freie Universität Berlin
Voigt	Silke	Institut für Geowissenschaften, Universität Frankfurt
Voigt	Janett	MARUM - Zentrum für Marine Umweltwissenschaften, Universität Bremen
Wagner	Bernd	Institut für Geologie und Mineralogie, Universität Köln
Weber	Michael	Steinmann-Institut für Geologie, Mineralogie und Paläontologie, Universität Bonn
Weber	Tobias	GFZ, Helmholtz-Zentrum Potsdam, Deutsches GeoForschungsZentrum, Potsdam
Weckmann	Ute	GFZ, Helmholtz-Zentrum Potsdam, Deutsches GeoForschungsZentrum, Potsdam
Wefer	Gerold	MARUM - Zentrum für Marine Umweltwissenschaften, Universität Bremen
Westerhold	Thomas	MARUM - Zentrum für Marine Umweltwissenschaften, Universität Bremen
Wiersberg	Thomas	GFZ, Helmholtz-Zentrum Potsdam, Deutsches GeoForschungsZentrum, Potsdam
Wilson	Paul A.	University of Southampton, Ocean & Earth Science, National Oceanography Centre, Southampton
Wittke	Andreas	Institut für Mineralogie, Universität Münster
Wonik	Thomas	Institut für Mineralogie, Universität Hannover
Yilmaz	Tim	Department für Geo- und Umweltwissenschaften, Universität München
Zhang	Chao	Institut für Mineralogie, Universität Hannover

ABSTRACTS UND FAHRTBERICHTE

FAHRTBERICHTE:

AUTOR	TITEL	SPP	SEITE
E. Albers, W. Menapace and the Expedition 366 Scientists	IODP Expedition 366: Mariana convergent margin & South Chamorro seamount	IODP	16
R. M. Kurzawski, J.C. Schindlbeck, F.M. van der Zwan, and IODP expeditions 367/368 Scientists	IODP Expedition 367/368: South China Sea Rifted Margin	IODP	17
H.-J. Brumsack, R. Hobbs, B. Huber, K. Bogus, and IODP Exp 369 Scientific Party	IODP Expedition 369: Australia Cretaceous Climate and Tectonics	IODP	19
E. Dallanave, T. Westerhold, R. Sutherland, G.R. Dickens, P. Blum and Expedition 371 Scientists	IODP Expedition 371: Tasman Frontier Subduction Initiation and Paleogene Climate	IODP	20
K. Heeschen, M. Brunet, J. Elger and Expedition 372 and 375 Shipboard Scientific Party	IODP Expedition 372: Creeping Gas Hydrate Slides and LWD for Hikurangi Subduction Margin	IODP	21

ABSTRACTS:

AUTOR	TITEL	SPP	SEITE
R. R. Adhikari, V. B. Heuer, M. Elvert, J. Kallmeyer, A. Kitte, L. Wörmer, K.-U. Hinrichs	First insights into the deep life in Bengal Fan sediment	IODP	23
K. Adler, M. Alawi, H.-M. Schulz, B. Plessen, D. Wagner, K. Mangelsdorf	Impact of geogenic CO ₂ on deep microbial ecosystems in the Hartoušov mofette system, NW Bohemia	ICDP	23
A. A. Andreev, P. E. Tarasov, V. Wennrich, M. Melles	Millennial-scale vegetation and climate history of the north-eastern Russian Arctic during the Mammoth Subchron inferred from the Lake El'gygytgyn pollen record	ICDP	24
T. Bauersachs, N. Lorbeer, L. Schwark	Cyanobacterial blooms and their role in the formation of bottom water hypoxia in the Baltic Sea	IODP	25
F. Bergmann, T. Schwenk, V. Spiess, B. Reily, C. France-Lanord and IODP Expedition 354 Scientific Party	Channel-levee evolution and stratigraphy at the middle Bengal Fan – Integrating multichannel-seismic data and IODP Expedition 354 results	IODP	25
T. Bickert, S. Krastel, P. Wilson A. Crocker, L. Dupont, S. Mulitza, E. Schefuss, M. Urlaub, T. Westerhold	IODP Proposal Neogene climate, productivity, and sediment transport on the NW African continental margin	IODP	26
P. Blaser, J. Lippold, M. Gutjahr, J. M. Link, F. Pöppelmeier, M. Frank, N. Frank	Deglacial deep water circulation and Nd isotope changes in the Nordic Seas and subpolar North Atlantic	IODP	27
M. E. Böttcher, H.-J. Brumsack, I. Schmiedinger	The stable water isotope geochemistry of interstitial fluids from the eastern Mediterranean Sea (ODP Leg 160)	IODP	27
A. Bornemann, O. Friedrich, K. Moriya, H. Scher	From the reef into the abyss – the Albian to Turonian record of IODP Site U1407 (Southeast Newfoundland Ridge)	IODP	28
P. A. Brandl, M. D. Hannington	A new MagellanPlus workshop proposal on drilling in the New Ireland Basin (PNG): Understanding the interactions between tectonism, volcanism, ore formation and the deep biosphere	IODP	28
L. Bretschneider, E. C. Hathorne, M. Frank, J. Lübbers, K. Kochhann, A. Holbourn, W. Kuhnt, N. Andersen	Asian Monsoon induced erosion during the Miocene	IODP	29
S. Brzelinski, O. Friedrich, A. Bornemann	Mechanisms of glacial/interglacial climate variability during the 'mid'-Oligocene	IODP	29
T. Burschil, H. Bunness, D. Tanner, G. Gabriel	Seismic exploration of overdeepened Alpine valleys	ICDP	30

AUTOR	TITEL	SPP	SEITE
F. Cáceres, F. Wadsworth, B. Scheu, M. Colombier, K.-U. Hess, B. Ruthensteiner, D. B. Dingwell	Vesiculation processes in rhyolitic magma as a response to heating and slow decompression	ICDP	31
M. C. A. Catunda, A. Bahr, O. Friedrich	Evolution of the oceanic circulation in the North Atlantic across the Mid-Pleistocene Transition	IODP	32
A. Cvetkoska, E. Jovanovska, T. Hauffe, S. Tofilovska, T. H. Donders, A. Francke, H. Vogel, B. Wagner, Z. Levkov, T. Wilke	Global climate and local environmental influence on diatom community structure over time in ancient Lake Ohrid	ICDP	32
T. Davis, E. Rivalta	Magma Propagation directions in the Eger rift (Czech republic)	ICDP	33
H. Deik, L. Reuning, B. Petrick	Hardened faecal pellets as a significant component in deep water, non-tropical marine environments	IODP	33
D. De Vleeschouwer, G. Auer, K. Bogus, B. Christensen, J. Groeneveld, B. Petrick, J. Henderiks, I. Castañeda, E. O'Brien, S. J. Gallagher, C. S. Fulthorpe, H. Pälike	The amplifying effect of Indonesian Through-flow heat transfer on Late Pliocene Southern Hemisphere climate cooling	IODP	34
C. Dinske, M. Müller, M. Voigt, J. Kummerow, S.A. Shapiro	Rupture Processes and Magnitude Statistics of the 2014 M5.5 Earthquake Sequence Below a Gold Mine in Orkney, South Africa	ICDP	34
W. Düsing, A. Asrat, V. Foerster, H. Krämer, H. Lamb, N. Marwan, F. Schäbitz, M. H. Trauth	Trends, rhythms and transitions during the Late Quaternary in southern Ethiopia	ICDP	35
W. Dummann, S. Steinig, P. Hofmann, S. Flögel, A. Osborne, J.O. Herrle, M. Frank, T. Wagner	Gateway history of the Early Cretaceous South Atlantic derived from Nd-isotope signatures	IODP	35
J. Elger, C. Berndt, F. Kästner, S. Pierdominici, J. Kück	First results on Core-Log-Seismic-Integration in hard-rock environments using the ICDP drilling project COSC-1, Sweden	ICDP	36
D. Elsner, S. Beil, J. Jöhnck, J. Lübbers, A. Holbourn, W. Kuhnt, Y. Rosenthal, D. Kulhanek and Expedition 363 Scientists	New insights into the Neogene evolution of the Australian Monsoon from IODP Expedition 363 "Western Pacific Warm Pool"	IODP	36
C. Flechsig, T. Günther, T. Nickschick	Large-scale geoelectrical survey in the eger rift zone (W-Bohemia) at a proposed pier-ICDP fluid monitoring drill sites to image fluid-related conductivity structures	ICDP	37
V. E. Foerster, A. Asrat, A. S. Cohen, D. M. Deocampo, A. Deino, W. Düsing, C. Günter, H. Krämer, H. F. Lamb, S. Opitz, H. M. Roberts, F. Schaebitz, M. H. Trauth & Hspdp Science Team	Authigenic minerals in the HSPDP-Chew Bahir sediment cores (southern Ethiopia): Using mineral alteration as sensitive paleoclimate proxy	ICDP	38
A. Friese, J. Kallmeyer, C. Glomitza, A. Vuillemin, R. Simister, S. Nomosatryo, K. Bauer, V. B. Heuer, C. Henny, S. A. Crowe, D. Ariztegui, S. Bijaksana, H. Vogel, M. Melles, J. M. Russell, D. Wagner and the Towuti Drilling Project Science Team	Methanogenesis predominated microbial organic matter mineralization in the ferruginous sediments of Earth's early oceans	ICDP	38
W. H. Geissler, J. Knies, J. Matthiessen, A. C. Gebhardt, C. Vogt	The Opening of the Arctic-Atlantic Gateway: Tectonic, Oceanographic and Climatic Dynamics – Status of the IODP Initiative	IODP	39
E. Gischler, F. S. Anselmetti	Geomorphology of the Belize Barrier Reef margin: A survey for IODP drilling	IODP	99
J. Grützner, G. Uenzelmann-Neben, I. A. Hall	The Indian-Atlantic Ocean gateway during the Pliocene: Current dynamics and changing sediment provenance	IODP	39
J. Grützner, F. J. Jimenez Espejo, N. Lathika, G. Uenzelmann-Neben	A new seismic stratigraphy for the Agulhas Plateau resembles major paleo-oceanographic changes in the Indian-Atlantic Ocean gateway since the late Miocene	IODP	40

AUTOR	TITEL	SPP	SEITE
P. Grunert, Á. García-Gallardo, B. Balestra, C. Richter, G. Auer, M. Van Der Schee, J.-A. Flores, F. J. Sierro, F. Jiménez-Espejo, C.A. Zarikian, U. Röhl, A. Bahr, S. Kaboth, W. E. Piller	Pliocene variability of Mediterranean-Atlantic exchange	IODP	41
F. Gu, K. A. F. Zonneveld, C. M. Chiessi, H. W. Arz, J. Pätzold, H. Behling	Late Quaternary palaeoenvironmental dynamics inferred from marine sediment cores of the western South Atlantic	IODP	41
N. Gussone, M. Inoue, Y. Yokoyama, A. Suzuki, H. Kawahata, S. Galer	Incorporation of Ca and Sr isotopes in scleractinian corals from culture experiments and the Great Barrier Reef	IODP	42
T. Haberzettl, G. Daut, T. Kasper, N. Schulze, V. Spiess, J. Wang, L. Zhu, Nam Co Science Team	Towards an ICDP drilling at Lake Nam Co (Tibet)	ICDP	43
M. Hallenberger, L. Reuning, H. Iwatani	Formation of an Pleistocene aragonite lowstand wedge along the North West Shelf of Australia (NWS), insights from Site U1461 of IODP Expedition 356	IODP	43
A. K.M. Hasberg, M. Melles, P. Held, V. Wennrich, J. Just, S. Opitz, M.A. Morlock, H. Vogel, J. M. Russell, S. Bijaksana and the ICDP-TDP Scientific Party	Geochemical characterization and genetic interpretation of mass movement deposits at TDP Site 2, Lake Towuti, Indonesia	ICDP	44
E. Hathorne, K. Thirumalai, D. Gebregiorgis, L. Giosan, B. N. Nath, M. Frank	Character of the enhanced South Asian Monsoon during the mid Holocene revealed by oxygen isotope analysis of individual foraminifera	IODP	44
C. Heubeck and the base team	Barberton Archean Surface Environments (BASE)	ICDP	45
K. Hochmuth, K. Gohl, G. Leitchenkov, I. Sauerlich, J. Whittaker, L. Desantis, E. Olivio, G. Uenzelmann-Neben, B. Davy	Paleobathymetric grids of the Cenozoic Southern Ocean – paving the way towards improved reconstructions of the Southern Ocean's past	IODP	45
C. Hübscher, T. Druitt, P. Nomikou, D. Papanikolaou, et al.	Volcanic, tectonic and hydrothermal processes in an island-arc caldera environment. Development of an IODP Drilling Proposal at Santorini-Kolumbo Marine Volcanic System	IODP	46
K. A. Jakob, P. A. Wilson, J. Pross, J. Fiebig, O. Friedrich	Early Quaternary stabilisation of the East Antarctic Ice Sheet linked to Northern Hemisphere ice volume	IODP	46
J. Jöhnck, W. Kuhnt, A. Holbourn, N. Andersen	Deciphering the late Miocene evolution of the Indian Monsoon in IODP Expedition 353 Sites U1447 and U1448 (Andaman Sea)	IODP	47
S. Kaboth, A. Bahr, C. Zeeden, S. Toucanne, F. Eynaud, F. Jiménez-Espejo, U. Röhl, O. Friedrich, J. Pross, L. Löwemark, L. Lourens	Continuous monsoonal forcing of European ice-sheet dynamics during the Late Quaternary	IODP	48
J. Kallmeyer, F. Schubert, T. Treude, IODP Exp. 370 Scientific Party	Exploring microbial sulphate reduction under high temperature and pressure – Results of a pilot study on samples from IODP Exp. 370	IODP	48
J. Kallmeyer, P. A. Baker, S. C. Fritz	The Trans-Amazon Drilling Project – A Joint ICDP/IODP Project To Unravel The History Of the Amazon Basin	ICDP	49
T. Kasper, T. Haberzettl, J. Wang, A. Schwalb, G. Daut, B. Plessen, L. Zhu, R. Mäusbacher	Indian Summer Monsoon record from Nam Co reveals a switching relation to Pacific climate oscillation during the Holocene	ICDP	49
F. Kästner, S. Pierdominici, J. Elger, C. Berndt, J. Kück	Core-Log-Seismic-Integration (CLSI) in hard-rock environments using the ICDP drilling project COSC-1, Sweden: project outline	ICDP	50
J. Krüger, M. Hofreiter, R. Tiedemann, M. H. Trauth, V. Foerster, S. Hartmann, K. Havenstein	Ancient DNA and Metagenomics of Lake Sediments	ICDP	50
S. Kotov, H. Pälike	Enhanced Principal Tensor Analysis as a tool for 3-way geological data reconstructions	IODP	51

AUTOR	TITEL	SPP	SEITE
I. Kousis, A. Koutsodendris, O. Peyron, N. Leicher, A. Francke, B. Wagner, M. Knipping, J. Pross	Centennial-scale vegetation dynamics and climate variability in SE Europe during Marine Isotope Stage 11 based on a pollen record from Lake Ohrid	ICDP	51
A. Kowatsch, S. Reiche, A. Thomas, S. Back	Forward modeling of prograding depositional sequences at the new jersey shallow shelf	IODP	52
M. Kriegerowski, S. Cesca, M. Ohrnberger, F. Krüger	How near source region double difference attenuation in North-West Bohemia can benefit from ICDP borehole seismometry	ICDP	99
R. Kühn, M. Stipp, B. Leiss, J. Kossak-Glowczewski, J. H. Behrmann	Texture and modelled elastic anisotropy of oceanic crust formed at the slow-spreading mid-Atlantic ridge at Atlantis Massif, sampled during IODP Expedition 357 – First results	IODP	53
R. M. Kurzwaski, A. R. Niemeijer, M. Stipp, D. Charpentier, J. H. Behrmann, C. J. Spiers	Shallow subduction channel deformation at the Costa Rica erosive convergent continental margin: frictional behavior of subduction input sediments	IODP	53
S. Kutterolf, J. C. Schindlbeck	Traces of explosive eruptions in Cretaceous to Quaternary Indian Ocean sediments	IODP	54
F. Lamy, G. Winckler, R. Anderson, H. W. Arz, G. Cortese, O. Esper, K. Gohl, I. Hall, C.D. Hillenbrand, C. Hübscher, C. Lange, L. Lembke-Jene, A. Martinez-Garcia, U. Ninnemann, D. Nürnberg, K. Pahnke, A. Polonia, J. Stoner, R. Tiedemann, G. Uenzelmann-Neben	IODP Expedition 383: Dynamics of the Pacific Antarctic Circumpolar Current (DYNAPACC)	IODP	54
S. Lauterbach, N. Andersen, T. Blanz, P. Martinez, R. Schneider	Centennial- to millennial-scale intervals of weak Indian summer monsoon intensity during the last 70 kyr reconstructed from stable isotope ratios of terrestrial n-alkanes in sediments from the Bay of Bengal (IODP site U1446)	IODP	55
V. Lay, S. Buske, S. B. Bodenbun, J. Townend, R. Kellett, M. Savage, J. Eccles, D. Schmitt, A. Constantinou, M. Bertram, K. Hall, D. Lawton, A. Gorman and DFDP Whataroa 2016 Science Team	3D-VSP experiment at the Alpine Fault DFDP-2 drill site in Whataroa, New Zealand	ICDP	56
N. Leicher, B. Wagner, G. Zanchetta, B. Giaccio, A. Francke, R. Sulpizio, S. Nomade, J. Just	Tephrostratigraphy and chronology of the Lake Ohrid DEEP site record of the last 1.4 Ma	ICDP	57
J. M. Link, P. Blaser, M. Gutjahr, F. Pöppelmeier, J. Lippold, K. A. Jakob, AH. Osborne, E. Böhm, M. Frank, O. Friedrich, N. Frank	North Atlantic Deep Water Provenance during the past one million years	IODP	58
S. A. Linsler, R. R. Almeev, F. Holtz	Crystallization conditions of fore-arc basalts from the Izu-Bonin-Mariana island arc: new experimental constraints	IODP	59
J. Lübbers, W. Kuhnt, A. E. Holbourn, C. T. Bolton, E. Gray, K. G. D. Kochhann, N. Andersen	Evidence of an intense middle to late Miocene “Carbonate Crash” in the Indian Ocean (IODP Site 1443)	IODP	61
J. Matthiessen, M. Schreck, S. De Schepper, C. Zorzi, A. De Vernal	Quaternary dinoflagellate cyst stratigraphy in the Arctic Ocean: potential and limitations	IODP	61
J. McCormack, T. R. R. Bontognali, A. Immenhauser, O. Kwiecien	Cyclic dolomite formation in Lake Van – mechanisms and links to abrupt climate change	ICDP	62
D. Mock, B. Ildefonse, D. Garbe-Schönberg, S. Müller, D. A. Neave, J. Koepke, and Oman Drilling Project Phase 1 Science Party	Understanding lower crust accretion at fast-spreading mid-ocean ridges: new insights from drill cores obtained by the ICDP Oman Drilling Project: First Results	ICDP	62
C. Möller, A. Bornemann, B. Rieger, J. Mutterlose	Coccolith size variations - potential tool for understanding the late Valanginian ocean perturbation	IODP	63

AUTOR	TITEL	SPP	SEITE
S. Mueller, J. Hasenclever, D. Garbe-Schönberg, J. Koepke, K. Hoernle	A Crystallization-Temperature Profile Through Paleo-Oceanic Crust (Wadi Gideah Transect, Oman Ophiolite): Application Of The Ree-In-Plagioclase-Clinopyroxene Partitioning Thermometer & Implications For A Refined Crustal Accretion Model	ICDP	63
B. Najdahmadi, M. Bohnhoff, Y. Ben-Zion, E. Görgün, H. Alp, E. Yalçinkaya	Ganos Fault Zone network: Imaging North Anatolian Fault Zone in the western Marmara region, Turkey, based on a dense local seismic network	ICDP	64
N. Nowaczyk, J. Rohrmüller, H. Kämpf, E. Geiß, J. Großmann, I. Grun, J. Mingram, J. Mrlina, B. Plessen, M. Stebich, C. Veress, A. Wendt	Reconnaissance study of an inferred Quaternary maar structure in the western part of the Bohemian Massif near Neualbenreuth, NE-Bavaria (Germany)	ICDP	64
K. Panagiotopoulos, J. Holtvoeth, R. D. Pancost, B. Wagner, M. Melles	Early Pleistocene vegetation and environmental history from Lake Ohrid	ICDP	65
B. F. Petrick, G. Auer, A. Martinez-Garcia, D. De Vleeschouwer, B. A. Christensen, C. Stolfi, L. Reuning, T. Buckley, S. J. Gallagher, C. S. Fulthorpe, K. Bogus, G. Haug	Heat exchange through the Indonesian Throughflow during the Middle Pleistocene Transition	IODP	65
S. Pierdominici, A. M. Schleicher, J. Kück, D. T. Rodbell, M. B. Abbott and the ICDP Lake Junín working group	Linking downhole logging data and clay mineralogy analysis in the ICDP Lake Junín drilling Project, Peru	ICDP	66
F. Pöppelmeier, M. Gutjahr, P. Blaser, L. D. Keigwin, J. Lippold	Origin of the deepest NW Atlantic water masses during the Last Glacial Maximum and deglaciation	IODP	66
M. Portnyagin, R. Almeev, D. Garbe-Schönberg	Evidence for mantle plume origin of the Shatsky Rise from systematics of chalcophile and siderophile elements in volcanic glasses	IODP	67
S. Prader, U. Kotthoff, F. M. G. Mccarthy, G. Schmiedl, T. H. Donders, D. R. Greenwood	Floristic and climatic characterization of the New Jersey hinterland during the Oligocene-Miocene transition in relation to major glaciation events	IODP	67
S. Prader, U. Kotthoff, D. Bunzel, Y. Milker, F. M. G. Mccarthy, G. Schmiedl, D. R. Greenwood	Orbital-driven paleovegetation changes in the New Jersey hinterland during a short time interval (300.000 yrs) of the Burdigalian	IODP	68
A. Prokopenko	North American Plio-Pleistocene sedimentary record from the extinct paleo-Lake Idaho, USA – a progress report	IODP	69
R. Reifenhöther, C. Münker, B. Scheibner	Evidence for selective tungsten enrichment in altered oceanic crust	IODP	69
L. Reuning, K. Sparwasser	Sedimentology and geochemistry of peritidal sediments from the Northwest Shelf of Australia and Abu Dhabi	IODP	70
A. Reusch, V. Spieß, H. Keil, C. Gebhardt, K. Abdrakhmatov	Long term tectonic and paleoclimatic history of Lake Issyk-Kul, Kyrgyzstan	ICDP	70
U. Riller, F. Schulte, M. Poelchau, A. S. P. Rae, R. A. F. Grieve, J. Lofi, J. Morgan, N. Mccall, S. P. C. Gulick	Target-rock fluidization during peak-ring formation of the Chicxulub impact crater inferred from Expedition 364 drill core	IODP	71
J. C. Schindlbeck	South China Sea tephra and sedimentary basement provenance	IODP	71
B. Schuck, C. Janssen, A. M. Schleicher, V. G. Toy, G. Dresen	Fault core deformation mechanisms deduced from microstructures, mineralogy and geochemistry of the Alpine Fault, New Zealand	ICDP	72
F. M. Schulte, S. Jung, U. Riller	Impact melt dynamics during peak-ring formation of the Chicxulub crater, Mexico	ICDP	72

AUTOR	TITEL	SPP	SEITE
N. Schulze, V. Spiess, J. Van Der Woerd, G. Daut, T. Haberzettl, J. Wang, L. Zhu	The tectonic system at Lake Nam Co, Tibetan Plateau – Results from high-resolution 2D seismic data	ICDP	73
A. Schwalb, V. Wittig, R. Bracke, U. Harms	Hipercorig – A modular Direct Push Coring Rig for extended reach in unconsolidated sediments on- and offshore and its operation	ICDP	74
T. Schwenk, V. Junge, V. Spiess, and Expedition 353 Scientists	A new stratigraphy of the middle Bengal Fan – results from correlation of seismic data with Site U1444, Expedition 353	IODP	74
H. Simon, F. Krauß, S. Buske, R. Giese, P. Hedin, C. Juhlin	Pre-stack depth migration in an anisotropic crystalline environment at the COSC-1 borehole, central Sweden	ICDP	75
H. Simon, S. Buske, T. Fischer	High-resolution seismic survey at a planned PIER-ICDP fluid-monitoring site in the Eger Rift zone, Czech Republic	ICDP	76
K. Stanislawski, M. J. Ikari	Frictional behavior of Juan de Fuca sediments approaching the Cascadia subduction zone	IODP	78
S. Steinig, W. Dummamann, S. Flögel, W. Park, T. Wagner, J. O. Herrle, P. Hofmann	Early Cretaceous South Atlantic opening - modelling the effects of geography, bathymetry and radiative forcing	IODP	78
L. Steinmann, V. Spiess, M. Sacchi	3D deep seismic imaging of the magmatic-hydrothermal system and architecture of the Campi Flegrei caldera to complement an amphibian ICDP/IODP drilling effort	ICDP	79
M. Stranghoener, A. Schippers, S. Dultz, H. Behrens	Microbially mediated alteration and Fe mobilization from basaltic rocks of the HSDP2 drill core, Hilo, Hawaii	ICDP	80
F. Sufke, F. Pöppelmeier, P. Blaser, M. Gutjahr, T. Goepfert, J. Grützner, B. Antz, J. Lippold	Changes of the Atlantic meridional overturning circulation of the past 30 ka recorded in a depth transect at the Blake Outer Ridge	IODP	81
D. Tangunan	Coccolithophore productivity and carbonate budget at the Indian-Atlantic Ocean Gateway since the Miocene	IODP	81
A. Thomas, S. Reiche, M. Riedel, S. Buske	Facies derived compaction trends integrated into a new jersey shelf hydrogeological model	IODP	82
R. Tjallignii, M. J. Schwab, M. Ahlborn, Y. Ben Dor, M. Armon, Y. Enzel, J. Hasan Shoqeir, A. Brauer and Palex Scientific Team	Holocene Paleohydrology and Extreme Floods in the Dead Sea Region	ICDP	82
M. H. Trauth, A. Asrat, W. Duesing, V. Foerster, H. Kraemer, H. Lamb, N. Marwan, M. A. Maslin, F. Schaebitz and the HSDP2 Science Team	Classifying past climate variation in the Chew Bahir basin, southern Ethiopia, using recurrence quantification analysis	ICDP	83
A. Türke, W.-A. Kahl, W. Bach	Subsurface Observatory at Surtsey, SUSTAIN Drilling Project	ICDP	83
G. Uenzelmann-Neben	Prydz Bay sediment drifts: Archives of modifications in East Antarctic climatic and oceanographic conditions	IODP	84
A. Ulfers, K. Hesse, T. Wonik	Paleoenvironmental indications and cyclostratigraphic studies of sediments from tropical Lake Towuti obtained from downhole logging	ICDP	84
J. Umlauf, H. Flores-Estrella, M. Korn	Imaging fluid channels using ambient seismic noise (Hartoušov Mofette Field, CZ)	ICDP	85
F. M. Van Der Zwan, S. Petersen	First basaltic melts and early hydrothermal processes at continental breakup - IODP Expeditions 367/368: South China Sea Rifted Margin	IODP	85

AUTOR	TITEL	SPP	SEITE
C. Vogt	The Plio-Pleistocene ACEX (Leg 302) record revisited – A high resolution mineralogical record	IODP	86
J. Voigt	Clumped isotope thermometry and $\delta^{18}\text{O}$ seawater composition of key climate events during the Oligocene	IODP	87
A. Vuillemin, R. Wirth, H. Kemnitz, J. A. Schuessler, L. G. Benning, A. Friese, A. Luecke, C. Mayr, C. Henny, K. Bauer, J. M. Russell, S. Bijaksana, H. Vogel, S. A. Crowe, J. Kallmeyer and the ICDP Towuti Drilling Project Science Team	Diagenetic siderites and vivianites in ferruginous sediment from Lake Towuti, Indonesia	ICDP	88
B. Wagner, B. Giaccio, N. Leicher, G. Mannella, S. Nomade, E. Regattieri, T. Wonik, G. Zanchetta,	Tephrochronology of a 415 ka sediment record from the Fucino Basin, Central Italy	ICDP	88
M. Wang, O. Namur, R. Almeev, B. Charlier, F. Holtz	Petrogenesis of Snake River Plain basalts from the Kimama core: An experimental study on ferrobasalts	IODP	90
M. E. Weber, M. Raymo, Y. M. Martos, C. Allen, S. Belt, P. U. Clark, M. Garcia, M. Gutjahr, I. Hall, G. Kuhn, F. Bohoyo, G. Lohmann, N. Mccave, J. X. Mitrovica, R. Schneider, D. Sprenk, J. Stoner, A. Timmermann, T. Williams, N. R. Golledge, R. Deconto, R. Gladstone, A. Hein, K. Hendry, A. Levermann, J. Pike, D. Pollard, V. Peck	IODP Expedition 382 – Iceberg Alley Paleocceanography & South Falkland Slope Drift	IODP	92
T. Weber, C. Drinkorn, J. Saynisch, G. Uenzelmann-Neben, M. Thomas	Transport, Removal and Accumulation of sediments Numerically Simulated for Paleo-Oceans and Reconstructed from cores of The Eirik Drift (TRANSPORTED)	IODP	92
U. Weckmann, G. Muñoz, J. Pek, S. Kováčiková, R. Klanica	Regional two-dimensional magnetotelluric profile in West Bohemia/Vogtland reveals deep conductive channel into the earthquake swarm region	ICDP	93
T. Westerhold, U. Röhl, R. H. Wilkens	A new high-resolution Maastrichtian to Late Campanian cyclostratigraphic record from equatorial Atlantic ODP Sites 1258 and 1259	IODP	94
T. Wiersberg, S. Hammerschmidt, T. Toki, A. Kopf, J. Erzinger	Fluid migration in the Nankai Trough Kumano forarc basin	IODP	95
A. Wittke, N. Gussone, D. Derigs, M. Schälling, C. März, B.M.A. Teichert	Ca isotope geochemistry in marine deep sea sediments of the Eastern Pacific	IODP	96
T. I. Yilmaz, K.-U. Hess, J. Vasseur, F. B. Wadsworth, H. A. Gilg, S. Nakada, D. B. Dingwell	Thermal Expansivity Between 150 and 800°C of Hydrothermally Altered Conduit Dyke Samples from USDP-4 Drill Core (Mt Unzen, Shimabara, Japan)	ICDP	97
C. Zhang, J. Koepke, O. Namur, S. Feig	Melt-peridotite interaction at crust-mantle boundary: An experimetal perspective	IODP	98

Fahrtberichte

IODP Expedition 366: Mariana convergent margin & South Chamorro seamount

E. ALBERS^{1,2}, W. MENAPACE²

AND THE EXPEDITION 366 SCIENTISTS

¹Department of Geosciences, University of Bremen, Bremen, Germany

²MARUM – Center for Marine Environmental Research, University of Bremen, Germany

Little is known about geologic processes occurring in forearcs of convergent plate margins. While inputs into subduction zones and deep processes are directly accessible by probing downgoing plates prior to subduction and outputs such as magmas and volatiles in volcanic arcs and backarc basins, respectively, there are no such means to sample and study forearc systems. Forearcs are, however, key areas where geologic processes affect geochemical cycling and fluxes, crustal and mantle evolution, seismicity and natural hazards, and the deep biosphere. Understanding shallow subduction zone mechanisms is hence extremely important. The Mariana convergent margin, where the Pacific plate subducts beneath the Philippine Sea plate, provides a window into this zone. Here, vast active mud volcanoes have formed by the eruption of fluids and sediments released from the subducting plate or picked up during the fluids' rise to the seafloor via deep-rooted faults.

Primary scientific objectives of IODP Exp. 366 were to assess (1) mass transport processes in the Mariana forearc, (2) spatial and compositional variability of slab-derived fluids, (3) the metamorphic and tectonic history and physical properties of the subduction zone, (4) biological activity associated with deep-derived subduction zone materials.

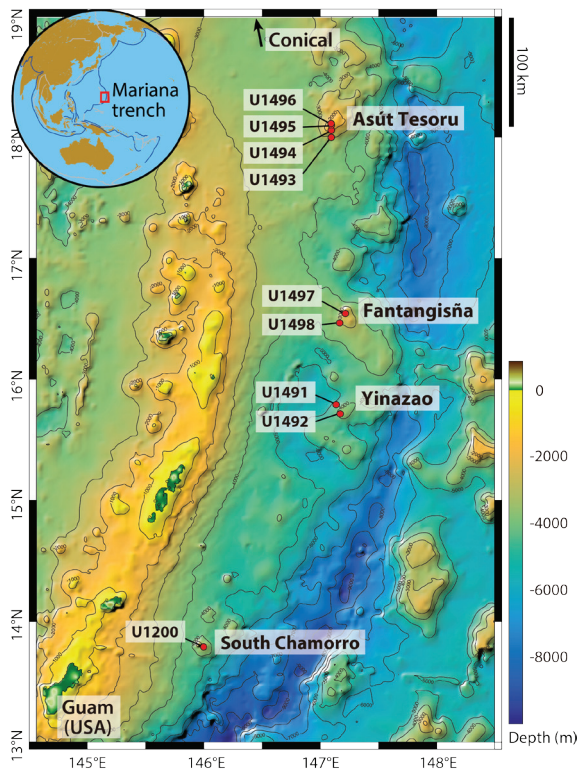


Fig. 1: Study area in the Mariana forearc region and IODP Exp. 366 Sites (after Fryer et al., 2017).

Expedition 366 set sail aboard D/V *JOIDES Resolution* in Guam (USA) on 8 Dec. 2016 and ended in Hong Kong on 7 Feb. 2017. During the expedition, we drilled and cored summits and flanks of three mud volcanoes (Yinazao, Fantangisña, and Asút Tesoru; Fig. 1). These structures are located at varying distances to the trench, i.e., varying depth to the subducting slab. A continuous down-subduction profile covering slab depths of about 13 to 19 km and slab temperatures of estimated 80 to 250–350°C (Maekawa et al., 1993; Fryer et al., 2006; Gharib, 2006; Oakley et al., 2007, 2008; Oakley, 2008; Hulme et al., 2010) is now available when integrating the results of Exp. 366 into the ones from two additional mud volcanoes drilled during earlier campaigns (Conical and South Chamorro seamounts, Leg 125 and 195, respectively).

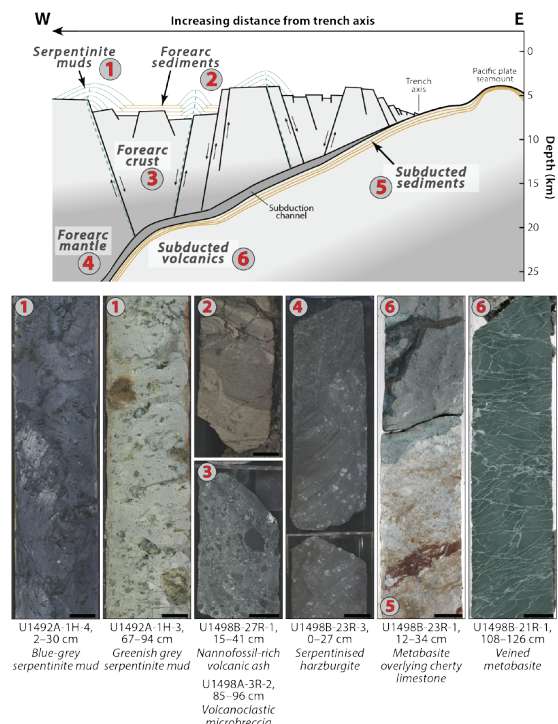


Fig. 2: Idealised cross-section of the Mariana forearc, including the relative positioning of serpentinite mud volcanoes. Tectonic zones 1 through 6 in the forearc subduction zone complex are keyed to drill core images (after Fryer et al., 2017).

Recovered materials are mostly serpentinite muds containing millimetre- to metre-sized clasts of ultramafic mantle material, derived from the forearc mantle and variably serpentinized by the rising, slab-derived fluids (Fig. 2; Fryer et al., 2017). Forearc sediments, composed of pelagic materials and volcanic ash deposits, as well as clasts of mafic forearc crust are minor components of the cored units. In addition, we encountered clasts of lithified sediments, alkali basalt, and limestone interpreted as recycled parts of the subducted Pacific plate (Fryer et al., 2017). The variably serpentinised ultramafic rock and mud materials are largely uniform in major element composition but vary considerably in terms of their trace element contents. These variations reflect changes in temperature and pressure conditions in the underlying subduction channel. Likewise, pore fluids hold signatures consistent with the processes taking place in the downgoing plate with increasing depth, i.e., sediment compaction, opal-CT dehydration, clay diagenesis, and decarbonation. Fluid discharge rates and dissolved gases (H_2 , CH_4 , C_2H_6) are highest at Asút Tesoru, the mud volcano furthest away from the trench. The gas-rich fluids presumably

support active microbial communities; extensive sampling for shore-based work was conducted during the expedition. Porosity and bulk density data of serpentinite muds vary strongly over the drilled sites. Both parameters are higher than expected for some of the summit sites coherent with active fluid discharge, which inhibits mud compaction, and with recent sediment expulsion. Thermal measurements revealed considerably higher heat flow on the seamounts' flanks compared to their summits.

In addition to coring operations, we installed three screened borehole casings with ROV landing platforms at the summits of Yinazao, Fantangisña, and Asüt Tesoru and removed a CORK body at South Chamorro seamount that was deployed during Leg 195. Plans for future *in situ* observatories and sampling through the implementation of CORK-Lite systems (simplified CORK plug systems) are currently underway.

References:

- Fryer PB, Gharib J, Ross K, Savov I & Mottl MJ (2006) Variability in serpentinite mudflow mechanisms and sources: ODP drilling results on Mariana forearc seamounts. *Geochem Geophys Geosyst* 7, Q08014.
- Fryer P, Wheat G, Williams T & the Expedition 366 Scientists (2017) Expedition 366 preliminary report: Mariana convergent margin and South Chamorro seamount. *International Ocean Discovery Program*.
- Gharib J (2006) Clastic metabasites and authigenic minerals within serpentinite protrusions from the Mariana forearc: implications for sub-forearc subduction processes. PhD Thesis, University of Hawai'i (HI), USA.
- Hulme SM, Wheat CG, Fryer PB & Mottl MJ (2010) Pore water chemistry of the Mariana serpentinite mud volcanoes: a window to the seismogenic zone. *Geochem Geophys Geosyst* 11, Q01X09.
- Maekawa H, Masaya S, Ishill T, Fryer P & Pearce JA (1993) Blueschist metamorphism in an active subduction zone. *Nature* 364, 520–523.
- Oakley AJ (2008) A multi-channel seismic and bathymetric investigation of the central Mariana convergent margin. PhD Thesis, University of Hawai'i (HI), USA.
- Oakley AJ, Taylor B, Fryer PB, Moore GF, Goodliffe AM & Morgan JK (2007) Emplacement, growth, and gravitational deformation of serpentinite seamounts on the Mariana forearc. *Geophys J Int* 170, 615–634.
- Oakley AJ, Taylor B & Moore GF (2008) Pacific plate subduction beneath the central Mariana and Izu-Bonin fore arcs: new insights from an old margin. *Geochem Geophys Geosyst* 9, Q06003.

Expedition report for IODP Expeditions 367/368: South China Sea Rifted Margin

R. M. KURZAWSKI^{1,3}, J. C. SCHINDLBECK², F. M. VAN DER ZWAN^{1,3}
AND IODP EXPEDITIONS 367/368 SCIENTISTS

¹GEOMAR Helmholtz Centre for Ocean Research Kiel, 24148 Kiel, Germany

²Institute of Earth Sciences, University of Heidelberg, 69120 Heidelberg, Germany

³Institute of Geosciences, Christian-Albrechts-University, 24118 Kiel, Germany

Expeditions 367 and 368 of the International Ocean Discovery Program (IODP) were implemented to study the mechanisms of lithosphere extension and continental breakup at a non-volcanic (magma-poor) rifted margin, and in particular to test the scientific hypothesis of “Iberia-type” continental breakup at the northern South China Sea (SCS) margin. Rifting style and history, as well as the interplay with early magmatic pulses and the onset of full oceanic spreading are to be compared to other non-volcanic rifted margins, such as e.g. the Newfoundland-Iberia conjugate rifted margins prominently exhuming serpentinitized mantle lithosphere at the sea floor. This project was carried out as a single science program with 114 days of drilling operations spread across two IODP expeditions as outlined in the Expedition 367/368 Scientific Prospectus (Sun et al., 2016).

The drill sites lie on a ~150 km wide transect crossing the Continent-Ocean Transition (COT) of the western South China Sea rifted margin (Sun et al., 2016) and target the four main tectonic features: the Outer Margin High (OMH) and its small rift basins (interpreted as continental crust) and the nature of the three ridges within the distal margin (Ridges A, B, and C that form the COT up to full oceanic spreading) (Figs. 1, 2).

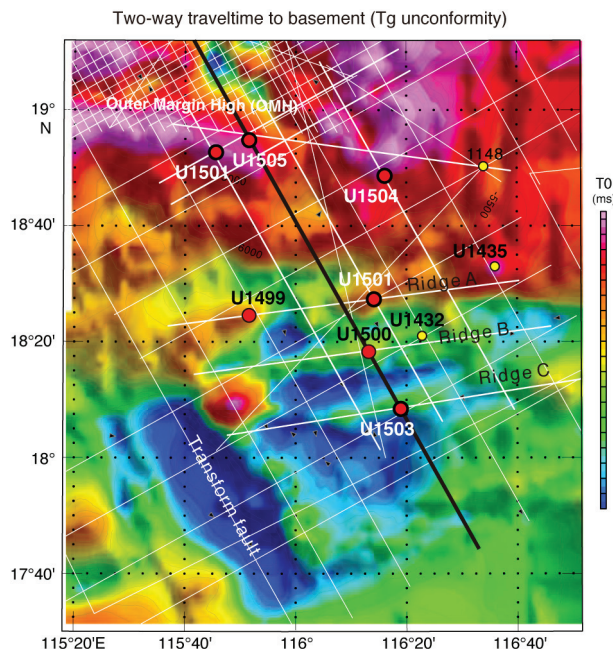


Fig. 1: Two-way travelttime to basement (Tg unconformity). The drilling transect is marked by a thick black line. Colored circles show ODP and IODP drill site locations. Locations of the Outer Margin High (OMH) and the Ridges A, B and C are shown relative to the drill sites. The figure is modified after Jian et al. (in press).

The expeditions took place from February to June 2017 and set sail from Hong Kong harbour to the first drill site. Expedition 367 drilled IODP Sites U1499 and U1500 (Figs. 1, 2; Sun et al., in press). Site U1499 is located on basement Ridge A within the South China Sea COT about 60 km seaward and SE of the Outer Margin High. Site U1500 is located on Ridge B, and it is the most seaward site that Expedition 367 drilled within the South China Sea continent-ocean transition (COT). Ridge B is located ~80 km seaward of the Outer Margin High, and ~20 km seaward of Ridge A where Site U1499 was drilled (Fig. 1). Expedition 368 drilled at five sites (Sites U1501-U1505; Figs. 1, 2; Jian et al., in press), and completed in total operations at four sites (U1501, U1502, U1504, U1505). The expedition drilled the two primary Sites U1501 and U1503 at the OMH and Ridge C (interpreted as full oceanic crust), respectively. For Site U1502, Expedition 368 chose to insert an alternate site on Ridge A based on the drilling results of Expedition 367. Site U1503, however, was not completed beyond casing to 990 m due to technical problems with the drilling equipment that limited the expedition to operate with a drill string not longer than 3400 m. The new alternate Sites U1504 and U1505 met this operational condition. Site U1504 was an alternate site located between the OHM and Ridge A, U1505 was an alternate site for the already drilled Site U1501.

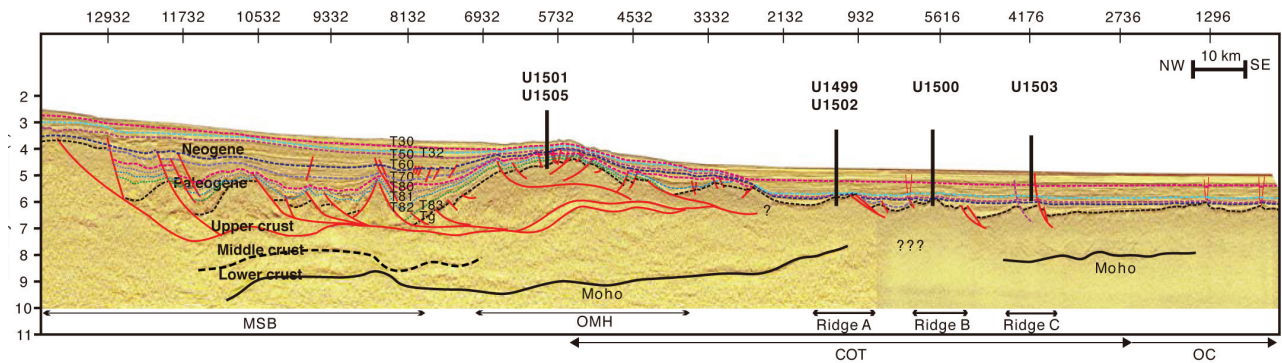


Fig. 2: Deep crustal time-migrated seismic reflection data with interpretation. COT= Continent–ocean boundary; OMH= Outer margin high. The major seismic unconformities are shown in purple and blue. Seismic data is from Line 04ec1555-08ec1555 (courtesy of the Chinese National Offshore Oil Corporation [CNOOC]).

We conducted operations in two holes at Site U1499. Hole U1499A penetrated from the seafloor to 659.2 m by advanced piston corer (APC) and the extended core barrel (XCB) coring and recovered 417.05 m (63%). We installed casing in Hole U1499B to 651 m followed by rotary core barrel (RCB) coring that penetrated from 655.0 to 1081.8 m and recovered 150.64 m (35%). Coring terminated in gravels before deteriorating drilling conditions prevented further penetration—no crystalline basement was encountered. Despite challenging conditions in the lowermost part of Hole U1499B, two successful wireline logging runs were conducted from 652 to 1020 m. Two holes were drilled at Site U1500. In Hole U1500A, we drilled without coring from the seafloor to 378.2 m, cored from 378.2 to 494.6 m and recovered 26.5 m (23%), drilled without coring from 494.6 to 641.2 m, and finally cored from 641.2 to 854.6 m and recovered 67.2 m (31%). After installation of a casing in Hole U1500B, we continuously cored the sediment sequence from 846.0 to 1379.1 m (533.1 m cored, 164.7 m recovered, 31%), and then continuously cored 149.9 m into the underlying crystalline basement from 1379.1 to 1529.0 m (114.92 m recovered, 77%). This made Hole U1500B the eighth deepest hole that the JOIDES Resolution has drilled. Three downhole logging strings were run in Hole U1500B from 842 to 1133 m. At Site U1501, four holes were drilled, from which Holes U1501A and U1501B recovered a full core barrel but missed the mudline and Hole U1501C was drilled to 461.8 m deep with a recovery of 447.8 m (96.3%). In Hole U1501D the expedition drilled without coring from the seafloor to 433.5 m to 644.3 m recovering 78.8 m of core (37.4%). Hole U1501D was logged with a triple combo tool string downhole from 113 to 299.3 m. At Site U1502, we conducted operations in two holes. In Hole U1502A we penetrated 758.2 m deep, and cored onwards from 375.0 m depth, recovered 176.81 m (46%). In Hole B we set 727.7 m of casing and cored from this depth to 920.95 m depth from the sediment-basement transition 180 m into the basement, recovering 128 m (70%). We collected downhole log data from 785.3 to 875.3 m and seismic data through the 10³/₄ inch casing. At Site U1503, we penetrated 995.1 m, setting 991.5 m of 10³/₄ inch casing, but no cores were taken. At Site U1504, we took 40 cores over two holes, both reaching crystalline basement. The cored interval was 165.5 m with 32% (52.77 m) recovery in Hole U1504A. An 88.2 m interval was drilled without coring in Hole U1504B, which is located 200 m southeast of Hole U1504A; subsequently cores were taken down to 200 m, recovering 21.48 m (19%). Four holes were drilled at Site U1505. Hole 1505A was mis-fired and recovered only 0.3 m and 3.23 m deep Hole U1505B was recovered for future education and outreach activities.

Both Holes U1505C and U1505D cored from the seafloor to 480.2 and 184.5 m respectively recovering 480.15 m (100%) and 191.43 (104%) of sediment. Logging data was collected from 80.1 to 341.2 m. Except for Sites U1503 and U1505, we drilled to acoustic basement, which prior to the expedition, except for Site U1501, had been interpreted to be crystalline basement.

A continuous sediment sequence from Pleistocene nannofossil-rich clay and calcareous ooze to pre-Miocene sandstones and breccia has been recovered at Site U1499. At Site U1500 we recovered Miocene claystones to sandstones overlying crystalline basement. At Site U1501 on the OMH, coring ~45 m into the acoustic basement sampled highly lithified sandstone to conglomerate of presumed Mesozoic age overlain by siliciclastic Eocene pre- to synrift sediments of Oligocene age and topped by primarily carbonaceous postrift sediments of early Miocene to Pleistocene age. At Site U1502, we recovered 180 m of crystalline basement below deep-marine sediments of Oligocene to late Miocene age. Coring was not performed within the upper 380 m (~Pliocene–Pleistocene) at Site U1502. Coring at Site U1504 on the OMH ~45 km east of Site U1501 recovered basement samples below late Eocene (?) carbonate rocks (partly reef debris) and early Miocene to Pleistocene sediments. At Site U1505, we cored to 480.15 m through Pleistocene to late Oligocene mainly carbonaceous ooze followed at depth by early Oligocene to late Eocene siliciclastic sediments.

After 4 months of drilling Expeditions 367/368 ended after a 4-day transit to Shanghai harbour.

References:

- Sun Z., Stock J., Jian Z., McIntosh K., Alvarez-Zarikian C., Klaus A. (2016) Expedition 367/368 scientific prospectus: South China Sea rifted margin. International Ocean Discovery Program. doi:10.14379/iodp.sp.367368.2016
- Sun Z., Stock J., Klaus A. and the Expedition 367 Scientists, in press. Expedition 367 Preliminary Report: South China Sea Rifted Margin. International Ocean Discovery Program. doi:https://doi.org/10.14379/iodp.pr.367.2017
- Jian, Z., Larsen, H.C., Alvarez Zarikian, C., and the Expedition 368 Scientists, in press. Expedition 368 Preliminary Report: South China Sea Rifted Margin. International Ocean Discovery Program. https://doi.org/10.14379/iodp.pr.368.2017

Report on IODP Expedition 369: Australia Cretaceous Climate and Tectonics

H.-J. BRUMSACK¹, R. HOBBS², B. HUBER³, K. BOGUS⁴
AND IODP EXP 369 SCIENTIFIC PARTY

¹Institut für Chemie und Biologie des Meeres (ICBM), Universität Oldenburg

²Department of Earth Sciences, University of Durham, GB

³Smithsonian Institution, Washington DC, USA

⁴IODP, Texas A&M University, College Station, USA

Expedition 369 “Australia Cretaceous Climate and Tectonics” began on September 26th 2017 in Hobart and ended on November 26th 2017 in Fremantle, Australia. It aimed at understanding the paleoceanography and tectonics of the Naturaliste Plateau (NP) and Mentelle Basin (MB) off SW Australia. Five sites (Fig. 1) in water depths between 850 and 3900 m (U1512 to U1516) were successfully drilled to investigate: (1) The rise and collapse of the Cretaceous hothouse; (2) the controls on oceanic anoxic events during major carbon cycle perturbations; (3) Cretaceous paleoceanography including deep and intermediate water circulation; (4) Cenozoic to recent paleoceanography including influence of the Tasman gateway opening and Indonesian gateway restriction; and (5) the tectonic, volcanic, and depositional history of the NP and MB prior to Gondwana breakup, as well as after separation from India and subsequently Antarctica.

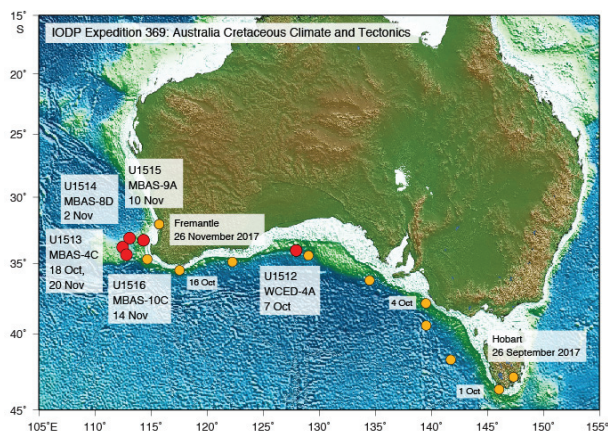


Fig. 1: Location of sites drilled during Exp 369.

The objective for drilling Site **U1512** was to obtain a continuous Upper Cretaceous record of marine black shales in the Great Australian Bight (GAB) across Oceanic Anoxic Event (OAE) 2, which straddles the Cenomanian-Turonian Boundary (CTB) interval. Site U1512 lies in 3000 m of water on the continental slope at 34°1.6407'S, 127°57.7604'E. The drilled sedimentary sequence is divided into two main lithostratigraphic units. These include 10.06 m of calcareous ooze with sponge spicules (Unit I) of Pleistocene age and 691.32 m of silty clay/silty claystone of Late Cretaceous (Santonian to Turonian) age with thin to medium beds of glauconitic and sideritic sandstone disseminated throughout (Unit II). Lithostratigraphic Unit II is further subdivided into Subunits II-a (silty clay) and II-b (silty claystone) based on the degree of sediment lithification. Site U1512 was the only site drilled during Exp 369, where larger quantities of interstitial gas (methane) were encountered below ca. 90 m CSF-A, paralleled by the almost complete depletion of interstitial water sulfate. For Unit II total organic carbon (TOC) ranges from 0.20 to 1.42 wt% with dominating Type III kerogen. The CTB interval (OAE-2) was absent at this site.

Site **U1513** (33°47.6084' S, 112°29.1338' E) lies at 2800 m water depth on the western margin of the MB. Particularly important goals were to obtain a complete OAE-2 sequence across the CTB, and to obtain basalt from the base of the sedimentary sequence to provide stratigraphic control on the age and nature of the pre-Gondwana breakup succession.

The cored section is divided into six lithostratigraphic units, five sedimentary and one igneous, based on a combination of data from Holes U1513A, U1513B, U1513D and U1513E. Unit I is a 64.93 m-thick sequence of light gray to pale yellow calcareous ooze and nannofossil ooze with sponge spicules of Pleistocene to late Miocene age. Unit II is a 182.93 m-thick sequence of Campanian–Cenomanian white to greenish gray calcareous and nannofossil ooze/chalk, clayey nannofossil chalk and silicified limestone. Unit III is a 21.87 m-thick sequence of alternating greenish gray, light gray and black nannofossil-rich claystones that are Cenomanian in age. Unit IV is a 187.12 m-thick sequence of black claystone and nannofossil-rich claystone that is Cenomanian to Albian in age. The interval from Sample U1513D 16R-CC, 15-20 cm through 20R-CC, 17-22 cm contains a succession that spans the CTB. Unit V is a 234.25 m-thick sequence of sandstone with siltstone and silty claystone of Aptian–Valanginian age. Unit VI is a 82.20 m-thick alternation of basalt flows and breccia intruded by a diabase dike, all with so far unknown ages.

Since sulfate was present in interstitial waters throughout the whole cores, methane levels were low. The chemistry of interstitial waters is governed by carbonate recrystallization in Unit I and basement alteration reactions at depth with strong depletions in Mg, K, and Na and high Ca and Sr concentrations.

Site **U1514** is the northernmost (33° 7.2443' S, 113° 5.4799' E) and deepest site targeted during Expedition 369, lying at 3850 m water depth. The greater paleodepth of the site relative to other sites cored in the MB, which is adjacent to the NP, provides the opportunity to characterize the evolution of deep water masses and deep ocean circulation during the final phase of breakup among the Gondwana continents. The sedimentary sequence recovered at Site U1514 is divided into three main lithostratigraphic units. Unit I is a 81.20 m-thick sequence of very pale brown to pale yellow nannofossil ooze, foraminiferal ooze and sponge spicule-rich nannofossil ooze that is Pleistocene–Eocene in age. Unit II is Eocene–Paleocene in age and consists of a 308.01 *m-thick sequence of* light greenish-gray clayey nannofossil ooze, sponge spicule-rich clay, nannofossil-rich clay that gradationally transitions into clayey nannofossil chalk and nannofossil-rich claystone. Unit III is Paleocene–Albian in age and consists of a 126.43 m thick sequence of greenish-gray, brown and black claystone. Soft sediment deformation, including convoluted and overturned bedding, is present in Subunit IIIa. Decreases in interstitial water salinity in Subunit IIIb seem to be associated with fluids associated with deformation processes.

Site **U1515** is the westernmost (33°16.1890' S, 114°19.3666' E) and shallowest site targeted during Expedition 369, lies at 861 m water depth, with the primary objective to provide evidence of the pre-breakup rifting history in the region prior to the final separation of Greater India and Antarctica. The sedimentary sequence recovered at Site U1515 is divided into two main lithostratigraphic units. Unit I is a sequence of light greenish gray calcareous ooze and calcareous chalk with sponge spicules, silicified limestone, chert and sandstone that is Pleistocene to upper Campanian in age. Unit II (age unknown, possibly Jurassic) consists of a sequence of gray to black silty sand and sandstones with glauconite, and silty sandstone and claystone

with variable abundances of organic matter. Due to the limited recovery, the thickness of each unit could not be specified.

Site **U1516** (34°20.9155' S, 112°47.9585' E) lies at 2666 m water depth in the south central MB. The basin is adjacent to the NP and was located at ~60°S paleolatitude during the mid-Cretaceous. The sedimentary sequence recovered is divided into four main lithostratigraphic units with Unit I further divided into three subunits. Unit I is Pleistocene to Paleocene in age and consists of a sequence of white, pinkish gray, and gray calcareous-foraminiferal-nannofossil ooze/chalk, and pale yellow to grayish green nannofossil-rich claystone (sometimes with chert) and claystone. Unit II is Turonian in age and consists of a 38.29 m-thick sequence of white, light olive brown, and light gray calcareous chalk interbedded with chert that gradually transitions into light greenish gray and greenish gray nannofossil chalk with clay that is interbedded with chert. Unit III consists of a 10.11 m-thick sequence of Cenomanian claystone with nannofossils, nannofossil-rich claystone and clayey nannofossil chalk that regularly alternates in color. Unit IV spans the Cenomanian to the Albian and is a 60.90 m-thick sequence of black and dark greenish gray claystone that is sometimes nannofossil-rich. The CTB was successfully recovered in Holes C and D. The diagenetic regime is characterized by carbonate recrystallization and basement alteration reactions. A prominent feature in IW chemistry is the strong depletion in salinity in Unit III, possibly associated with downslope movement of larger sedimentary sequences and fluid mobilization within faults.

Overall most of the objectives of Expedition 369 were achieved, even though weather conditions in part were rough. The Cenomanian/Turonian OAE- 2 could be recovered from two sites. In total 230 IW samples were analyzed to characterize the diagenetic regime.

IODP Expedition 371: Tasman Frontier Subduction Initiation and Paleogene Climate

E. DALLANAVE¹, T. WESTERHOLD², R. SUTHERLAND³, G. R. DICKENS⁴,
 P. BLUM⁵ AND EXPEDITION 371 SCIENTISTS

¹Dept. Earth and Environmental Sciences, Ludwig Maximilians University München, Theresienstrasse 41, 80333 München, Germany

²MARUM – Center for Marine Environmental Sciences, University of Bremen, Leobener Straße 8, 28359 Bremen, Germany

³Department of Geography, Environment, Earth Sciences, Victoria University Wellington, Kelburn PO Box 600, Wellington, New Zealand

³Department of Earth Science, Rice University, 6100 Main Street, Houston TX 77005, USA

³International Ocean Discovery Program, Texas A&M University, 1000 Discovery Drive, College Station TX 77845-9547, USA

The Cenozoic tectonic evolution of the Southwest Pacific area between the Tasman Sea and the Tonga-Kermadec arc (Fig. 1A) is complex and still not completely resolved. A recent appraisal of seismic reflectors across the Tasman and Northern Zealandia area revealed the occurrence of a widespread middle Eocene convergent deformation, reverse faulting, and uplift, followed by a late Eocene–Oligocene large-magnitude subsidence (>1 km; Fig. 1B; Sutherland et al., 2017). This particular Tectonic Event of the Cenozoic in the Tasman Area (TECTA) is interpreted to be related with the Tonga-Kermadec subduction initiation (Fig. 1C). Intriguingly, this major tectonic change may also coincide with the global Eocene climate turnover from the warming trend peaking with the early Eocene climate optimum (EECO) to the ensuing general middle–late Eocene cooling. Pacific Plate westward-dominated subduction beneath oceanic crust, instead of subduction only occurring be-

neath the continental crust of the American cordillera, might have caused a significant drop in pCO₂ (Lee et al., 2013) and thus global cooling.

IODP Expedition 371 (27 July – 26 September 2017) cored 2506 m of sediment and volcanic rock at six sites located in the northern Zealandia and Tasman sea area to constraining the age of the tectonic deformation and to quantify the uplift/subsidence related the Tonga-Kermadec subduction initiation as well as to improve paleoceanographic reconstructions since the Eocene.

At sites U1506 to U1510 nannofossil and foraminiferal ooze or chalk were drilled containing volcanic or volcanoclastic intervals, with variable clay content. At the final Site U1511, a sequence of abyssal clay and diatomite was recovered with only minor carbonate. The ages of strata at the base of each borehole were between middle Eocene and Cretaceous. For the first time the new drill sites provide a substantial basis defining formal lithostratigraphic units that can be mapped across a considerable part of northern Zealandia and related to onshore records of New Caledonia and New Zealand. The primary science objectives of the voyage were successfully completed. All six sites provided new stratigraphic and paleogeographic information that can be put into context through regional seismic-stratigraphic interpretation, and hence provide strong constraints on geodynamic models of subduction zone initiation. New observations from Exp. 371 can be directly related to the timing of plate failure, magnitude and timing of vertical motions, and the timing and type of volcanism. Sedimentological indication of shallow-water seas and land helps evaluating the amount of vertical movement. Furthermore, relative variations of iron oxides in the carbonate-free sediments of the Tasman plain abyssal Site, originated on the Australian continent and transported here via aeolian media, will give information about the weathering style and intensity on land through the early–middle Eocene. This can help evaluating the role of the chemical weathering of silicate to buffer CO₂ variations during time of global climate change (Dallanave et al., 2010). Secondary paleoclimate objectives were not all completed as planned, but significant new records of southwest Pacific climate were obtained and are the subject of post-voyage research.

Expedition 371 had significant media activity (international TV, radio, web, newspapers) associated with both port calls and during the cruise. Stories ran in the major newspapers of many countries (e.g., New York Times, Le Figaro, Vanguardia, Sydney Morning Herald, etc.). A total of 53 ship to shore video links were established with 41 different international education institutions with approximately 2600 students and teachers participating. Several video clips were uploaded to YouTube, and the JOIDES Resolution website covering different topics from leaving port in Townsville, drone footage of the ship, and drilling and core sampling process.

References:

- Sutherland, R. et al. Widespread compression associated with Eocene Tonga-Kermadec subduction initiation. *Geology* 45, 355–358 (2017).
 Lee, C.-T. A. et al. Continental arc–island arc fluctuations, growth of crustal carbonates, and long-term climate change. *Geosphere* 9, 21–36 (2013).
 Dallanave, E., Tauxe, L., Muttoni, G. & Rio, D. Silicate weathering machine at work: Rock magnetic data from the late Paleocene-early Eocene Cicogna section, Italy. *Geochemistry Geophys. Geosystems* 11(7), (2010).

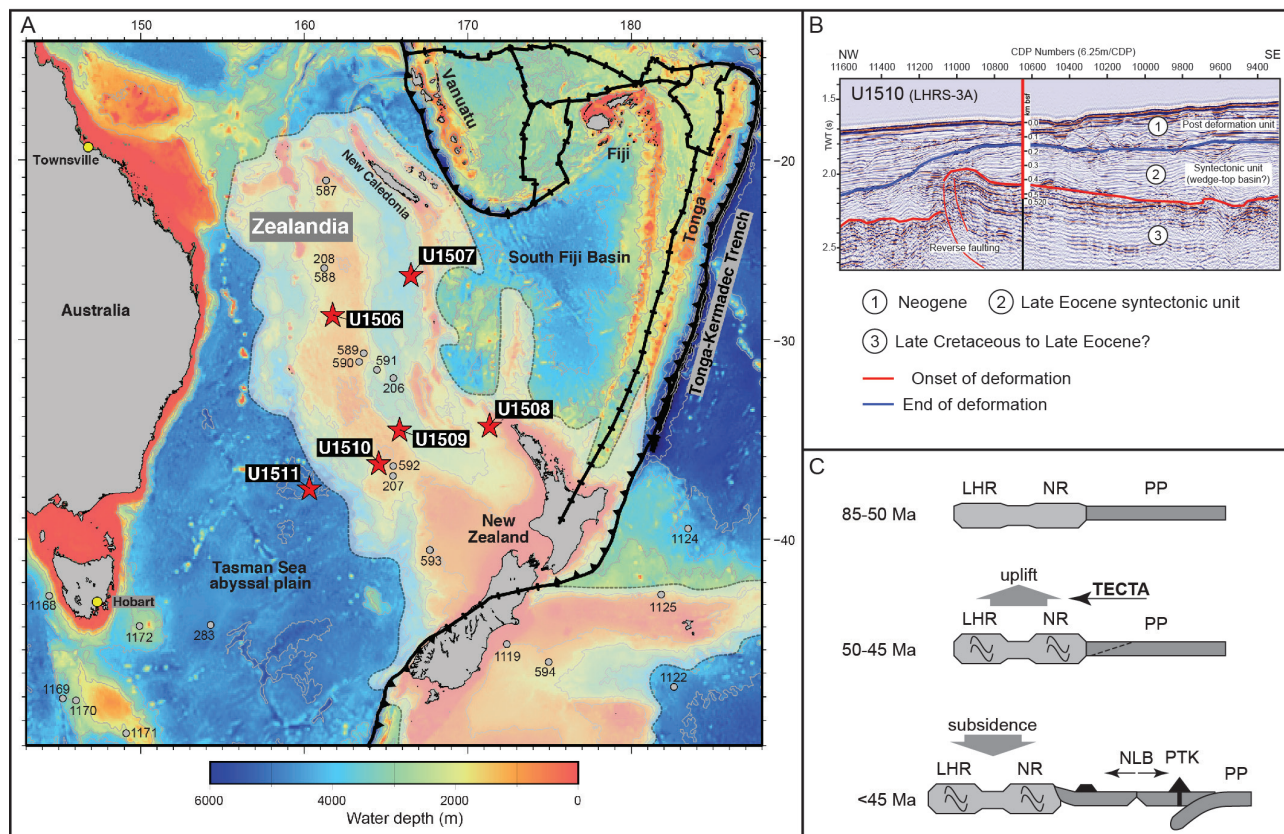


Fig. 1: A) Bathymetry of the Southwest Pacific-Tasman area. Stars indicate sites drilled during Exp. 371; the black dashed line envelops the northern part of Zealandia. B) Example of seismic profile (Site U1510), with indication of the main seismic reflectors. C) Schematic model for the Tonga-Kermadec subduction initiation¹. LHR and NR= Lord Howe Rise and Norfolk Ridge; PP= Pacific Plate; TECTA= tectonic event of the Cenozoic in the Tasman area; NLB and PTK= North Loyalty basin and proto-Tonga Kermadec arc.

Links to video clips:

- HIGH ABOVE THE JOIDES RESOLUTION, <http://joidesresolution.org/video-link-high-above-the-joides-resolution-exp-371>
- THE ADVENTURE BEGINS: EXPEDITION 371-TASMAN SEA FRONTIER, <http://joidesresolution.org/video-link-the-adventure-begins-expedition-371-tasman-sea-frontier>
- EXPLORING ZEALANDIA-EXPEDITION 371 TASMAN SEA FRONTIER, <http://joidesresolution.org/video-link-exploring-zealandia-expedition-371-tasman-sea-frontier>
- DRILLING 101-EXPEDITION 371 TASMAN SEA FRONTIER, <http://joidesresolution.org/video-link-drilling-101-expedition-371-tasman-sea-frontier>
- FIRST DRILL-EXPEDITION 371 TASMAN SEA FRONTIER, <http://joidesresolution.org/video-link-first-drill-expedition-371-tasman-sea-frontier>
- LAST CORE ON DECK-EXPEDITION 371 TASMAN SEA FRONTIER, <http://joidesresolution.org/video-link-last-core-on-deck-expedition-371-tasman-sea-frontier>

IODP Expedition 372 Cruise Report: Creeping Gas Hydrate Slides and LWD for Hikurangi Subduction Margin

K. HEESCHEN¹, M. BRUNET², J. ELGER³ AND THE EXPEDITION 372
AND 375 SHIPBOARD SCIENTIFIC PARTY

¹Institut für Geowissenschaften der Christian-Albrechts-Universität zu Kiel, Ludwig-Meynstraße 10-14, 24118 Kiel, Germany

²MARUM - Center for Marine Environmental Sciences, University of Bremen, 28359 Bremen, Germany

³GEOMAR - Helmholtz-Zentrum für Ozeanforschung Kiel, Wischhofstr. 1-3, 24148 Kiel, Germany

ODP Expedition 372 (26 Dec 2017 - 04 Jan 2018) is one of two related expeditions on the northern Hikurangi subduction margin (HSM) offshore the North Island of New Zealand. The joint proposal for both expeditions focusses on the slow slip events (SSE) on subduction faults with Expedition 372 undertaking logging while drilling (LWD) and Expedition 375 conducting coring and the emplacement of CORK observatories. Based on the shallow and frequent SEEs every 1.5 – 2.0 years (Wallace and Beavan, 2010), the northern Hikurangi Margin offers the opportunity to resolve key questions regarding the generation of slow slip and the mechanics of subduction interface thrusts (Barnes et al., 2017). The second objective of Expedition 372 is to investigate the role of gas hydrates in the slow, “creeping” deformation of the Tuaheni Landslide Complex (TLC) as postulated from seismic images and gas hydrate stability considerations (Mountjoy et al., 2014; Barnes et al., 2017). Drilling at the TLC site covered LWD, coring, and the deployment of a temperature-pressure probe.

During Expedition 372 a total of four sites were drilled with 190 m of cores being recovered at the TLC Site U1517 and LWD conducted at all sites. The HSM sites include HSM-01A (U1519) targeting a mid-slope basin on the continental plate, Site HSM-15A (U1518; 2636 m water depth) on the frontal accretionary wedge close to the deformation front, and HSM-05A (U1520) on the subducting sequence on the incoming plate. The HSM sites will be cored on Expedition 375 and CORK observatories will be installed at Sites U1518 and U1519 to record pressure, temperature and fluid flow transients associated with SSE-propagated strains. The LWD data will be integrated with seismic reflection data sets to guide coring during Expedition 375 and support the interpretation of sedimentary and chemical characteristics as well as the interpretation of stress regimes.

The LWD bottom-hole assembly (BHA) was composed of a maximum of six tools attached behind the bit: geoVISION, NeoScope, StethoScope, TeleScope, SonicScope, and proVISION. These tools successfully provide data on the gamma ray (from geoVISION and NeoScope), resistivity (from geoVISION and NeoScope), porosity (from NeoScope and proVISION), and compressional and shear wave velocity (from SonicScope). The formation pressure measurements at Site U1518 using the StethoScope tool was unsuccessful.

LWD data from Site U1518 covered the upper 600 m of the sediment package, resolving six main units using physical properties. The thrust fault was interpreted close to the predicted depth from the seismic data, where significant changes in density and porosity occur. Higher electrical resistivities at various depths of roughly 300 to 500 m indicate the presence of gas hydrates. Borehole U1519A acquired data over a range of 650 m and has been divided into three main logging units. Intervals of increased washout were encountered at shallower depths whereas resistive layers and borehole breakouts were identified in the lower part of the borehole. Fractures occur sparsely throughout the borehole. Site U1520 acquired data down to 750 mbsf, distinguishing nine main logging units. The log data within each unit shows significant variations in physical properties reflecting changes in the clastic trench sequence and inferred upper pelagic sequence. Bedding is mostly shallowly dipping.

At the TLC site (U1517) we logged 205 mbsf with an almost full core recovery to 190 mbsf, just below the base of the gas hydrate stability zone. The core is characterized by a clayey silt lithology with sandy intervals and subdivided into five units. The stratigraphic succession includes bedded turbidite sequences and mass transport deposits, as well as background sedimentation with the upper ~67 mbsf being within the TLC. Porosities are unusually low. Increased resistivities in the LWD data at depth between 110-150 mbsf indicate the presence of gas hydrates. Chlorinity measurements indicate gas hydrates at depths of ~135 to 165 mbsf.

The main focus of the German participants is on the TLC site. The first objective is to characterize the gas hydrates and their role for the observed creep and shear strength of the sediments packages. The second focus is to better constrain composition and origin of the sedimentary record and characterize creeping deformation based on micro structures.

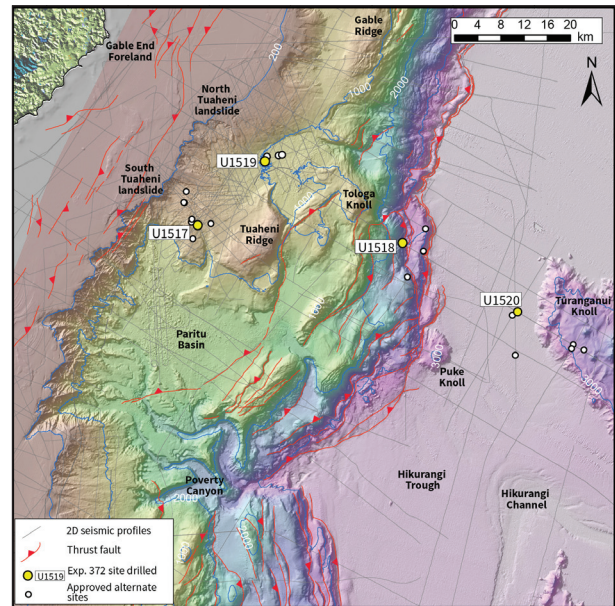


Fig. 1: Drill sites of Expedition 372 offshore New Zealand. Bathymetry data: NIWA, New Zealand.

References:

- Barnes, P. M., Pecher, I., and LeVay, L.J., 2017, Creeping Gas Hydrate Slides and LWD for Hikurangi Subduction Margin: coring and logging while drilling to unravel the mechanisms of creeping landslides and subduction slow slip events at the Hikurangi subduction margin, New Zealand, Intern. Ocean Discovery Program Scientific Prospectus, 372.
- Mountjoy, J. J., Pecher, I., Henrys, S., Crutchley, G., Barnes, P. M., and Plaza-Faverola, A., 2014, Shallow methane hydrate system controls ongoing, downslope sediment transport in a low velocity active submarine landslide complex, Hikurangi Margin, New Zealand: *Geochem. Geophys. Geosyst.*, v. 15, no. 11, p. 4137–4156.
- Wallace L.M. and J. Beavan, 2010, Diverse slow slip behavior at the Hikurangi subduction margin, New Zealand, *J. Geophys. Res.*, 115, B12402, doi.org/10.1029/2010JB007717.

Abstracts

IODP

First insights into the deep life in Bengal Fan sediment

R. R. ADHIKARI¹, V. B. HEUER¹, M. ELVERT¹, J. KALLMEYER², A. KITTE², L. WÖRMER¹, K.-U. HINRICH¹

¹MARUM - Center for Marine Environmental Sciences, University of Bremen, Leobener Str. 8, 28359 Bremen, Germany

²Geomicrobiology, Helmholtz Centre Potsdam, GFZ German Research Centre for Geosciences, Telegrafenberg, 14473 Potsdam, Germany

It is widely accepted that the deep marine seafloor biosphere plays a major role in global elemental cycles. However, the state of investigations of the deep biosphere in different marine subsurface environments is rather limited, for example, seafloor biosphere in the Indian Ocean has not been investigated in detail so far. During International Ocean Discovery Program Expedition 354 (February – March 2015, Singapore – Colombo, Sri Lanka) we sampled sediments from seven Sites U1449-U1455 along a 8°N transect. Here we present our first explorative results of seafloor life in the Bengal Fan sediments in the Indian Ocean. We quantified (i) prokaryotic cells using epifluorescence microscopy after detaching cells from the sediment, (ii) bacterial endospores by analyzing the diagnostic biomarker dipicolinic acid (DPA) through detection of fluorescence from the terbium-DPA complex, and (iii) microbial activity by analyzing hydrogen utilization potential based on the activity of hydrogenase enzymes, which are ubiquitous in subsurface microorganisms. We measured highest cell concentrations of ca. 10^7 cells cm^{-3} in shallow sediments close to the seafloor; these concentrations are lower than in most marine continental margin settings. At greater depth the concentrations followed global trend and decreased exponentially with depth. Endospore concentrations scattered between ca. 10^5 and 10^7 cells g^{-1} sediment. We could not observe a clear relationship of endospore concentrations and sediment depth; instead, it appears to be linked to lithology and total organic carbon content. Potential hydrogenase enzyme activity scattered in the nmolar to μmolar range of H_2 $\text{g}^{-1}\text{d}^{-1}$. Similar to previous observations, per-cell hydrogen utilization depends on vertical biogeochemical zones, which could be due to the differences in hydrogen utilization requirements/efficiency of the respective metabolic processes such as sulfate reduction, methanogenesis, fermentation etc. We observed interesting shifts in biogeochemical profiles, for example at around 110 mbsf at Site U1449 right below a hemipelagic sediment layer (0.8-1.3 Ma). Above and below such episode of sedimentation, turbidite deposits and thick sand layers dominated the lithology. Based on our recent observations, we suggest that the origin and quality of sedimentary material influenced microbial activity and the deep biosphere in Bengal Fan sediment, that are primarily dominated by terrigenous origin.

ICDP

Impact of geogenic CO_2 on deep microbial ecosystems in the Hartoušov mofette system, NW Bohemia

K. ADLER¹, M. ALAWI¹, H.-M. SCHULZ¹, B. PLESSEN¹, D. WAGNER¹, K. MANGELSDORF¹

¹GFZ German Research Centre for Geosciences – Helmholtz Centre Potsdam

A mofette is a natural cold either dry or wet gas vent releasing CO_2 -rich gases into the atmosphere. The Hartoušov mofette system is located in the northern Cheb Basin (NW Bohemia, Eger Rift). The area is characterized by active seismicity in form of periodically occurring swarm earthquakes and lithospheric mantle-derived gas emanations ($> 99\%$ CO_2). The exhaling free gas phase of the Bublak mofette, near the Hartoušov mofette system, is characterized by a subcontinental mantle helium isotope signature of 5.9 Ra and a d^{13}C signal of ca. 2 ‰ (Bräuer et al., 2011). The relatively high d^{13}C signal bears the opportunity to trace the incorporation of geogenic CO_2 into microbial biomass. The objective of this study is the investigation of the impact of geogenic CO_2 on deep microbial communities and their surrounding sedimentary life habitat. Therefore, the initial environmental conditions are characterized by sedimentological bulk parameters (TC, TOC, TIC, $\delta^{13}\text{C}_{\text{org}}$, TN, TOC/TN) and past microbial biomarker signals (Glycerol Dialkyl Glycerol Tetraethers - GDGTs, Hopanoids) are compared to microbial life markers (Phospholipid Fatty Acids – PLFAs, intact Phospholipids - PL). A further focus is placed on carbonate precipitations in consequence of the interaction of the exhaling CO_2 with the sedimentary life habitat.

In early 2016 a 108.5 m deep borehole was drilled by GFZ as a preliminary study for the PIER-ICDP study - drilling the Eger Rift (DFG Alawi, AL 1898/1). The drilling was performed in a mofette system near the village of Hartoušov. During drilling CO_2 -rich sediments were recovered between 71 m and 81 m depth and at 78.5 m depth a CO_2 blow out occurred suggesting a CO_2 reservoir in this core interval related to an aquifer between 79 m – 85 m. In consequence the core interval between 65 m and 95 m was selected for further investigations. Lithologically, this core section is composed of three different units that are (from the bottom to the top): a weathered Palaeozoic mica schist (95 m – 91.5 m depth), a compact, sandy Miocene claystone with lignite fragments and root structures suggesting soil horizons and deposition in a swamp environment (91.5 m – 78.5 m) as well as a laminated to bedded, calcareous, sandy or peaty Miocene mudstone interbedded with bioclastic carbonates, dolomite beds and gypsum layers of lacustrine origin (78.5 m – 65 m). The sediments exhibit natural deformation structures in form of small faults, dykes and sills all indicating hydrofracturing and sediment fluidization resulting from high pore fluid pressures. The sediments in the vicinity of these deformation structures are infrequently cemented by carbonate or gypsum and can exhibit changes in color (Bussert et al., 2017).

Carbonate is present in all units, but nearly absent in areas with high CO_2 content. Carbonate minerals in the deeper Palaeozoic and Miocene swamp sediments are dominated by siderite whereas calcite predominates in lacustrine sediments. Siderite varies in size and zonation is caused by different Mg, Ca and Mn contents. A correlation of these zones may provide information about changes in formation water chemistry including a later control by CO_2 -rich waters.

TOC is absent in the Palaeozoic basement, increases towards the top of the swamp sediments, and is high but variable

the mPWP. However, the forested area decreased, while herb- and shrub dominated vegetation spread again between 3.236 and 3.223 Myr BP, suggesting a noticeable climatic deterioration and relatively cold and dry conditions during MIS KM6.

References:

- Andreev, A.A., Tarasov, P.E., Wennrich, V., Raschke, E., Herzschuh, U., Nowaczyk, N.R., Brigham-Grette, J., Melles, M., 2014. Late Pliocene and Early Pleistocene environments of the north-eastern Russian Arctic inferred from the Lake El'gygytyn pollen record. *Climate of the Past* 10, 1-23.
- Brigham-Grette, J., Melles, M., Minyuk, P., Andreev, A., Tarasov, P., DeConto, R., Koenig, S., Nowaczyk, N., Wennrich, V., Rosén, P., Haltia-Hovi, E., Cook, T., Gebhardt, C., Meyer-Jacob, C., Snyder, J., Herzschuh, U., 2013. Pliocene warmth, extreme polar amplification, and stepped Pleistocene cooling recorded in NE Russia. *Science* 340, 1421-1427.
- Melles, M., Brigham-Grette, J., Minyuk, P.S., Nowaczyk, N.R., Wennrich, V., DeConto, R.M., Anderson, P.M., Andreev, A., Coletti, A., Cook, T., Haltia-Hovi, E., Kukkonen, Lozhkin, A.V., Rosén, P., Tarasov, P., Vogel, H., Wagner, B., 2012. 2.8 Million Years of Arctic Climate Change from Lake El'gygytyn, NE Russia. *Science* 337, 315-320.

IODP

Cyanobacterial blooms and their role in the formation of bottom water hypoxia in the Baltic Sea

T. BAUERSACHS¹, N. LORBEER¹, L. SCHWARK¹

¹Christian-Albrechts-University, Institute of Geosciences, Department of Organic Geochemistry, Ludewig-Meyn-Straße 10, 24118 Kiel, Germany (email: thorsten.bauersachs@ifg.uni-kiel.de)

In the modern Baltic Sea, massive blooms of heterocystous cyanobacteria regularly occur during summer. Such blooms have considerably increased in frequency and intensity since the second half of the last century with worrisome consequences for the health of the Baltic Sea ecosystem as the massive export and decay of cyanobacterial biomass has resulted in the spread of bottom water hypoxia (dissolved oxygen < 2 mg/L) and anoxia. As a consequence, the Baltic Sea currently turns into one of the world's largest dead zones that experiences a significant loss of benthic faunal communities, the reduction of fish populations and major alterations of biogeochemical cycles (Conley, 2012). The increased anthropogenic loading of nutrients (in particular phosphorus) in the Baltic Sea is commonly considered to be responsible for the enhanced activity of cyanobacterial blooms but other factors that may control bloom formation (such as e.g. the influence of climate warming) are less well constrained.

Here, we analyzed sediments from the Little Belt, Bornholm Basin, Landsort Deep and Ångerman River Estuary obtained during IODP Expedition 347: Baltic Sea Paleoenvironment to determine the role of climate warming on the formation of cyanobacterial blooms and their role in the spread of bottom water hypoxia/anoxia in the Baltic Sea. Bulk geochemistry indicates a significant increase in primary productivity and preservation in the Baltic Sea with the establishment of brackish conditions at all sites with the Holocene Thermal Maximum (HTM), the Medieval Climate Anomaly (MCA) and the Modern Hypoxic Period (MHP) showing exceptional high concentrations of organic carbon (>8 wt%) and total sulfur (>3 wt%) burial. In combination with the simultaneously fine lamination of the sediments across the Baltic Sea basin, this suggests that the organic-rich deposits were formed in a highly productive ecosystem and under anoxic to euxinic conditions. Excursions to lighter nitrogen isotope values during the HTM, MCA and MHP at all four sites suggests a significant shift in the phytoplankton community with diazotrophic cyanobacteria constituting the majority of the preserved organic matter. This

observation is supported by concomitantly high abundances of heterocyst glycolipids, which represent specific biological markers for heterocystous cyanobacteria (Bauersachs et al. 2009; 2017) and in combination evidence the massive spread of cyanobacterial blooms during the HTM, MCA and MHP in the Baltic Sea. Interestingly, periods of increased cyanobacterial activity and enhanced bottom water anoxia are characterized by TEX₈₆^L reconstructed sea surface temperatures exceeding a threshold of 16 °C, indicating that climate warming played a major role in the formation of cyanobacterial blooms in the past Baltic Sea. Our results thus provide first evidence that heterocystous cyanobacteria do not only play a major role in the nitrogen cycling of the modern Baltic Sea but that they repeatedly formed massive blooms that stretched from the Kattegat to the Bothnian Sea and significantly impacted the ecosystem of the Baltic Sea by triggering the spread of bottom water hypoxia. The anthropogenic loading of nutrients in concert with an anticipated ~3 °C increase in sea surface temperature in the Baltic Sea until the end of this century (HELCOM, 2013) may thus result in a yet unprecedented spread of cyanobacteria in the Baltic Sea with yet unforeseen consequences for the Baltic Sea ecosystem.

References:

- Bauersachs, T., Compaoré, J., Hopmans, E.C., Stal, L.J., Schouten, S., Sinnighe Damsté, J.S. (2009) Distribution of heterocyst glycolipids in cyanobacteria. *Phytochemistry* 70, 2034-2039.
- Bauersachs, T., Talbot, H.M., Sidgwick, F., Sivonen, K., Schwark, L. (2017) Lipid biomarker signatures as tracers for harmful cyanobacterial blooms in the Baltic Sea. *PLOS ONE* 12, e0186360.
- Conley, D.J. (2012) Save the Baltic Sea. *Nature* 486, 463-464.
- HELCOM (2013) Climate change in the Baltic Sea area: HELCOM thematic assessment in 2013. *Baltic Sea Environment Proceedings*.

IODP

Channel-levee evolution and stratigraphy at the middle Bengal Fan – Integrating multichannel-seismic data and IODP Expedition 354 results

F. BERGMANN¹, T. SCHWENK¹, V. SPIESS¹, B. REILY², C. FRANCE-LANORD³
AND IODP EXPEDITION 354 SCIENTIFIC PARTY

¹Faculty of Geosciences, University of Bremen, Klagenfurter Strasse 2-4, 28359 Bremen, Germany

²College of Earth, Ocean and Atmospheric Sciences, Oregon State University, Corvallis OR 97331, USA

³Centre de Recherches Pétrographiques et Géochimiques, CNRS Université de Lorraine, BP 20, 54501 Vandoeuvre les Nancy, France

The Bengal Fan – the largest submarine fan on Earth – started to evolve as a direct response to the Indian-Asian collision and the concomitant Himalayan uplift (Curry et al., 2003). The fan is of particular scientific importance as it contains the most complete record of the tectonic and climate history of the Himalayan Mountains/Tibetan Plateau uplift as well as the evolution of the Asian monsoon from fan initiation in the early Eocene to present. In the modern situation, sediment is transported from the Himalayan area to the shelf mainly via Ganges and Brahmaputra rivers and further downslope via episodically occurring turbidity currents. Since the Late Miocene deposition on the Bengal Fan is dominated by channel-levee systems (CLSSs) initiated and further shaped by these downslope flowing turbidity currents (Schwenk and Spieß 2009). Frequent channel avulsions and reoccupation of older pathways resulted in a complex depositional system with lateral depocenter migration over the entire fan (Curry et al., 2003, Schwenk and Spieß 2009).

In order to further comprehend this depositional system, a prerequisite to ultimately draw inferences from the sink (Bengal

Fan) to changes in the source (Himalaya, Tibetan Plateau), the Bengal Fan was target of IODP Expedition 354 'Bengal Fan' in February/March 2015 drilling seven sites along a 400 km long west-east transect at 8°N. Main objectives were, amongst others, to get further insight into the emergence of the Himalaya and its link to the onset of fan deposition, the Miocene/Pliocene fan evolution, the monsoonal impact on sediment supply and flux, the role of the Bengal Fan in the global carbon cycle as well as the spatial variability of the depocenter.

Within the frame of DfG project SCHW 1551/7-2, IODP Expedition 354 drilling results are integrated with high-resolution multichannel-seismic (MCS) data gathered during cruises SO125/126 (1997) and SO188 (2006), allowing the correlation of stratigraphic time markers in between the 7 drill sites while also regarding for phases of sedimentation not covered by the drill sites. This study further aims to investigate the fan architecture, the stacking of channel-levee systems, and the succession of individual Pleistocene channel-levee systems with respect to environmental changes in the Bengal Basin.

One very prominent stratigraphic marker is a several meter thick layer of calcareous clay comprising the Brunhes/Matuyama (0.781 Ma) as well as the Cobb Mountain/Matuyama (1.185 Ma) boundary. This layer (HL1) has been recovered at all seven IODP sites and is present as constant layer throughout the full MCS dataset separating the transect into an upper and a lower part. Along the MCS Profile GeoB97-020+027 crossing all IODP 354 sites, 40 individual channel-levee systems occur above HL1. CLSs cluster on the western and eastern section of the profile while only small scale channels were found in the center. Based on thorough tracing of base reflections of all channel-levee systems a relative stacking pattern composed of two stages has been developed. The first stage starts with the transition from a hemiplegic dominated period at 8°N during the deposition of HL1 back to a turbiditic controlled regime and the formation of channel-levee systems in the center of the transect. Subsequently, the location of the active channel-levee system migrates laterally along the middle and eastern part of the profile. The distance between two successive systems is quite variable ranging between 5 km to >190 km.

The transition from stage one to stage two occurs around 0.2-0.3 Ma ago, while channel-levee formation concentrates now in the western third of the transect filling up available accommodation space, whereas the center and east of the transect is covered by a several meter thick hemipelagic drape. These large-scale depositional dynamics promote the concept of individual subfans or channel-levee complexes, introduced by Curray et al., 2003, which govern only parts of the Bengal Fan while other areas receive no or almost no fan sedimentation.

Average lifetime of CLSs during stage one is about 16-18 ka when disregarding different sizes of individual systems. This is significantly longer than average lifetimes known from e.g. the Amazon Fan where channel avulsion are associated with rapid variations in sea level (Maslin et al., 2006). The variable size of CLSs at the middle Bengal Fan, however, indicates a random distribution of the maturity of individual systems which in turn suggests autocyclic processes such as upfan avulsions as main control on the CLS lifetimes.

The CLSs are intercalated by inter-channel sediments (HARPs) composed of mainly silts and sands deposited from unchannelized turbidity currents. Calculating the proportion of channelized and unchannelized sediments (area covered along GeoB97-020+027) reveals a ratio of ~37% channelized deposition (CLSs) vs. ~63% of unchannelized deposition. This not only demonstrates the dominance of unchannelized sedimentation to the fan architecture but further shows that the sand

content in large submarine fans might be higher than expected. While the position of CLSs is variable and builds up topography, the deposition of the unchannelized sands control the preservation of a nearly flat surface/seafloor along the drilling transect..

References:

- Curray, J.R., Emmel, F.J., and Moore, D.G., 2003. The Bengal Fan: morphology, geometry, stratigraphy, history and processes. *Marine and Petroleum Geology*, 19(10):1191–1223.
- France-Lanord, C., Spiess, V., Klaus, A., Schwenk, T., and the Expedition 354 Scientists, 2016. Bengal Fan. Proceedings of the International Ocean Discovery Program, 354: College Station, TX (International Ocean Discovery Program). <http://dx.doi.org/10.14379/iodp.proc.354.2016>
- Maslin, M., Knutz, P.C., Ramsay, T., 2006. Millennial-scale sea-level control on avulsion events on the Amazon Fan. *Quaternary Science Reviews* 25, 3338–3345.
- Schwenk, T. & Spieß, V., 2009. Architecture and stratigraphy of the Bengal Fan as response to tectonic and climate revealed from high resolution seismic data. In Kneller, B., Martinsen, O.J., and McCaffrey, B., eds., *External Controls on Deep-Water Depositional Systems: SEPM Special Publication 92*, p. 107–

IODP

IODP Proposal Neogene climate, productivity, and sediment transport on the NW African continental margin

T. BICKERT¹, S. KRASTEL², P. WILSON³, A. CROCKER³, L. DUPONT¹, S. MULITZA¹, E. SCHEFUSS¹, M. URLAUB², T. WESTERHOLD¹

¹MARUM, Universitaet Bremen, 28334 Bremen, Germany

²Geowissenschaften, Universitaet Kiel, 24118 Kiel, Germany

³NOC, University Southampton, Southampton SO14 3ZH, UK

Within the frame of the IODP Science Plan 2013-2023 we propose a drilling expedition exploring Neogene climate, ocean productivity and mass sediment transport on the continental margin of NW Africa. Between Cap Bojador, southeast of the Canary Islands, and the deltas of Senegal and Gambia rivers, we propose to retrieve sediment cores in six study areas, that include also the Cap Verde and Sierra Leone Plateaus. One major objective, targeted with up to four primary sites, is to study Neogene North African hydroclimate and vegetation to reconstruct the timing and cause of late Miocene to early Pliocene aridification. Further sites with high- to very high sediment accumulation rates are planned to explore millennial- to orbital- scale climate change in the subtropics and related sediment transport regimes. We will focus on the Sahara and/or Mauretania Slides to constrain the causes and frequencies for submarine landslides at the continental slope. Drilled sediments from the target sites will also provide key records to study ocean productivity and ecosystem response to climate perturbations in the upwelling area off Cap Blanc. Among others, we intend to revisit the well-investigated high accumulation site ODP 658 in a position nearby, to allow for covering the missing mid to late Pleistocene transition sediment sequence. The planned investigations are related to projects of the MARUM Center for Marine Environmental Sciences, University of Bremen, the Institute for Geosciences, University of Kiel, the GEOMAR Helmholtz Centre for Ocean Research Kiel, and the National Oceanography Centre, University of Southampton, in close cooperation with many other partners.

IODP

Deglacial deep water circulation and Nd isotope changes in the Nordic Seas and subpolar North Atlantic

P. BLASER¹, J. LIPPOLD¹, M. GUTJAHR², J. M. LINK³, F. PÖPPELMEIER¹,
M. FRANK², N. FRANK³

¹Institute of Earth Sciences, Heidelberg University, Germany, contact: patrick.blaser@geow.uni-heidelberg.de

²GEOMAR Helmholtz Centre for Ocean Research, Kiel, Germany

³Institute of Environmental Physics, Heidelberg University, Germany

Neodymium (Nd) isotopes have become a valuable proxy for the reconstruction of past water mass provenance and mixing. However, the local water mass Nd isotope signature is a function of water mass advection and Nd fluxes from weathering and diagenesis. Consequently, Nd isotope signatures of water mass end members may vary under changing weathering regimes such as glacial-interglacial cycles. The accurate interpretation of Nd isotopes in terms of changing ocean circulation requires a precise knowledge of end-member isotopic compositions through time. North Atlantic Deep Water (NADW) presents a major link between the atmosphere and the deep ocean, but whether or not its Nd isotope composition remained constant through time or to which degree it varied over glacial cycles is debated. The northern North Atlantic is the source region of NADW and connects the Nordic Seas and the central Atlantic. Weathering fluxes and sources in the North Atlantic varied significantly through the last glacial cycle, potentially affecting local deep water Nd isotope compositions.

Aiming to provide improved (de-)glacial end member compositions, we reconstructed the deep water Nd isotope signatures from 10 ODP/IODP sites across the Nordic Seas and the subpolar North Atlantic from the last glacial to the late Holocene. For this task we scrutinised established methods for the extraction of archived seawater-derived Nd from marine bulk sediments by chemical leaching [1]. With an improved sediment leaching scheme we are able to reconstruct past deep water Nd isotope compositions from diverse sediments and verify their authigenic origin with the help of the elemental composition of the leachates. Comparison between sites and regions testifies the general integrity of this approach.

Our results show that the Nordic Seas were characterised by at least 3 epsilon units less radiogenic Nd isotope signatures during the Last Glacial than today. Furthermore, water mass exchange between the deep eastern and western subpolar North Atlantic basins was limited during the Last Glacial Maximum, probably due to the weakened admixture of overflow waters from the Nordic Seas. During the deglaciation, a strong overflow from the Nordic Seas into the North Atlantic was established, leading to the homogenisation of Nd signatures along the flow paths of the western boundary currents. The changes to weathering in a warmer climate during the early Holocene further led to a transient change in the Nd isotope signatures of the Nordic Seas and consequently of the overflow waters exported to the Atlantic Ocean. These changes in end member water mass Nd isotope signatures are crucial for more accurate interpretations of Nd isotope records throughout the Atlantic Ocean.

References:

[1] Blaser et al. (2016), *Chemical Geology*

IODP

The stable water isotope geochemistry of interstitial fluids from the eastern Mediterranean Sea (ODP Leg 160)

M. E. BÖTTCHER¹, H.-J. BRUMSACK², I. SCHMIEDINGER¹

¹Geochemistry & Isotope Biogeochemistry Group, Marine Geology Department, Leibniz IOW, Warnemünde, Germany

²Microbiogeochemistry, ICBM, University of Oldenburg, Germany

Interstitial waters were extracted from long sediment cores retrieved during Leg 160 of the Ocean Drilling Program (ODP) and analysed for the stable water isotope ($^2\text{H}/^1\text{H}$, $^{18}\text{O}/^{16}\text{O}$) composition. It was the aim to constrain hydrographic changes in the eastern Mediterranean Sea prior to modern time. Measurements include samples from ODP Sites 963 to 973, covering the geographical range between the Strait of Sicily and the eastern end of the Libyan Sea. At most sites, the measurements demonstrate downcore variations in both water isotope ratios covering overall dynamics of more than 1 ‰ ($\delta^{18}\text{O}$) and 8 ‰ ($\delta^2\text{H}$) (Sites 963-968).

The stable isotope results are compared to recent isotope measurements on modern Mediterranean surface waters from a transect between the Strait of Gibraltar and the Black Sea retrieved during RV Maria S. Merian cruise MSM 33. The Leg 160 pore waters from shallow sediment depths are close to a Mediterranean seawater evaporation trend as defined by salinity-stable isotope and $\delta^2\text{H}$ - $\delta^{18}\text{O}$ covariations found for the modern surface waters (Fig. 1). Trends for sites impacted by deep-seated salty solutions indicate a substantial variation towards a lighter water isotope composition.

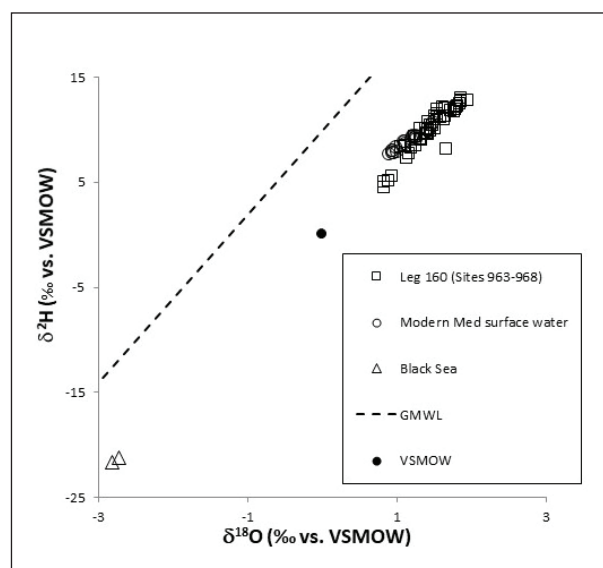


Fig. 1: First measurements of the water isotope composition of ODP Leg 160 pore waters (here: Sites 963-968) compared to surface waters taken on a transect through the modern Mediterranean Sea and the Black Sea water column.

In order to reconstruct the hydrographic evolution of the Mediterranean Sea hydrography and the composition of the deeper salty brines, it is further planned to apply an integrated advection-diffusion model. In addition, diagenetic reactions and the consequence of pore water compositions on developing O isotope signatures of dissolved sulfate will be addressed.

IODP

From the reef into the abyss – the Albian to Turonian record of IODP Site U1407 (Southeast Newfoundland Ridge)

 A. BORNEMANN¹, O. FRIEDRICH², K. MORIYA³, H. SCHER⁴
¹ Bundesanstalt für Geowissenschaften und Rohstoffe, Hannover, Germany

² Institut für Geowissenschaften, Ruprecht-Karls-Universität Heidelberg, Heidelberg, Germany

³ Department of Earth Sciences, Waseda University, Japan

⁴ Department of Earth and Ocean Sciences, University of South Carolina, Columbia, USA

Within the scope of IODP Expedition 342 a 270-m-thick sedimentary succession of Cretaceous and Paleogene age has been recovered at Site U1407 (Southeast Newfoundland Ridge). The two deepest holes U1407A and B cover the transition from fine grained pelagic marls to the basement formed by reefal sediments at ~270 CCSF. The basal short-cores of these two holes revealed a number of shallow-water fossils such as gastropods, corals, rudists and larger foraminifera (orbitulinids; Norris et al., 2014). In addition, a well-developed Cenomanian-Turonian Boundary (CTB) with its typical black shale expression of the Oceanic Anoxic Event 2 is also represented in the cores.

Here, we present a high-resolution carbon isotope record of the 40-m-thick succession from the top of the reef to the bathyal CTB black shales. Beside the typical $\delta^{13}\text{C}$ anomalies associated with the CTB we were able to identify the decline of $\delta^{13}\text{C}$ values related to the top of the Albian-Cenomanian boundary interval and the Mid-Cenomanian Event. We further present new biostratigraphic results based on calcareous nannofossils as well as $^{87}\text{Sr}/^{86}\text{Sr}$ isotope ages for the top of the reef analyzed on *Orbitulina*. These new data in combination with the identified, stratigraphically well-calibrated events allow for a detailed comparison with other mid-Cretaceous records around the world and provide new insights into the subsidence history of the western Atlantic margin off Newfoundland.

References:

Norris, R.D., Wilson, P.A., Blum, P. & Expedition 342 Scientists, 2014. Site U1407. Proceedings of the Integrated Ocean Drilling Program, Volume 342, doi:10.2204/iodp.proc.342.108.2014.

IODP

A new MagellanPlus workshop proposal on drilling in the New Ireland Basin (PNG): Understanding the interactions between tectonism, volcanism, ore formation and the deep biosphere

 P.A. BRANDL^{1*}, M.D. HANNINGTON¹
¹GEOMAR Helmholtz Centre for Ocean Research Kiel, Wischhofstr. 1-3, 24148 Kiel

*corresponding author: Tel. +49 431 600-1433, Email: pbrandl@geomar.de

Strategic metals such as Cu, Au, Ag, As, Tl are essential for our current economy especially with respect to the development of energy-efficient green technologies. The majority of these metals are mined from deposits related to major crustal-scale fault zones and/or crustal growth at convergent margins (e.g., Sillitoe, 2010). Thus, the formation of ore deposits ('metallo-geny') is closely linked to magmatism at convergent margins and the subsequent structural evolution of the crust. One area that is

globally unique in terms of regional metal endowment related to recent plate tectonic processes, is eastern Papua New Guinea (PNG). Here, a number of large porphyry Cu-Au deposits (e.g., Grasberg, Panguna, Ladolam etc.) formed within the Neogene (e.g., Sillitoe, 2010). However, the microplate tectonics that ultimately localise magmatism and ore formation remain poorly constrained.

A key area in the microplate mosaic of eastern PNG, is the Tabar-Lihir-Tanga-Feni (TLTF) island chain, that forms the subaerial expression of four alkaline volcanic centres (e.g., Wallace et al., 1983) in the sedimentary New Ireland Basin (Exon & Tiffin, 1984). This basin formed in a forearc setting relative to southward subduction of the Pacific Plate along the Manus-Kilinailau Trench prior to docking of the oceanic Ontong-Java Plateau and subduction reversal in the Miocene. Ladolam on Lihir is the 3rd largest porphyry-epithermal gold deposit in the world and all of the island groups in the TLTF chain except Tanga (at least to our current knowledge) are well endowed in Cu and Au.

The key process that lead to volcanism along the TLTF island chain is microplate rotation and lithospheric extension (e.g., McInnes & Cameron, 1994; Brandl & Hannington, in prep.) leading to melting of metasomatically enriched portions of the lithospheric mantle (e.g., McInnes & Cameron, 1994; Franz et al., 2002; Kamenov et al., 2008). The TLTF island chain is globally unique in that a sedimentary basin, previously located in a forearc setting is now being displaced, stretched and magmatically overprinted. However, the detailed geological processes are yet to be investigated and scientific deep drilling provide a unique opportunity to study the seafloor geology and to reconstruct the geological and geodynamic history of the region. The diverse range of scientific questions to be addressed in our pre-proposal offer the possibility of multi-disciplinary research and we consider this as the only way to resolve the regional tectonic, magmatic and metallogenic history. However, eastern PNG may work as a modern analogue for plate tectonic processes of the late Archean. Understanding the complexity of active microplate evolution may thus provide important insights into the processes of the Early Earth. Constraints gained from drilling in the TLTF regions will have a wide impact on research in the fields of structural and economic geology, understanding modern and ancient plate tectonics, microbiology (seafloor life linked to hydrocarbons and sulphur reduction) and paleoclimate (microfossil record and climate reconstruction).

References:

Exon, N.F., Tiffin, D.L., 1984. Geology of offshore New Ireland basin in Northern Papua New Guinea, and its petroleum prospects, in: Presented at the Transactions of the Third Circum-Pacific Energy and Mineral Resources Conference, Honolulu, pp. 623-630.

Franz, L., Becker, K.-P., Kramer, W., Herzig, P.M., 2002. Metasomatic Mantle Xenoliths from the Bismarck Microplate (Papua New Guinea)—Thermal Evolution, Geochemistry and Extent of Slab-induced Metasomatism. Journal of Petrology 43, 315-343.

Kamenov, G.D., Perfit, M.R., Mueller, P.A., Jonasson, I.R., 2008. Controls on magmatism in an island arc environment: study of lavas and sub-arc xenoliths from the Tabar-Lihir-Tanga-Feni island chain, Papua New Guinea. Contributions to Mineralogy and Petrology 155, 635-656.

McInnes, B.I.A., Cameron, E.M., 1994. Carbonated, alkaline hybridizing melts from a sub-arc environment: Mantle wedge samples from the Tabar-Lihir-Tanga-Feni arc, Papua New Guinea. Earth and Planetary Science Letters 122, 125-141.

Sillitoe, R.H., 2010. Porphyry Copper Systems. Economic Geology 105, 3-41.

Wallace, D.A., Johnson, R.W., Chappell, B.W., Arculus, R.J., Perfit, M.R., Crick, I.H., 1983. Cainozoic volcanism of the Tabar, Lihir, Tanga, and Feni Islands, Papua New Guinea: Geology, whole-rock analyses, and rock-forming mineral compositions (No. MF197), Report, Bureau of Mineral Resources, Geology and Geophysics. Canberra.

IODP

Asian Monsoon induced erosion during the Miocene

L. BRETSCHNEIDER¹, E. C. HATHORNE¹, M. FRANK¹, J. LÜBBERS²,
K. KOCHHANN^{2,3}, A. HOLBOURN², W. KUHN², N. ANDERSEN⁴

¹ GEOMAR Helmholtz Centre for Ocean Research Kiel, Germany

² Institute of Geosciences, Christian-Albrechts-University Kiel, Germany

³ Universidade do Vale do Rio dos Sinos, São Leopoldo, Brazil

⁴ Leibniz Laboratory for Radiometric dating and Stable Isotope Research, Christian-Albrechts-University Kiel, Germany

The development of the Indian or South Asian monsoon has been connected to Himalayan tectonic events, while others have suggested that the tectonics in the region have responded to monsoon induced erosion (e.g. Iaffaldano et al., 2011; Molnar et al., 1993). There is increasing evidence that the East Asian (e.g. Clift et al., 2008) and South Asian monsoons (Retallack et al., 2017) initiated or were already in existence during the early Miocene. The Miocene epoch (23–5.6 Ma) was characterised by remarkable global climate change with a period of global warmth followed by the development of permanent ice sheets on Antarctica after 13.9 Ma. Understanding how and when the monsoon first intensified and subsequently developed in relation to various forcing mechanisms is a key component for improving coupled ocean-atmosphere general circulation models. We are developing high resolution (<5 kyr) records across key climatic intervals of the Miocene to better understand the roles of tectonics, global climate and regional monsoon climate on the weathering and erosion of the watersheds feeding into the Bay of Bengal. The radiogenic Sr, Nd and Pb isotope compositions of clays are used as provenance tracers, because they reflect rock type and age. Their isotopic signature is transported within clay minerals into the central Bay of Bengal, revealing the source rocks of regional erosion. The Bay of Bengal receives discharge and sediments from the Ganga and Brahmaputra rivers, draining the Himalayas, and the Irrawaddy and Salween rivers, which supply sediments from the Indo-Burman Ranges. Previous studies suggest that especially the latter have served as an important source of material to Site U1443 during the Miocene (Ali et al., unpublished). This also corresponds to the locations of the highest modern-day monsoon rainfall over South Asia, indicating similar sediment sources during the Miocene and today.

In this study, we focus on seven key intervals in the Miocene for which continuous 500 kyr long records will be generated following the splice of IODP Site U1443. To date, we have analysed samples for two of these intervals: from 15.8 to 15.3 Ma within the Middle Miocene Climatic Optimum, and from 14 to 13.5 Ma across the first Miocene global cooling step. These new high resolution data show fluctuations on short timescales for all three isotope systems. These transient excursions reflect a changing balance of different sediment sources, which was most likely climatically driven. These new high resolution data suggest that tectonic events played a negligible role as such events occur on extended timescales, leading to long-term, gradual shifts in sources. Future work will include developing a regional climate record using paired $\delta^{18}\text{O}$ and Mg/Ca of planktonic foraminifera, in order to distinguish between regional and global climatic drivers of erosion.

References:

Ali, S., Hathorne, E. C. & Frank, M. Persistent South Asian Monsoon induced erosion over the past 26 million years, submitted, 2017.

Clift, P. D., Hodges, K. V., Heslop, D., Hannigan, R., Van Long, H., & Calves, G. (2008). Correlation of Himalayan exhumation rates and Asian monsoon intensity. *Nature geoscience*, 1(12), 875.

Iaffaldano, G., Husson, L., & Bunge, H. P. (2011). Monsoon speeds up Indian plate motion. *Earth and Planetary Science Letters*, 304(3–4), 503–510.

Molnar, P., England, P., & Martinod, J. (1993). Mantle dynamics, uplift of the Tibetan Plateau, and the Indian monsoon. *Reviews of Geophysics*, 31(4), 357–396.

Retallack, G. J., Bajpai, S., Liu, X., Kapur, V. V., & Pandey, S. K. (2018). Advent of Strong South Asian Monsoon by 20 Million Years Ago. *The Journal of Geology*, 126(1), 1–24.

IODP

Mechanisms of glacial/interglacial climate variability during the ‘mid’-Oligocene

S. BRZELINSKI¹, O. FRIEDRICH¹, A. BORNEMANN²

¹Sedimentology & Marine Paleoenvironmental Dynamics, Institute of Earth Sciences, Heidelberg University, Heidelberg, Germany

²Bundesanstalt für Geowissenschaften und Rohstoffe, Hannover, Germany

The transition from a world lacking large-scale continental ice sheets and rapid eustatic sea-level changes to a world dominated by these factors makes the Oligocene epoch one of the most interesting episodes of the Cenozoic. The Oligocene climate system was characterised by recurrent glaciations as evidenced by a pronounced variability in deep-water $\delta^{18}\text{O}$ [1, 2] and sea level (e.g. [3]). The pronounced glaciations of the early to ‘mid’-Oligocene resulted in sea-level drops of as much as 65 m [4], thus possibly being similar in magnitude to the sea-level decline at the E/O boundary (e.g., [5]). However, the existence of Northern Hemisphere ice sheets and their potential contribution to the deep-sea $\delta^{18}\text{O}$ signal is still controversially debated for large parts of the late Paleogene. Therefore, we have generated benthic foraminiferal oxygen-isotope ($\delta^{18}\text{O}$) and magnesium/calcium (Mg/Ca) records for two intervals of the ‘mid’-Oligocene from IODP Site 1406 in the Northern Atlantic. We utilize these data to constrain the magnitudes and durations of ice-volume and sea-level fluctuations. Our records, which have a temporal resolution of ~600–800 yr and comprise ~282 and ~185 kyr, respectively, are positioned between magnetostratigraphic C7A and C8 (25.20–25.98 Ma). Benthic foraminifera $\delta^{18}\text{O}$ values range between 1.03 and 2.67 ‰. The older interval (25.78–25.98 Ma) shows continuous, step-wise increases in benthic $\delta^{18}\text{O}$ values, with glacial episodes at 25.96, 25.92, 25.86, and 25.82 Ma that correspond to sea-level fluctuations of ~0–70 m. In contrast, the younger interval (25.20–25.48 Ma) is characterised by abrupt, “termination-like” decreases with four major terminations (25.32, 25.39, 25.43 and 25.47 Ma) marked by $\delta^{18}\text{O}$ increases that suggest a sea-level change of ~45–90 m. In both cases, the $\delta^{18}\text{O}$ variations point to persistent 41 kyr obliquity modulations of sea-level change during the ‘mid’-Oligocene, comparable in magnitude to the Oi-1 event [5]. The Mg/Ca-derived bottom-water temperatures document an only minor contribution of bottom-water cooling to the $\delta^{18}\text{O}$ signal. They show only a weak correlation to the $\delta^{18}\text{O}$ -based sea-level reconstruction; this might be due to an only very gradual change in bottom-water temperatures over time, whereas the ‘mid’-Oligocene cryosphere was responsive already on shorter time scales [6]. Considering the lack of large-scale ice sheets in the northern hemisphere during the Oligocene, our data indicate substantial, obliquity-paced ice-volume changes on Antarctica.

References:

[1] Paliike, H., Norris, R.D., Herrle, J.O., Wilson, P.A., Coxall, H.K., Lear, C.H., Shackleton, N.J., Tripathi, A.K., Wade, B.S., 2006. The Heartbeat of the Oligocene Climate System. *Science* 314, 1894–1898.

- [2] Zachos, J.C., Dickens, G.R., Zeebe, R.E., 2008. An early Cenozoic perspective on greenhouse warming and carbon-cycle dynamics. *Nature* 451, 279-283.
- [3] Miller, K.G., Wright, J.D., Fairbanks, R.G., 1991. Unlocking the Ice House - Oligocene-Miocene Oxygen Isotopes, Eustasy, and Margin Erosion. *Journal of Geophysical Research-Solid Earth and Planets* 96, 6829-6848.
- [4] Wade, B.S., Palike, H., 2004. Oligocene climate dynamics. *Paleoceanography* 19, 4.
- [5] Miller, K.G., Wright, J.D., Katz, M.E., Wade, B.S., Browning, J.V., Cramer, B.S., Rosenthal, Y., 2009. Climate threshold at the Eocene-Oligocene transition: Antarctic ice sheet influence on ocean circulation, in: Koeberl, C., Montanari, A. (Eds.), *The Late Eocene Earth—Hothouse, Icehouse, and Impacts*. Geological Society of America.
- [6] Cramer, B.S., Miller, K.G., Barrett, P.J., Wright, J.D., 2011. Late Cretaceous-Neogene trends in deep ocean temperature and continental ice volume: Reconciling records of benthic foraminiferal geochemistry ($\delta^{18}\text{O}$ and Mg/Ca) with sea level history. *Journal of Geophysical Research-Oceans* 116.

ICDP

Seismic exploration of overdeepened Alpine valleys

T. BURSCHIL¹, H. BUNESS¹, D. TANNER¹, G. GABRIEL¹

¹Leibniz Institute for Applied Geophysics, Stilleweg 2, 30655 Hannover

ject are (1) the distal Tannwald Basin, located about 50 km north of Lake Constance (Germany), and (2) the proximal Lienz Basin in Eastern Tyrol (Austria).

Shallow P-wave reflections, in combination with prestack depth migration processing, improve seismic imaging and enable us to reveal the structure of the basins and to distinguish different facies within the sediment succession. For the Tannwald Basin, we acquired a net of five P-wave profiles that were able to map the base of the basin. In combination with a research borehole, we characterise five seismic facies and various subfacies (Burschil et al., 2017). Two pure SH-wave and multicomponent sections also show structural parts of the basin infill that correlated with P-wave reflections.

The Lienz Basin (LB), which is one of the deepest Quaternary basins in the Eastern Alps, was covered by more than 1500 m ice during the last glacial maximum (Reitner, 2003). In the Lienz Basin (LB), we acquired four parallel profiles perpendicular to the valley axis, with different wave types (Fig. 1). All profiles comprise P-wave seismic methods, two of the profiles were surveyed by 1-component horizontal S-waves, and one with 6-component S-waves. In addition to LIAG equipment,

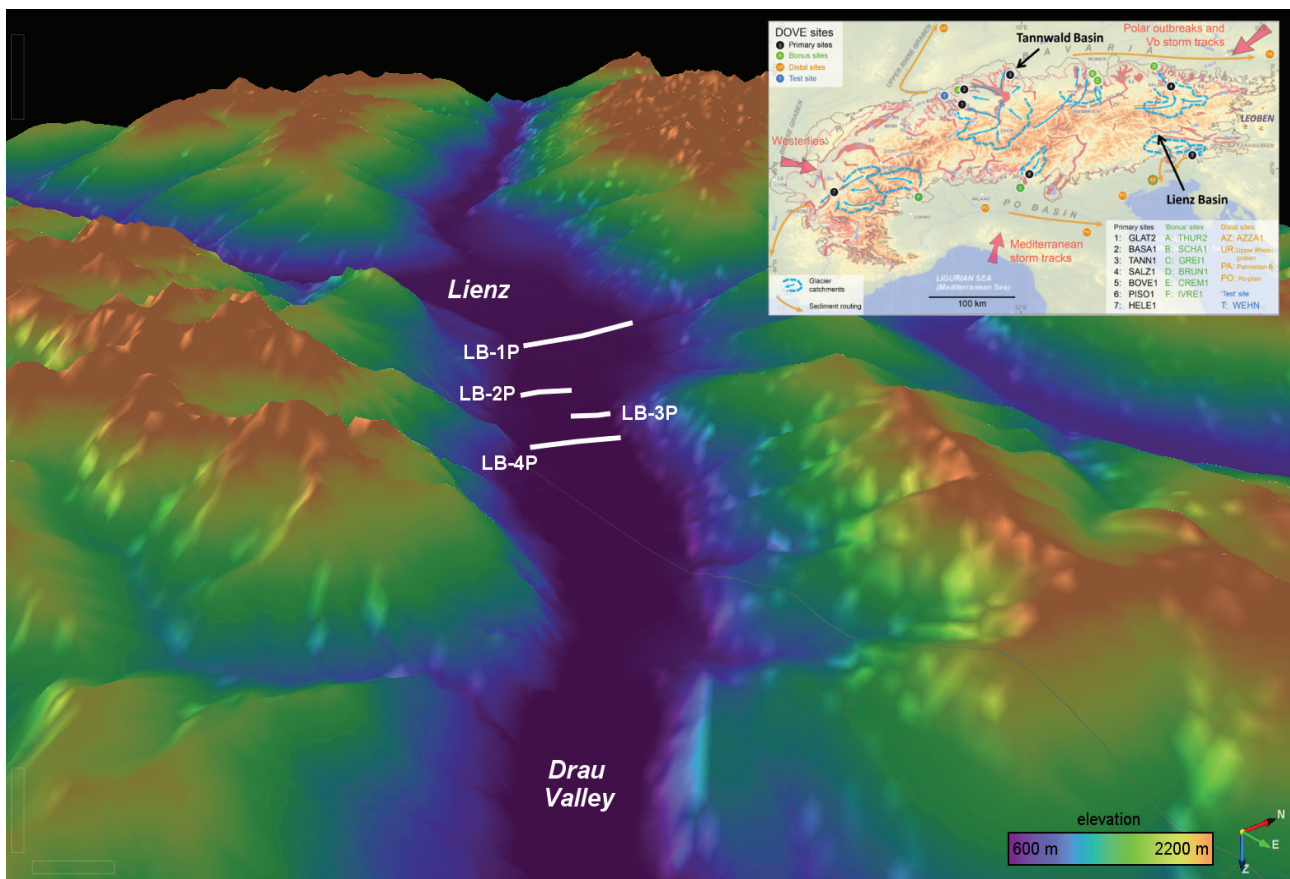


Fig. 1: Map of the DOVE sites (after Anselmetti et al., 2016) and 3-D view from SE into the Lienz Basin with locations of seismic profiles.

In the context of climate change and further challenges, the ICDP project Drilling Overdeepened Valleys (DOVE, Anselmetti et al., 2016) will analyse the sedimentary history of the glacial overdeepened valleys at seven primary drill sites in the European Alps. These sites comprise distal and proximal sediment successions. Boreholes at three locations are planned in a first stage to prove the feasibility of the methodology and a second phase will spread this concept over the entire Alpine ridge. Associated with DOVE is a DFG-funded project that investigates the benefit of high-resolution seismic reflection using modern multicomponent technology. Survey locations of the pro-

ject are (1) the distal Tannwald Basin, located about 50 km north of Lake Constance (Germany), and (2) the proximal Lienz Basin in Eastern Tyrol (Austria).

ject are (1) the distal Tannwald Basin, located about 50 km north of Lake Constance (Germany), and (2) the proximal Lienz Basin in Eastern Tyrol (Austria). we employed 60 data cubes from GFZ Geophysical Instrument Pool Potsdam, which improved imaging quality. The P-wave images the LB structure as well as internal seismic facies. The LB base reaches a maximum depth of 600 m and shows asymmetric flanks which dip approx. 27 to 41 degrees. All profiles show a comparable succession of different seismic facies (Fig. 2). We interpret the deepest facies, according to its reflection characteristic, as basal till. Above, parallel coherent reflections indicate basin fines. Varying thickness of the layer indicates compaction, e.g., due to Pleistocene ice load. Above, an unconformity marks a change in sedimen-

tation. Above that, a unit of chaotic seismic facies terminates about 70 m below surface. We interpret this unit as a till of a younger glaciation, which suggests at least two glaciations. At the top, a more chaotic facies completes the sediment succession. A 60 m groundwater well, which is the deepest borehole in LB until now, identifies this unit as coarse sand and gravels. Further features are present in the seismic sections: Slumps of various extent are present in the deepest facies at the flanks of the LB in profiles 1 and 4. Uplift of the internal horizons at the valley flank supports the theory of compaction on profile 3. On profile 4, we interpret a wedge at the northern valley flank as an alluvial fan. S-wave sections are not processed yet.

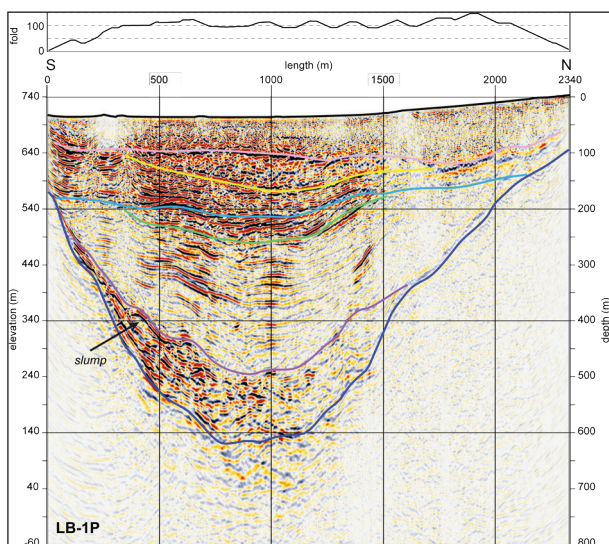


Fig. 2: P-wave seismic reflection profile LB-1P with interpretation (described in the abstract).

At both survey sites, seismic imaging show an remarkable quality for land seismic data that allows us to interpret various features in the sediment succession. According to the seismic data, a drill location was chosen for the Tannwald Basin and suggested for the LB. In addition to further processing of the 2-D S-wave and multicomponent data, a 3-D multicomponent survey will follow in the Tannwald Basin.

We acknowledge the GFZ Geophysical Instrument Pool Potsdam for providing seismic equipment, grant number GIPP201623.

References:

- Anselmetti et al. (2016). Drilling overdeepened Alpine Valleys (DOVE). ICDP Full Proposal, 174pp.
 Burschil et al. (2017). Facies Characterization of the Overdeepened Glacial Tannwald Basin. Extended Abstract EAGE Near Surface Geoscience 2017.
 Reitner (2003). Bericht 2000 über geologische Aufnahmen im Quartär auf Blatt 179 Lienz. Jahrbuch der Geologischen Bundesanstalt 143 (3), 389-395.

ICDP

Vesiculation processes in rhyolitic magma as a response to heating and slow decompression.

F. CÁCERES¹, F. WADSWORTH¹, B. SCHEU¹, M. COLOMBIER¹, K.-U. HESS¹,
 B. RUTHENSTEINER², D. B. DINGWELL¹

- ¹ Department of Earth and Environmental Sciences, Ludwig-Maximilians-Universität (LMU) München, Germany. (f.caceres@lmu.de),
² Bavarian State Collection of Zoology.

The degassing dynamics of a magma exerts a first order control on the potential for explosivity at erupting volcanoes as

it controls the overpressure of the magma in the shallow crust. Bubbles can grow both by gas expansion for instance due to decompression and by mass addition via volatile diffusion from the melt. Both of these mechanisms are dependent on pressure gradients during ascent, together with composition-dependent melt properties including volatile solubility, diffusivities and viscosity. Quite importantly, at (pre-)eruptive conditions volatile solubility is an increasingly strong function of pressure and temperature, such that both temperature increases or pressure decreases can cause magma vesiculation. Here we investigate the role of 1) heating and 2) slow decompression on rhyolite magma vesiculation. The experiments were conducted using cores of natural obsidians from Hrafninnuhryggur, Krafla volcano with different low initial water contents (0.11-0.15 wt%).

In a first series of experiments, we exposed the obsidian to slow and fast heating to temperatures of 800-1000°C and at 1 bar ambient pressure using an optical dilatometer. These heating experiments were conducted with initially cylindrical samples, which remained axisymmetrical in shape during vesiculation permitting the application of the solid-of-rotation to obtain continuous data of volume from ambient to final temperature. During heating, the volume of the sample increased nonlinearly as bubbles nucleated and grew. Selected samples were analysed by X-ray computed microtomography to determine vesicularity, bubble number density and bubble connectivity. In these experiments, the bubbles grew due to the temperature-induced supersaturation of water that drove nucleation and diffusion of water into bubbles. X-ray tomography revealed low bubble number densities (1-7 mm⁻³) consistent across a large range of vesicularities (6-60%). Even samples at the high end of the vesicularity range exhibit a low to very low vesicle connectivity, indicating isolated bubble growth in this unconstrained, slow vesiculation scenario. These continuous porosity-time data will be compared with numerical models for bubble growth in rhyolites.

In a second series of experiments, we are exposing the same composition of obsidian samples as well as synthetic hydrated samples (0.3-1.8 wt %) of Krafla obsidian to magmatic temperatures (750-900°C) and varying slow decompression scenarios, both linear and non-linear. In these experimental series we are exploring the effect of pressure changes on bubble nucleation and growth, to mimic the regimes and changes relevant for the shallow rhyolitic magma reservoir found at Krafla in Iceland. The decompression and heating textures will then be compared quantitatively. The results may shed light on the relative roles of decompression and heating in nucleation scenarios in nature.

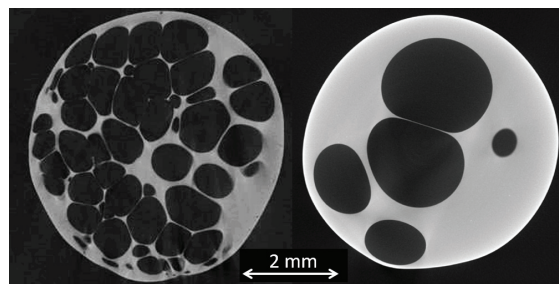


Fig. 1: 2D X-ray micro-tomography images showing the evolution of vesicularity in Krafla obsidians foamed at 1000°C during the first series of experiments using an optical dilatometer. The two samples shown here were quenched at different stages giving insight into vesiculation process.

IODP

Evolution of the oceanic circulation in the North Atlantic across the Mid-Pleistocene Transition

 M. C. A. CATUNDA¹, A. BAHR¹, O. FRIEDRICH¹
¹Institut für Geowissenschaften, Universität Heidelberg, Heidelberg, Deutschland.

The current global climate system underwent its last major reorganization during the so-called Mid-Pleistocene Transition (MPT). The development of present-day 100-kyr glacial cyclicity [1,2] traces back to this period, between Marine Isotopic Stages (MIS) 35–15, 1190 kyr - 620 kyr. The shift from the previous 41-kyr obliquity-paced glacial/interglacial rhythm is poorly understood, being still a matter of active debate in the scientific community. Apart from the change in cyclicity, the MPT is also marked by increased amplitudes in glacial-interglacial cyclicity and the enlargement of North Hemisphere ice sheets during glacial [3], which may have preconditioned the prolongation of the post-MPT glacial periods [1]. With respect to this, a mechanistic understanding of the impact of changes in oceanic heat transport in the northern Atlantic during the mid-Pleistocene waxing and waning of northern hemisphere ice sheets is essential for fully appreciating the dynamics of Quaternary climate evolution.

The North Atlantic Subtropical Gyre (NASG) plays a central role in the transport of heat and moisture into the higher-latitude North Atlantic. In this project we are exploring changes in the temperature and salt budget within the gyre and the strength and spatial configuration of its circulation pattern during MIS 35–15, to shed light on the dynamics of the mid-Pleistocene meridional heat transport. We are, therefore, generating combined subsurface $\delta^{18}\text{O}$ and Mg/Ca records from two marine sediment cores: IODP Site U1313 and ODP Site 1058. These two sites are strategically located at the current northern (U1313) and western (1058) boundaries of the NASG and thus, highly sensitive to variations in its extent and circulation strength.

Here, we present Mg/Ca-derived subsurface paleotemperatures (SubT) on the deep thermocline dweller *Globorotalia crassaformis* obtained on central North Atlantic IODP Site U1313. Our SubT record reveals the persistent establishment of cold ($\sim -4^\circ\text{C}$) subT during glacial after MIS 22, in contrast to relatively mild glacial subT of $\sim -6^\circ\text{C}$ before MIS 22. We attribute the post-MIS 22 subT cooling to the emerging presence of Glacial North Atlantic Intermediate Water (GNAIW) on thermocline level, leading to abrupt temperature decreases by up to 5°C . Between MIS 35-22 central North Atlantic thermocline temperatures were relatively stable, with only two major cooling events during early MIS 30 and 22. Also notably, variations in thermocline depth at Site U1313 (calculated from the difference of sea-surface temperatures [4] and subT) do not follow glacial-interglacial periodicity, but closely match fluctuations of dust input into the Eastern Mediterranean Sea [5]. We argue that phases of high dust input and, hence, pronounced aridity in the Eastern Mediterranean realm, were characterized by more vigorous formation of Levantine Intermediate Water (LIW) [6]. The LIW is the key driver of the warm and saline Mediterranean Outflow Water (MOW) [7], which is nowadays a major source of intermediate waters in the Northern Atlantic [8]. The increase of MOW production from MIS 24 onwards might have profoundly changed the status quo of Northern Atlantic upper ocean circulation as an enhanced MOW presence would have added heat and salinity to the Northern Atlantic, fueling the strength of NASG. A strong NASG in turn might have acted as a pathway for moisture transport into the higher latitudes.

Our results from IODP Site U1313 will be compared with currently generated deep dweller Mg/Ca and $\delta^{18}\text{O}$ records on *Globorotalia truncatulinoides* (sinistral) from ODP Site 1058, situated along the current Gulf Stream pathway. The combination of both records will generate a complete picture of the North Atlantic Subtropical Gyre evolution and thus will be instrumental for resolving the puzzle of amplified ice-sheet growth during the MPT.

References:

- [1] Clark, P. U., Archer, D., Pollard, D., et al., 2006, The middle Pleistocene transition: characteristics, mechanisms, and implications for long-term changes in atmospheric pCO_2 : *Quat. Sci. Rev.*, 25, 31503184.
- [2] McClymont, E. L., Sostian, S. M., Rosell-Melé, A., et al., 2013, Pleistocene sea-surface temperature evolution: Early cooling, delayed glacial intensification, and implications for the mid-Pleistocene climate transition: *Earth-Science Rev.*, 123, 173-193.
- [3] Raymo, M. E., Lisiecki, L. E., and Nisancioglu, K. H., 2006, Plio-Pleistocene ice volume, Antarctic climate, and the global $\delta^{18}\text{O}$ record: *Science*, 313, 492-495. 4. Sostian and Rosenthal, 2009
- [4] Naafs, B. D. A., Hefter, J., Acton, G., et al., 2012, Strengthening of North American dust sources during the late Pliocene (2.7 Ma): *EPSL*, 317, 8-19.
- [5] Larrasoana, J. C., Roberts, A. P., Rohling, E. J., Winkhofer, M., Wehausen, R., 2003. Three million years of monsoon variability over the northern Sahara. *Clim. Dyn.* 21, 689-698.
- [6] Bahr, A., Kaboth, S., Jiménez-Espejo, F., Sierro, F., Voelker, A., Lourens, L., Röhl, U., Reichert, G., Escutia, C., Hernández-Molina, F., Pross, J., Friedrich, O. (2015), Persistent monsoonal forcing of Mediterranean Outflow Water dynamics during the late Pleistocene: *Geology*, 43: 951-954.
- [7] Rogerson, M., Rohling, E.J., Bigg, G.R., and Ramirez, J., 2012, Paleoceanography of the Atlantic - Mediterranean exchange: Overview and first quantitative assessment of climatic forcing: *Reviews of Geophysics*, v. 50, RG2003, doi:10.1029/2011RG000376.
- [8] Talley L. D., Pickard G. L., Emery W. J., Swift J. H., 2011. *Descriptive Physical Oceanography: An Introduction (Sixth Edition)*, Elsevier, Boston, 560 pp.

ICDP

Global climate and local environmental influence on diatom community structure over time in ancient Lake Ohrid

 A. CVETKOSKA¹, E. JOVANOVSKA¹, T. HAUFFE¹, S. TOFILOVSKA²,
 T.H. DONDRS³, A. FRANCKE⁴, H.VOGEL⁵, B. WAGNER⁶, Z. LEVKOV²,
 T. WILKE¹
¹Department of Animal Ecology and Systematics, Justus Liebig University, Giessen, Germany

²Institute of Biology, Faculty of Natural Sciences, Skopje, R. of Macedonia

³Palaeoecology, Department of Physical Geography, Faculty of Geosciences, Utrecht University, Utrecht, The Netherlands

⁴Wollongong Isotope Geochronology Laboratory, School of Earth and Environmental Sciences, University of Wollongong, Wollongong, Australia

⁵Institute of Geological Sciences & Oeschger Centre for Climate Change Research, University of Bern, Bern, Switzerland

⁶Institute of Geology and Mineralogy, University of Cologne, Cologne, Germany

Biological diversity is characterized by a heterogeneous spatial-temporal distribution, shaped by the complex interplay of ecological and evolutionary processes. Despite numerous studies on present-day diversity and community patterns, very few ecosystems, such as ancient lakes, offer the potential to understand the environmental drivers of community structure on long temporal scale. The SCOPSCO project (Scientific Collaboration on Past Speciation Conditions in Lake Ohrid) is among the first integrative ICDP campaigns that closely combines geology and biology aiming to understand the drivers of the unique biodiversity and endemism in an ancient lake setting. The 584 m long sediment record from the DEEP site is unique in the preservation of diatoms (Bacillariophyceae), particularly for the interval 0-1.4 Ma. Due to the depth of the cor-

ing location (i.e., 243 m) in the centre of the lake, planktonic diatom taxa dominate the microfossil record. We here present the stratigraphic succession of planktonic diatom diversity and test how global climate and local environmental drivers shaped the community structure over time.

Our biostratigraphic record shows that three types of major planktonic communities have existed in the lake since the onset of full lacustrine conditions, ca. 1.4 Ma ago. Low species richness and the dominance of distinct endemic taxa characterized each community. Community turnovers occurred at glacial-interglacial transitions, caused by the extinction of dominant endemic species and emergence and/or increase in the relative abundance of newly evolved ones.

We tested the influence of the climatic and environmental drivers for each major type of community individually. The results show that different global and local drivers affected the community structure over time. The diatom community present in the lowermost stratigraphic interval, between 440 and 330 m core depth, is primarily structured under the influence of local habitat structure and nutrient availability, whereas global-scale climate variability had relatively low effects. The 100 ka cycle, global and Mediterranean climate variability became more important during the second section, between 330 and 80 m depth. However, local variations in precipitation, depositional environment, catchment dynamics, nutrient availability and lake mixing were predominant factors driving community dynamics. The last community turnover at the MIS 7/6 boundary, ca. 190 ka ago, marks a complete change of the prevailing drivers, with global-scale changes in temperature, and regional changes in precipitation having a large effect on the local environment. Diatom community structure from ca. 185 ka until present appears thus driven by global and Mediterranean climate change causing, however, no extinction events or irreversible community turnovers.

Our results demonstrate that diatom community structure in Lake Ohrid was influenced by local environmental and global-scale factors, changing their relative importance over the entire lake history. This study thus provides a better understanding of the complex role of the environment in structuring community and diversity patterns over long temporal scales.

ICDP

Magma Propagation directions in the Eger rift (Czech republic)

T. DAVIS, E. RIVALTA¹

¹ GFZ German Research Centre for Geosciences, Section 2.1, Physics of earthquakes and volcanoes.

We have developed a 3D boundary element code to simulate magma propagation paths through a heterogeneous stress field. The code has been benchmarked against analytical solutions for removal/addition of topographic loads. It is shown this is accurate in computing both the magnitude and direction of the principal stresses. In our model we approximate dyke trajectories by aligning these parallel with the most compressive stress in the system. In this sense, our model is an end member, where the path is not deflected due to magma buoyancy or internal viscous flow. Boundary conditions are applied such that the stress state for the rift system is a combination of topographic loading/unloading and far field tectonic stresses, in 3D. A dyke is seeded at a point with a given start depth and its trajectory to the surface is calculated. Using this model we aim to resolve the most likely combination of parameters that

result in the observed vent locations in the Eger rift. We hope to constrain the parameter space further using geodynamical models, dykes alignments and geochemical constraints. The aim of such modelling to help constrain physical parameters driving the crustal evolution of the area. This should in turn allow for a better knowledge of the source for crustal fluids in the area and the stresses controlling the damage within the rock volume hosting these.

IODP

Hardened faecal pellets as a significant component in deep water, non-tropical marine environments

H. DEIK¹, L. REUNING¹, B. PETRICK²

¹EMR-Group, Geological Institute, RWTH Aachen University

²Max-Planck-Institute for Chemistry, Mainz

Hardened faecal pellets are classically interpreted to form in shallow, tropical environments. However, faecal pellets deposited in deep, non-tropical marine conditions are poorly studied. IODP Site U1460 on the Carnarvon Ramp (SW Shelf of Australia, 214.4m water depth) recovered a nearly continuous Pliocene to recent record of outer shelf sediments deposited at the transition between cool and warm water environments. Below a depth of ~20 CSF-A the relative abundance of sand-sized faecal pellets varies between 0 and 69 %. The origin and composition of the faecal pellets were investigated using scanning electron microscopy, binocular microscope and X-ray diffraction (XRD). The faecal pellets have a uniform size and shape and tend to occur mainly in relatively deeper water during interglacial times. They are mainly composed of skeletal fragments such as ascidians spicules, planktic foraminifera, sponge spicules and coccolith plates in a micritic matrix. The pellets therefore show an identical composition compared to the surrounding matrix, indicating that they have formed in situ. X-ray diffraction shows that the faecal pellets consist of aragonite, low-Mg calcite and dolomite. The aragonite at this study reaches up to 30% of the total bulk sediment and generally decreases with depth due to either dissolution or platform progradation. Aragonite dissolution within the faecal pellets is visible e.g. at the tips of the ascidian spicules. The presence of framboidal pyrite within the pellets indicates bacterial-sulfate reduction (BSR). BSR likely explains the observed aragonite dissolution, which is accompanied by an alkalinity increase and in consequence by the precipitation of calcite and dolomite cements. The occurrence of pyrite in a depth starting at 5 CSF-A (m), indicates that aragonite dissolution and calcite cementation already started in the very shallow burial environment. We suggested that the faecal pellets are hardened due to this early cementation by calcite and therefore can be preserved in the fossil record.

IODP

The amplifying effect of Indonesian Through-flow heat transfer on Late Pliocene Southern Hemisphere climate cooling.

D. DE VLEESCHOUWER¹, G. AUER², K. BOGUS³, B. CHRISTENSEN⁴,
 J. GROENEVELD¹, B. PETRICK⁵, J. HENDERIKS⁶, I. CASTAÑEDA⁷,
 E. O'BRIEN⁸, S. J. GALLAGHER⁹, C. S. FULTHORPE¹⁰, H. PÁLIKE¹

¹ MARUM-Center for Marine and Environmental Sciences, University of Bremen, Klagenfurterstraße 2-4, Bremen, 28359, Germany

² Department of Biogeochemistry, Japan Agency for Marine-Earth Science and Technology (JAMSTEC), Kanagawa, 237-0061, Japan

³ International Ocean Discovery Program, Texas A&M University, College Station, 77845-9547, USA

⁴ Environmental Studies Program, Adelphi University, Garden City, New York

⁵ Max-Planck-Institut für Chemie, Mainz, 55128, Germany

⁶ Department of Earth Sciences, Uppsala University, Uppsala, 75236, Sweden

⁷ Department of Geosciences, University of Massachusetts at Amherst, Amherst, MA 01003, USA

⁸ Department of Geology and Geophysics, Texas A&M University, College Station, TX 77843, USA

⁹ School of Earth Sciences, University of Melbourne, Melbourne, 3010, Australia

¹⁰ Institute for Geophysics, Jackson School of Geosciences, University of Texas at Austin, Austin, 78758-4445, USA

An unusually short glaciation interrupted the warm Pliocene around 3.3 Ma (Marine Isotope Stage (MIS) M2). Different hypotheses exist to explain why this glaciation event was so pronounced, and why the global climate system returned to warm Pliocene conditions relatively quickly. One of these proposed mechanisms is a reduced equator-to-pole heat transfer, in response to a tectonically reduced Indonesian Throughflow (ITF). The ITF is a critical part of the global thermohaline ocean circulation, transporting heat from the Indo-Pacific Warm Pool to the Indian Ocean. When ITF connectivity is reduced, the water and heat supply for the Leeuwin Current, flowing poleward along Australia's west coast, is also diminished. To assess the possible relationship between mid-Pliocene glaciations and latitudinal heat transport through the Indonesian Throughflow, we constructed a multi-proxy orbital-scale record for the 3.9 - 2.7 Ma interval from International Ocean Discovery Program (IODP) Site U1463. The comparison of the Site U1463 record with paleoclimate records from nearby Site 763 (Karas et al., 2011) and West Pacific Warm Pool Site 806 (Wara et al., 2005; O'Brien et al. 2014) allows for a detailed regional reconstruction of Pliocene paleoceanography and thus for testing the proposed hypothesis.

The U1463 oxygen isotope record of the planktonic foraminifer *Globigerinoides sacculifer* correlates exceptionally well with the sea surface temperature (SST) record from Site 806 in the West Pacific Warm Pool, even during MIS M2. Hence, Site U1463 preserves an uninterrupted ITF signal even during Pliocene glaciations. However, the U1463 $\delta^{18}\text{O}_{\text{G.sacculifer}}$ record exhibits a 0.5‰ offset with the nearby Site 763A record around MIS M2. This implies that Site 763A, about 500 km west of U1463, more closely tracks Indian Ocean SST records across MIS M2. The U1463 data thus reveal that heat-transport through the Indonesian Throughflow did not shut down completely during MIS M2, but rather its intensity decreased, causing Site 763A to temporarily reflect an Indian Ocean, rather than an ITF signal. We conclude that ITF variability significantly influenced latitudinal heat transport by means of the Leeuwin Current and hence contributed to the relative intensity of MIS M2. We propose the ITF valve between the Pacific and Indian Ocean as a positive feedback mechanism, in which reduced ITF heat transport

amplifies global cooling by advancing the thermal isolation of Antarctica.

References:

- Karas, C., Numberg, D., Tiedemann, R., Garbe-Schonberg, D., 2011. Pliocene Indonesian Throughflow and Leeuwin Current dynamics: Implications for Indian Ocean polar heat flux. *Paleoceanography* 26. doi:10.1029/2010pa001949
- O'Brien, C.L., Foster, G.L., Martinez-Boti, M.A., Abell, R., Rae, J.W.B., Pancost, R.D., 2014. High sea surface temperatures in tropical warm pools during the Pliocene. 7, 606. doi:10.1038/ngeo2194
- Wara, M.W., Ravelo, A.C., Delaney, M.L., 2005. Permanent El Niño-like conditions during the Pliocene warm period. *Science* 309, 758-761. 10.1126/science.1112596

ICDP

Rupture Processes and Magnitude Statistics of the 2014 M5.5 Earthquake Sequence Below a Gold Mine in Orkney, South Africa

C. DINSKE¹, M. MÜLLER¹, M. VOIGT¹, J. KUMMEROW¹, S. A. SHAPIRO¹

¹Freie Universität Berlin, FR Geophysik, Malteserstr. 74-100, 12249 Berlin

Despite our general understanding of earthquake processes, it is still not fully understood how earthquake ruptures nucleate and propagate and why they stop. Furthermore, the controlling factors of the frequency and the size of earthquakes are subject of ongoing research. We address these questions with a comprehensive study of seismicity from deep South African gold mines. Here, we find the unique situation that the seismicity consists of both mining-induced earthquakes and aftershocks triggered by the M5.5 Orkney earthquake in August 2014 (Moyer et al., 2017). We hypothesize that the finiteness and geometry of the volume of stress perturbation, either by mining activities or by a main shock, controls the nucleation and propagation of ruptures and influences the frequency-magnitude distribution. To test our hypothesis, we apply novel approaches to the seismicity from the deep mines which involve both waveform-based and probabilistic methods. These methods were recently elaborated and successfully applied to fluid injection induced earthquakes and include rupture propagation imaging (Folesky et al., 2015), rupture directivity analysis (Folesky et al., 2016), and studies of the scaling of the earthquakes magnitude statistics (Shapiro et al., 2013, Dinske et al., 2017). We test the applicability of these approaches to the seismicity in deep South African mines which also occurs in finite volume where the in-situ stress is perturbed. It contributes to a better understanding of seismogenic processes and, in particular, to an improved assessment and mitigation of seismic hazard in mining environment. First results indicate a unilateral rupture of the M5.5 main shock, which is in agreement with previous results (Ogasawara et al., 2017), and we find a clear spatial separation of aftershock hypocenters and the induced seismicity in the different mining horizons.

References:

- Dinske, C. and Shapiro, S. A. (2017). Scaling of injection-induced earthquake magnitude statistic and implications for seismic hazard assessment. *J Geoph Res*, in revision.
- Folesky, J., Kummerow, J., and Shapiro, S. A. (2015). Microseismic rupture propagation imaging. *Geophysics*, 80(6):WC107-WC115.
- Folesky, J., Kummerow, J., Shapiro, S. A., Haering, M., and Asanuma, H. (2016). Rupture directivity of fluid induced microseismic events: Observations from an enhanced geothermal system. *J Geoph Res*, 121(11):8034-8047.
- Ogasawara, H. and the ICDP DSeis Team (2017). Drilling to probe quasi-static and dynamic seismic ruptures in deep South African gold mines from cm- to km-scale. *Schatzalp Workshop on Induced Seismicity*. Davos, Switzerland, March 2017.
- Shapiro, S. A., Krüger, O. S., and Dinske, C. (2013). Probability of inducing given-magnitude earthquakes by perturbing finite volumes of rocks. *J Geophys Res*, 118(7):3557-3575.

ICDP

Trends, rhythms and transitions during the Late Quaternary in southern Ethiopia

W. DÜSING¹, A. ASRAT², V. FOERSTER³, H. KRÄMER⁴, H. LAMB⁵,
N. MARWAN⁴, F. SCHÄBITZ³, M. H. TRAUTH¹

¹Institute of Earth and Environmental Science, University of Potsdam, Potsdam, Germany

²Addis Ababa University, School of Earth Sciences, Addis Ababa, Ethiopia

³Institute of Geography Education, University of Cologne, Köln, Germany

⁴Potsdam Institute of Climate Impact Research, Potsdam, Germany

⁵Aberystwyth University, Department of Geography and Earth Sciences, Aberystwyth, UK

This project aims at statistically analyzing the long (~278 m) sediment record of the Chew Bahir basin, as part of the ICDP-funded Hominin Sites and Paleolakes Drilling Project (HSPDP). The aim of the project is (1) to establish a robust age-depth model for the sediment cores, (2) to correlate the Chew Bahir record with other records within and outside HSPDP, (3) to detect trends, rhythms and events in the environmental record of the basin, and (4) identify recurrent, characteristic types of climate transitions in the time series, as compared with the ones of the other HSPDP sites and climate records outside HSPDP. The work presented here will provide first results of age-depth modelling, including cyclostratigraphy, of the long Chew Bahir cores. Second, it gives an overview of the first results from evolutionary spectral analysis to detect changes in the response of the Chew Bahir to orbital forcing during the last 550 kyr. Third, the results of a change point analysis will be presented to define the amplitude and duration of past climate transitions and their possible influence on the development of early modern human cultures.

IODP

Gateway history of the Early Cretaceous South Atlantic derived from Nd-isotope signatures

W. DUMMANN¹, S. STEINIG², P. HOFMANN¹, S. FLÖGEL², A. OSBORNE²,
J. O. HERRLE^{3,4}, M. FRANK², T. WAGNER⁵

¹Institute of Geology and Mineralogy, University of Cologne, Zùlpicher Str. 49a, 50674 Cologne, Germany

²GEOMAR Helmholtz Centre for Ocean Research Kiel, Wischhofstr. 1-3, 24148 Kiel, Germany

³Institute of Geosciences, Goethe-University Frankfurt, Altenhõferallee 1, 60438 Frankfurt am Main, Germany

⁴Biodiversity and Climate Research Centre (BIK-F), Senckenberganlage 25, 60325 Frankfurt am Main, Germany

⁵Sir Charles Lyell Centre, School of Energy, Geoscience, Infrastructure and Society, Heriot-Watt University, Edinburgh, EH14 4AS, UK

Young ocean basins emerging during the break-up of supercontinents provide favorable conditions for drawdown and burial of atmospheric CO₂. Extensive black shale deposition, the formation of petroliferous sedimentary basins along continental margins and carbon cycle modelling suggest that the young South Atlantic (subdivided by the Wavis Ridge/Rio Grande Rise into the Cape-Argentine-Basin to the south and the Angola-Brazil-Basin to the north) and the Southern Ocean acted as important carbon sinks during the Early Cretaceous break-up of Gondwana.

We present a consistent stratigraphic framework for several South Atlantic (DSDP Sites 361, 327, 511, 364, 363) and Sou-

thern Ocean deep sea drilling sites (DSDP Site 249 and ODP Site 693) based on high resolution ¹³C tuning. Our data provide the temporal data basis for an ongoing modelling approach attempting to quantify the contribution of local carbon burial within these young emerging basins to the global carbon budget (see abstract of Steinig et al.). Source regions, modes, and flow paths of deep water are reconstructed based on a twofold approach combining sea water-derived neodymium (Nd) isotope signatures and a novel general circulation model (Steinig et al.). Bulk geochemical parameters (i.e., total organic carbon content) are used to investigate the relationship between deep water circulation and carbon burial.

Our results show that during the lowermost Aptian, prior to 124 Ma, the Falkland Plateau hindered water mass exchange between the South Atlantic (south of the Wavis Ridge/Rio Grande Rise) and the Southern Ocean as indicated by divergent Nd-isotopic signatures. General circulation model simulations (Steinig et al.) indicate that the anti-estuarine, salinity-driven overturning circulation within the silled South Atlantic was restricted to intermediate water depths (South Atlantic Intermediate Water) and largely stagnant within the deep Cape Basin at that time. The slow replenishment of oxygen to the deep Cape Basin promoted marine carbon burial and the periodic expansion of bottom water euxinia as indicated by organic carbon contents of up to 20 %, abundant sulfur, and enrichment of redox-sensitive trace metals. Similar redox conditions prevailed within the semi-enclosed Falkland Basin, which was confined by the African continent to the North, the Maurice Ewing Bank to the East, and the Falkland Island basement high to the West. The Angola Basin north of the Wavis Ridge/Rio Grande Rise was filled with a hypersaline water mass imprinted with unradiogenic Nd isotopic signatures probably derived from local erosional input of dissolved Nd from the Congo Craton.

From 124 Ma onwards, the progressive westward drift and subsidence of the Falkland Plateau permitted intermediate water mass outflow of South Atlantic Intermediate Water through the Falkland Basin into Southern Ocean as recorded by a clear shift in redox conditions and Nd-isotopic composition. The radiogenic Nd isotope signature of the outflowing intermediate water mass is consistent with a formation region along the shelves south of the Wavis Ridge/Rio Grande Rise as proposed by the general circulation model. Nd isotopic gradients between South Atlantic Intermediate Water and the deep water within in the Cape Basin indicate a stratified water column persistently maintaining bottom water anoxia/ euxinia.

Around 122 Ma, the occurrence of planktonic foraminifera and a redox shift towards suboxic conditions marks the first marine incursion into the Angola Basin. From this time on, the progressive oxygenation and a long-term trend towards more radiogenic Nd isotope signatures indicates the admixture of an oxic water mass overprinting the local water mass signature. Although the source region of this water mass remains to be identified, the clear offset between Nd isotope signatures north and south of the Wavis Ridge/Rio Grande Rise argues against significant water mass exchange between the southern South Atlantic and the Angola Basin.

By ~116 Ma, Nd isotope signatures within the Southern Ocean, the Falkland Basin, and the Cape Basin converge indicating significant water mass mixing between all sub-basins. At the same time, anoxic conditions abated and carbon burial decreased within the deep South Atlantic and Southern Ocean denoting the onset of an efficient overturning circulation. This marks the opening of the deep Georgia Basin Gateway due to the detachment of the Maurice Ewing Bank from the African continent. Distinct Nd isotope signatures in the South Atlan-

tic north and south of the Wavis Ridge/Rio Grande Rise until at least Cenomanian times indicate the continued presence of hydrologically separated sub-basins.

Our combined geochemical and modelling approach generated a consistent circulation history of the young South Atlantic and Southern Ocean emphasizing the importance of marine gateways. The improved stratigraphic framework will provide the chronology for the non-transient biogeochemical model enabling us to investigate the global impact of local carbon burial.

ICDP

First results on Core-Log-Seismic-Integration in hard-rock environments using the ICDP drilling project COSC-1, Sweden

J. ELGER¹, C. BERNDT¹, F. KÄSTNER², S. PIERDOMINICI², J. KÜCK²

¹Helmholtz Centre for Ocean Research Kiel

²Helmholtz Centre Potsdam GFZ German Research Centre for Geosciences

Core-Log-Seismic-Integration (CLSI) is an interdisciplinary strategy to integrate core measurements, logging data either from wireline or core logs or both, and seismic data to bridge scales from the sub millimetre-scale of core investigations to metre scale of seismic data. This method has been developed for soft sediments and non-metamorphic lithified sediments and has been successfully applied in marine and lake environmental (e.g. Gaillot et al., 2007; Riedel et al., 2013).

As part of the ICDP priority program “Collisional Orogeny of the Scandinavian Caledonides (COSC)” we are investigating the geophysical properties of the rocks from the Seve Nappe Complex (SNC) using the COSC-1 borehole (Sweden). This project has two main objectives. The first, geological aim is to establish a high-resolution seismic stratigraphy applying CLSI to a metamorphic setting in order to improve our understanding of the tectonic and structural geological processes that led to the formation of the SNC in particular how shear was partitioned and how it affected the geophysical properties. The second objective is methodological. Here, we aim at learning how the CLSI techniques can be applied for metamorphic rocks although they have been developed mainly for hydrocarbon reservoirs in lithified sediment rocks but also for high-resolution combination of shallow sediment cores and ultra-high resolution seismic data.

In a first step we use information from two sets of wire line logs and tie them to 3D seismic survey from the SNC (Hedin et al., 2016), a multi-azimuthal walkaway vertical seismic profile (Simon et al., 2016), and a high-resolution zero-offset vertical seismic profile (Krauß et al., 2016), and combine them in the Log-Seismic-Integration (LSI). From density and sonic information we have generate synthetic seismograms and compared them to zero offset seismic traces which are extracted from the processed surface 3D seismic data at the location of the bore hole.

As expected the results show significant deviations between synthetic and measured seismograms. These deviations are due to imperfect coupling of the tools in the boreholes and uncertainty in the depth measurements during logging, seismic wave propagation artefacts, anisotropy in the seismic velocities and noise both in the seismic data and in the log data. In the following steps we will minimize the mismatch and analyze depth intervals at which the mismatch is particularly large in order to deduce where samples should be taken for seismic anisotropy

measurements as previous work (Simon et al., 2017) have shown that anisotropy can be up to 15% in these metamorphic rocks.

References:

- Gaillot, P., Brewer, T., Pezard, P., Yeh, E.-C., 2007. Contribution of Borehole Digital Imagery in Core-Log-Seismic Integration. *Scientific Drilling*, No. 5, 50-53.
- Hedin, P., Almqvist, B., Berthet, T., Juhlin, C., Buske, S., Simon, H., Giese, R., Krauss, F., Rosberg, J.-E., Alm, P.-G., 2016. 3D reflection seismic imaging at the 2.5km deep COSC-1 scientific borehole, central Scandinavian Caledonides. *Tectonophysics*, 390, 301-319.
- Krauß, F., Hedin, P., Almqvist, B., Simon, H., Giese, R., Buske, S., Juhlin, C., Lorenz, H., 2016. Borehole seismic in crystalline environment at the COSC project in Central Sweden. *Geophysical Research Abstracts*, vol. 18, EGU2016-8018, EGU General Assembly 2016, Vienna.
- Riedel, M., Bahk, J.J., Kim, H.S., Yoo, D.G., Kim, W.S., Ryu, B.J., 2013. Seismic facies analyses as aid in regional gas hydrate assessments. Part-I: Classification analyses. *Marine and Petroleum Geology*, 47, 248-268.
- Simon, H., Krauß, F., Hedin, P., Buske, S., Giese, R., Juhlin, C., 2016. The derivation of an anisotropic velocity model from combined surface and borehole seismic experiments at the COSC-1 borehole, central Sweden. *Geophysical Research Abstracts* Vol. 18, EGU2016-2820, EGU General Assembly 2016, Vienna.
- Simon, H., Buske, S., Krauß, F., Giese, R., Hedin, P., Juhlin, C., 2017. The derivation of an anisotropic velocity model from a combined surface and borehole seismic survey in crystalline environment at the COSC-1 borehole, central Sweden. *Geophysical Journal International*, 210, 1332-1346.

IODP

New insights into the Neogene evolution of the Australian Monsoon from IODP Expedition 363 “Western Pacific Warm Pool”

D. ELSNER¹, S. BEIL¹, J. JOHNNCK¹, J. LÜBBERS¹, A. HOLBOURN¹,
 W. KUHN¹, Y. ROSENTHAL², D. KULHANEK³
 AND EXPEDITION 363 SCIENTISTS

¹Institute of Geosciences, Christian-Albrechts-University, 24118 Kiel, Germany.

²Department of Marine and Coastal Services, Rutgers, The State University of New Jersey, New Brunswick NJ 08901-8521, USA.

³International Ocean Discovery Program, Texas A&M University, College Station TX 77845, USA.

Pre-Quaternary records of the Australian monsoon are extremely scarce and little is known about the timing of the onset of modern patterns of rainfall seasonality. Specifically, the sensitivity of the Australian monsoon to changing climate boundary conditions such as global ice volume and greenhouse gas concentrations, the response to changes in interhemispheric thermal asymmetry as well as the dynamic cross-equatorial coupling with the Indo-Asian monsoon remain highly enigmatic. During IODP Expedition 363, two extended (sedimentation rate: ~6 cm/ky at Site U1482 and ~10 cm/ky at Site U1483), undisturbed hemipelagic successions spanning the late Miocene to Holocene were retrieved from the NW Australian continental margin, at the southwestern edge of the present day Western Pacific Warm Pool (Rosenthal, Holbourn, Kulhanek et al., 2016). These carbonate- and clay-rich sequences are ideal to chart the monsoon’s evolution through several episodes of fundamental climate re-organization that were driven by internal changes in the response of the ocean/climate system and/or by changes in external forcing. The late Miocene to Pliocene interval and the Mid-Pleistocene Transition offer, in particular, a challenging opportunity to explore climate-carbon cycle dynamics on a warmer-than-present Earth, thus, helping to guide models and constrain predictions of climate change and sensitivity. The U1482 and U1483 records will additionally shed light on the temporal and regional coupling between different monsoon subsystems, including the timing of major re-organizations in wind (driving upwelling and productivity) and precipitation

(salinity and terrigenous runoff) patterns. These records will provide a Southern Hemisphere perspective, complementing the overarching goal of several recent IODP expeditions to unravel the Neogene evolution and variability of Indo-Asian-Australian monsoon subsystems over multiple timescales.

Preliminary results at Site U1482 (15°3.32'S, 120°26.10'E, water depth: 1466 m), based on XRF-scanning terrigenous runoff proxy and grain size data over the interval 523 to 208 m ccsf (~8.6 to 4.4 Ma) reveal a major climate shift at ~7 Ma from an obliquity-controlled phase of precipitation and terrestrial runoff to a more seasonal monsoonal regime paced by precession, which lasted until ~5 Ma and coincided with a period of global climate cooling and drying (Herbert et al., 2016). This was followed by a massive intensification in terrestrial runoff during the early Pliocene warm period (~5 to 4.4 Ma) during an interval of global warmth, characterized by a reduced latitudinal temperature contrast and prominent 41-kyr climate rhythms. We are currently developing an orbitally-tuned age model at Site U1482 (based on high-resolution benthic $d^{18}O$ records) and will then integrate our XRF-derived runoff records with sea surface temperature and salinity reconstructions (based on planktic foraminiferal stable isotopes and Mg/Ca) to comprehensively explore relationships between regional rainfall patterns, high-latitude climate variations and eastern Indian Ocean surface hydrology. We will extend these analyses to the base of the core (604 m ccsf) to obtain a continuous climate record back to -10.7 Ma.

References:

- Herbert, T. D., Lawrence, K. T., Tzanova, A., Peterson, L. C., Caballero-Gill, R., & Kelly, C. S. (2016). Late Miocene global cooling and the rise of modern ecosystems. *Nature Geoscience*, 9(11), 843-847.
- Rosenthal, Y., Holbourn, A.E., Kulhanek, D.K., and the Expedition 363 Scientists, 2017. Expedition 363 Preliminary Report: Western Pacific Warm Pool. International Ocean Discovery Program. <http://dx.doi.org/10.14379/iodp.pr.363.2017>.

ICDP

Large-scale geoelectrical survey in the Eger Rift zone (W-Bohemia) at a proposed PIER-ICDP fluid monitoring drill site to image fluid-related conductivity structures

C. FLECHSIG¹, T. GÜNTHER², T. NICKSCHICK¹

¹ Institut für Geophysik und Geologie, Universität Leipzig, Talstraße 35, 04103 Leipzig

² Leibniz-Institut für Angewandte Geophysik, Stilleweg 2, 30655 Hannover

The NW-Bohemia/Vogtland region is an intra-continental non-volcanic region and is characterized by outstanding geodynamic activities, which result in earthquake swarms and significant CO₂ emanations. Because of these phenomena, the Eger Rift area is a unique site for interdisciplinary drilling programs to study the fluid-earthquake interaction. The ICDP project PIER (Probing of Intra-continental magmatic activity: drilling the Eger Rift) will set up an observatory, consisting of five monitoring boreholes (Dahm et al., 2013).

In preparation for one major drill, a large-scale geoelectric survey has been carried out to characterize the projected fluid-monitoring drill site at the CO₂ degassing mofette field near Hartoušov, Czech Republic. We used the dipole-dipole configuration (CC-PP). Non-polarizable Cu/CuSO₄ and Ag/AgCl electrodes were used as potential probes. Transmitter and receiver units were physically separated. The transmitter generates the artificial electric field and synchronized automatic

data recorders collect the readings of the observed voltage at the remote receiving dipole. To record the data, 24 single channel transient recorders REFTEK Texan 125 and ten 3-channel custom data loggers from LIAG were used in the experiment.

The profile, measured in late June of 2016 by LIAG Hannover and Leipzig university, features a total length of about 6.5 km (see Fig. 1). The central part around the Hartoušov mofette field consists of 33 electrode pairs with a spacing of 100 m each. The outer parts consist of an additional ten and eleven electrode pairs of 150 m spacing in the west and east, respectively. A total of 47 current injections, using two high-voltage transmitter were realized during the survey.

Data analysis and processing of the recorded signals after extracting the significant injection time sections from the whole time series, included drift correction and low pass filtering and was performed in order to minimize the influences of industrial and cultural noise. Selective stacking was applied to improve the signal quality by reducing incoherent noise for all data sets. Additionally, recorded signals were exemplarily analyzed using a Lock-In approach and a Fast Fourier Transformation approach (FFT), according to Oppermann and Günther (in review).

The quality of the data can be described as good (Fig 1.), only few datasets with very large spacings between injection and potential measurements were disturbed by noise, especially near the small village Kacerov in the east. As a next step, we will invert the data and carry out the next planned survey about 5 km north of this profile. Integration of data from other sources (magnetotelluric data from U. Weckmann, GFZ; seismic data from S. Buske, TU Freiberg, borehole and geologic data) and modelling will allow an investigation of the subsurface below the fluid system to a depth of about 500-700m.

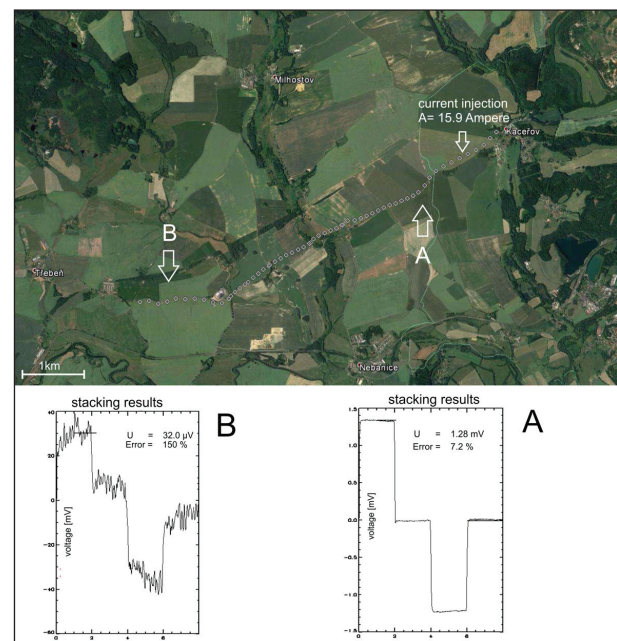


Fig. 1: Location and data processing results of the 6.5 km large-scale geoelectric survey. The signal can be traced over the whole profile length after applying filtering and stacking algorithms A and B mark two respective voltages from the current injection in the east.

References:

- Oppermann, F., Günther, T.: A remote-control datalogger for large-scale resistivity surveys and robust processing of its signals using a software Lock-In approach, *Geosci. Instrum. Method. Data Syst. Discuss.*, <https://doi.org/10.5194/gi-2017-37>, in review, 2017.
- Dahm, T., Hrubcova, P., Fischer, T., Horálek, J., Buske, S., Wagner, S., 2013. Eger Rift ICDP: An observatory for the study of non-volcanic, midcrustal earthquake swarms and accompanying phenomena. *Scientific drilling* 16, 93-99.

ICDP

Authigenic minerals in the HSPDP-Chew Bahir sediment cores (southern Ethiopia): Using mineral alteration as sensitive paleoclimate proxy

V. E. FOERSTER¹, A. ASRAT², A. S. COHEN³, D. M. DEOCAMPO⁴, A. DEINO⁵, W. DÜSING⁶, C. GÜNTHER⁶, H. KRÄMER⁶, H. F. LAMB⁷, S. OPITZ⁸, H. M. ROBERTS⁷, F. SCHAEBITZ¹, M. H. TRAUTH⁶ & HSPDP SCIENCE TEAM

¹University of Cologne, Institute of Geography Education, Cologne Germany

²Addis Ababa University, School of Earth Sciences, Addis Ababa, Ethiopia

³University of Arizona, Department of Geosciences, Tucson AZ, USA

⁴Georgia State University, Department of Geosciences, Atlanta, USA

⁵Berkeley Geochronology Center, Berkeley, USA

⁶University of Potsdam, Institute of Earth and Environmental Science, Potsdam, Germany

⁷Aberystwyth University, Department of Geography and Earth Sciences, Aberystwyth, UK

⁸University of Cologne, Institute of Geography, Cologne, Germany

Through Continental Scientific Drilling, six sites in Ethiopia and Kenya, all adjacent to key paleoanthropological sites have been investigated as part of the Hominin Sites and Paleolakes Drilling Project (HSPDP), aiming at an enhanced understanding of climatic influences on human physical and cultural evolution. Together the sites cover the last ~3.5 Ma of climate change. Initial results show that sediment core records archive environmental change during diverse milestones in human evolution, and times of dispersal and technological and cultural innovation. The 280 m-long Chew Bahir lacustrine record, recovered from a tectonically-bound basin in the southern Ethiopian rift in late 2014, covers the past ~550 ka of environmental history, a time period that includes the transition to the Middle Stone Age, and the origin and dispersal of modern *Homo sapiens*.

To develop a continuous climate history based on sediment core composition is challenging due to the complex relationship between climate and sedimentary deposits. Our composite core record represents >90% recovery, verified through multi-proxy inter-core correlation, together with high-resolution μ XRF, XRD, and sedimentological data. Initial results suggest mineralogical and geochemical proxies are potential climate indicators of wet, dry and hyper-arid climate intervals. Mineral assemblages include salinity indicators such as zeolitic alteration and authigenic clay minerals. Understanding and determining the degree of authigenic mineral alteration in the Chew Bahir records will enable interpretation of μ XRF-derived proxies (e.g. K indicating aridity), and provide direct paleohydrologic data. The high quality geochronology, nearly continuous record, and our growing understanding of site-specific proxy formation will provide a robust environmental history on decadal to orbital timescales. This will enable us to test current hypotheses of the impact of climate change and variability on human evolution and dispersal.

ICDP

Methanogenesis predominated microbial organic matter mineralization in the ferruginous sediments of Earth's early oceans

A. FRIESE¹, J. KALLMEYER¹, C. GLOMITZA^{2,3}, A. VUILLEMIN^{1,4}, R. SIMISTER⁵, S. NOMOSATRYO^{1,7}, K. BAUER⁵, V. B. HEUER⁶, C. HENNY⁷, S. A. CROWE⁵, D. ARIZTEGUI⁸, S. BIJAKSANA⁹, H. VOGEL¹⁰, M. MELLES¹¹, J. M. RUSSELL¹², D. WAGNER¹ AND THE TOWUTI DRILLING PROJECT SCIENCE TEAM

¹GFZ German Research Centre For Geosciences, Section 5.3. Geomicrobiology, D-14473 Potsdam, Germany

²NASA Ames Research Center, Mofett Field, CA, USA

³Center For Geomicrobiology, Aarhus University, Denmark

⁴Ludwig-Maximilians-Universität München, Department of Earth&Environmental Sciences, Paleontology & Geobiology, Munich, Germany

⁵Department of Microbiology & Immunology and Department of Earth, Ocean, and Atmospheric Sciences, University of British Columbia,

Vancouver, Canada

⁶MARUM – Center for Marine Environmental Sciences, University of Bremen, Leobener Str. 8, 28359 Bremen, Germany

⁷Research Center for Limnology, Indonesian Institute of Sciences

⁸Department of Earth Sciences, University of Geneva, rue des Maraichers 13, 1205 Geneva, Switzerland

⁹Faculty of Mining and Petroleum Engineering, Institut Teknologi Bandung, Jl. Ganesha 10, 40132 Bandung, Jawa Barat, Indonesia

¹⁰Institute of Geological Sciences & Oeschger Centre for Climate Change Research, University of Bern, Baltzerstrasse 1-3, 3012 Bern, Switzerland

¹¹Institute of Geology and Mineralogy, University of Cologne, Zùlpicher Str. 49a, D-50674 Cologne, Germany

¹²Department of Earth, Environmental, and Planetary Sciences, Brown University, 85 Waterman Street, Providence, RI, USA

Lake Towuti is a tropical, weakly stratified, 200m deep tectonic lake, with anoxic conditions below 130m water depth. Its catchment is mainly composed of ultramafic rocks and lateritic soils. As a result Lake Towuti sediment is Fe-rich and can contain more than 20 weight percent iron(oxy)hydroxides. Sulfate concentrations in the anoxic bottom water and at the sediment water interface are exceptionally low (<20 μ M). Such physical and chemical characteristics lead to a depositional environment partly analogous to those of the ferruginous oceans that persisted throughout the Precambrian eons. Even though these conditions prevailed through much of Earth's history, models of the biogeochemical processes that occurred under these conditions remain largely conceptual, as modern analogue environments are rare. In spring 2015 the Towuti Drilling Project retrieved a ~115 m long sediment core for geomicrobiological investigations. We characterized the biogeochemistry of this ferruginous environment by analyzing cat- and anions dissolved in the pore water and by modeling net reaction rates of elements and compounds involved in microbial organic matter degradation. We further analyzed the concentration and isotopic composition of pore water methane and quantified the total microbial abundance in the sediment.

Lake Towuti's sediment has low concentrations of the electron acceptors nitrate and sulfate. Total microbial abundance in Lake Towuti sediment is relatively high and decreases from 10⁸ cells cm⁻³ at the top of the core to 10⁵ cells cm⁻³ at ~50m and remains constant below. Given the lack of nitrate and sulfate we suggest that the high microbial abundance is supported by metabolisms like fermentation and methanogenesis. Methane accumulates to ~200 μ M over the upper 20 m and appears to remain constant below this depth, even though there is substantial variability that comes from sediment degassing due to pressure loss after core retrieval. Despite relatively high total

iron concentrations in Lake Towuti's sediment, modeled rates of methanogenesis exceeded those of all other metabolisms considered, indicating that methanogenesis is the dominant process in microbial organic matter degradation. This implies that microbes do not readily utilize the iron that is present in minerals; together with the scarcity of sulfate and lack of nitrate this likely indicates that there is no appreciable anaerobic oxidation of methane (AOM). The $\delta^{13}\text{C}$ values of CH_4 in Lake Towuti sediment range from -73 ‰ to -64 ‰ whereas $\delta\text{D}_{\text{CH}_4}$ values are very heavy with values between -176 ‰ and -160 ‰. Such isotopic compositions are characteristic for hydrogenotrophic methanogenesis but do not rule out a contribution from acetoclastic or methylotrophic methanogens. The prevalence of methanogenesis even in this very iron-rich modern environment implies that methanogenesis may play an important role in biogeochemical cycling in ferruginous environments more broadly including in the oceans of the Precambrian eons.

IODP

The Opening of the Arctic-Atlantic Gateway: Tectonic, Oceanographic and Climatic Dynamics – Status of the IODP Initiative

W. H. GEISSLER¹, J. KNIES^{2,3}, J. MATTHIESSEN¹, A. C. GEBHARDT¹, C. VOGT⁴

¹Alfred Wegener Institute Helmholtz Centre for Polar and Marine Research, 27568 Bremerhaven, Germany

²Geological Survey of Norway, 7491 Trondheim, Norway

³Centre for Arctic Gas Hydrate, Environment and Climate, University of Tromsø, 9037 Tromsø, Norway

⁴Crystallography, Geosciences, University of Bremen, 28334 Bremen, Germany

The modern polar cryosphere reflects an extreme climate state with profound temperature gradients towards high-latitudes. It developed in association with stepwise Cenozoic cooling, beginning with ephemeral glaciations and the appearance of sea ice in the late middle Eocene. The polar ocean gateways played a pivotal role in changing the polar and global climate, along with declining greenhouse gas levels. The Arctic Ocean was an isolated basin until the early Miocene when rifting and subsequent sea-floor spreading started between Greenland and Svalbard, initiating the opening of the Fram Strait / Arctic-Atlantic Gateway (AAG). Although this gateway is known to be important in Earth's past and modern climate, little is known about its Cenozoic development. The opening history and AAG's consecutive widening and deepening must have had a strong impact on circulation and water mass exchange between the Arctic and the North Atlantic Oceans. To study the AAG's complete history, ocean drilling sites in the Boreas Basin and along the East Greenland continental margin are proposed. These sites will provide unprecedented sedimentary records that will unveil the history of shallow-water exchange between the Arctic and the North Atlantic Oceans, and the development of the AAG to a deep-water connection and its influence on the global climate system.

Getting a continuous record of the Cenozoic sedimentary succession that recorded the evolution of the Arctic-North Atlantic horizontal and vertical motions, and land and water connections will also help better understanding the post-breakup evolution of the NE Atlantic conjugate margins and associated sedimentary basins.

IODP

The Indian-Atlantic Ocean gateway during the Pliocene: current dynamics and changing sediment provenance

J. GRÜTZNER¹, G. UENZELMANN-NEBEN¹, I. A. HALL²

¹Alfred-Wegener-Institut, Helmholtz-Zentrum für Polar- und Meeresforschung, Bremerhaven, Germany

²School of Earth and Ocean Sciences, Cardiff University, Cardiff, United Kingdom

The Pliocene epoch represents a discrete interval which reversed a long-term trend of late Neogene cooling and is also the most recent geological interval in which global temperatures were several degrees warmer than today. It is therefore often considered as the best analogue for a future anthropogenic greenhouse world. However, there is growing evidence that the Pliocene was not a stable period but can rather be subdivided in several distinct climate phases. Our understanding of Pliocene climate variability in the Southern Hemisphere, and especially in the Atlantic-Indian ocean gateway, is limited by scarce marine records and poor age control on existing terrestrial climate archives. At five drilling locations IODP Exp. 361 recovered high resolution complete late Miocene to Pleistocene sections (Hall et al., 2017). Our research proposal is based on the Sites U1474 (Natal Valley), U1475 (Agulhas Plateau), and U1479 (Cape Basin) forming a latitudinal transect. The main focus is on the interplay between northern and southern sourced deep water masses in the Atlantic-/Indian Ocean gateway during the Pliocene and combines chemical, physical property and seismic methods. Our research is driven by three working hypotheses:

Seismic stratigraphies for the last 6 Ma and sediment drift growth in the Atlantic-Indian gateway are mainly controlled by bottom water flow changes

Using the sediment archives and physical property records from IODP Exp. 361 (Hall et al., 2017) we aim to construct and compare detailed seismic stratigraphies for the Agulhas Plateau, the Natal valley and the Cape basin for the last 6 Ma. At all Exp. 361 sites *P*-wave velocity and density records enable detailed correlations of drilling results and site survey data through the calculation of synthetic seismograms. Our working hypothesis implies that seismic reflection patterns and sediment accumulation during the Pliocene are closely linked to deep water circulation changes associated with climate Pliocene phases. Furthermore four distinct high latitude Pliocene glaciation events have been identified. We speculate that these phases and events have led to deep water circulation changes in Agulhas region, have altered the sediment physical properties and thus may be recognized as reflectors in the seismic profiles. How did the sediment input of terrigenous vs. biogenic sediment components in the gateway change during these events? Are these changes driven by dilution, dissolution, or productivity? We strive to answer these questions by interpreting edited and in-situ corrected physical core scanning records in combination major element variability derived from post cruise XRF-scanning.

Trajectories and intensities of deep water masses in the Agulhas region during the Pliocene were influenced by Antarctic ice volume rather than by the closure of the Central American Seaway.

The Exp. 361 drill sites offer the possibility to inter-correlate different flow speed proxies and to derive a detailed picture of flow changes during the Pliocene. By comparing core-measurements of sortable silt (SS), physical properties and XRF-core scanning data with seismic features we will tie the major

flow speed changes to our seismic grid covering the Agulhas Plateau such that changing current intensities and pathways can be mapped together. Here we hypothesize that these changes are mainly driven by climate (Antarctic ice volume). How have the sedimentation patterns changed under the growing influence of North Atlantic Deep Water (NADW) during the Pliocene? What were the main changes associated with the instability of Antarctic ice sheets and was the production of Antarctic Bottom Water (AABW) reduced or enhanced during these intervals? Was there also a potential influence of tectonic processes on the flow changes in the Agulhas region? Especially the closure of the Central American Seaway (CAS) in various phases between ~14 and ~2.7 Ma is thought to have had a profound impact on climate.

Changes in physical and chemical sediment properties in the Agulhas region are largely controlled by earth's orbital variations and allow a significant improvement of age models by cyclostratigraphy.

Another primary objective of our research is the detection and characterization of orbital and sub-orbital cycles in the Agulhas sedimentary environment in relation to paleoceanographic changes. The presence of orbital cycles in ocean sediments has widely been used to derive high resolution age models in Cenozoic sediments. Typically orbital chronologies are based on benthic oxygen isotope records ($d^{18}O$) that are correlated to astronomical forcing functions ("orbital tuning"). However, the generation of such records at high resolution over long time intervals is time consuming and will likely not be completed for the Exp. 361 sites over the next years. In the absence of $d^{18}O$ records cyclic changes in high resolution measurements of physical (e.g. density, colour reflectance, magnetic susceptibility) and chemical (major elements from XRF core scanning) parameters have been successfully used for orbital tuning. At the Exp. 361 Sites very regular cyclic amplitude changes are evident in the Pliocene sections (Gruetzner et al., 2017), but up to now have not been further investigated. Which orbital frequency do these cycles represent and how do the dominant frequencies change over time? What is the potential of the observed cycles for stratigraphic purposes? We will analyse those cyclicities in the depth and time domain and strive to generate orbitally tuned time series of sediment provenance.

References:

- Gruetzner, J., Lathika, N., Jiménez-Espejo, F., Uenzelmann-Neben, G., IODP Exp. 361 Scientific Party Team, 2017. Changing sediment physical properties at the Agulhas Plateau (IODP Site U1475): indications for the long-term variability of deepwater circulation over the last 7 Ma, EGU General Assembly 2017, Vienna, Austria, hdl:10013/epic.50654.d001
- Hall, I.R., Hemming, S.R., LeVay, L.J., and the Expedition 361 Scientists, 2017. *South African Climates (Agulhas LGM Density Profile)*. Proceedings of the International Ocean Discovery Program, 361: College Station, TX (International Ocean Discovery Program). <http://dx.doi.org/10.14379/iodp.proc.361.2017>

IODP

A new seismic stratigraphy for the Agulhas Plateau resembles major paleo-oceanographic changes in the Indian-Atlantic Ocean gateway since the late Miocene

J. GRUETZNER¹, F. J. JIMENEZ ESPEJO², N. LATHIKA³,
 G. UENZELMANN-NEBEN¹

¹Alfred-Wegener-Institut, Helmholtz-Zentrum für Polar- und Meeresforschung, Bremerhaven, Germany

²Institute of Biogeosciences, Japan Agency for Marine-Earth Science and Technology (JAMSTEC), Yokosuka, Japan

³Ice Core Laboratory, National Centre for Antarctic and Ocean Research (NCAOR), Vasco-da-Gama, Goa, India

The exchange of shallow and deep water masses between the Indian Ocean and the Atlantic constitutes an integral inter-ocean link in the global thermohaline circulation. In the gateway south of South Africa long-term changes in deep water flow during the Cenozoic have been initially studied using seismic reflection profiles. But the seismic stratigraphy was poorly constrained and not further resolved within the time period from the late Miocene to present. In particular, there were limited Pliocene records that could be used to investigate the influence of climatic (e.g. Antarctic ice volume) and tectonic (e.g. closure of the Central American seaway) on the deep-water variability. In 2016 the International Ocean Discovery Program (IODP) Expedition 361 ("SAFARI") recovered complete high-resolution Plio-/Pleistocene sediment sections at six drilling locations on the southeast African margin and in the Indian-Atlantic ocean gateway (Gruetzner et al., 2017). Here, we present results from Site U1475 (Agulhas Plateau), a location proximal to the entrance of North Atlantic Deep Water (NADW) to the Southern Ocean and South Indian Ocean (Hall et al., 2017). The site is located over a sediment drift in 2669 m water depth and comprises a complete carbonate rich (74 – 85%) stratigraphic section of the last ~7 Ma. We edited high-resolution data sets of density, velocity and natural gamma radiation measured at Site U1475 and corrected them to in-situ conditions. Cross correlations show that acoustic impedance contrasts and thus the formation of seismic reflectors are mainly due to density changes that are caused by climate-induced variations in biogenic vs. terrigenous sediment input. The calculated synthetic seismograms show an excellent correlation of drilling results with the site survey seismic field record, provide an accurate traveltime to depth conversion, and allow preliminary age assignments (± 0.3 Ma) based on the shipboard bio- and magnetostratigraphy. The most prominent reflectors are associated with compositional changes related to late Pleistocene glacial/interglacial variability, the middle Pleistocene transition, and the onset of the northern hemisphere glaciation. Furthermore, a peculiar early Pliocene interval (~ 5.3 – 4.0 Ma) bounded by two reflectors is characterized by 3-fold elevated sedimentation rates (> 10 cm/ka) and the occurrence of sediment waves. We argue that this enhanced sediment transport to the Agulhas Plateau was caused by a reorganization of the bottom current circulation pattern due to maximized inflow of NADW. Rhythmic bedding within the Pliocene sediment wave sequence likely reflects the 100-kyr orbital cycle. On the other hand, colour reflectance and natural gamma radiation show highest variability in the precession band. The very regular response of the core logging data to orbital forcing suggests that the shipboard age model can be significantly improved by cyclostratigraphy.

References:

- Gruetzner, J., Just, J., Koutsodendris, A., Tanguan, D., Hall, I.R., Hemming, S.R., LeVay, L.J., and the Expedition 361 Scientists, 2017. IODP Expedition 361 – Southern African Climates and Agulhas LGM Density Profile, Gemeinsames Kolloquium - DFG-Schwerpunktprogramme ICDP (International Continental Scientific Drilling Program) und IODP (International Ocean Discovery Program), Braunschweig.
- Hall, I.R., Hemming, S.R., LeVay, L.J., Barker, S., Berke, M.A., Brentegani, L., Caley, T., Cartagena-Sierra, A., Charles, C.D., Coenen, J.J., Crespin, J.G., Franzese, A.M., Gruetzner, J., Han, X., Hines, S.K.V., Jimenez Espejo, F.J., Just, J., Koutsodendris, A., Kubota, K., Lathika, N., Norris, R.D., Periera dos Santos, T., Robinson, R., Rolinson, J.M., Simon, M.H., Tanguan, D., van der Lubbe, J.J.L., Yamane, M., Zhang, H., 2017b. Site U1475, in: Hall, I.R., Hemming, S.R., LeVay, L.J., and the Expedition 361 Scientists (Ed.), South African Climates (Agulhas LGM Density Profile), Proceedings of the International Ocean Discovery Program, 361. International Ocean Discovery Program, College Station, TX.

IODP

Pliocene variability of Mediterranean–Atlantic exchange

P. GRUNERT¹, Á. GARCÍA-GALLARDO², B. BALESTRA³, C. RICHTER⁴,
G. AUER⁵, M. VAN DER SCHEE⁶, J.-A. FLORES⁶, F. J. SIERRO⁶,
F. JIMÉNEZ-ESPEJO⁵, C. ALVAREZ ZARIKIAN⁷, U. RÖHL⁸, A. BAHR⁹,
S. KABOTH⁹,
W. E. PILLER²

- ¹ Institute of Geology and Mineralogy, University of Cologne, Zùlpicher StraÙ 49a, 50674 Cologne, Germany
- ² Institute of Earth Sciences, University of Graz, NAWI Graz, Heinrichstrasse 26, 8010 Graz, Austria
- ³ Institute of Marine Sciences, University of California Santa Cruz, United States of America
- ⁴ School of Geosciences, University of Louisiana at Lafayette, United States of America
- ⁵ Department of Biogeochemistry, Japan Agency for Marine–Earth Science and Technology (JAMSTEC), Yokosuka, Japan
- ⁶ Department of Geology, University of Salamanca, Spain
- ⁷ International Ocean Discovery Program, Texas A&M University, College Station, TX 77845, United States of America
- ⁸ MARUM – Center for Marine Environmental Sciences, University of Bremen, Germany
- ⁹ Institute of Geoscience, University of Heidelberg, Im Neuenheimer Feld 234, 69120 Heidelberg, Germany

The opening of the Gibraltar Strait at 5.3 Ma ago marked the beginning of renewed water mass exchange between the Mediterranean Sea and the Atlantic Ocean. Mediterranean Outflow Water (MOW) is a considerable source of heat and salt for today's North Atlantic and is considered to contribute to maintaining the Atlantic meridional overturning circulation (AMOC). There is evidence that MOW intensity varied on glacial/interglacial and stadial/interstadial timescales in the past, and that phases of MOW intensification potentially preconditioned thermohaline circulation for its interglacial mode in the late Pleistocene. Until recently, however, efforts towards a better understanding of MOW behavior through time and potential climatic feedback mechanisms between MOW, the African Monsoon, AMOC, and eustatic sea-level fluctuations have been impeded by the limitation of available sample material largely to the uppermost Pleistocene and Holocene. In 2011/12, IODP Expedition 339 drilled several sites in the Gulf of Cadiz and off the western Iberian Margin, recovering a total of 4.5 km of Pliocene to Holocene contouritic deposits of MOW.

In this paper, we summarize new findings on early MOW history and Mediterranean–Atlantic exchange from IODP Sites U1387 and U1389, specifically its onset after the Messinian Salinity Crisis and its behavior at the transition from the Pliocene warmhouse to Pleistocene icehouse climate. Micropalaeontological and geochemical data suggest that Mediterranean water

reached IODP Site U1387 shortly after the opening of the Gibraltar Strait and before the onset of contourite drift deposition, representing the first indications of Mediterranean–Atlantic exchange (García Gallardo et al., 2017). At IODP Site U1389, a refined age model for the time interval between 3.6 and 2.5 Myrs allows the evaluation of long- and short-term trends in data from XRF core-scanning and stable isotope analyses, and their comparison to proxy records from the Mediterranean and North Atlantic (Grunert et al., 2017). Cyclostratigraphic analysis of Zr/Al records and grain-size data in well-recovered intervals suggest that the long-term strengthening of MOW at the onset of Northern Hemisphere Glaciation is punctuated by a strong precessional control on bottom current strength. Intensified Mediterranean–Atlantic exchange is further indicated by flat gradients of planktic $\delta^{18}\text{O}$ for the severe glacial Marine Isotope Stage (MIS) M2 and the initiation of the NHG (MIS G22, G14, G6–104) (García Gallardo et al., under review). These periods correlate with the occurrence of ice-rafted debris (IRD) at low latitudes and weakening of the Atlantic Meridional Overturning Circulation (AMOC). Our results may thus suggest the development of a negative feedback between AMOC and exchange rates at the Strait of Gibraltar in the latest Pliocene as it has been proposed for the late Quaternary.

Research for this study was funded through project P25831-N29 of the Austrian Science Fund FWF (2013–2017), ECORD (2014) and the Max Kade Foundation (2014–2015).

References:

- García Gallardo, A., Grunert, P., Van der Schee, M., Sierro, F.J., Jiménez-Espejo, F.J., Alvarez-Zarikian, C.A., Piller, W.E., 2017. Benthic foraminifera-based reconstruction of the first Mediterranean–Atlantic exchange in the early Pliocene Gulf of Cadiz. *Palaeogeography, Palaeoclimatology, Palaeoecology* 472, 93–107. <https://doi.org/10.1016/j.palaeo.2017.02.009>.
- García Gallardo, A., Grunert, P., Piller, W.E., under review. Variations of Mediterranean–Atlantic exchange across the late Pliocene climate transition. *Climate of the Past*, discussion paper. <https://doi.org/10.5194/cp-2017-134>.
- Grunert, P., Balestra, B., Richter, C., Flores, J.-A., Auer, G., García Gallardo, A., Piller, W.E., 2017. Revised and refined age model for the upper Pliocene of IODP Site U1389 (IODP Expedition 339, Gulf of Cadiz). *Newsletters on Stratigraphy*. <https://doi.org/10.1127/nos/2017/0396>.

IODP

Late Quaternary palaeoenvironmental dynamics inferred from marine sediment cores of the western South Atlantic

F. GU¹, K. A. F. ZONNEVELD², C. M. CHIESSI³, H. W. ARZ⁴, J. PATZOLD²,
H. BEHLING¹

- ¹University of Goettingen, Department of Palynology and Climate Dynamics, Untere Karspùle 2, 37073 Göttingen, Germany,
- ²University of Bremen, MARUM – Center for Marine Environmental Sciences, Leobener Str. 8, 28359 Bremen, Germany
- ³University of São Paulo, School of Arts, Sciences and Humanities, Rua Arlindo Bettio, 1000, CEP03828-000 São Paulo, SP, Brazil
- ⁴Leibniz Institute for Baltic Sea Research Warnemünde (IOW), Marine Geology Department, SeestraÙe 15, 18119 Rostock-Warnemünde, Germany

1400 km long transect have been studied by pollen, spores, fresh water algae and dinoflagellate cysts to reconstruct vegetation, climate and ocean environmental dynamics since the early last glacial period.

During glacial times, in particular during the last glacial maximum (LGM), grassland was the dominant vegetation in southeastern South America, indicating cold and dry climatic conditions. *Araucaria* trees were relatively frequent on the southern Brazilian highland between 73.5 and 65 cal kyr BP, similar to the late Holocene, suggesting not so cold and dry

climatic conditions. The Atlantic rainforest started to expand in northern South Brazil at 14 cal kyr BP while in southern South Brazil the stronger expansion to the south occurred due to wetter conditions after 5 cal kyr BP.

The dinoflagellate cysts indicate the stronger presence of warm surface water of the Brazil Current since 15 cal kyr BP in the northern South Brazil and since 9 cal kyr BP in the southern South Brazil.

Dinocysts suggests that cold water masses transported by the sub-polar Malvinas Current and Brazil Coastal Current had a markedly stronger influence during the glacial period, in particular during the LGM period. The occurrence of *Nothofagus* pollen in the marine cores, which derived from the southern South America, suggests an efficient transport by the southern westerlies and Argentinean rivers, then by the Malvinas Current and finally by the BCC to the study sites.

Studies on the three marine sediment cores contributes to a better understanding of vegetation dynamics, climate change, marine surface water and ocean current changes in southeastern South America over long time periods.

References:

- Gu F, Zonneveld KA, Chiessi CM, Arz HW, Pätzold J, Behling H. 2017. Long-term vegetation, climate and ocean dynamics inferred from a 73,500 years old marine sediment core (GeoB2107-3) off southern Brazil. *Quaternary Science Reviews*, 172: 55-71.
- Gu F, Chiessi CM, Zonneveld KA, Behling H. 2018. Late Quaternary environmental dynamics inferred from marine sediment core GeoB6211-2 off southern South Brazil. *Palaeogeography, Palaeoclimatology, Palaeoecology*, (accepted).

IODP

Incorporation of Ca and Sr isotopes in scleractinian corals from culture experiments and the Great Barrier Reef

N. GUSSONE¹, M. INOUE^{1,2}, Y. YOKOYAMA³, A. SUZUKI⁴, H. KAWAHATA³, S. GALER⁵,

¹Institut für Mineralogie, Westfälische-Wilhelms-Universität Münster, Germany

²Graduate School of Natural Science and Technology, Okayama University, 3-1-1 Tsushima-naka, Okayama 700-8530, Japan

³Atmosphere and Ocean Research Institute, The University of Tokyo, 5-1-5 Kashiwanoha, Kashiwa, Chiba 277-8564, Japan

⁴Geological Survey of Japan, National Institute of Advanced Industrial Science and Technology (AIST), 1-1-1 Higashi Tsukuba, AIST Tsukuba Central 7, Ibaraki 305-8567, Japan

⁵Max-Planck-Institut für Chemie, Hahn-Meitner-Weg 1, 55128 Mainz

Scleractinian reef corals play an important role within the System Earth and for unraveling past changes in climate dynamics. As one of the main producers of continental shelf carbonates, coral growth is of great relevance, because of their social-economic importance e.g. in coastal protection, as they can stabilize shore areas, and because of their great potential as recorder for paleoclimatic information. Several geochemical and isotopic proxies, such as Sr/Ca or oxygen isotope ratios have been developed and successfully applied for temperature and salinity reconstructions on coral material. For instance, paleoenvironmental fluctuations during the last glacial termination have been reconstructed with fossil *Porites* corals from Tahiti during IODP Exp. 310 (e.g., Felis et al., 2012). However, corals do not only record changes in the climate system, but due to their large contribution to the oceanic CaCO₃ formation, they are linked to the global C-cycle and thus related to environmental changes. One important parameter affecting the oceanic C chemistry is the Ca concentration of the seawater, as it controls via the CaCO₃ solubility the precipitation of Ca carbonate mi-

nerals, and subsequently the fixation of carbon. During calcium carbonate precipitation, light Ca and Sr isotopes are enriched in the solid phase, leading to a relative enrichment of heavy isotopes in the residual fluid. The Ca and Sr isotopic composition of past seawater, recorded in marine carbonates can therefore be used as tool to reconstruct changes in the oceanic Ca and Sr budgets through time. Following this approach, a careful determination of isotope fractionation of marine biogenic carbonates is necessary to determine the isotopic composition of the sedimentary Ca and Sr output fluxes, as well as for the calculation of the isotopic composition of past seawater from fossil carbonate shells. Because corals belong to the dominant marine CaCO₃ producers, the determination of their isotope fractionation in response to environmental changes, as well as gaining an understanding of the fractionation mechanisms involved in biomineralisation, is of special importance.

Experiments on multiple colonies of *Porites* corals cultured under temperature, pH and light controlled environments that investigated the relationship between $\delta^{44}\text{Ca}$ in coral skeleton grown during the culture period and each environmental parameters, showed that only temperature has a significant effect on the Ca isotope fractionation during coral biomineralisation (Inoue et al. 2015), consistent with observations for other coral species (cf. Böhm et al. 2006). The small temperature sensitivity of 0.02‰/°C observed for the temperature range from 21 to 29°C is similar to inorganic aragonite (Gussone et al. (2003), but the degree of isotope fractionation is about +0.4 ‰ offset in corals relative to inorganic aragonite. $^{88}\text{Sr}/^{86}\text{Sr}$ ratios analysed on these samples do not demonstrate a significant dependence on temperature. Due to coral-specific biomineralization processes, the overall mean $\delta^{44}\text{Ca}$ of scleractinian corals including results from previous studies are different from other biogenic aragonites like sponges and pteropods, which resemble inorganic aragonite. Apparently, coral Ca isotope ratios are more similar to those of calcitic coccolithophores, which Ca isotope composition was suggested to be governed by biological fractionation processes. Other factors such as pH (7.4 to 8.0) and photon flux density were shown not to influence the Ca isotopic composition of the coral skeleton (Inoue et al. 2015) or the $^{88}\text{Sr}/^{86}\text{Sr}$ ratio.

To investigate, if the experimentally determined Ca and Sr isotope fractionation characteristics also apply to natural corals from downcore material, we determined Ca and Sr isotope ratios of natural *Acropora* sp. and *Isopora* sp. corals drilled during IODP expedition 325 from the shelf edge seaward of the modern Great Barrier Reef, covering the time between 24 and 11 ka (Yokoyama et al., 2011). Calcium and Sr isotope ratios were determined by TIMS double spike techniques at the University of Münster and MPI Mainz, respectively. Our results show a gradual increasing of $\delta^{44}\text{Ca}$ from the LGM towards the Holocene and no shift in the Sr isotopes. Given the small temperature dependence of Ca isotope fractionation in corals, the temperature rise towards the holocene can account for half the $\delta^{44}\text{Ca}$ increase observed at the Great Barrier Reef. The remaining $\delta^{44}\text{Ca}$ signal can most likely be attributed to $\delta^{44}\text{Ca}$ changes of the local seawater by increased surface or subsurface discharge related to weathering of the exposed carbonate shelf during the LGM. This observation suggests a significant Ca flux to the ocean and points to potential bias in near shore proxy archives.

References:

- Böhm, F., Gussone, N., Eisenhauer, A., Dullo, W.-C., Reynaud, S., Paytan, A. (2006) Calcium Isotope Fractionation in Modern Scleractinian Corals. *Geochimica et Cosmochimica Acta* 70, 4452-4462.
- Felis, T., Merkel, U., Asami, R., et al. (2012) Pronounced interannual variability in tropical South Pacific temperatures during Heinrich Stadial 1. *Nat. Commun.* 3:965, doi: 10.1038/ncomms1973.

Gussone, N., Eisenhauer, A., Heuser, A., Dietzel, M., Bock, B., Böhm, F., Spero, H. J., Lea, D. W., Bijma, J., and Nägler, Th.F. (2003) Model for Kinetic Effects on Calcium Isotope Fractionation ($\delta^{44}\text{Ca}$) in Inorganic Aragonite and Cultured Planktonic Foraminifera. *Geochimica et Cosmochimica Acta* 67 (7) 1375-1382.

Gussone, N., Nehrke, G., Teichert, B.M.A. (2011) Calcium isotope fractionation in ikaite and vaterite. *Chem. Geol.* 285, 194–202.

Inoue, M., Gussone, N., Koga, Y., et al. (2015) Controlling factors of Ca isotope fractionation in scleractinian corals evaluated by temperature, pH and light controlled culture experiments. *Geochim. Cosmochim. Acta*, 167, 80–92.

Yokoyama, Y., Webster, J. M., Cotterill, C., Braga, J. C., Jovane, L., Mills, H., Morgan, S., Suzuki, A. and the IODP Expedition 325 Scientists (2011) IODP Expedition 325: Great Barrier Reefs Reveals Past Sea-Level, Climate and Environmental Changes Since the Last Ice Age. *Scientific Drilling* 12, 32-45. doi:10.2204/iodp.sd.12.04.2011.

ICDP

Towards an ICDP drilling at Lake Nam Co (Tibet)

T. HABERZETTL^{1,2}, G. DAUT¹, T. KASPER¹, N. SCHULZE³, V. SPIESS³, J. WANG⁴, L. ZHU⁴, NAM CO SCIENCE TEAM⁵

¹Physical Geography, Institute of Geography, Friedrich-Schiller-University Jena, Löbdergraben 32, 07743 Jena, Germany

²Physical Geography, Institute of Geography and Geology, University of Greifswald, Friedrich-Ludwig-Jahn Str. 16, 17487 Greifswald, Germany

³Department of Geosciences, University of Bremen, P.O. Box 330440, 28334 Bremen, Germany

⁴Institute of Tibetan Plateau Research, Chinese Academy of Sciences, Beijing 100101, China

⁵Potential Workshop participants listed in approved proposal

Nam Co is one of the largest and deepest lakes on the Tibetan Plateau. Due to this location at the intersection of Monsoon (increased precipitation) and Westerlies (increased evaporation, Fig. 1) paleoclimate proxies derived from sediments of Nam Co clearly reflect the spatial and temporal interplay and thus the dominance of one of the two circulation systems. Considering that almost one third of the population of the world depends on the water supply from the Tibetan Plateau the future hydrological development which is dependent on the interplay of the two systems will clearly have a major societal impact. To define parameters for future climate change scenarios (IPCC) and their consequences for ecosystems, it is of paramount importance to improve our knowledge of timing, duration, and intensity of past climatic variability and environmental impact, especially on long geologic time scales. Situated on the central Tibetan Plateau, Nam Co is also ideally located to fill a gap of missing long-term paleoclimate information in two ICDP/IODP transects (Fig. 1) to allow comparisons of climatic evolution/behavior on a continental scale.

Seismic data show an infill of >800 m of well layered undisturbed sediments in the central part of the lake. Sediment accumulation rates measured on a 10.4 m reference core, seismic stratigraphic investigations, and molecular clock analyses suggest an age of the seismically imaged sequence of >1 Mio years. However, a basement reflector has only been found occasionally indicating even older sequences. Multiproxy studies on the reference core provide an excellent high-resolution paleoclimate record covering the past 24 ka cal BP validated by extensive modern process studies and multi-dating approaches.

Furthermore, the Tibetan Plateau is characterized by a high degree of endemism of organisms that are dependent on continuously existing water bodies. Nam Co likely served as a dispersal centre for these organisms, as other shallower lakes desiccated during dry glacial periods of the Cenozoic. Nam Co appears to be a first class example for studying the link between geological and biological evolution in highly isolated Tibetan

Plateau ecosystems including the deep biosphere over long time scales. A continuous, high-resolution, record for these long time scales from Nam Co will further enable to study sediment budget changes under varying climatic and tectonic settings, and contribute to a better understanding of the Quaternary geomagnetic field.

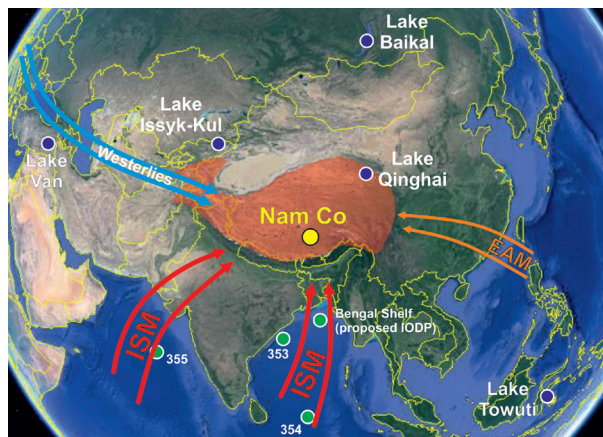


Fig. 1: Strategic location of Nam Co on the Tibetan Plateau (orange) with respect to further potential and drilled ICDP/IODP sites. Numbers represent IODP expeditions, ISM: Indian Summer Monsoon, EAM: East Asian Monsoon. map: Google Earth 2014.

An ICDP workshop was funded and will be held in Beijing from 22 to 24 May 2018. Participants from Canada, China, Denmark, France, Germany, Iceland, India, Israel, Italy, Spain, Switzerland, The Netherlands, UK and USA will bring in their expertise in logistics, seismics, tectonics, drilling, core curation, down-hole logging, various dating methods (incl. ^{14}C -, optical, ^{10}Be -, U-Th- and AAR-dating), chronological modelling, paleomagnetism, environmental magnetism, geochemistry, sedimentology, micropaleontology, palynology, pigments, DNA/RNA analysis, data management as well as outreach. This will be complemented by medical experts interested in high-altitude medicine from the German Aerospace Center (DLR).

IODP

Formation of an Pleistocene aragonite lowstand wedge along the North West Shelf of Australia (NWS), insights from Site U1461 of IODP Expedition 356

M. HALLENBERGER¹, L. REUNING¹, H. IWATANI²

¹Energy and Mineral Resources Group (EMR), Geological Institute, RWTH Aachen University, Aachen, Germany

²School of Biological Sciences, The University of Hong Kong, Hong Kong SAR, China

The widely used “highstand shedding” concept predicts that carbonate production on flat-topped platforms and distally-steepened ramps peak during sea-level highstand when the inner platform is flooded. In contrast, surface-sediment sampling at the distally steepened ramp of the North West Shelf of Australia (NWS) indicate that very little aragonite mud is produced during modern highstand conditions. Instead it has been proposed that considerable amounts of aragonite have been produced during the last glacial maximum forming a regional aragonite lowstand wedge with a volume which could rival typical highstand systems. To test this hypothesis, we investigated the upper 70 m of Site U1461, which has been cored during IODP

Expedition 356, using a combination of geophysical log interpretation, thin-section and SEM petrography, stable oxygen and carbon isotope analysis, and XRD derived mineralogy ($n > 100$). XRD data has been further used to calibrate a nearly continuous XRF-Scan, providing a high resolution record of mineralogical variation (e.g. aragonite).

The investigated section displays a distinct pattern with alternating changes in core color from dark to light. Dark sections are dominated by a calcitic mineralogy and elevated amounts of siliciclastics, while the lighter sections are mainly aragonitic with little to no amounts of siliciclastics. Based on texture the aragonite rich sections are further subdivided into parts which are rich in mud and parts which contain high amounts of non-skeletal grains such as peloids and ooids. Ooids, although not well developed, are a clear indication for a very shallow paleo water depth as well as a high carbonate saturation. They are proposed to have formed during glacials, when elevated aridity and a low sea-level guaranteed favorable conditions for ooid formation along the NWS. The first ooid rich section in particular is thought to have formed during the last glacial maximum (LGM), when a large fall in sea-level (-120 m) brought Site U1461 within very shallow water depths.

Crystal morphology, isotope signatures and mineralogical composition of aragonite micrite indicate formation as a seawater precipitate at times of elevated carbonate saturation. Micrite production and redeposition is therefore proposed to have peaked during sea-level lowstands.

During sea level highstands (i.e. interglacials) a combination of strong riverine input, the unimpeded influence of strong oceanic currents, and a low salinity hindered aragonite production. Instead a calcitic pelagic ooze forms, presently overlying the aragonitic lowstand wedge.

ICDP

Geochemical characterization and genetic interpretation of mass movement deposits at TDP Site 2, Lake Towuti, Indonesia

A. K. M. HASBERG¹, M. MELLES¹, P. HELD¹, V. WENNRICH¹, J. JUST², S. OPITZ³, M. A. MORLOCK⁴, H. VOGEL⁴, J. M. RUSSELL⁵, S. BIJAKSANA⁶
 AND THE ICDP-TDP SCIENTIFIC PARTY

¹Institute of Geology and Mineralogy, University of Cologne, Zùlpicher Str. 49a, 50674 Cologne, Germany

²Geoscience University Bremen, GEO-Building, Klagenfurter Straße, 28359 Bremen, Germany

³Geographical Institute, University of Cologne, Zùlpicher Str. 45, 50674 Cologne, Germany

⁴Institute of Geological Sciences & Oeschger Centre for Climate Change Research, University of Bern, Baltzerstr. 1+3, 3012 Bern, Switzerland

⁵Department of Earth, Environmental, and Planetary Sciences, Brown University, 324 Brook St. BOX, 1846, Providence, RI 02912, USA

⁶Faculty of Mining and Petroleum Engineering, Institut Teknologi Bandung, Jalan Ganesa 10, Bandung, 40291, Indonesia

Within the scope of our DFG funded project “Decadal- to orbital-scale climate variability in the Indo-Pacific Warm Pool during the past ca. 650,000 years” we successfully investigated the tropical Lake Towuti (2.5°S, 121.5°E), which is of tectonically origin and situated on Sulawesi Island (southeastern Indonesia), within the heart of the Indo-Pacific Warm Pool (IPWP). The oligotrophic lake got drilled at three sites by the International Continental Scientific Drilling Program (ICDP) Towuti Drilling Project (TDP) in late spring 2015 with a total sediment core recovery of ~1100 m.

The major aims of the TDP are the reconstructions of: (i) the major climate changes in the region during the past ca. 600 ka, their frequency, and their triggering mechanism, (ii) the development of the lake basin and the hydrological lake history, and (iii) the special faunal and floral Fe-dominated microbiological setting as well as the biological evolution of the dominating endemic flora and fauna. Our part of the project focuses on the development of the lake, especially on the hydrological connectivity of the upstream Lakes Matano and Mahalona via the Petea and Mahalona River to Lake Towuti. Consequently, our analyses focus on TDP Site 2, which is located within the Mahalona River Delta area and in the upper 60 m of the 136 m long drill core contains sediments dominated by mass movement deposits.

Here, we present the results of high-resolution (5 mm) XRF half-core measurements and of wider spaced analyses of the grain-size distribution, the mineralogical composition, and the total organic carbon (TOC), total sulfur (TS), and total nitrogen (TN) concentrations, which were conducted on the composite sediment cores from TDP Sites 2A, B, and C at the laboratories of the University of Cologne (UoC). The data are compared to spectroscopy data measured at the Brown University, Providence (USA). The results are evaluated by statistical analyses as well as Principle Component Analysis (PCA) using the Excel software add-in XLSTAT, and by endmember modeling using the Matlab software package ‘AnalySize’.

The geochemical and mineralogical data show distinct groups of 355 mass movement deposits appearing within the upper 60.5 m of the TDP Site 2 composite profile. Geochemical endmember modelling suggests two potential trigger areas combined with different processes: (i) mass movements from the Mahalona River Delta, and (ii) slope failure at the north-eastern part of Lake Towuti shoreline. The source areas of the turbidites can be identified based on provenance analyses that have been conducted on an extensive surface sediment data sets from Lake Towuti. However, the results are partly hampered by insufficient information concerning the source rocks in the Towuti Lake catchment.

IODP

Character of the enhanced South Asian Monsoon during the mid Holocene revealed by oxygen isotope analysis of individual foraminifera

E. HATHORNE¹, K. THIRUMALAI², D. GEBREGIORGIS³, L. GIOSAN⁴, B. N. NATH⁵, M. FRANK¹

¹GEOMAR Helmholtz Centre for Ocean Research Kiel,

Wischhofstr. 1-3, 24148 Kiel, Germany (ehathorne@geomar.de)

²Brown University, Providence RI, USA

³Georgia State University, Department of Geosciences, Atlanta, USA

⁴Woods Hole Oceanographic Institute, USA

⁵National Institute of Oceanography Goa, India

The South Asian Monsoon (SAM) is a seasonal climatic phenomenon with distinctive inter-annual and decadal modes of variability that have significant impacts on human timescales. The monsoon provides vital water resources for billions of people but has proven difficult to predict. With only one century of instrumental data for the Indian Monsoon we must look to palaeoclimate proxy records to better understand past SAM variability and improve future predictions. As some planktonic foraminifera species calcify the major part of their shells within lunar periods, the analysis of many single shells has the

potential to reveal the range of conditions prevailing on sub-seasonal, seasonal, and inter-annual timescales. The SAM causes a strong seasonal salinity signal in the Andaman Sea where the NGHP Site 17 and IODP U1447 and U1448 sediment cores were obtained. We have measured oxygen isotope compositions of many individual *N. dutertrei* and *G. sacculifer* shells and have modelled individual foraminifera pseudo- $\delta^{18}\text{O}$ data based on observational time series for this location (Thirumalai et al., 2013). The distribution of individual shell oxygen isotopes from a nearby core top sample agrees very well with the modelled distribution providing confidence in this technique to reconstruct past variability. The recent and last glacial maximum $\delta^{18}\text{O}$ distributions are relatively similar although the mean values are offset as expected. In contrast, the distributions from three samples from the early to mid Holocene exhibit a significant skew towards negative values reflecting increased freshwater addition to the mixed layer. Kurtosis is a measure of the „curvedness“ of a distribution and provides a useful approach to infer past monsoon variability. For these early-to-mid Holocene samples, this statistic supports stronger monsoon variance and indicates heightened variability of mixed layer salinity.

Reference:

Thirumalai, K., J. W. Partin, C. S. Jackson, and T. M. Quinn (2013), *Paleoceanography*, 28(3), 401-412..

ICDP

Barberton Archean Surface Environments (BASE)

C. HEUBECK¹ AND THE BASE TEAM

¹Institut für Geowissenschaften, Friedrich-Schiller-Universität Jena, Burgweg 11, 07749 Jena

We report on a submitted ICDP Full Proposal with the objective to drill sedimentary rocks of the Early Archean Barberton Greenstone Belt, South Africa. There, sedimentary (and minor volcanic) units of the Moodies Group (~3.22 Ga, ~3.7 km thick) were deposited within ~1-14 Ma and thus record at very high resolution Archean surface processes in fluvial to prodeltaic depositional environments. Despite tight regional folding, metamorphic grade is only lower greenschist-facies; widespread early-diagenetic silicification preserved abundant micro- and macrot textures virtually without strain. Moodies strata thus allow the regional and temporal contextualization of high-resolution analytical data, in many aspects equal or superior to Pilbara strata. They record numerous bio-geo-atmo-hydrosphere interactions and are ideal to investigate Archean terrestrial-marine transitions, particularly those related to diverse and well-documented microbial life. These “earth system” and “global environmental change” topics provide an excellent match to the themes of a nascent UNESCO world heritage site to be declared in the Barberton Mountain Land.

We conducted a field workshop in October 2017 in which 48 scientists from 11 countries participated. We inspected, discussed and prioritized potential sections. Four focus groups (life, paleoenvironment, “hard rock”, and sedimentation dynamics) defined eight inclined drillholes of 300-600m length each, targeting transitions between thick tidal microbial mats, fluvial and coastal gypsiferous paleosols, shoreline systems, delta complexes, potentially eolian strata, and prodeltaic jaspilites and banded-iron formation.

Principal questions include:

(1) Is there a stratigraphic rhythmicity preserved in the fine-grained prodelta sediments? What is the origin of its clay minerals? How do coastal BIFs and jaspilites relate to nearby tidal microbial mats?

(2) What is the ecology, 3-D morphology and metabolism(s) of the abundant (oxygenic photosynthetic?) microbial mats in minimally compacted tidal-facies sandstones? What is their C-isotope microstratigraphy, preservation pathway(s), origin of early diagenetic chert, and the degree of thermal overprint? Can we constrain net O₂ production rates and the early N cycle?

(3) What global surface conditions can be inferred? What was the redox state (sulfate, redox-sensitive metal isotopes), temperature and composition of ocean water and of early diagenetic fluids, and the relevance and processes of weathering and early diagenesis by paleosols formation?

(4) What does the paleomagnetic record imply about the strength of the Earth’s magnetic field?

(5) What is the association between a thick mid-section lava and Moodies basin collapse? Can high-precision U-Pb dating of air-fall tuffs quantify rates of sedimentation and subsidence on a permobile lithosphere dominated by vertically-dominated tectonics?

IODP

Paleobathymetric grids of the Cenozoic Southern Ocean – paving the way towards improved reconstructions of the Southern Ocean’s past

K. HOCHMUTH¹, K. GOHL¹, G. LEITCHENOV², I. SAUERMLICH³, J. WHITTAKER³, L. DESANTIS⁴, E. OLIVIO⁴, G. UENZELMANN-NEBEN¹, B. DAVY⁵

¹Alfred Wegener Institute, Helmholtz-Center for Polar and Marine Research, Bremerhaven, Germany

²All Russia Scientific Research Institut for Geology and Mineral Resources of the Ocean, St.-Petersburg, Russia

³Institute of Marine and Antarctic Studies, University of Tasmania, Hobart, Australia

⁴Instituto Nazionale di Oceanografia e di Geofisica Sperimentale, Trieste, Italy

⁵GNS Science, Lower Hutt, New Zealand

Paleo-ocean circulation models of the Southern Ocean suffer from missing boundary conditions, which accurately describe the geometries of the seafloor surfaces at their geological epoch and their dynamics over time-scales. The accurate parameterisation of these models controls the meaning and implications of regional and global paleo-climate models. Existing paleobathymetric models consider only the top of the oceanic basement based on paleo-age models from magnetic seafloor spreading anomalies or simplify the sedimentary cover by outdated isopach maps. Therefore, the available multichannel seismic reflection (MCS) data have been re-evaluated and linked to DSDP, ODP or IODP drill sites to calculate paleobathymetric grids for the Cenozoic. This project is a community-based effort and with our wide network of cooperation partners, who provide additional data as well as interpreted horizon data, we successfully unified the seismic stratigraphy of the Southern Ocean. The ultimate goal for the final year of this project is to enable the reconstruction the paleobathymetric grids in approx. 2 m.y. steps throughout the Cenozoic in order to match the time periods used by ice sheet and paleoceanographic modellers. The calculated grids for time-slices such as i.e. the Eocene-Oli-

gocene transition or the Mid-Miocene Climate Optimum will be made available by publications linked with data repository entries such as in PANGAEA.

Drill site information is of the utmost importance to provide reliable reconstructions of the geometry of the sedimentary cover. Therefore, we carefully re-evaluated the physical sedimentary parameters, downhole-logging data and age information of more than 200 drill sites recovered by IODP and its predecessor programs DSDP and ODP within the Southern Ocean. The current efforts of IODP within the Ross Sea (Exp. 374) and the Amundsen Sea (Exp. 379), will supply much needed further constraints on the sediment composition within the West Antarctic sector within the next years, which can be integrated swiftly into the created database.

The Eocene/Oligocene Boundary marks a drastic change within the Southern Ocean. The opening of the Drake Passage as well as of the Tasman Gateway, allows the establishment of the Circum Antarctic Current, finalizing the isolation of the Antarctic continent from the other continents of Gondwana. Additionally, this boundary marks the onset of the continental glaciation of Antarctica and therefore introduces the Antarctic ice sheets as crucial players in the regime of the Southern Ocean. Paleobathymetric maps of this timeframe show the extent of the ocean gateways and the important role of magmatic edifices such as Large Igneous Provinces (e.g. Kerguelen Plateau) but also seamount provinces (e.g. Marie Byrd Seamounts) in shaping the sedimentation and circulation patterns. To enable more sophisticated reconstructions the Antarctic continent prior to the immense erosion of a continental ice sheet, we calculated sedimentary thickness maps describing the glacially derived amount of sedimentation and the sedimentation prior to glaciation. Those charts also pinpoint the areas of immense sedimentation and shelf progradation since the onset of glaciation. The position of the shelf break proves to be a vital ingredient in paleocurrent modelling, e.g. leading to enhanced bottom water production throughout the Southern Ocean.

IODP

Volcanic, tectonic and hydrothermal processes in an island-arc caldera environment. Development of an IODP Drilling Proposal at Santorini-Kolumbo Marine Volcanic System

C. HÜBSCHER¹, T. DRUITT², P. NOMIKOU³, D. PAPANIKOLAOU³ ET AL

¹University of Hamburg, Germany. Email: christian.huebscher@uni-hamburg.de

²Clermont-Auvergne University, France

³National and Kapodistrian University of Athens, Greece

The relationships between tectonics, sea level change and volcanism are fundamental questions in modern Earth Sciences. How do volcanoes react to external forcings, how sensitive are these interactions, and what are the feedbacks? The Christianna-Santorini-Kolumbo (CSK) volcanotectonic line in the Southern Aegean Sea (Greece) is an excellent natural laboratory for the study of these questions, lying as it does in a 100-km-long, 45-km-wide rift zone that cuts across the Hellenic Volcanic arc. The line hosts volcanic centres including the extinct Christianna Volcano, Santorini caldera with its intracaldera Kameni Volcano, Kolumbo seamount, and 25 other submarine cones of the Kolumbo chain. It is one of the most important volcanic fields in Europe, having produced more than 100 explosive eruptions in the last 400,000 years, the mass flows from which have poured into the surrounding submarine basins. Drilling the

fills of these basins will enable access to a complete record of the sedimentary, environment, tectonic and volcanic evolution of the CSK line since the Pliocene, enabling high-resolution reconstruction of the evolution of the rift and its volcanoes.

A MagellanPlus workshop in Athens on 21-23 November 2017 assembled a working group to prepare a drilling proposal for submission to the International Ocean Discovery Programme (IODP). The meeting was extremely productive, and created strong support for the CSK line as an outstanding drilling target for addressing fundamental issues related to volcanism in a rifted arc environment. A pre-proposal will be submitted to IODP on 2 April 2018.

The drilling initiative is founded on many years of intensive onland and offshore research on the rift and its volcanoes. Several geophysical campaigns since 2001 have generated a dense network of sub-seafloor seismic reflection profiles, and high-resolution bathymetric surveys have imaged volcanic edifices, tectonic fault zones and caldera floors.

Six sites with existing seismic coverage of high quality were selected as most appropriate for addressing the science questions (Fig. 1), including:

- (1) the volcanic histories of the volcanic centres of the CSK line,
- (2) the tectonic, sedimentary and sea-level histories of the rifts,
- (3) the links between volcanism, tectonics and sea level,
- (4) the mechanisms of shallow to emergent volcanism,
- (5) the effects of the iconic ~1630 BCE eruption of Santorini on the late Bronze-Age Mediterranean world,
- (6) the generation and evolution of CSK magmas,
- (7) the mechanisms of caldera collapse, and
- (8) hydrothermal and deep microbial activity within volcanic accumulations.

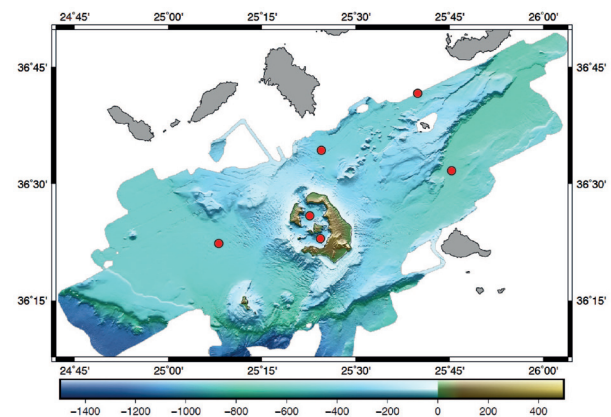


Fig. 1: Synthetic topographic map of Christianna-Santorini-Kolumbo (CSK) volcanic line (modified from Hooft et al., 2017, *Tectonophysics* 712–713, 396–414), showing the proposed drilling sites in red.

IODP

Early Quaternary stabilisation of the East Antarctic Ice Sheet linked to Northern Hemisphere ice volume

K. A. JAKOB¹, P. A. WILSON², J. PROSS¹, J. FIEBIG³, O. FRIEDRICH¹

¹Institute of Earth Sciences, Heidelberg University, Im Neuenheimer Feld 234–236, 69120 Heidelberg, Germany

²National Oceanography Centre Southampton, University of Southampton, European Way, Southampton SO14 3ZH, UK

³Institute of Geosciences, Goethe-University Frankfurt, Altenhöferallee1, 60438 Frankfurt, Germany

Sea-level rise resulting from the instability of polar continental ice sheets represents a major socio-economic hazard associated with future anthropogenic warming (IPCC, 2014). While the response of the Greenland (GIS) and West Antarctic (WAIS) ice sheets to global warming is relatively well understood, the behavior of the largest component of the Earth's cryosphere – the East Antarctic Ice Sheet (EAIS) – is more uncertain (Hanna et al., 2013). Recent studies consider atmospheric CO₂ concentrations (*p*CO₂) to be the dominant factor in controlling EAIS stability, questioning its stability under Anthropocene-like *p*CO₂ (~400 parts per million by volume [ppmv]; Cook et al., 2013; DeConto & Pollard, 2016) and suggesting that a return toward preindustrial *p*CO₂ (~280 ppmv) may allow the EAIS to stabilize (Foster & Rohling, 2013).

The transition from the Pliocene to the Quaternary represents the most recent interval in Earth's history that captures the range of *p*CO₂ levels from those that are suggested to promote EAIS instability (i.e., Anthropocene-like values ~400 ppmv) to those that have been postulated to allow for a stable ice sheet (i.e., “standard-Quaternary”, preindustrial-like levels ~250–300 ppmv; Seki et al., 2010). This *p*CO₂ decline goes along with progressive cooling and finally led to the expansion of Northern Hemisphere ice sheets (Lisiecki & Raymo, 2005; DeConto et al., 2008) – a time interval termed the “intensification of Northern Hemisphere Glaciation” (iNHG), typically being considered to span ~3.6–2.4 Ma (Mudelsee & Raymo, 2005). In this study, we test EAIS behaviour during the final phase of iNHG. Therefore, we quantified sea-level/ice-volume changes via generating new, high-resolution (~375–1500 yr) benthic foraminiferal (*Oridorsalis umbonatus*) Mg/Ca and oxygen-isotope ($\delta^{18}\text{O}$) data from a sediment core recovered by IODP Expedition 306 in the North Atlantic (Site U1313) for the latest Pliocene to earliest Quaternary (~2.75–2.4 Ma, Marine Isotope Stages [MIS] G7–95).

The sea-level values that we reconstructed from our proxy records fluctuate between a maximum of ~50 ± 25 m above present-day sea-level during MIS 101 and a minimum of ~120 ± 25 m below modern values during MIS 96. Our sea-level record indicates a clear glacial-interglacial cyclicity, with lower amplitudes before MIS 100 (typically ~50–90 m) and higher fluctuations from MIS 100 onward (typically ~80–120 m).

Complete melting of the present-day GIS and WAIS can only account for a 12.4 m higher-than-modern sea level (Lythe & Vaughan, 2001; Vaughan, et al. 2013). Sea-level highstands of ~25 to 50 m above modern values as resulting from our data indicate a substantial melt of the EAIS (by at least ~24 % relative to its present size) during late Pliocene interglacials MIS G7 and G1 and early Quaternary interglacial MIS 101. Therefore our record suggests that the EAIS was highly unstable even under preindustrial-like *p*CO₂ and responded dynamically to glacial-interglacial cycles until the earliest Quaternary (~2.5 Ma). It only stabilized with the final phase of the iNHG. In this context, we propose that ocean-cryosphere interactions play a decisive role in controlling EAIS (in)stability: A drop in mean-state sea level due to an increase in global ice-volume not only during glacials, but also during interglacials since MIS 100 as documented by our data indicates that the marine-based margin of the EAIS that existed during Pliocene interglacials (DeConto & Pollard, 2016) became extremely reduced, turning the EAIS into a predominantly land-based ice sheet from that time onward. As a consequence, basal melt became less effective, which stabilized the EAIS since MIS 100. To conclude, our data suggest a fundamental link between EAIS (in)stability and Northern Hemisphere ice volume, thereby providing evidence

that another pivotal factor except *p*CO₂ – i.e., basal melt – controlled EAIS dynamics.

References:

- Cook, C.P. et al. (2013). Dynamic behaviour of the East Antarctic ice sheet during Pliocene warmth. *Nature Geoscience* 6, 765–769.
- DeConto, R.M. et al. (2008). Thresholds for Cenozoic bipolar glaciation. *Nature* 455, 652–656.
- DeConto, R.M. & Pollard, D. (2016). Contribution of Antarctica to past and future sea-level rise. *Nature* 531, 591–597.
- Foster, G.L. & Rohling, E.J. (2013). Relationship between sea level and climate forcing by CO₂ on geological timescales. *Proceedings of the National Academy of Sciences* 110, 1209–1214.
- Hanna, E. et al. (2013). Ice-sheet mass balance and climate change. *Nature* 498, 51–59.
- IPCC (2014). *Climate Change 2014: Synthesis Report*. IPCC, Geneva, Switzerland, 151 pp.
- Lisiecki, L.E. & Raymo, M.E. (2005). A Pliocene-Pleistocene stack of 57 globally distributed benthic $\delta^{18}\text{O}$ records. *Paleoceanography* 20, PA1003.
- Lythe, M.B. & Vaughan, D.G. (2001). BEDMAP: A new ice thickness and subglacial topographic model of Antarctica. *Journal of Geophysical Research: Solid Earth* 106, 11335–11351.
- Mudelsee, M. & Raymo, M.E. (2005). Slow dynamics of the Northern Hemisphere Glaciation. *Paleoceanography* 20, PA4022.
- Seki, O. et al. (2010). Alkenone and boron-based Pliocene *p*CO₂ records. *Earth and Planetary Science Letters* 292, 201–211.
- Vaughan, D.G. et al. (2013). Observations: Cryosphere. In *Climate Change 2013: The Physical Science Basis*. Contribution of Working Group I to the Fifth Assessment Report of the Intergovernmental Panel on Climate Change (edited by T.F. Stocker et al.), Cambridge University Press, pp. 317–382.

IODP

Deciphering the late Miocene evolution of the Indian Monsoon in IODP Expedition 353 Sites U1447 and U1448 (Andaman Sea)

J. JÖHNCK¹, W. KUHN¹, A. HOLBOURN¹, N. ANDERSEN²

¹Institute of Geosciences, Christian-Albrechts-University, 4118 Kiel, Germany

²Leibniz Laboratory for Radiometric Dating and Stable Isotope Research, Christian-Albrechts-University, 24118 Kiel, Germany

The long- and short-term variability and drivers of Indo-Asian-monsoonal circulation and precipitation patterns remain intensely debated. In particular, the sensitivity of the Indian Monsoon to insolation forcing and to changing climate boundary conditions in the Earth's most important geographic regime of monsoonal influence, the margins of the Bay of Bengal, is still poorly understood. Two sites from IODP Expedition 353 (iMonsoon) drilled in the Andaman Sea, U1448 (10°38.03'N/93°00.00'E, 1098 m water depth) and U1447 (10°47.40'N/93°00.00'E, 1392 m water depth), provide extended upper Miocene successions, thus offering an outstanding opportunity to assess the timing and boundary conditions of Indian monsoonal circulation and high-latitude climate change during the late Miocene (Clemens et al., 2016). This interval is characterized by transient Northern Hemisphere cooling events (TG Events) with mean-state background climate conditions close to today's. We are currently developing an orbitally tuned isotope stratigraphy based on a composite record of Sites U1447 and U1448 over the interval 10 to 5 Ma as well as high-resolution monsoonal run-off records from XRF-scanning elemental data coupled with sea surface temperature/salinity reconstructions from paired stable isotopes and Mg/Ca paleothermometry. We applied minor adjustments to the ship-board splice and generated new tie points based on comparison of XRF-derived Log(Ca/Fe) and benthic stable isotope data. Cold stages T4 to TG34 were identified in the interval between 5 and 6 Ma, which are associated with obliquity minima and maxima in precession parameter (Northern Hemisphere cooling). These TG Events are strongly imprinted in Indian Ocean

temperature records from surface and intermediate waters. During TG Events, decreasing Log(Ca/Fe) values indicate minima in carbonate production and decreasing Log(K/Ti) values suggest that the erosion of the Himalayan foothills became less intense due to summer monsoon failure, as during Pleistocene glacial stages.

References:

Clemens, S.C., Kuhnt, W., LeVay, L.J., Anand, P., Ando, T., Bartol, M., Bolton, C.T., Ding, X., Gariboldi, K., Giosan, L., Hathorne, E.C., Huang, Y., Jaiswal, P., Kim, S., Kirkpatrick, J.B., Littler, K., Marino, G., Martinez, P., Naik, D., Peketi, A., Phillips, S.C., Robinson, M.M., Romero, O.E., Sagar, N., Tala-day, K.B., Taylor, S.N., Thirumalai, K., Uramoto, G., Usui, Y., Wang, J., Yamamoto, M., and Zhou, L., 2016. Site U1447, Site U1448. In Clemens, S.C., Kuhnt, W., LeVay, L.J., and the Expedition 353 Scientists, *Indian Monsoon Rainfall*. Proceedings of the International Ocean Discovery Program, 353: College Station, TX (International Ocean Discovery Program). <http://dx.doi.org/10.14379/iodp.proc.353.107.2016>.

IODP

Continuous monsoonal forcing of European ice-sheet dynamics during the Late Quaternary

S. KABOTH¹, A. BAHR², C. ZEEDEN³, S. TOUCANNE⁴, F. EYNAUD⁵, F. JIMÉNEZ-ESPEJO⁶, U. RÖHL⁷, O. FRIEDRICH², J. PROSS², L. LÖWEMARK¹, L. LOURENS⁸

¹ Department of Geosciences, National Taiwan University, Taipei City 106, Taiwan

² Institute of Earth Sciences, Heidelberg University, 69210 Heidelberg, Germany

³ IMCEE, Observatoire de Paris, PSL Research University, Paris 75014, France

⁴ Ifremer, Centre Bretagne, UR Geosciences Marines, Plouzané Cedex 29280, France

⁵ Université de Bordeaux, Pessac Cedex 33607, France

⁶ Department of Biogeochemistry, Japan Agency for Marine-Earth Science and Technology (JAMSTEC), Yokosuka-city 237-0061, Japan

⁷ MARUM—Center of Marine Environmental Sciences, University of Bremen, 28359 Bremen, Germany

⁸ Department of Earth Sciences, Utrecht University, Utrecht 3584CD, The Netherlands

The dynamics of Northern Hemisphere ice-sheets during Late Quaternary glacials have so far been dominantly examined from a Laurentide Ice sheet perspective. The resulting insights have shaped the idea of moisture-starved glacials and small-scale ice volume variability. However, the waxing and waning of European Ice Sheets (EIS) cast doubt on this perception. A mechanistic understanding of EIS dynamics is crucial because its melt-water masses have the capacity to influence global climate by weakening deep-water formation in the North Atlantic Ocean. Here we show that the advection of subtropical water towards the continental margin of western Europe lead to enhanced moisture availability on the continent and fuelled the rapid re-growth of EIS during glacials. Our results from IODP 339 Site U1389 document precession-driven pulses of warm water masses reaching up to ~40°N caused by enhanced Mediterranean Outflow Water (MOW) production that dragged subtropical surface waters towards the European margin. The increased thermal gradient between warm waters and cold land-masses thereby invoked snow accumulation over continental Europe boosting ice growth. As MOW dynamics are driven by the North African monsoon this mechanism presents a hitherto unrecognized marine-terrestrial pathway that allows low-latitude forcing to shape high-latitude glaciations.

IODP

Exploring microbial sulphate reduction under high temperature and pressure –Results of a pilot study on samples from IODP Exp. 370

J. KALLMEYER¹, F. SCHUBERT¹, T. TREUDE²,
 IODP EXP. 370 SCIENTIFIC PARTY

¹GFZ Potsdam, Potsdam, Germany

²UCLA, Los Angeles, United States

Sulphate reduction is the quantitatively most important process in the anaerobic degradation of organic matter in the sea floor. Due to cryptic sulphur cycling it can proceed even if sulphate concentrations are near or below our detection limits. While the effects of elevated pressure and temperature on microbial sulphate reduction have been studied for decades, almost all studies were carried out in hydrothermal systems like Guaymas Basin, whereas sedimentary non-hydrothermal systems did not receive much attention.

Expedition 370 (Temperature Limit of the Deep Biosphere off Muroto) of the Integrated Ocean Drilling Program (IODP) was specifically planned to explore the upper temperature limit of life in a sedimentary system off the coast of Japan (Heuer et al., 2017).

Due to the high heat flow in the area the geothermal gradient is high enough (ca. 100°C km⁻¹) to sample the putative temperature-dependent biotic–abiotic transition zone at relatively shallow sediment depth but still sufficiently gradual for the establishment of distinct, thick depth horizons (>10 m) with suitable conditions for psychrophilic (optimal growth temperature range: < 20°C) mesophilic (20–45°C), thermophilic (45–80°C) and hyperthermophilic (>80°C) microorganisms. Site C0023 allows exploring the putative biotic fringe at a relatively shallow depth, but with high resolution of the temperature gradient. Radiotracer measurements of microbial turnover was one of the key aspects of this expedition, and each parameter that can be measured by radiotracer (methanogenesis, anaerobic oxidation of methane, hydrogenase enzyme activity, sulphate reduction) will be measured by a different group that has specialized in this kind of analysis.

Due to several logistical limitations it was decided to carry out those experiments mostly on shore, only for methanogenesis and sulphate reduction a small subset of samples was incubated at their approximate in-situ temperature and atmospheric pressure.

The sulphate reduction rate samples from the on-board incubations were processed at GFZ Potsdam to guide subsequent incubations with radioisotopes. Further experiments with additions of electron donors (e.g. volatile fatty acids, methane) explored not just the upper temperature limit of this important biogeochemical process but also the transition from mesophilic to thermophilic communities. Together with previous data from ODP Leg 190, Site 1174, which was drilled in close proximity to Exp. 370 site C0023, sulphate reduction could be detected down to over 1000 mbsf.

Acknowledgements:

This research used samples and data provided by the International Ocean Discovery Program (IODP). The authors would like to thank all personnel involved in the operations of DV Chikyu during Expedition 270 and the support team at the Kochi Core Center

References:

Heuer, V.B., Inagaki, F., Morono, Y., Kubo, Y., Maeda, L., and the Expedition 370 Scientists, 2017. Expedition 370 Preliminary Report: Temperature Limit of the Deep Biosphere off Muroto. International Ocean Discovery Program. <http://dx.doi.org/10.14379/iodp.pr.370.2017>

ICDP/IODP

The Trans-Amazon Drilling Project – a joint ICDP/IODP project to unravel the history of the Amazon Basin

J. KALLMEYER¹, P. A. BAKER^{2*}, S. C. FRITZ^{3*}

¹GFZ German Research Center for Geosciences, Potsdam, Germany (kallm@gfz-potsdam.de)

²Duke University, Durham, USA

³University of Nebraska–Lincoln, USA

*Lead PIs

The Amazon/Andes of tropical South America is a key region on Earth, and its rainforests host over half of all terrestrial plant species. The forests and their biota have evolved together with the physical landscape, closely linking processes in the Earth's interior with surface climate and landscapes, ecosystems, and biodiversity. The proposed Trans-Amazon Drilling Project will address fundamental questions about the geologic and biotic evolution of the Amazon, focusing on (1) how Cenozoic climate and geologic history, including uplift of the Andes and development of the Amazon fluvial system, influenced the origins of the Amazon rainforest and its incomparable biodiversity; and (2) the origin of the Amazonian "Pentecaua" diabase sills, one of Earth's largest intrusive complexes, and the impacts of this intrusion on the atmospheric gas composition and mass extinction at the Triassic/Jurassic boundary. These goals require long sedimentary records, which, in most of the Amazon region, can only be obtained by drilling. We propose to drill the entire Cenozoic sequence in three continental sites in different ancient sedimentary basins that are aligned along the modern Amazon River and that transect the entire near-equatorial Amazon region of Brazil, from the Andean foreland to the Atlantic Ocean. The transect of sites is essential for distinguishing basin-wide and continental-scale patterns of climate, landscape, and biotic evolution; evaluating questions about west-to-east gradients and hydrologic connectivity; and correlating the continental strata with a site dated using marine biostratigraphy. In addition, in the Amazonas Basin, we propose to drill both the Cenozoic sedimentary sequence and the entire 1100 m thick underlying diabase sequence along with its interbedded host meta-sediments. Drill sites have been chosen that are all near large navigable rivers of the Amazon or roads that are easily accessible from these rivers. This transect, coupled with proposed IODP sites on the Amazon continental margin, will span 40°W to 73°W, thus encircling nearly 10% of Earth's equatorial circumference. We believe that this work will provide transformative understanding of Amazonian geological and biotic evolution that addresses important and long-standing questions about the linkages between the geophysical environment and its biotic history. ICDP granted this project in 2017, currently the proponents are submitting proposals to their national funding agencies to obtain the required co-funding. There are plans among the proponents from Switzerland, Austria and Germany to prepare a joint D-A-CH proposal. The plan is to start drilling in 2020. The complementary IODP proposal is still under revision.

ICDP

Indian Summer Monsoon record from Nam Co reveals a switching relation to Pacific climate oscillation during the Holocene

T. KASPER¹, T. HABERZETTL¹, J. WANG², A. SCHWALB³, G. DAUT¹, B. PLESSEN⁴, L. ZHU², R. MAUSBACHER¹

¹Department of Physical Geography, Institute of Geography, Friedrich-Schiller-University Jena, Loebdergraben 32, 07743 Jena, Germany

²Institute of Tibetan Plateau Research, Chinese Academy of Sciences, Beijing 100101, China

³Institute of Geosystems and Bioindication, Technische Universität Braunschweig, Langer Kamp 19c, 38106 Braunschweig, Germany

⁴Helmholtz Centre Potsdam, GFZ German Research Centre for Geosciences, Telegrafenberg, Building C, 14473 Potsdam, Germany

Although in recent observations the Indian Summer Monsoon (ISM) and the Pacific climate oscillation known as El Niño-Southern Oscillation (ENSO) reveal mutual influence, evidence for a link between both systems on millennial time scales is still missing. Based on minerogenic input into lacustrine systems on the Tibetan Plateau, a high-resolution reconstruction of Holocene ISM variability is derived. This reveals a distinct decoupling from lake level (volume) reconstructed from bulk stable isotope data, emphasizing the need of process-oriented precipitation proxies, because lake levels are not directly linked to ISM rainfall intensity on the TP. Compared to long-term ENSO records from the tropical Pacific, ISM changes reveal an in-phase pattern during the Early and mid-Holocene from 11,000 to ca. 5,000 cal BP. This is likely driven by the synchronicity of insolation in both regions. During this period, phases of ISM strengthening were concurrent with phases of more frequent and stronger El Niño events (=in-phase). This coupling was reversed to an anti-phase pattern with strong and frequent El Niño phases and a weakened ISM, most likely caused by the inversion of the insolation parameters after ca. 5,000 cal BP. A remarkable shift to strong El Niño contemporaneous with dry conditions in the ISM region at 2,000 cal BP highlights this climatic teleconnection during the Late Holocene.

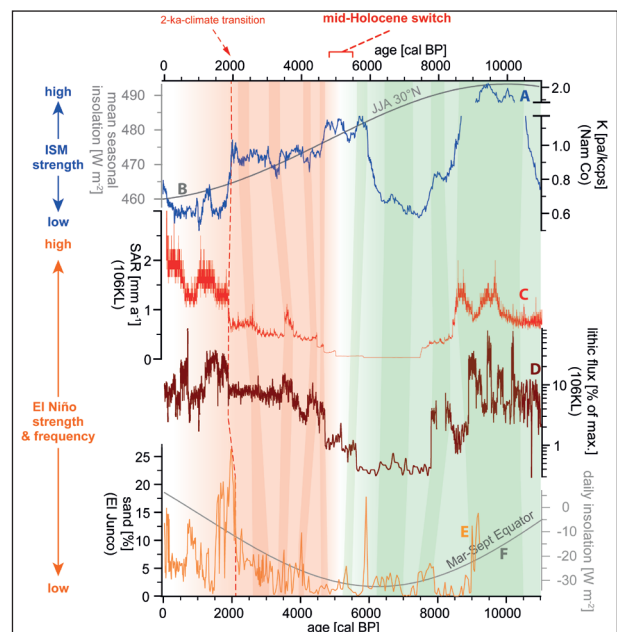


Fig. 1: ISM variations during the Holocene derived from Nam Co (A) with the mean JJA insolation at 30° N (B) as main driver. Records from the Tropical Pacific reflecting El Niño strength and frequency variations (lithic flux from marine sediment core 106KL off Peru

(Rein et al., 2005) (D), sand content El Junco lacustrine sediment record from the Galapagos archipelago (Conroy et al., 2008) (E)).

References:

- Conroy, J. L., Overpeck, J. T., Cole, J. E., Shanahan, T. M., and Steinitz-Kannan, M., 2008, Holocene changes in eastern tropical Pacific climate inferred from a Galapagos lake sediment record: *Quaternary Science Reviews*, v. 27, no. 11-12, p. 1166-1180.
- Kasper, T., Haberzettl, T., Wang, J., Daut, G., Zhu, L., and Mäusbacher, R., 2015, Hydrological variations on the Central Tibetan Plateau since the LGM and their teleconnection to inter-regional and hemispheric climate variations: *Journal of Quaternary Science*, v. 30, no. 1, p. 70-78.
- Rein, B., Lückge, A., Reinhardt, L., Sirocco, F., Wolf, A., and Dullo, W.-C., 2005, El Niño variability off Peru during the last 20,000 years: *Paleoceanography*, v. 20, no. 4, p. PA4003.

ICDP

Core-Log-Seismic-Integration (CLSI) in hard-rock environments using the ICDP drilling project COSC-1, Sweden: project outline

F. KÄSTNER^{1,2}, S. PIERDOMINICI², J. ELGER³, C. BERNDT^{2,3}, J. KÜCK¹

¹Helmholtz-Zentrum Potsdam, Deutsches GeoForschungsZentrum GFZ

²Christian-Albrechts-Universität zu Kiel

³Helmholtz-Zentrum für Ozeanforschung Kiel, GEOMAR

As part of the ICDP priority program “Collisional Orogeny of the Scandinavian Caledonides (COSC)” we investigate the integration and linkage of geophysical properties of the subsurface by laboratory investigations, borehole measurements and reflection seismic data.

The COSC project aims to better understand the deep orogenic processes in mountain belts in a major mid-Paleozoic orogen in western Scandinavia (Gee et al., 2010). The COSC-1 borehole was drilled in 2014 as the first of two proposed scientific boreholes in the Jämtland region, close to the town of Åre in central Sweden. It was drilled into the lower part of the Seve Nappe Complex (SNC) of the middle allochthon of the central Scandinavian Caledonides, which is characterized by ultra-high pressure metamorphism. The almost 2.5 km deep, almost fully cored borehole is dominated by homogenous gneisses with only subordinate mafic bodies and an unexpectedly thick basal thrust zone (> 800 m), whereas the lowermost section of the Seve Nappe is mainly composed of lower-grade metasedimentary rocks and garnetiferous mylonites (Lorenz et al., 2015).

In a multi-scale approach, we aim to construct a high-resolution seismic stratigraphy of the SNC at the COSC-1 drill site and nearby areas by core-log-seismic integration (CLSI) method. Together with a 100 percent core recovery, the COSC project provides an excellent coverage of seismic, borehole, and core data, and therefore represents the ideal case study for CLSI. Although the method of CLSI has been already successfully applied in marine and lake environments (e.g., Thu et al., 2002), this is the first application of CLSI in a crystalline, hard-rock environment and it represents a scientific challenge.

The investigation across multiple scales of data such as seismic (two- and three-dimensional information reflecting regional geologic structures), downhole logging (continuous information at intermediate scale, in the direct vicinity of the borehole), and core data (small-scale, detailed petrophysical properties and geological age information), contributes to improve the confidence of each data set. Integration of core-log-seismic data needs careful adjustments and calibration. Especially, synthetic seismograms created from density and velocity data (downhole and laboratory) are used to correlate and link the different datasets during the integration process. Thus, three

main steps are required for a robust and reliable investigation: (1) core-log integration providing essential rock-physical and in-situ geophysical properties, (2) log-seismic integration and calibration providing a synthetic seismic trace based on reflection coefficient series which subsequently may be used to (3) create a 3D geological model of the 2D or 3D seismic reflection data using different inversion techniques.

Ongoing work focuses on collecting and calibrating the different datasets. Moreover, P-wave velocities are determined from the drill core with a multi-sensor core logger (MSCL, provided by BGR core repository in Spandau, Berlin), which, due to technical issues, were not measured on site. These high-resolution velocity data will be used to select a set of core samples for small-scale anisotropy measurements in the laboratory. The combination of core and log measurements provides fundamental information about geological formation and its physical properties, while its usage is twofold: First, integrate the dataset from different measurement methods, and second, bridges scales from the sub millimeter-scale of core samples to the decimeter scale of logging data, which investigate a different volume of rock (e.g., Lovell et al., 1998). Essentially, the primary purpose of core-log integration is to control the log evaluation using data measured under laboratory conditions (e.g., MSCL). Another requirement is to reconcile the different vertical resolutions by, for instance, depth averaging of core data or signal enhancement of log data. Important to this process is the adoption of so-called key intervals (e.g., prominent horizons or stratigraphic markers) as control zones for data integration. These procedures can reduce uncertainties, which can be transferred to the evaluation of the subsurface by a better petrophysical definition of the lithological units. Consequently, it can help to better understand the seismic response of the complex nappe tectonics and its evolution.

References:

- Gee, D.G., Juhlin, C., Pascal, C., Robinson, P., 2010. Collisional Orogeny in the Scandinavian Caledonides (COSC). *Gff* 132, 29–44. doi:10.1080/11035891003759188
- Lovell, M.A., Harvey, P.K., Jackson, P.D., Brewer, T.S., Williamson, G., Williams, C.G., 1998. Interpretation of core and log data—integration or calibration? *Geol. Soc. London, Spec. Publ.* 136, 39–51. doi:10.1144/GSL.SP.1998.136.01.05
- Lorenz, H., Rosberg, J.-E., Juhlin, C., Bjelm, L., Almqvist, B.S.G., Berthet, T., Conze, R., Gee, D.G., Klonowska, I., Pascal, C., Pedersen, K., Roberts, N.M.W., Tsang, C.-F., 2015. COSC-1 – drilling of a subduction-related allochthon in the Palaeozoic Caledonide orogen of Scandinavia. *Sci. Drill.* 19, 1–11. doi:10.5194/sd-19-1-2015
- Thu, M.K., Tamaki, K., Kuramoto, S.-I., Tada, R., Saito, S., 2002. High-resolution seismic stratigraphy of the Yamato Basin, Japan Sea and its geological application. *Isl. Arc* 11, 61–78. doi:10.1046/j.1440-1738.2002.00352.x

ICDP

Ancient DNA and Metagenomics of Lake Sediments

J. KRÜGER¹, M. HOFREITER¹, R. TIEDEMANN², M. H. TRAUTH³, V. FOERSTER⁴, S. HARTMANN¹, K. HAVENSTEIN²,

¹Unit of Evolutionary Adaptive Genomics, Institute for Biochemistry and Biology, University of Potsdam

²Unit of Evolutionary Biology/Systematic Zoology, Institute for Biochemistry and Biology, University of Potsdam

³Institute of Earth and Environmental Science, University of Potsdam

⁴Institute of Geography Education, University of Cologne

Ongoing advances in DNA extraction and sequencing have made it possible to obtain sequences of organisms, that have died up to hundreds of thousands of years ago.¹ This ancient

DNA (aDNA) reveals insights into evolutionary processes and past population distributions², often with surprising results and conflicting with conclusions, that are based on modern samples alone.

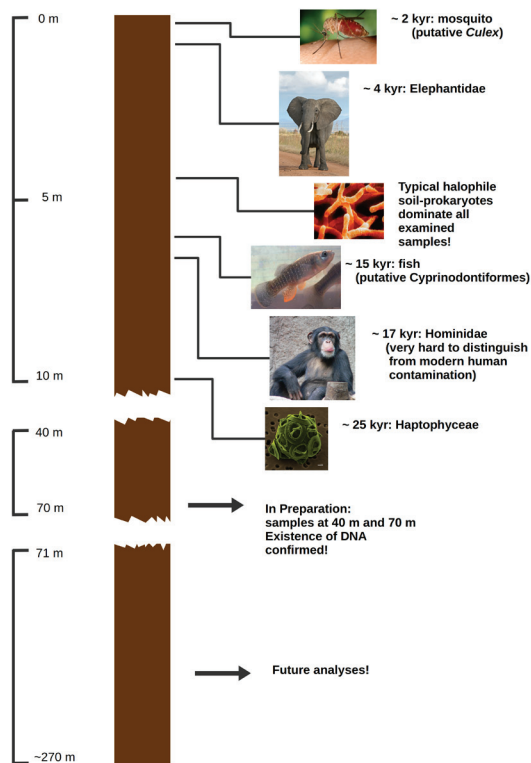


Fig. 1: Scheme of the sediment core. Selected samples of the upper 10 m have been roughly analyzed. A detailed analysis, using “hybridization capture”⁴ will follow and include samples of the upper 70 m.

The Chew Bahir Drilling Project³ is a good example for the usage of aDNA in a palaeoclimatic and evolutionary context. The main aim of the project is to recover aDNA from two ~270 m long sediment cores that have been retrieved from a lake in the Ethiopian desert. Since the sampling site is known for many fossils of early humans, the examination of these sediment cores might provide interesting information about climate, flora and fauna at important stages of human evolution. The genetic analysis of selected samples of the cores aims at providing evidence for the presence of certain taxa of animals, algae and plants, which are informative about environmental conditions.

References:

1. Dabney, J., Meyer, M. & Pa, S. Ancient DNA Damage. *Cold Spring Harb Perspect Biol* 5, 1–7 (2013).
2. Hofreiter, M., Serre, D., Poinar, H. N., Kuch, M. & Pääbo, S. *Ancient DNA*. 2, 3–9 (2001).
3. Chew Bahir Drilling Project. <http://www.geo.uni-potsdam.de/chew-bahir-drilling-project-dfg.html>. (2017-09-13).
4. Walker, J. M. *METHODS IN MOLECULAR BIOLOGY*TM. Life Sciences 531, (2009).

IODP

Enhanced Principal Tensor Analysis as a tool for 3-way geological data reconstructions

S. KOTOV¹, H. PÄLIKE¹

¹MARUM, Bremen Uni., Leobener Str. 8, 28359 Bremen, Germany

Principal tensor analysis (PTA) is considered as a potentially useful tool in geosciences, particularly for reconstructions of paleo-climate multi-way (time -- space -- proxies) datasets. Possible restrictions and main reasons of the method limitation are discussed. We introduce an advanced method of PTA: PTA enhanced with Singular Spectrum Analysis (SSA). The method has been applied to 4-way data tensor (time -- space -- proxies -- delay-time) constructed from marine sediment proxies. The algorithm has been implemented as an R function.

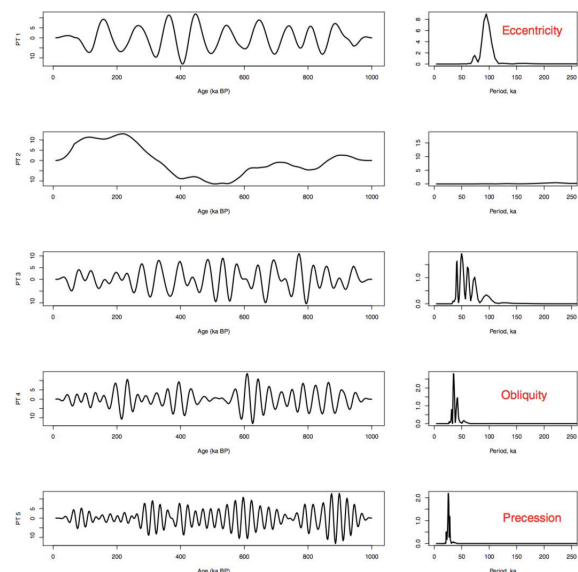


Fig. 1: Scores of 4-way PTA vs age. On the right side - periodograms (period vs amplitude).

References:

- Kotov, S., Pälike, H., 2017. Principal Tensor Analysis as a Tool for Paleoclimatic Reconstructions. In: 18th International Association for Mathematical Geosciences Conference 2017. IAMG, Perth, p. 67.

ICDP

Centennial-scale vegetation dynamics and climate variability in SE Europe during Marine Isotope Stage 11 based on a pollen record from Lake Ohrid

I. KOUSIS¹, A. KOUTSODENDRIS¹, O. PEYRON², N. LEICHER³, A. FRANCKE^{3,4}, B. WAGNER³, M. KNIPPING⁵, J. PROSS¹

¹Paleoenvironmental Dynamics Group, Institute of Earth Sciences, Heidelberg University, Heidelberg

²ISEM, Université de Montpellier, CNRS, IRD, EPHE, Montpellier

³Institute of Geology and Mineralogy, University of Cologne, Cologne

⁴Wollongong Isotope Geochronology Laboratory, School of Earth and Environmental Sciences, University of Wollongong, Wollongong

⁵Institute of Botany, University of Hohenheim, Stuttgart

To better understand climate variability during Marine Isotope Stage (MIS) 11, we present a new, centennial-scale-resolution pollen record from Lake Ohrid (Balkan Peninsula). Our palynological data are derived from sediment cores retrieved

during an International Continental Scientific Drilling Program (ICDP) campaign in 2013. Augmented by quantitative pollen-based reconstructions, they provide insight into the vegetation dynamics and thus also climate variability in SE Europe during one of the best orbital analogues for the Holocene. The comparison of our palynological results with other proxy data from Lake Ohrid as well as with regional and global climate records shows that the vegetation in SE Europe responded sensitively both to long- and short-term climate change during MIS 11. Our study indicates that MIS 11c (~426–398 ka) was the warmest interval of the MIS 11 interglacial, with mean annual temperature (TANN) ranging between 5 and 13°C and mean annual precipitation (PANN) between 340 and 1000 mm. The younger part of the interglacial (i.e., MIS 11b–11a; ~398–377 ka) exhibits a gradual cooling trend. It is characterized by lower TANN values than MIS 11c, ranging from 3 to 9°C, and higher PANN values between 600 and 1200 mm. This interval is marked by considerable millennial-scale variability as documented by six sub-millennial- to millennial-scale forest contractions. Interestingly, a profound, ca. 2-kyrs-long forest setback centered at ~405 ka occurred during full interglacial conditions of MIS 11c. This event was characterized by a substantial reduction in PANN and was likely associated with strong seasonality as suggested by the combination of high summer and low winter insolation. The integration of our data with other regional records suggests that the onset of millennial-scale variability during MIS 11 in Southern Europe was ca. 7 kyrs before the end of MIS 11c, which is earlier than in the marine realm where such a variability occurred only from MIS 11b onwards. This conclusion gains support by the detection of a new tephra layer (i.e., Vico- α , 415±6 ka (Marra et al. (2011)) within MIS 11c, which unequivocally supports the orbitally tuned age model for the Lake Ohrid record (Francke et al., 2016). Finally, our study provides new insight into the presence of several vegetation elements from Europe during the Middle Pleistocene that are now rare and/or extinct, including thermophilous taxa (i.e., *Carya*, *Cedrus*, *Parrotia*, *Pterocarya* and *Tsuga*) and Tertiary relics (i.e., *Picea omorika*, *Zelkova*). Our observations underscore the notion that the Lake Ohrid region served as a refugium for tree taxa during Pleistocene glacials.

References:

- Francke, A., Wagner, B., Just, J., Leicher, N., Gromig, R., Baumgarten, H., Vogel, H., Lacey, J.H., Sadori, L., Wonik, T., Leng, M.J., Zanchetta, G., Sulpizio, R., Giaccio, B., 2016. Sedimentological processes and environmental variability at Lake Ohrid (Macedonia, Albania) between 637 ka and the present. *Biogeosciences* 13, 1179–1196.
- Marra F, Deocampo D, Jackson MD & Ventura G. 2011. The Alban Hills and Monti Sabatini volcanic products used in ancient Roman masonry (Italy): An integrated stratigraphic, archaeological, environmental and geochemical approach. *Earth-Science Reviews*, 108, 115–136.

IODP

Forward modeling of prograding depositional sequences at the New Jersey shallow shelf

A. KOWATSCH¹, S. REICHE¹, A. THOMAS¹, S. BACK²

¹Institute for Applied Geophysics and Geothermal Energy, RWTH Aachen University, Mathieustrasse 10, 52074 Aachen, Germany.

²Institute of Geology & Paleontology, RWTH Aachen University, Wuellnerstrasse 2, 52056 Aachen, Germany.

The flow of terrestrial groundwater to the sea is an important part of the hydrological cycle. One of the best-documented examples of an offshore groundwater system is the occurrence of low-salinity groundwater below the New Jersey continental

shelf, US. This region was targeted by several drilling campaigns (AMCOR, ODP Expedition 150, 174A and IODP Expedition 313) revealing the presence of a complex, low-salinity groundwater distribution up to 400 m below the sea floor. To gain insight and further knowledge on this freshwater system, we aim to perform groundwater flow simulations at the New Jersey shelf using a detailed three-dimensional subsurface model based on seismic, core and logging data. The meaningfulness of such a groundwater model is strongly dependent on the input data and the geological model building workflow applied. To determine the geometrical patterns of geological objects and their associated petrophysical properties, spatial prediction and interpolation techniques must be applied. Kriging, for instance, is a widely-used modeling technique that assumes sediment or rock properties at two points likely to be more similar if these points are located closely together. Correspondingly, as the distance between two points increases, a distance may be reached where a spatial correlation no longer exists. Since well data offshore New Jersey is sparse, often with large distances between individual sites, conventional geostatistical techniques may not be suitable for generating a hydrogeological model.

In this study we test an alternative approach, based on stratigraphic forward modeling in order to reproduce the lateral distribution of sedimentary facies by following a process-based approach. This modeling technique uses the principles of sequence stratigraphy, based on the concept that the depositional record can be subdivided into unconformity-bound units that reflect the sedimentological response to sea-level changes, subsidence, and sediment supply. The value of sequence stratigraphy is to predict the sedimentary facies distribution within the hydrogeological model domain.

The deterministic stratigraphic forward modeling software Dionisos (Granjeon & Joseph, 1999) is used to generate a subsurface model of Miocene prograding sequences by simulating geological processes from late Aquitanian to late Serravallian times. Input parameters and boundary conditions incorporated in the modeling process are derived from seismic and well interpretations and literature data. The simulation is based on gravity- and water-driven diffusive transport processes for different lithologies in continental and marine environments. At each time step, Dionisos accounts for accommodation, sediment supply and sediment transport. As an alternative approach to conventional geostatistical modeling techniques and by honoring key factors such as eustasy, subsidence/uplift and sediment supply, we are presenting a preliminary facies model calibrated to available well data as a basis for subsequent groundwater flow simulations.

References:

- Granjeon, D., Joseph, P., 1999. Concepts and applications of a 3-D multiple lithology, diffusive model in stratigraphic modeling. *Numerical Experiments in Stratigraphy: Recent Advances in Stratigraphic and Sedimentologic Computer Simulations*, SEPM Special Publications No. 62.

IODP

Texture and modelled elastic anisotropy of oceanic crust formed at the slow-spreading mid-Atlantic ridge at Atlantis Massif, sampled during IODP Expedition 357 – First results

R. KÜHN¹, M. STIPP², B. LEISS³, J. KOSSAK-GLOWCZEWSKI⁴,
J. H. BEHRMANN¹

¹Geomar Helmholtz Centre for Ocean Research Kiel, Dep. Marine Geodynamics, Wischhofstr. 1-3, 24148 Kiel, Germany

²Institute of Geology, University of Innsbruck, Innrain 52 f, 6020 Innsbruck, Austria

³Department of Structural Geology and Geodynamics, University of Göttingen, Goldschmidtstraße 3, 37077 Göttingen, Germany

⁴Steinmann Institute, University of Bonn, Poppelsdorfer Schloss, 53115 Bonn, Germany

At slowly spreading ridges discontinuous melt flow is counterbalanced by movement along large faults and shear zones, which can lead to the exhumation of upper mantle rocks. At such locations, ultramafic and mafic rocks are highly altered, resulting in new mineralogies, e.g. talc-amphibole-chlorite schists and serpentinites. Most minerals in these altered lithologies have high single crystal anisotropies, prominent examples being antigorite and talc. Plastic deformation of these rocks leads to a pronounced crystallographic preferred orientation (=texture), predicting high bulk rock elastic anisotropies. IODP Expedition 357 to the Atlantis Massif sampled sheared and altered ultramafic and mafic rocks on an east-west transect across the southern wall of the Massif.

Texture analysis reveals the degree of crystallographic preferred orientation from which the texture-related portion of the elastic anisotropy in these rocks can be modeled. Because of large differences in grain size of fresh and altered rocks, two different methods were used. Neutron texture analysis was applied for coarse grained fresh rocks like gabbros. Experiments were conducted at the SKAT texture goniometer at the Frank Laboratory for Neutron Physics in Dubna, Russia. This instrument is especially suited for large sample volumes necessary to quantitatively determine the texture of coarse-grained rocks. Neutron diffraction, however, cannot be successfully applied to hydrated rocks, like talc schists or serpentinites because neutrons are absorbed. Thus, finer grained, hydrated samples were measured using synchrotron radiation at beamline ID11 at the European Synchrotron Research Facility in Grenoble, France. To compensate for the small beam size of ~1 mm, several slices of the samples were measured in transmission, i.e. measuring the full sample diameter of 15 – 20 mm. Data of both methods were analyzed using Rietveld Texture Analysis leading to the calculation of orientation distribution functions of the major constituent mineral phases, which are then combined with single crystal elastic constants, to model the elastic anisotropy of the rocks studied.

First results show no or weak texture for gabbro, with probably magnetically aligned plagioclase crystals causing the weak texture. This results in weak elastic anisotropies of ~1%. Talc-amphibole-chlorite schists show a strong texture of the included phyllosilicates, a result of ductile shearing in detachment zones. This generates a strong seismic anisotropy of these rocks. Serpentinites so far analyzed show only a weak texture and resulting elastic anisotropy. This unexpected effect may be caused by unconventional lattice disorder of some of the constituent serpentine minerals.

We suppose that syntectonic alteration leading to talc-bearing lithologies might be important in defining shear zones of high seismic anisotropy. Shear zone abundance in the upper-

most layer of hydrated mantle could, therefore, potentially be used as proxy for seismic anisotropy and vice versa. The pattern of seismic anisotropy at slow-spreading ridges is very heterogeneous and localized. This has to be discussed with regard to seismic tomography data from slow-spreading ridges, generally showing lower elastic anisotropy than for oceanic crust and lithosphere created at fast-spreading ridges.

IODP

Shallow subduction channel deformation at the Costa Rica erosive convergent continental margin: frictional behavior of subduction input sediments

R. M. KURZAWSKI^{1,2}, A. R. NIEMEIJER³, M. STIPP⁴, D. CHARPENTIER⁵,
J. H. BEHRMANN¹, C. J. SPIERS³

¹GEOMAR Helmholtz Centre for Ocean Research Kiel, Wischhofstr. 1-3, 24148 Kiel, Germany

²Institute of Geosciences, University of Kiel (CAU), Otto-Hahn-Platz 1, 24118 Kiel, Germany

³HPT-Laboratory, Utrecht University, Budapestlaan 4, 3584 CD Utrecht, The Netherlands

⁴Institute of Geology, University of Innsbruck, Innrain 52, 6020 Innsbruck, Austria

⁵Université de Franche-Comté, 16 Route de Gray, 25030 Besancon Cedex, France

The Costa Rica Seismogenesis Project (CRISP; IODP Expeditions 334 and 344) was designed to study fault zone behavior during earthquake nucleation and rupture propagation at a convergent plate boundary characterized by tectonic erosion. In particular, lithological controls on the onset of seismicity at the updip limit of the seismogenic zone were in the focus of attention. The CRISP study area is located offshore Osa Peninsula (Costa Rica), where active and long-lived subduction erosion occurs along the Middle America Trench. This area is characterized by low sediment supply, fast convergence rate, abundant plate interface seismicity, and a change in subducting plate relief along strike.

The spectrum of slip modes occurring along shallow portions of the plate boundary décollement in subduction zones includes aseismic slip, slow slip, and seismogenic slip. The factors that control slip modes directly influence the hazard potential of subduction zones for generating large magnitude earthquakes and tsunamis. Here, we report on results from hydrothermal rotary shear experiments conducted on simulated fault gouges prepared from CRISP samples. The velocity dependence of friction was explored using all major lithologies, and covering a wide range of conditions representative for the initial stages of subduction. Temperature, effective normal stress, and pore fluid pressure were varied systematically up to 140 °C, 110 MPa and 120 MPa respectively. Sliding velocities up to 100 µm/s, relevant for earthquake rupture nucleation and slow slip, were investigated. The only sediment type that produced frictional instabilities (i.e. laboratory earthquakes) was the calcareous ooze carried by the incoming Cocos Plate, which by virtue of its slip weakening behaviour is also a likely candidate for triggering slow slip events. We evaluate this mechanism of producing unstable slow slip and consider alternatives. Locking and unlocking of plate boundary megathrusts are not only related to variations in pore fluid pressure, but may also depend on the presence of pelagic carbonate-rich lithologies. Subduction systems containing such input are likely low-latitude, with buoyant (i.e. young and/or thick) lower plates.

IODP

Traces of explosive eruptions in Cretaceous to Quaternary Indian Ocean sediments

 S. KUTTEROLF¹, J. C. SCHINDLBECK²
¹GEOMAR, Helmholtz Center for Ocean Research, Kiel

²Institute of Earth Sciences, University of Heidelberg, 69120 Heidelberg, Germany

IODP Expeditions 353 and 362 drilled in the Indian Ocean, ~800 km west of the volcanic front of the Sunda arc. The recovered sediments are intercalated with tephra layers that reach down to the Campanian.

The objectives of the cruises were to determine the material properties causing the seismogenic slip (362) and to reconstruct and understand changes in Indian monsoon circulation (353).

In this project we aim to establish a marine tephrostratigraphic framework for the entire region by correlating widespread tephra layers between the different sites and if possible, to terrestrial eruptions. Therefore we will combine the tephra records of Expeditions 353 and 362 with marine tephra layers from previous ODP drillings from the whole Indian Ocean, and on the Ninetyeast Ridge in particular. Geochemical, petrological and volcanological approaches for tephra and sediment characterization will be used to quantitatively and qualitatively decrypt their provenance and the eruption succession. Additionally, we will perform absolute age dating to improve and confirm the existing age models. Robust age models are needed to study the temporal and spatial changes in eruption processes, magnitudes and frequencies of large volcanic eruptions from the Sunda arc, or so far unknown volcanic sources.

This study will help to learn more about the temporal evolution of different volcanic systems and establish long time series of explosive volcanism in this region. Within our record we will identify large, known, but also previously unknown, eruptions, which will enable us to study the respective recurrence rates from Pleistocene volcanic centres of the Sumatran arc and to elaborate on cyclicities in the tephra record. Finally, we will also study the Miocene to Pleistocene sediment record of the Nicobar Fan to detect potential episodes of enhanced volcanism or single events hidden in the background sedimentation.

Especially the determination of the amount and character of volcanic matter that is incorporated in the sediments is important to characterize the material and how it acts, when it is subducted at the seismogenic and tsunamogenic Sumatran convergent margin.

IODP

IODP Expedition 383: Dynamics of the Pacific Antarctic Circumpolar Current (DYNAPACC)

 F. LAMY*¹, G. WINCKLER*², R. ANDERSON², H. W. ARZ³, G. CORTESE⁴, O. ESPER¹, K. GOHL¹, I. HALL⁵, C. D. HILLENBRAND⁶, C. HÜBSCHER⁷, C. LANGE⁸, L. LEMBKE-JENE¹, A. MARTINEZ-GARCIA⁹, U. NINNEMANN¹⁰, D. NÜRNBERG¹¹, K. PAHNKE¹², A. POLONIA¹³, J. STONER¹⁴, R. TIEDEMANN¹, G. UENZELMANN-NEBEN¹ *Co-CHIEF SCIENTISTS

¹AWI, Bremerhaven, Germany

²Lamont-Doherty Earth Observatory, Columbia University, Palisades, NY, USA

³Leibniz Institute for Baltic Sea Research, Rostock-Warnemünde, Germany

⁴GNS Science, Lower Hutt, New Zealand

⁵School of Earth and Ocean Sciences, Cardiff University, Cardiff, CF10 3AT, UK

⁶British Antarctic Survey, Cambridge, UK

⁷University of Hamburg, Germany

⁸COPAS/IDEAL, University of Concepción, Concepción, Chile

⁹Max-Planck-Institut für Chemie, Mainz, Germany

¹⁰University of Bergen, Norway

¹¹GEOMAR Helmholtz-Zentrum für Ozeanforschung, Kiel, Germany

¹²ICBM, University of Oldenburg, Germany

¹³ISMAR/CNR - Institute of Marine Sciences, Bologna, Italy

¹⁴Oregon State University, Corvallis, USA.

IODP Expedition 383 will investigate the Pliocene-Pleistocene atmosphere-ocean-cryosphere dynamics of the Pacific Antarctic Circumpolar Current (ACC), and their role in regional and global climate and atmospheric CO₂ based on sediment records with the highest possible stratigraphic resolution.

The ACC is the world's largest current system connecting all three major basins of the global ocean (the Pacific, Atlantic and Indian Oceans) integrating and responding to climate signals throughout the globe. By inducing strong upwelling and formation of new water masses, the ACC also fundamentally affects the global meridional overturning circulation (MOC) and the stability of Antarctica's ice sheets, and has been recognized as a key mechanism in regulating variations in atmospheric CO₂ and global climate.

The expedition will test two major scientific hypotheses: (1) ACC dynamics and Drake Passage throughflow conditioned the global Meridional Overturning Circulation and high-low climate linkages on orbital and submillennial time-scales since the Pliocene. (2) Variations in the Pacific ACC determine the physical and biological characteristics of the oceanic carbon pump and atmospheric CO₂.

IODP Expedition 383 will target six primary sites on a transect in the central South Pacific between the modern Polar Front and the Subantarctic Zone, and at the Chilean Margin close to the Drake Passage. Central Pacific sites will document the Plio-Quaternary ACC paleoenvironmental history at water depths ranging from 5100 to 3600 m. At the Chilean Margin the sites provide a depth transect (~1000–3900 m) across the major Southern Ocean water masses that will document Plio-Pleistocene changes in the vertical structure of the ACC—a key issue for understanding the role of the Southern Ocean in the global carbon cycle.

The planned drilling strategy is designed for recovering sediment sequences suitable for ultra-high-resolution studies. The proposed sites are located at latitudes and water depths where sediments will allow the application of a wide range of siliciclastic, carbonate, and opal-based proxies for reconstructing surface to deep ocean variations and their relation to atmosphere and cryosphere changes with unprecedented stratigraphic detail.

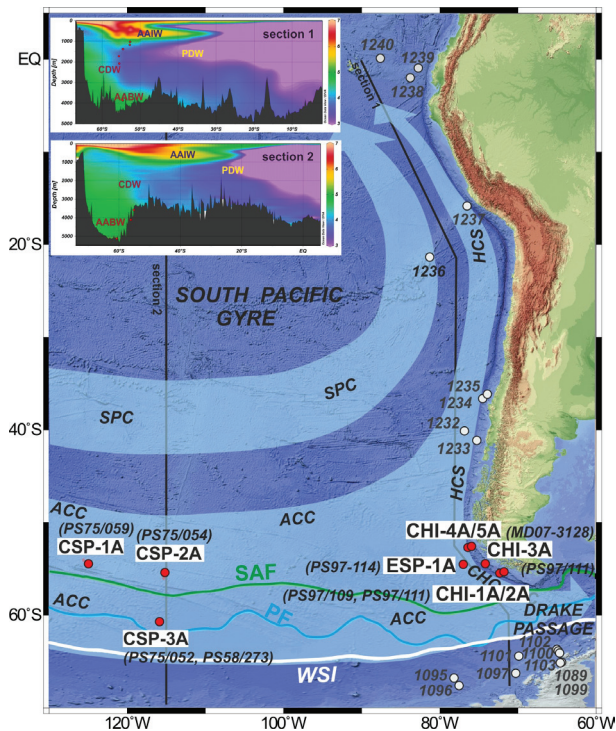


Fig. 1: Map showing the location of the proposed drilling sites in the Pacific ACC (CSP, ESP, and CHI) proposed sites with site survey cores; red dots) and of previously collected cores during various expeditions in the eastern Pacific referred to in text (white dots; ODP Leg 202 Sites 1232–1240; ODP Leg 178 Sites 1095–1102) in context of the modern oceanography. WSI=winter sea-ice; SAF=Subantarctic Front, modern locations after Orsi et al. (1995) and Reynolds (2002; 2007); dotted lines show inferred LGM positions; SPC= South Pacific Current; HCS= Humboldt Current System; CHC= Cape Horn Current; EPR= East Pacific Rise. Small inset figures show vertical water mass structure along two transects in the central and eastern South Pacific (oxygen content; AABW=Antarctic Bottom Water; AAIW=Antarctic Intermediate Water; CDW=Circumpolar Deep Water; PDW=Pacific Deep Water).

IODP

Centennial- to millennial-scale intervals of weak Indian summer monsoon intensity during the last 70 kyr reconstructed from stable isotope ratios of terrestrial *n*-alkanes in sediments from the Bay of Bengal (IODP site U1446)

S. LAUTERBACH¹, N. ANDERSEN¹, T. BLANZ², P. MARTINEZ³,
R. SCHNEIDER^{1,2}

¹Christian-Albrechts-University of Kiel, Leibniz Laboratory for Radiometric Dating and Stable Isotope Research, Max-Eyth-Str. 11–13, 24118 Kiel, Germany

²Christian-Albrechts-University of Kiel, Institute of Geosciences, Ludewig-Meyn-Str. 10–14, 24118 Kiel, Germany

³Université de Bordeaux, UMR CNRS 5805 – Environnements et Paléoenvironnements Océaniques et Continentaux (EPOC), Allée Geoffroy Saint-Hilaire, CS 50023, 33615 Pessac CEDEX, France

Understanding the global climate system and its large-scale climatic teleconnections and feedback mechanisms in the past provides key information for assessing its future behaviour under the influence of anthropogenic climate change and the resulting consequences for modern societies and economies more reliably. This is particularly true for the Asian monsoon

system, whose variability influences the daily life of billions of people and is consequently also of major importance for global economy. Regarding the evidence for past changes in monsoonal rainfall intensity, there are already many long marine proxy records of Indian summer monsoon (ISM) variability from the Arabian and South China Sea available (e.g. Clemens & Prell, 2003; Schulz et al., 1998; Sirocko et al., 1993; Wang et al., 1999), but the number of comparable records from the Bay of Bengal, i.e. from the core zone of the ISM, is still rather limited. In addition, the latter either provide only information about monsoon-driven paleoceanographic changes (e.g. ocean surface salinity; Kudrass et al., 2001), cover only relatively short time intervals (Contreras-Rosales et al., 2014) or suffer from low temporal resolution, consequently leaving important uncertainties regarding long- and short-term changes of the ISM as well as their terrestrial impact.

Nonetheless, previous studies on Asian palaeomonsoon archives, particularly on Chinese and Indian speleothems (e.g. Cai et al., 2015; Kathayat et al., 2016; Wang et al., 2001) but also on marine sediments (e.g. Saraswat et al., 2013), have provided evidence for centennial- to millennial-scale reductions in monsoonal precipitation across Asia, so-called weak monsoon intervals (WMIs). These WMIs occurred synchronously to cold Heinrich events in the North Atlantic realm. This points towards a large-scale climatic teleconnection between the North Atlantic and the Asian monsoon system also on shorter than orbital time scales and thus a different forcing than Northern Hemisphere summer insolation. However, the exact mechanisms behind this relationship as well as possible influences of low-latitude and/or Southern Hemisphere forcing on ISM variability are still not fully understood.

Drilled during Leg 353 in January 2015, IODP site U1446 (Clemens et al., 2016) provides a well-suited marine sediment record from the northwestern Bay of Bengal that will be analysed for the stable hydrogen and carbon isotope composition ($\delta^2\text{H}$, $\delta^{13}\text{C}$) of terrestrial leaf wax *n*-alkanes preserved in the sediments, aiming to reconstruct ISM variability during the last 70 kyr at centennial-scale resolution. IODP site U1446 is characterized by a very high sedimentation rate ($\sim 16 \text{ cm kyr}^{-1}$; Clemens et al., 2016) and is ideally located at a relatively near-shore position, ensuring high input of terrestrial organic matter via river runoff. As it is furthermore located within the reach of the Ganges–Brahmaputra river system, which drains a large part of the ISM core zone, $\delta^2\text{H}$ and $\delta^{13}\text{C}$ records of terrestrial leaf wax *n*-alkanes from IODP site 1446 are supposed to directly reflect past precipitation and vegetation changes on the Indian subcontinent at high temporal resolution. In combination with other proxy data obtained from the same sediment core (e.g. μXRF , pollen, alkenone-based U^k_{37} , sea surface temperature) and in comparison with other regional proxy records, the project is therefore expected to provide a comprehensive view on ISM changes and their trigger mechanisms during the last 70 kyr and particularly on centennial- to millennial-scale WMIs.

References:

- Cai, Y., Fung, I.Y., Edward, R.L., An, Z., Cheng, H., Lee, J.-E., Tan, L., Shen, C.-C., Wang, X., Day, J.A., Zhou, W., Kelly, M.J. & Chiang, J.C.H. (2015): Variability of stalagmite-inferred Indian monsoon precipitation over the past 252,000 y. *Proc. Natl. Acad. Sci. U. S. A.* 112, 2954–2959.
- Clemens, S.C., Kuhnt, W., LeVay, L.J. & the Expedition 353 Scientists (2016): Indian Monsoon Rainfall. *Proceedings of the International Ocean Discovery Program 353*. College Station, TX (International Ocean Discovery Program).
- Clemens, S.C. & Prell, W.L. (2003): A 350,000 year summer-monsoon multiproxy stack from the Owen Ridge, Northern Arabian Sea. *Mar. Geol.* 201, 35–51.
- Contreras-Rosales, L.A., Jennerjahn, T., Tharammal, T., Meyer, V., Lückge, A., Paul, A. & Scheffuß, E. (2014): Evolution of the Indian Summer Monsoon and terrestrial vegetation in the Bengal region during the past 18 ka. *Quat. Sci. Rev.* 102, 133–148.

- Kathayat, S.W., Cheng, H., Sinha, A., Spötl, C., Edwards, R.L., Zhang, H., Li, X., Yi, L., Ning, Y., Cai, Y., Lui, W.L. & Breitenbach, S.F.M. (2016): Indian monsoon variability on millennial-orbital timescales. *Sci. Rep.* 6, 24374.
- Kudrass, H.R., Hofmann, A., Doose, H., Emeis, K. & Erlenkeuser, H. (2001): Modulation and amplification of climatic changes in the Northern Hemisphere by the Indian summer monsoon during the past 80 k.y. *Geology* 29, 63–66.
- Saraswat, R., Lea, D.W., Nigam, R., Mackensen, A. & Naik, D.K. (2013): Deglaciation in the tropical Indian Ocean driven by interplay between the regional monsoon and global teleconnections. *Earth Planet. Sci. Lett.* 375, 166–175.
- Schulz, H., von Rad, U. & Erlenkeuser, H. (1998): Correlation between Arabian Sea and Greenland climate oscillations of the past 110,000 years. *Nature* 393, 54–57.
- Sirocko, F., Sarnthein, M., Erlenkeuser, H., Lange, H., Arnold, M. & Duplessy, J.C. (1993): Century-scale events in monsoonal climate over the past 24,000 years. *Nature* 364, 322–324.
- Wang, L., Sarnthein, M., Erlenkeuser, H., Grimalt, J., Grootes, P., Heilig, S., Ivanova, E., Kienast, M., Pelejero, C. & Pflaumann, U. (1999): East Asian monsoon climate during the Late Pleistocene: high-resolution sediment records from the South China Sea. *Mar. Geol.* 156, 245–284.
- Wang, Y.J., Cheng, H., Edwards, R.L., An, Z.S., Wu, J.Y., Shen, C.-C. & Dorale, J.A. (2001): A high-resolution absolute-dated Late Pleistocene monsoon record from Hulu Cave, China. *Science* 294, 2345–2348.

ICDP

3D-VSP experiment at the Alpine Fault DFDP-2 drill site in Whataroa, New Zealand

V. LAY¹, S. BUSKE¹, S. B. BODENBURG¹, J. TOWNEND², R. KELLETT³, M. SAVAGE², J. ECCLES⁴, D. SCHMITT⁵, A. CONSTANTINO⁶, M. BERTRAM⁷, K. HALL⁷, D. LAWTON⁷, A. GORMAN⁸ AND DFDP WHATAROA 2016 SCIENCE TEAM

¹Institute of Geophysics and Geoinformatics, TU Bergakademie Freiberg, 09596 Freiberg

²Victoria University Wellington, Wellington, New Zealand

³GNS Science, Lower Hutt, New Zealand

⁴University of Auckland, Auckland, New Zealand

⁵University of Alberta, Edmonton, Canada

⁶Schlumberger, London, United Kingdom

⁷University of Calgary, Calgary, Canada

⁸University of Otago, Dunedin, New Zealand

Introduction

The plate-bounding Alpine Fault in New Zealand is an 850 km long transpressive continental fault zone that is late in its earthquake cycle. The Deep Fault Drilling Project (DFDP) aims to deliver insight into the geological structure of this fault zone and its evolution by drilling and sampling the Alpine Fault at depth (Townend et al., 2009). Results from the drilling reveal an active hydrothermal circulation system in the hanging wall with a wider damage zone around the main Alpine Fault core (Townend et al., 2017), however, the detailed structures of the fault system remain unknown.

Previously analysed 2D reflection seismic data image the main Alpine Fault reflector at a depth of 1.5–2.2 km with a dip of approximately 48° to the southeast below the DFDP-2 borehole (Lay et al., 2016). Additionally, there are indications of a more complex 3D fault structure with several fault branches which have not yet been clearly imaged in detail.

Data Set

For that reason we acquired a 3D-VSP seismic data set at the DFDP-2 drill site in January 2016. A zero-offset VSP and a walk-away VSP survey were conducted using a Vibroseis source. Within the borehole, a permanently installed “Distributed Acoustic Fibre Optic Cable” (down to 893 m) and a 3C Sercel slimwave tool (down to 400 m) were used to record the seismic wavefield. A first analysis of both borehole data sets shows a good correlation of both recording systems (Constantinou et al., 2016). Furthermore, the velocity features coincide with results obtained previously from borehole logging.

In addition, various receiver systems recorded the seismic wavefield at the surface: (i) an array of 160 three-component receivers, moved successively along the valley during the survey, (ii) two lines of 400 Aries vertical-component receivers parallel to source lines, (iii) five Reftek stations and (iv) a small-aperture far-offset vertical-component geophone array.

In the following, we will discuss the data set for the three-component receiver array in more detail. First, the receivers were widely distributed within the Whataroa valley during the multi-offset source lines. This data set is used to verify and improve the existing velocity model derived from a previously acquired 2D reflection line (Lay et al., 2016).

Second, a source loop with 71 different source locations was acquired with a total of 3502 sweeps. The 160 receivers were set up as an array with a spacing of 10 m perpendicular and 20 m parallel to the main strike of the Alpine Fault. The whole array was moved successively along the valley twelve times to record reflections from the main Alpine Fault zone over a broad depth range. Altogether, 1916 receiver locations were recorded for the 71 source locations. Thus, the detailed 3C array densely covers an area within Whataroa valley of approximately 1800 m inline along the river (i.e., perpendicular to the fault strike) and 600 m crossline perpendicular to the river (i.e., parallel to the fault strike).

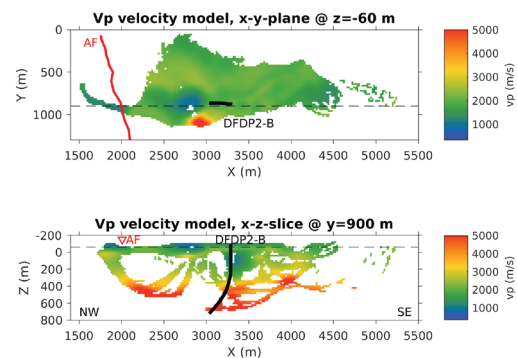


Fig. 1: The tomographic P-wave velocity model using all subsets of the data set is shown for parts with sufficient ray coverage. The borehole trajectory of the DFDP-2B borehole (black) and the assumed Alpine Fault surface trace (red) are marked. Top: x-y plane at a depth of $z = -60$ m. Bottom: x-z slice at $y = 900$ m. Note that the location of the respective other slice is marked by a dashed line.

Processing and Results

A detailed 3D velocity model was derived by first arrival tomographic inversion (see Fig. 1). Subsets of the whole data set were analysed separately to estimate the corresponding ray coverage and the reliability of the observed features in the obtained velocity model. After testing various inversion parameters and starting models, the final detailed near surface velocity model reveals the significance of the old glacial valley structures. Shallow high velocities correlate with the southwestern valley flanks (circa at $y = 1100$ m) and indicate 3D structures that were not detectable with the previous 2D data set. Additionally, analyses of the first-arrivals recorded in the borehole show systematically slower P-wave velocities in comparison to arrivals at surface recorders. Taking into account the different raypaths, this can be explained by anisotropy which would be in agreement with the geologically identified foliated schists and mylonites dipping $\sim 50^\circ$ to the Southeast (Toy et al., 2017).

First simple data processing results shows clear reflections on both inline and crossline profiles. Correlating single reflection

events enables us to identify the origin of reflections recorded in the data and reveal their 3D character. Already preliminary interpretations from this array data set reveal strong evidence for reflections coming presumably from the steeply dipping valley flanks along the Whataroa river side, possibly from the valley flanks. Further detailed analysis is ongoing and will help to understand the 3D subsurface structures causing these reflections.

Outlook

The data will be further analysed using advanced seismic imaging methods to derive a 3D structural image of the valley and the Alpine fault zone at depth. Finally, the results will provide a detailed basis for a seismic site characterization at the DFDP-2 drill site. The existing borehole did not intersect the Alpine Fault at depth, but ended within 200-400 m distance of the principal slip zone, i.e. the fault plane (Toy et al., 2017). Thus, detailed seismic images will be of crucial importance for further structural and geological investigations of the architecture of the Alpine Fault zone in this area.

References:

- Constantinou, A., D. R. Schmitt, R. Kofman, R. Kellest, J. Eccles, D. Lawton, M. Bertram, K. Hall, J. Townend, M. Savage, S. Buske, V. Lay and A. R. Gorman, (2016), Comparison of Fibre Optic Sensor and Borehole Seismometer VSP surveys in a Scientific Borehole - DFDP-2B, Alpine Fault, New Zealand, *SEG Technical Program Expanded Abstracts 2016*: pp. 5608-5612, doi: 10.1190/segam2016-13946302.1
- Lay, V., S. Buske, A. Lukács, A. R. Gorman, S. Bannister, and D. R. Schmitt (2016), Advanced seismic imaging techniques characterize the Alpine Fault at Whataroa (New Zealand), *J. Geophys. Res. Solid Earth*, 121, doi:10.1002/2016JB013534
- Townend, J., Sutherland, R., and V.G. Toy (2009), Deep Fault Drilling Project Alpine Fault, New Zealand, *Scientific Drilling*, 8, Sept 2009, 75-82, doi: 10.2204/iodp.sd.8.12.2009
- Townend, J., Sutherland, R., Toy, V. G., et al., (2017), Petrophysical, Geochemical, and Hydrological Evidence for Extensive Fracture-Mediated Fluid and Heat Transport in the Alpine Fault's Hanging-Wall Damage Zone. *Geochemistry, Geophysics, Geosystems*, doi:10.1002/2017GC007202.
- Toy, V. G., Sutherland, R., Townend, J., et al., (2017), Bedrock geology of DFDP-2B, central Alpine Fault, New Zealand. *New Zealand Journal of Geology and Geophysics*, 60(4), 497-548.

ICDP

Tephrostratigraphy and chronology of the Lake Ohrid DEEP site record of the last 1.4 Ma

N. LEICHER¹, B. WAGNER¹, G. ZANCHETTA², B. GIACCIO³, A. FRANCKE^{1,4}, R. Sulpizio^{5,6}, S. NOMADE⁷, J. JUST^{1,8}

¹ University of Cologne, Institute of Geology and Mineralogy, Cologne, Germany

² Dipartimento di Scienze della Terra, University of Pisa, Pisa, Italy

³ Istituto di Geologia Ambientale e Geoingegneria, CNR, Roma, Italy

⁴ University of Wollongong, Wollongong Isotope Geochronology Laboratory, Wollongong, Australia

⁵ Dipartimento di Scienze della Terra e Geoambientali, University of Bari, Bari, Italy

⁶ Istituto per la Dinamica dei Processi Ambientali (IDPA) CNR, Milan, Italy

⁷ Laboratoire des sciences du climat et de l'environnement, CEA/CNRS/UVSQ, Gif-Sur-Yvette, France

⁸ Faculty of Geosciences, Marine Geophysics, University of Bremen, Germany

The sedimentary archive of Lake Ohrid, located on the Balkan Peninsula, was drilled in 2013 within the scope of the International Continental Scientific Drilling Program (ICDP) and the Scientific Collaboration on Past Speciation Conditions in Lake Ohrid (SCOPSCO) project. It is one of the very few terrestrial archives that cover the last 1.4 Ma continuously and provide high-resolution information about the regional geologi-

cal and paleoclimatic processes, as well as triggers of evolutionary patterns and endemic biodiversity.

At the main drill site DEEP in the centre of the lake a continuous composite profile (584 m) has been compiled out of 4 neighbouring bore holes and was logged (XRF, MSCL) and subsampled for biogeochemical (TIC, TOC, TN, TS) and sedimentological (grain size) analyses. Lithological information from the DEEP site record implies shallow water conditions between 584 and 456 m. The deposition of this sedimentary facies is correlated to the establishment of the lake between 1.9 and 1.4 Ma ago, after the Ohrid basin formed, according to geotectonic, seismic, and biological information, by transtension during the Miocene and opened during the Pliocene and Pleistocene. Since 1.4 Ma (ca. 456 m sediment depth), biogeochemical, and sedimentological proxy data indicate pelagic sedimentation that reflects global glacial/interglacial variability, with warm periods being characterized by high TIC and TOC concentrations and cold periods by negligible TIC and low TOC contents, respectively.

Within the upper 456 m of the sequence 56 tephra horizons were identified so far, 48 of which are macroscopic tephra layers. Juvenile glass fragments of all of these layers were analysed for their major element composition using SEM-EDS/WDS systems (see Leicher et al., 2016 for details). Their geochemical fingerprint suggests a volcanic origin exclusively from the Italian comagmatic provinces. Their active volcanic centres during this time include: the Vulsini, Vico, Sabaitini, Colli Albani, Ernici-Roccamonfina, Pontine Islands, Vulturne, the Aeolian Islands, and unknown-Campanian volcanoes.

The tephrostratigraphic work and correlation of tephra to other records is limited as only few other Mediterranean records cover the period from the Early Pleistocene up to recent times continuously. These records include the Calabrian Ridge core KC01B (Lourens, 2004; Insinga et al., 2014) and the peat record from Tenaghi Philippon, Greece (St. Seymour et al., 2004; Tzedakis et al., 2006; Pross et al., 2015). However, tephrostratigraphic information of these two records are published for the late Pleistocene (max. ca. 192 ka) so far only, from which also additional information from other shorter records exist. The tephrostratigraphic knowledge about the period older 200 ka is based on individual, non-continuous records from various mid-distal Italian intermountain continental basins or continental margin marine basins only (e.g. such as Sulmona, Acerno, Mercure, or Montalbano Jonico) and still relatively poorly understood. Therefore, the Lake Ohrid record provides the unique opportunity to investigate the distal dispersal of tephra from the Italian volcanoes in a continuous record covering the last 1.4 Ma for the first time.

In the interval between 456 and 248 m, representing 1.4 – 0.65 Ma, 15 tephra layers were identified, three of which – between 290 and 267 m could successfully be correlated with ⁴⁰Ar/³⁹Ar dated tephra layers from the Sulmona basin (e.g. Giaccio et al., 2015). These tephra layers bracket the Brunhes/Matuyama transition in both archives and allow a detailed investigation of the timing of the last magnetic pole reversal across different archives. The (so far) uncorrelated tephra layers provide valuable new information about the volcanic activity especially for the time interval >0.8 Ma, and could become important first marker horizons for future tephrostratigraphic work in the region. Additional age control for the lower part of the DEEP site section is given by the detection of the base of the Jaramillo subchron at 374 m (1.07 Ma). Unfortunately, the diagenetic formation of greigite in the sediments mask the top of the Jaramillo subchron (0.99 Ma).

The upper 248 m (<0.65 Ma) contain 41 tephra layers that are important chronological tie points and marker horizons. Thirteen of those layers are described and correlated to known tephra layers in other records in Leicher et al. (2016). New investigations could also allow the correlation of two tephra layers in MIS 6 with eruptions originating from Pantelleria, which were also found in ODP Site 963A in the Sicily Channel (Tamburrino et al., 2012). Trace element compositions of single glass shards of tephra layers from unknown volcanic eruptions were studied by LA-ICP-MS in order to obtain more information about the origin of these eruptions. We could identify new, so far unknown eruptions from the Italian volcanic centres e.g. of Ischia, the Aeolian Arc, or Roccamonfina. In combination with isotopic studies (Sr, Nd) this methodological approach shall also be applied for tephra layers of the interval older 0.65 Ma.

First cryptotephra studies of selected intervals of the DEEP site record emphasize the tephrostratigraphic potential of the Lake Ohrid record. Downcore XRF data indicate six cryptotephra horizons within the sediments of the last 15 ka. Their isochrone position was precisely determined by physical separation and glass shard concentration counting. During MIS 11, the recognition of a cryptotephra correlated with the Vico α eruption (ca. 415 ka) is fundamental for a high-resolution pollen study (Kousis, this issue).

Tephrochronology and magnetostratigraphy are the pivotal tools to develop a chronology for the upper 456 m of the DEEP site sequence. Age modelling is based on the chronological approach that was already successfully applied for the upper 247 m (Francke et al., 2016). The small grain size of crystals of the Lake Ohrid tephra layers has so far prevented direct radioisotopic dating of these layers, but ages of radioisotopically dated equivalent tephra from more proximal sites were imported to the Ohrid record. As the published $^{40}\text{Ar}/^{39}\text{Ar}$ ages come from different laboratories and were processed with different constants and standards, we recalculated all ages with the same constants and flux standards in order to obtain a homogenous set of ages. The tephrochronological and the paleomagnetic age information provide first order tie points for the age-depth model. Second order tie points from tuning biogeochemical proxy data to orbital parameters support the age model down to 456 m. The partly independent and well-established chronology is the backbone to fulfil the major aims of the SCOPSCO project and e.g. allows paleoenvironmental reconstructions or investigations of the origin of Lake Ohrid.

References:

- Francke A, Wagner B, Just J, Leicher N, Gromig R, Baumgarten H, Vogel H, Lacey JH, et al. 2016. Sedimentological processes and environmental variability at Lake Ohrid (Macedonia, Albania) between 637 ka and the present. *Biogeosciences*, 13, 1179-1196.
- Giaccio B, Regattieri E, Zanchetta G, Nomade S, Renne PR, Sprain CJ, Drysdale RN, Tzedakis PC, et al. 2015. Duration and dynamics of the best orbital analogue to the present interglacial, *Geology*, 43, 603-606.
- Insinga DD, Tamburrino S, Lirer F, Vezzoli L, Barra M, De Lange GJ, Tiepolo M, Vallefucio M, et al. 2014. Tephrochronology of the astronomically-tuned KC01B deep-sea core, Ionian Sea: insights into the explosive activity of the Central Mediterranean area during the last 200 ka. *Quaternary Science Reviews*, 85, 63-84.
- Leicher N, Zanchetta G, Sulpizio R, Giaccio B, Wagner B, Nomade S, Francke A & Del Carlo P. 2016. First tephrostratigraphic results of the DEEP site record from Lake Ohrid (Macedonia and Albania). *Biogeosciences*, 13, 2151-2178.
- Lourens LJ. 2004. Revised tuning of Ocean Drilling Program Site 964 and KC01B (Mediterranean) and implications for the $\delta^{18}\text{O}$, tephra, calcareous nannofossil, and geomagnetic reversal chronologies of the past 1.1 Myr. *Paleoceanography*, 19, PA3010.
- Pross J, Christanis K, Fischer T, Fletcher WJ, Hardiman M, Kalaitzidis S, Knipping M, Kotthoff U, et al. 2015. The 1.35-Ma-long terrestrial climate archive of Tenaghi Philippon, northeastern Greece: Evolution, exploration, and perspectives for future research. *Newsletters on Stratigraphy*, 48, 253-276.
- St. Seymour K, Christanis K, Bouzinos A, Papazisimou S, Papatheodorou G, Moran E & Denes G. 2004. Tephrostratigraphy and tephrochronology in

the Philippi peat basin, Macedonia, Northern Hellas (Greece). *Quaternary International*, 121, 53-65.

- Tamburrino S, Insinga DD, Sprovieri M, Petrosino P & Tiepolo M. 2012. Major and trace element characterization of tephra layers offshore Pantelleria Island: insights into the last 200 ka of volcanic activity and contribution to the Mediterranean tephrochronology. *Journal of Quaternary Science*, 27, 129-140.
- Tzedakis PC, Hooghiemstra H & Palike H. 2006. The last 1.35 million years at Tenaghi Philippon: revised chronostratigraphy and long-term vegetation trends. *Quaternary Science Reviews*, 25, 3416-3430.

IODP

North Atlantic Deep Water Provenance during the past one million years

J. M. LINK¹, P. BLASER², M. GUTJAH³, F. PÖPPELMEIER², J. LIPPOLD², K. A. JAKOB², A. H. OSBORNE³, E. BÖHM⁴, M. FRANK³, O. FRIEDRICH², N. FRANK^{1,2}

¹Institute of Environmental Physics, Heidelberg University, Germany

²Institute of Earth Sciences, Heidelberg University, Germany

³GEOMAR Helmholtz Centre for Ocean Research Kiel, Kiel, Germany

⁴LSCE, Gif-sur-Yvette, France

The North Atlantic Ocean plays a crucial role in the global climate as it is one of the regions, where the atmosphere and the deep ocean are in direct contact. Therefore, the understanding of the (paleo)oceanography of this region is one of the key challenges for climate research.

Neodymium (Nd) isotopes are a powerful tool to track past changes of water mass pathways. They are expressed as ϵ_{Nd} , which is the deviation of the measured ratio of $^{143}\text{Nd}/^{144}\text{Nd}$ from that of the chondritic uniform reservoir times 10,000. The continental Nd isotope signal is imprinted into the oceans and therefore different water masses can be distinguished. To establish a record of the past ocean circulation, the Nd isotopic composition can be retrieved from sediment cores. Here, the authigenic ferromanganese coatings of sediment particles, which carry the Neodymium isotopic signature of the past bottom water, are extracted via the protocol of Blaser et al. (2016).

In this project, a sediment core from the Northwest Atlantic, ODP Site 1063 located at the Bermuda Rise at 4584m water depth, was studied. The already existing ϵ_{Nd} record for the past 150 ka (Böhm et al., 2015; Gutjahr and Lippold, 2011; Roberts et al., 2010) was extended back to one million years. For homogeneity and continuity reasons, the previous age model of Poirier and Billups (2014) (250-1030 ka) was complemented by a new age model for the time period between 150 and 250 ka. Therefore, the $\delta^{18}\text{O}$ signal of the benthic foraminifera species *Oridorsalis umbonatus* and *Cibicides wuellerstorfi* was aligned to the LR04 stack of Lisiecki and Raymo (2005). In this way, a continuous and homogeneous age model from 150 to 1030 ka was established.

The neodymium isotope signal at the core site shows in general a typical record of glacial-interglacial variability. During most of the glacial of the past 900 ka, ϵ_{Nd} values between -11 to -12 are recorded, which point to an enhanced presence of a water mass with southern origin (southern-sourced water, SSW). An exception to this typical pattern of more radiogenic ϵ_{Nd} values during glacial maxima is MIS 14, during which the ϵ_{Nd} signal remained unusually unradiogenic. However, this possible absence of SSW at the core site fits well with other climate records from the Northern Hemisphere, which identified MIS 14 as an exceptionally mild and weak glacial (Hao et al., 2015; Lang and Wolff, 2011).

Before MIS 22, which displays the first glacial accompanied by a strong incursion of more SSW to the core site, the

glacials are characterized by rather unradiogenic water mass values.

During each glacial termination (except T-VI), the retrieved ϵ_{Nd} signal changes to unradiogenic values, which indicates the shift to northern-sourced water masses. Hereby, more negative values (ϵ_{Nd} of -16 to -17) were recorded at the start of each interglacial, but usually returned to more modern-like values in their course until they start to fluctuate again during the glacial inception. However, during MIS 11 and 13, the local water masses stayed markedly unradiogenic for an unusually long time period. Those values indicate that there must have been a stronger influence of the northeastern American continent and of (a potentially ice-free) Greenland to the ϵ_{Nd} signal compared to today.

References:

- Blaser, P., Lippold, J., Gutjahr, M., Frank, N., Link, J. M., and Frank, M., 2016, Extracting foraminiferal seawater Nd isotope signatures from bulk deep sea sediment by chemical leaching: *Chemical Geology*, 439, p. 189-204.
- Böhm, E., Lippold, J., Gutjahr, M., Frank, M., Blaser, P., Antz, B., Fohlmeister, J., Frank, N., Andersen, M. B., and Deininger, M., 2015, Strong and deep Atlantic meridional overturning circulation during the last glacial cycle: *Nature*, 517, p. 73-76.
- Gutjahr, M., and Lippold, J., 2011, Early arrival of Southern Source Water in the deep North Atlantic prior to Heinrich event 2: *Paleoceanography*, 26, p. PA2101.
- Hao, Q., Wang, L., Oldfield, F., and Guo, Z., 2015, Extra-long interglacial in Northern Hemisphere during MIS 15-13 arising from limited extent of Arctic ice sheets in glacial MIS 14: *Scientific Reports*, 5, p. 12103.
- Lang, N., and Wolff, E. W., 2011, Interglacial and glacial variability from the last 800 ka in marine, ice and terrestrial archives: *Climate of the Past*, 7, p. 361-380.
- Lisiecki, L. E., and Raymo, M. E., 2005, A Pliocene-Pleistocene stack of 57 globally distributed benthic $\delta^{18}\text{O}$ records: *Paleoceanography*, 20, p. PA1003.
- Poirier, R. K., and Billups, K., 2014, The intensification of northern component deepwater formation during the mid-Pleistocene climate transition: *Paleoceanography*, 29, p. 1046-1061.
- Roberts, N. L., Piotrowski, A. M., McManus, J. F., and Keigwin, L. D., 2010, Synchronous deglacial overturning and water mass source changes: *Science*, 327, p. 75-78.

IODP

Crystallization conditions of fore-arc basalts from the Izu-Bonin-Mariana island arc: new experimental constraints

S. A. LINSLER¹, R. R. ALMEEV¹, F. HOLTZ¹,

¹Institute of Mineralogy, Leibniz Universität Hannover, Callinstr. 3, 30167 Hannover, Germany

The process of subduction is considered as one of the major manifestations of a dynamic Earth. However, little is known about how subduction starts and proceeds. According to one of the first conceptual model of Stern and Bloomer (1992), in the course of subduction initiation, the old and relatively dense oceanic lithosphere begins to sink into the asthenosphere. Lithosphere in the upper plate adjacent to the sinking lithosphere rapidly extends into the gap left as the dense lithosphere sinks. In this setting, mantle flows into the nascent mantle wedge and interacts with a small and variable contribution of fluids from the sinking plate. Melting induced by the fluid augments that resulting from decompression, leading to a higher degree of melting than at mid-ocean ridges. These MORB-like lavas with arc-signatures originating in this setting have been recently termed as *forearc basalts* (FABs, Reagan et al. 2010). Combination of rapid decompression melting with fluid enhanced lowering of the solidus leads to more extensive melting of the shallow asthenospheric wedge, creating refractory Mg-rich and Si-rich lavas such as *boninites* and high-Mg andesites and leaving an extremely refractory harzburgitic residue (Shervais, 2001). In the Stern-Bloomer model, the presence of boninites

at the top of a FAB lava sequence is a major indicator of a subduction-initiation setting (Pearce, 2014). **Thus, the knowledge on the main changes in magma origin and magma evolution conditions at the transition from FAB to boninite is crucial to understand the general process of subduction initiation, the role of mantle reorganization and specifics of mantle melting regimes.**

In 2014 IODP Expedition 352 successfully recovered 1.22 km of igneous basement of FABs and boninites at four drilling sites (Expedition 352 Scientists, 2015). The expected sequence of FABs underlain by boninites was however not encountered. In contrast, dikes at the base of FABs (Sites U1440 and U1441) and boninite (Sites U1439 and U1442) sections provided rather an indication for independent conduit systems for FABs and boninite magmas which were offset more horizontally than vertically (Expedition 352 Scientists, 2015). Here we present the results of petrological and experimental investigations of the recovered fore-arc basalts.

FABs are typically aphyric to sparsely phyrlic, plagioclase-pyroxene-phyric basalts and dolerites. Olivine phenocrysts are not present in lavas, only sporadically crystals have been met in less differentiated glassy samples with more than 8wt% MgO. Its composition ranges from 81 to 76 mol% Fo. Anorthite contents of plagioclase and Mg# number of clinopyroxene pheno- and subphenocrysts cores are ranging from 86 to 60 (mol%) and from 0.86 to 0.53 respectively. Across the Hole U 1440 An in Plag and Mg# in Cpx behaves s-shaped in which the units 2, 3, 7, 8 and 14 show higher An and #Mg values than the remaining units of 3, 6 and 13. Bigger units like 7, 8 and 14 exhibit a higher variability of these values between different sample cores.

The whole rock compositions of FAB lavas erupted at Sites U1440 and U1441 range between 5 and 8 wt% MgO. FAB glass compositions are generally in the range of whole rock compositions. However, they have slightly higher FeO and systematically lower Al_2O_3 , Na_2O and K_2O contents. The differentiation trends obtained from whole rock major element compositions (from basalt to andesite) indicate that the analyzed samples can only be derived from slightly different parental magma compositions. For example, the most primitive FAB magmas from UNIT 3 are too poor in TiO_2 to be parental for the less evolved magmas from other groups. Results of our phase equilibria simulations conducted for several representative starting compositions indicate that a slight variability in primitive FAB magmas is required to let them follow natural liquid lines of descent and match the natural glass compositions. It should be noted that all calculations have been conducted in the range of low melt H_2O contents (0.1 to 0.8 wt%). This low water content was confirmed by FTIR analyses of the dissolved H_2O in naturally quenched glasses. An interesting feature of the FABs is the very narrow compositional range of glass compositions sampled at the top (UNIT 2), the middle (UNITs 7 and 8) and bottom (UNIT 14) of the core in site U1440, indicative of similar magma storage conditions over time. However, this homogeneity of magma storage conditions is sometimes interrupted as demonstrated by the eruption of magmas representative of Units 6 (andesites) and 13 (H_2O -rich). The most evolved glasses from UNIT 6 and intermediate Al_2O_3 -enriched glasses from UNIT 13 cannot be produced by fractional crystallization of primitive melts from the UNITs 2, 7, 8 and 14 and require even more contrasting parental melt compositions. The Unit 6 andesite also requires more than 85% fractionation of magnetite-bearing phase assemblage and has trace element pattern somewhat different from other FABs. The basaltic glass from UNIT 13 strongly differs from other FABs showing anomalously high H_2O contents

(~2 wt%), higher Al₂O₃ and lower FeO indicative of crystallization under hydrous conditions (Danyushevsky, 2001).

The good match of modelled and natural liquid lines of descent observed for UNITS 2, 7, 8 and 14 demonstrate that modelled intensive parameters can be considered as pre-eruptive conditions: low H₂O (0.1-0.8 wt%), and low-pressure (most likely below 100-200 MPa). The low pressure conditions (~100 MPa) have been confirmed by the modelling the conditions of multiple saturation in less differentiated glasses saturated with olivine, plagioclase and clinopyroxene (using the approach from Almeev et al., 2008). It should be noted, however, that application of cpx-melt and plag-melt geothermobarometers (Putirka, 2008) revealed systematically higher pressures and also a larger pressure range of partial crystallization (200-600 MPa). However, such higher pressures are not realistic. At high pressure, FAB melts with their high CaO/Al₂O₃ ~0.9 (in MORBs: CaO/Al₂O₃ < 0.85) should exhibit clinopyroxene alone crystallization on their liquidus. This contradicts with natural observation of the presence of both clinopyroxene and plagioclase (+ olivine in some primitive samples) phenocrysts in lavas.

Crystallization experiments in FABs were designed to address three major goals:

(1) Determination of liquidus phases: in our calculations we were not able to produce Olivine-free Plag-Cpx cotectic crystallization. The modeling predicts that olivine crystallization is expected over a long crystallization interval, even after 30-40% crystallization with melts having 6 to 8 wt% MgO contents, which is predominant in natural FABs. However, olivine is rare in the natural samples and natural FABs with similar MgO concentrations are olivine-free lavas. Therefore one important question is to understand which parameters control the near-liquidus phase assemblage Plag-Cpx in primitive FAB;

(2) Determination of depth of magma storage: the experimental constraints are helpful to resolve the discrepancy in pressure estimates obtained from phase equilibria simulations of FAB crystallization (model COMAGMAT) and from results of mineral-melt geothermobarometry (using Putirka, 2008 formulations);

(3) Determine the role of fractional crystallization in genesis of the FAB magmas.

Two synthetic analogues of the FAB glasses 352-U1440B-12R-2W-67cm and 352-U1440B-24R-1W-13cm (with 8.5 and 7.5 wt% MgO respectively) have been used to determine experimentally equilibrium phase assemblages at 100 MPa under nominally dry conditions in internally heated pressure vessels under intrinsic oxygen fugacity conditions. Two capsule configurations were used to model (a) anhydrous (<0.1 wt% H₂O) and reduced (FMQ-1) conditions using Pt-lined graphite capsules and (b) low H₂O (~0.6 wt% H₂O) and oxidized (FMQ) conditions in Fe-saturated Au₂₀Pd₈₀ capsules. Plagioclase and clinopyroxene were present in products at 1175, 1150 and 1125°C under both anhydrous and low H₂O conditions. This perfectly fits to the phenocrysts assemblage observed in natural FABs. The experimental liquid lines of descent are in a good agreement with those defined by natural glass compositions (Figure 1). This allows us to conclude that thermodynamic conditions utilized in our experiments (100 MPa; 1175-1125°C; FMQ-1 < logfO₂ < FMQ+0.5) can be potentially considered as conditions of partial crystallization of the Units 7-8-14 and 13 FABs. However natural mineral compositions are not fully reproduced (experimental plagioclase is too calcic and clinopyroxenes are too magnesian). In addition, clinopyroxene alone was observed in experiments at high temperature (1200°C) and not the cotectic assemblage Cpx+Plag, which is always observed in the natural Plag+Cpx bearing FAB lavas. This incon-

sistency can be explained either by (1) too high experimental pressure which favours crystallization of the clinopyroxene, or (2) by slight differences between our synthetic starting compositions and the natural FAB glasses. However, strong deviations of the starting compositions from the natural glasses are not observed and the most important changing parameter is the CaO/Al₂O₃ ratio (0.92 in the starting materials and 0.9 in natural counterpart).

To check and constrain the effect of pressure, additional set of experiments at 50 and 200 MPa have been conducted for both dry and low H₂O conditions. At both pressures, only clinopyroxene was observed at 1200°C. Due to the submarine character of FAB magma eruptions, there is no geological evidence to assume partial pressure of crystallization below 50 MPa. Therefore the problem of early Cpx crystallization can be attributed to the slight discrepancy between synthetic starting material and natural glass composition. This does not affect the general results of our experimental simulations (e.g., equilibrium compositions between melts and minerals). However, our observations show that very small variations of CaO/Al₂O₃ ratio influence significantly the phase equilibria and possible the trace element distributions in residual melts.

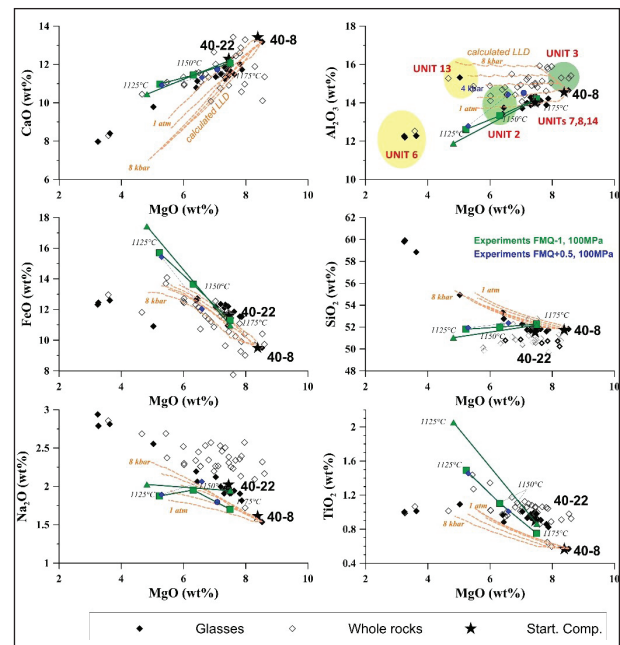


Fig. 1: Comparison of natural FAB whole rock compositions (open diamonds, whole rocks, on-board data, Expedition 352), natural FAB glasses (grey diamonds, microprobe data), residual melt compositions produced in experiments at 100 MPa on 40-8 and 40-22 starting FABs (blue – under FMQ, and green – under CCO redox conditions (~FMQ-1)). Orange dashed lines are liquid lines of descent calculated for starting composition 40-8 in the range of pressures from 1 atm to 800 MPa.

In summary, according to our experimental investigations and results of the modelling we suggest that crystallization of typical FAB magmas should have proceeded in shallow level systems at ~100 MPa. The H₂O content of melts with 6-8 wt% MgO is low (<0.8%). Our experimental data show that residual liquids produced under FMQ-1 and FMQ conditions are nearly identical on Harker diagrams, indicating that variations of redox conditions in the range FMQ-1 - FMQ + 0.5 (corresponding to reducing conditions) are not expected to influence significantly liquid lines of descent. The similar liquid lines of descent are mostly explained by the absence of magnetite in the crystallizing phase assemblage, which is only expected at more

reducing conditions. An additional constraint on the prevailing oxygen fugacity could be obtained by comparing the $\text{Fe}^{2+}/\text{Fe}^{3+}$ ratios in the natural and experimental glasses.

References:

- Almeev, R. R., Holtz, F., Koepke, J., Haase, K. M. & Devey, C. W. (2008). Depths of Partial Crystallization of H₂O-bearing MORB: Phase Equilibria Simulations of Basalts at the MAR near Ascension Island (7°-11°S). *Journal of Petrology* 49 (1), 25-45.
Expedition 352 Scientists. (2015) IODP Prel. Rept. 352.
Danyushevsky, L. V. (2001). The effect of small amounts of H₂O on crystallization of mid-ocean ridge and backarc basin magmas. *Journal of Volcanology and Geothermal Research* 110 (3-4), 265-280.
Pearce, J.A. (2014) Immobile Element Fingerprinting of Ophiolites. *ELEMENTS* 10, 101-108.
Putirka, K. D. (2008). Thermometers and Barometers for Volcanic Systems. *Reviews in Mineralogy and Geochemistry* 69 (1), 61-120.
Reagan, M.K., et al. (2010) Fore-arc basalts and subduction initiation in the Izu-Bonin-Mariana system. *Geochemistry, Geophysics, Geosystems* 11, Q03X12.
Shervais, J.W. (2001) Birth, death, and resurrection: The life cycle of suprasubduction zone ophiolites. *Geochem. Geophys. Geosyst.* 2.

IODP

Evidence of an intense middle to late Miocene “Carbonate Crash” in the Indian Ocean (IODP Site 1443)

J. LÜBBERS¹, W. KUHN¹, A. E. HOLBOURN¹, C. T. BOLTON², E. GRAY²,
K. G. D. KOCHHANN^{1,3}, N. ANDERSEN⁴

¹Institute of Geosciences, Christian-Albrechts-University, 24118 Kiel, Germany

²Aix-Marseille Univ, CNRS, IRD, Coll de France, INRA, CEREGE, 13545 Aix en Provence, France

³Technological Institute of Micropaleontology, Unisinos University, 93022-750 São Leopoldo, Brazil

⁴Leibniz Laboratory for Radiometric Dating and Stable Isotope Research, Christian-Albrechts-University, 24118 Kiel, Germany.

We present high-resolution X-ray fluorescence (XRF) elemental data, carbonate accumulation rates and benthic foraminiferal stable isotopes at an average temporal resolution of ~4.5 kyr from IODP Expedition 353 Site U1443 (5° 23.01'N, 90° 21.7'E; at 2925 m water depth) on the northern extension of the Ninetyeast Ridge in the northeastern Indian Ocean. Comparison of overlapping high-resolution XRF and benthic isotope data initially confirmed that the shipboard sediment splice is accurate and only needed minor adjustment across tie points. We then generated a new chronology by correlating the benthic $\delta^{18}\text{O}$ and $\delta^{13}\text{C}$ curves from IODP Sites U1443 and 1146 (South China Sea, Holbourn et al., 2013), using a minimal tuning approach. The benthic $\delta^{18}\text{O}$ curve reveals a pronounced warming episode at 10.8-10.7 Ma, which was previously reported from ODP Site 1146 and is used as a primary tiepoint between the two records. This transient warming coincides with a marked negative $\delta^{13}\text{C}$ shift and is reminiscent of high-amplitude thermal events, which are paced by 100 kyr variability and characterize the warmer climate mode of the “Miocene Climatic Optimum” (~16.4–14.6 Ma).

Our new records closely track changes in the carbonate cycle and climate during the late middle and early late Miocene (~13.5 to ~7.5 Ma). Decreasing carbonate content together with a marked decrease in sedimentation rates from 0.6 to 0.2 cm/kyr at ~13.2 Ma signal the onset of a prolonged and intense carbonate dissolution episode in the northeastern tropical Indian Ocean, which lasted until ~8.5 Ma and correlates with the “Carbonate Crash” identified in the Equatorial Pacific and Atlantic Oceans (Lyle et al., 1995; Diester-Haass et al., 2004; Preiss-Daimler et al., 2013). The middle to late Miocene

carbonate crash in the tropical Indian Ocean exhibits a two-phase evolution. An older substage is characterized by a series of intensifying carbonate dissolution events and low Log(Ba/Ti), indicating low primary production. At ~11.4 Ma carbonate preservation starts to improve again, Ba/Ti increases markedly, and sedimentation rates show a gradual increase in the second phase of the carbonate crash. The end of the carbonate crash (~8.5 Ma) is marked by increased carbonate preservation, MARs and sedimentation rates.

Global carbonate dissolution events in the open deep ocean may be related to either (1) shelf-basin partitioning of carbonate accumulation, resulting in preferential carbonate deposition on the shelves and depletion of the deep sea carbonate reservoir during periods of sea-level highstands or (2) transient changes in ocean chemistry such as enhanced deep sea carbonate dissolution following regressions, when organic carbon from shallow-marine/terrestrial carbon reservoirs was transferred to the deep ocean, or (3) northward expansion of corrosive southern-sourced water masses following the growth of the East Antarctic ice sheet during the middle to late Miocene. We speculate that carbonate dissolution during the late Miocene carbonate crash was associated with sea level regressions and related release of organic carbon to the ocean system from transient shallow marine-terrestrial carbon reservoirs (e.g., shallow marine organic-rich sediments, marshes, swamps, soil and forests) and/or northward advection of corrosive southern-sourced water masses. In contrast, early to middle Miocene “hyperthermal” dissolution events during the “Miocene Climatic Optimum” (~16.4–14.6 Ma) appear to have been linked to deep ocean acidification, sustained by shelf-basin partitioning of carbonate during periods of overall higher sea-level.

References:

- Diester-Haass, L., Meyers, P. A., and Bickert, T. (2004). Carbonate crash and biogenic bloom in the late Miocene: Evidence from ODP Sites 1085, 1086, and 1087 in the Cape Basin, southeast Atlantic Ocean. *Paleoceanography* 19(1). Doi:10.1029/2003PA000933.
Holbourn, A. E., Kuhn, W., Clemens, S., Prell, W., Andersen, N., 2013. Middle to late Miocene stepwise climate cooling: Evidence from a high-resolution deep water isotope curve spanning 8 million years. *Paleoceanography* 28, 688–699.
Lyle, M., Dadey, K. A., and Farrell, J. W. (1995). 42. The Late Miocene (11–8 Ma) Eastern Pacific Carbonate Crash: evidence for reorganization of deep-water Circulation by the closure of the Panama Gateway. *Proceedings of the Ocean Drilling Program, Scientific Results* 138.
Preiss-Daimler, I. V., Henrich, R., & Bickert, T. (2013). The final Miocene carbonate crash in the Atlantic: Assessing carbonate accumulation, preservation and production. *Marine Geology*, 343, 39-46.

IODP

Quaternary dinoflagellate cyst stratigraphy in the Arctic Ocean: potential and limitations

J. MATTHIESSEN¹, M. SCHRECK², S. DE SCHEPPER³, C. ZORZI⁴,
A. DE VERNAL⁴

¹ Alfred Wegener Institute Helmholtz Centre for Polar and Marine Research, Bremerhaven, Germany

² Department of Geosciences, University of Tromsø – The Arctic University, Tromsø, Norway

³ Bjerknes Centre for Climate Research, Bergen, Norway

⁴ Université du Québec à Montréal, Centre GEOTOP, Montréal, Québec, Canada

Dinoflagellate cysts are valuable microfossils for both biostratigraphy and paleoenvironmental reconstructions in the high northern latitudes. Initial studies on sub-arctic sequences with excellent independent chronostratigraphy demonstrate that robust numerical ages may be defined for bioevents in the Neogene and Quaternary but the biostratigraphic potential has

not been evaluated in the Arctic Ocean. Dinoflagellate cysts are more continuously present in the marginal seas (e.g. Barents Sea, Bering Sea) than in the Arctic Ocean itself throughout the Quaternary. Most species have long stratigraphic ranges, are temporarily absent and show abundance variations on glacial-interglacial timescales. Of the more than 30 taxa recorded, only *Habibacysta tectata* and *Filisphaera filifera* became extinct in the Pleistocene, and their highest persistent occurrences at ca. 1.8 Ma and at ca. 2.0 Ma, respectively, can be used for supra-regional stratigraphic correlation between the Arctic Ocean and adjacent basins. These events corroborate a slow sedimentation rate model for the Quaternary section on the central Lomonosov Ridge but a combination of different methods will have to be applied to provide a detailed chronostratigraphy for the central Arctic Ocean.

ICDP

Cyclic dolomite formation in Lake Van – mechanisms and links to abrupt climate change

J. McCORMACK¹, T. R. R. BONTOGNALI^{2,3}, A. IMMENHAUSER¹,
O. KWIECIEN¹

¹Sediment and Isotope Geology, Ruhr University Bochum, 44801 Bochum, Germany

²Department of Earth Sciences, ETH-Zurich, 8092 Zurich, Switzerland

³Space Exploration Institute, 2000 Neuchâtel, Switzerland

Despite more than 200 years of research, the key factors controlling dolomite occurrence in geological records remain speculative and debated. Modern dolomite-forming environments are often limited to evaporitic settings such as lagoons and sabkhas. Beside microbial mediation, high temperatures and Mg²⁺ concentrations in solution are factors considered important in aiding dolomite formation. Accordingly, episodic occurrence of dolomite in lacustrine successions is commonly uncritically associated with enhanced evaporation, low lake levels and a higher Mg/Ca ratio. This was also the case for the presence of dolomite within deep sediments of alkaline Lake Van (Turkey) (Degens et al., 1984; Landmann et al., 1996; Lemcke & Sturm, 1997; Çağatay et al., 2014).

We systematically studied Lake Van's carbonate inventory in a sedimentary profile covering the last ca. 250 kyr, recovered during the ICDP PALEOVAN drilling campaign in 2010. We document, by means of XRD, SEM and stable isotope ($\delta^{18}\text{O}$ and $\delta^{13}\text{C}$) mass spectrometry, a cyclic occurrence of dolomite-rich intervals (20 – 85 % relative carbonate content). A comparison with published data (ICDP PALEOVAN) suggests that these intervals coincide with periods of high lake level and increased humidity related to suborbital climate variability (Dansgaard-Oeschger cycles). Here, we propose a link between abrupt climate change and dolomite formation.

Combined evidence of SEM imaging showing large, euhedral dolomite crystals interwoven with clay minerals, individual crystals grown together, and heavy $\delta^{18}\text{O}$ signature indicate early diagenetic formation within the sediment below a thick water column at constantly low temperatures (ca. 3 °C). This interpretation is supported by lake level reconstructions (Tomonaga et al., 2017) claiming water depth of at least 150 m at the coring site throughout the interval of interest.

Taking advantage of the independent ICDP PALEOVAN proxy data we investigated the relationship between dolomite nucleation and environmental factors. Early diagenetic, deep water and low temperature dolomite in Lake Van questions the

necessity of evaporative conditions for this mineral formation. We propose that dolomite precipitation in Lake Van (with or without a precursor phase) is a product of a microbially influenced process triggered by ecological stress resulting from episodic re-ventilation of the water-sediment interface following the lake level fall. Independently from the validity of this hypothesis, our results call for a re-evaluation of the palaeoenvironmental conditions often invoked for early diagenetic dolomite-rich intervals within ancient sedimentary sequences (e.g., periods of enhanced aridity and evaporation). False environmental association and overlooking dolomite occurrence in sedimentary records, can compromise carbonate-based palaeolimnological and palaeoclimatic interpretations.

References:

- Çağatay, M. N., Ögretmen, N., Damcı, E., Stockhecke, M., Sancar, Ü., Eriş, K. K., & Özeren, S. (2014). Lake level and climate records of the last 90 ka from the Northern Basin of Lake Van, eastern Turkey. *Quaternary Science Reviews*, 104, 97-116.
- Degens, E. T., Wong, H. K., Kempe, S., & Kurtman, F. (1984). A geological study of Lake Van, eastern Turkey. *Geologische Rundschau*, 73(2), 701-734.
- Landmann, G., Reimer, A., & Kempe, S. (1996). Climatically induced lake level changes at Lake Van, Turkey, during the Pleistocene/Holocene transition. *Global biogeochemical cycles*, 10(4), 797-808.
- Lemcke, G., & Sturm, M. (1997). $\delta^{18}\text{O}$ and trace element measurements as proxy for the reconstruction of climate changes at Lake Van (Turkey): Preliminary results. *NATO ASI Series*, 149, 653-678.
- Tomonaga, Y., Brennwald, M. S., Livingstone, D. M., Kwieciën, O., Randlett, M. E., Stockhecke, M., ... & Schubert, C. J. (2017). Porewater salinity reveals past lake-level changes in Lake Van, the Earth's largest soda lake. *Scientific Reports*, 7, 1-10.

ICDP

Understanding lower crust accretion at fast-spreading mid-ocean ridges: new insights from drill cores obtained by the ICDP Oman Drilling Project: First Results

D. MOCK¹, B. ILDEFONSE², D. GARBE-SCHÖNBERG³, S. MÜLLER³,
D.A. NEAVE¹, J. KOEPKE¹ AND OMAN DRILLING PROJECT PHASE 1 SCIENCE PARTY

¹Institut für Mineralogie, Leibniz Universität Hannover
(d.mock@mineralogie.uni-hannover.de)

²Géosciences Montpellier, Université de Montpellier 2

³Institut für Geowissenschaften, Christian-Albrechts-Universität zu Kiel

The Samail Ophiolite in the Sultanate of Oman and the United Arab Emirates is regarded as the largest and best-exposed analogue of fast-spreading oceanic crust on land. During two drilling phases (December 2016 to March 2017 and November 2017 to March 2018), nine drill cores, each with a length of either 300 or 400 m, were obtained. These cores sample the lower gabbros (GT1), lower to mid-level gabbros (GT2), the dyke-gabbro transition (GT3), listvenites and the basal thrust (BT1), active alteration zones (BA sites) and the crust-mantle boundary (CM sites). The cores of drilling Phase 1 (GT1–GT3 and BT1) were described by the Oman Drilling Project Phase 1 Science Party in summer 2017 on board the Japanese IODP drilling vessel CHIKYU, establishing a close link between IODP and the Oman Drilling Project (OmanDP).

Here, we present the very first results of a project that aims to constrain details of the accretion of the lower oceanic crust, by using two OmanDP cores GT1 and GT2 obtained in the Wadi Jidya (Wadi Tayin Massif, Samail ophiolite). The quantification of textural, petrological and geochemical features should provide information about the origins of different layering types in the lower oceanic crust (e.g., modal layering, cryptic layering, grain size layering) at fast-spreading mid-ocean ridges.

Furthermore, our results will be interpreted in terms of lower crustal formation mechanisms, taking the two most popular end-member models *sheeted sill model* [1] and *gabbro glacier model* [2] into account.

In order to study layer-forming processes, samples of different lithologies and of coherent layer transitions were chosen. In addition to measuring major and trace element compositions, we aim to quantify crystallographic preferred orientations (CPO) and to estimate crystallisation temperatures of the samples, applying a new REE-in-plagioclase-clinopyroxene thermometer [3]. Analyses will be performed in Hannover (electron probe microanalysis), Kiel (laser ablation inductively-coupled plasma mass spectrometry) and Montpellier (France; electron back-scattered diffraction).

The primary lithologies observed in GT1 and GT2 range from gabbros to olivine-rich gabbros; thin ultramafic layers of troctolite or wehrlite can also be observed, which represents a significant improvement in sample quality compared to sampling strongly weathered outcrops at the surface. Moreover, they fundamentally improve the coherence of the crustal section in terms of lithological representativeness. Secondary features like hydrothermal veins or fault zones are very common in the cores. Both cores show clear modal layering at mm- to m-scales. Grain size layering is observed as well, but is not as common as modal layering. Changes in grain size are not necessarily correlated with changes in modal proportions. Beside the main phases plagioclase, clinopyroxene and olivine, small amounts of spinel and orthopyroxene are observable in some individual samples. First mineral analyses reveal Mg# ((Mg / Mg+Fe)*100; molar basis) between 83 and 86 in clinopyroxene and an anorthite content in plagioclase varying between 80 and 87 mol%. Due to secondary alteration processes, most of the olivine grains are strongly serpentinized and therefore not analysable for primary compositions. Single grains in the uppermost samples of the profile have a Mg# of 80. Chemical zoning is observed in plagioclase and clinopyroxene, while olivine shows constant major element contents in core and rim.

References:

- [1] Kelemen, P. B., Koga, K., & Shimizu, N. (1997). Geochemistry of gabbro sills in the crust-mantle transition zone of the Oman ophiolite: Implications for the origin of the oceanic lower crust. *Earth and Planetary Science Letters*, 146(3-4), 475-488.
- [2] Henstock, T. J., Woods, A. W., & White, R. S. (1993). The accretion of oceanic crust by episodic sill intrusion. *Journal of Geophysical Research: Solid Earth*, 98(B3), 4143-4161.
- [3] Sun, C., & Liang, Y. (2017). A REE-in-plagioclase-clinopyroxene thermometer for crustal rocks. *Contributions to Mineralogy and Petrology*, 172(4), 24.

IODP

Coccolith size variations - potential tool for understanding the late Valanginian ocean perturbation

C. MÖLLER¹, A. BORNEMANN², B. RIEGER³, J. MUTTERLOSE³

¹Università degli Studi di Milano, Dipartimento di Scienze della Terra "A. Desio", Via Mangiagalli 34, 20133 Milano, Italy

²Bundesanstalt für Geowissenschaften und Rohstoffe, Stilleweg 2, 30655 Hannover

³Ruhr-Universität Bochum, Fakultät für Geowissenschaften, Institut für Geologie, Mineralogie und Geophysik, Universitätsstr. 150, 44780 Bochum

Strata of late Valanginian age (Early Cretaceous, 139.8-132.9 Ma) record a 1.5 ‰ positive carbon isotope excursion (CIE), the Weissert Event. This event is thought to be related to the volcanic activity of the Paraná-Etendeka large igneous

province. In contrast to the Mesozoic Oceanic Anoxic Events (OAEs), black-shales, organic-rich marine sediments related to perturbations of the marine carbon-cycle, are not commonly associated with the Weissert Event.

Recent biometric studies observed size reductions of certain calcareous nannofossil species along with global environmental perturbations in the Cretaceous. Dwarfism has specifically been described for the mid Cretaceous (~125 - 90 Ma) OAE1a and OAE2. Our biometric analyses of selected nannofossil taxa in samples from the Western Atlantic (DSDP Site 534A), northern Germany (Scharrel 10, Wiedensahl 2), and sections in southern France revealed size reduction of *Biscutum constans* coccoliths in the upper Valanginian.

The implications of coccolith size changes for paleoceanographic questions are still a matter of debate. The paleoenvironmental factors that possibly induced the production of smaller coccoliths include ocean acidification due to excess atmospheric CO₂, high concentrations of toxic trace metals in the ocean water because of strong submarine volcanism, as well as the availability of light and/or nutrients resulting from changes in climate and continental weathering regimes.

ICDP

A Crystallization-Temperature Profile Through Paleo-Oceanic Crust (Wadi Gideah Transect, Oman Ophiolite): Application of the REE-in-Plagioclase-Clinopyroxene Partitioning Thermometer & Implications for a Refined Crustal Accretion Model

S. MUELLER¹, J. HASENCLEVER², D. GARBE-SCHÖNBERG¹, J. KOEPKE³, K. HOERNLE⁴

¹University of Kiel, Institute of Geosciences, Kiel, Germany,

²University of Hamburg, Institute of Geophysics, Hamburg, Germany,

³Leibniz University of Hannover, Institute of Mineralogy, Hannover, Germany,

⁴GEOMAR Helmholtz Centre for Ocean Research Kiel, Kiel, Germany

The accretion mechanisms forming oceanic crust at fast spreading ridges are still under controversial discussion. Thermal, petrological, and geochemical observations predict different end-member models, i.e., the gabbro glacier and the sheeted sill model. They all bear implications for heat transport, temperature distribution, mode of crystallization and hydrothermal heat removal over crustal depth. In a typical MOR setting, temperature is the key factor driving partitioning of incompatible elements during crystallization.

LA-ICP-MS data for co-genetic plagioclase and clinopyroxene in gabbros along a transect through the plutonic section of paleo-oceanic crust (Wadi Gideah Transect, Oman ophiolite) reveal that REE partitioning coefficients are relatively constant in the layered gabbro section but increase for the overlying foliated gabbros, with an enhanced offset towards HREEs. Along with a systematic enrichment of REE's with crustal height, these trends are consistent with a system dominated by in-situ crystallization for the lower gabbros and a change in crystallization mode for the upper gabbros.

Sun and Liang (2017) used experimental REE partitioning data for calibrating a new REE-in-plagioclase-clinopyroxene thermometer that we used here for establishing the first crystallization-temperature depth profile through oceanic crust that facilitates a direct comparison with thermal models of crustal accretion. Our results indicate crystallization temperatures

of about $1220 \pm 8^\circ\text{C}$ for the layered gabbros and lower temperatures of $1175 \pm 8^\circ\text{C}$ for the foliated gabbros and a thermal minimum above the layered-to-foliated gabbro transition. Our findings are consistent with a hybrid accretion model for the oceanic crust. The thermal minimum is assumed to represent a zone where the descending crystal mushes originating from the axial melt lens meet with mushes that have crystallized in situ. These results will be used to verify and test thermal models (e.g., MacLennan et al., 2004, Theissen-Krah et al., 2016) and their predictions for heat and fluid flow and temperature distribution in the oceanic crust.

The current project provides support for the ICDP Oman Drilling Project (<http://www.omandrilling.ac.uk/> and <https://twitter.com/OmanDrillProj>), which started its active phase in December 2016, with drilling of the crustal transects in the Wadi Gideah (Wadi Tayin Massif, Oman ophiolite). We performed several field campaigns, in order to provide a reference frame for the individual crustal drillings within the Oman Drilling Project. Our current project within the SPP ICDP aims to provide constraints on the accretion and evolution of the Oman paleocrust with focus on depth logs with respect to (1) petrology, (2) major and trace element geochemistry on rocks and minerals, (3) crystallographic preferred orientations (CPO), (4) the evolution of hydrothermal alteration and (5) the sulfur cycle. More than 400 collected samples cover the whole oceanic crust from the mantle/crust boundary up to the dike/gabbro transition zone.

References:

- MacLennan, J., Hulme, T., & Singh, S. C. (2004), *G3*, 5(2).
 Sun, C., & Liang, Y., (2017), *CMP*, 172(4).
 Theissen-Krah, S., Rüpke, L. H., & Hasenclever, J. (2016), *GRL*, 43(3).

ICDP

Ganos Fault Zone network: Imaging North Anatolian Fault Zone in the western Marmara region, Turkey, based on a dense local seismic network

B. NAJDAHMADE¹, M. BOHNHOFF^{1,2}, Y. BEN-ZION³, E. GÖRGÜN⁴,
 H. ALP⁴, E. YALÇINKAYA⁴

¹Section 4.2: Geomechanics and Rheology, Helmholtz-Centre Potsdam, GFZ German Centre for Geosciences, Potsdam, Germany

²Institute of Geological Sciences, Free University Berlin, Berlin, Germany

³Department of Earth Sciences, University of Southern California, Los Angeles, California, USA

⁴Department of Geophysical Engineering, Istanbul University, Istanbul, Turkey

The Ganos fault has been activated in a M7.4 event in 1912 and is believed to be a first-order linear and vertical fault that is currently locked down to ~15 km depth. A 40-station seismic network has been deployed in September 2017 at the northeastern part of the Ganos Fault to study the fault-zone geometry at depth. The station layout comprises a higher station density on top of the fault core/damage zone as well a larger inter-station distance away from the fault in different azimuths to ensure both high-resolution fault-zone imaging and good azimuthal coverage for locating local seismic events. Having a network across the fault is an efficient tool to gain a high resolution image of the fault at depth for example by using signals such as fault zone head waves (Najdahmadi et al., 2016) to explore bimaterial interfaces across the fault. The progress report on

the waveform analysis from this network will be presented and discussed.

References:

- Najdahmadi, B., Bohnhoff, M., & Ben-Zion, Y. (2016). Bimaterial interfaces at the Karadere segment of the North Anatolian Fault, northwestern Turkey. *Journal of Geophysical Research: Solid Earth*, 121, 931–950. <https://doi.org/10.1002/2015JB012601>

ICDP

Reconnaissance study of an inferred Quaternary maar structure in the western part of the Bohemian Massif near Neualbenreuth, NE-Bavaria (Germany)

N. NOWACZYK¹, J. ROHRMÜLLER², H. KÄMPF³, E. GEISS⁴,
 J. GROSSMANN⁴, I. GRUN^{1,5}, J. MINGRAM¹, J. MRLINA⁶, B. PLESSEN¹,
 M. STEBICH⁷, C. VERESS⁴, A. WENDT^{8,1}

¹ GFZ German Research Centre for Geosciences, Section 5.2, Telegrafenberg, 14473 Potsdam, Germany

² Bayerisches Landesamt für Umwelt / Bavarian Environment Agency, Leopoldstraße 30, 95615 Marktredwitz, Germany

³ GFZ German Research Centre for Geosciences, Section 3.2, Telegrafenberg, 14473 Potsdam, Germany

⁴ Bayerisches Landesamt für Umwelt / Bavarian Environment Agency, Haunstätter Straße 112, 86161 Augsburg, Germany

⁵ Institute of Earth and Environmental Science, University of Potsdam, Germany

⁶ Institute of Geophysics CAS, Boci II 1401, 141 31 Praha 4, Czech Republic

⁷ Senckenberg Research Station of Quaternary Palaeontology Weimar, 99423 Weimar, Germany

⁸ University of Greifswald, Institute of Geography and Geology, 17489 Greifswald, Germany

The Neualbenreuth dry maar, discovered just a few years ago, turned out to be a complete climate archive for the penultimate glaciation in middle Europe. The former maar lake is hidden in a spruce forest close to the small Upper Palatinate village Neualbenreuth. It aligns along a tectonic fault zone, together with two scoria cones, Železná hůrka and Komorní hůrka, already known for some hundred years, and another dry maar close to Mýtina, just discovered 10 years ago. First evidence for a possible maar eruption were provided by geological/tectonic investigations. By a comprehensive field-geophysical survey, using gravimetric and geomagnetic probing as well as seismic and geoelectric profiling by the Bavarian Environment Agency a hidden maar structure could be discovered close to the german village Neualbenreuth. Finally, a scientific drill core recovered by the Bavarian Environment Agency revealed a sequence of 100 m of lake sediments.

The geophysical, sedimentological, and geochemical analyses of this drill core were performed at the German Georesearch Centre (GFZ) Potsdam. Palynological investigations at the Senckenberg Research Station for Quaternary Palaeontology Weimar supplied additional informations on the vegetational history.

The joint analyses of first results could show that the eruption that formed the Neualbenreuth dry maar must have occurred about 280.000 to 300.000 years ago. The subsequently formed lake compiled sediments with time and got finally silted up about 85.000 years ago. Thus, this recently discovered climate archive provides detailed information about the environmental history of the penultimate glaciation, the so-called ‚Saalian glacial‘ and the subsequent interglacial, the ‚Eemian‘ warm period. Due to advancing glaciers during the last glacial in middle

Europe this time interval was documented only fragmentarily up to now.

Based on the results obtained from the Neualbenreuth drill core, for the first time, geoscientists now could prove the existence of three pronounced warm phases within the ‚Saalian‘ glacial, characterized by a mixed deciduous forest, alternating with a glacial steppe vegetation.

These new findings were obtained within the project **“DRILLING THE EGER RIFT – Crust, mantle, and deep biosphere processes in an active continental rift”**, mainly funded by the International Continental Scientific Drilling Project (ICDP), focussing on the active geodynamics (swarm earthquakes, rising magma, volcanism), the deep-biosphere, and the climate dynamics in the German-Czech borderland.

References:

- J. Rohrmüller, H. Kämpf, E. Geiß, J. Großmann, I. Grun, J. Mingram, J. Mrlina, B. Plessen, M. Stebich, C. Veress, A. Wendt, N. Nowaczyk (2017): Reconnaissance study of an inferred Quaternary maar structure in the western part of the Bohemian Massif near Neualbenreuth, NE-Bavaria (Germany). *International Journal of Earth Science (Geologische Rundschau)*, DOI: 10.1007/s00531-017-1543-0

ICDP

Early Pleistocene vegetation and environmental history from Lake Ohrid

K. PANAGIOTOPOULOS¹, J. HOLTVOETH², R. D. PANCOST², B. WAGNER¹, M. MELLES¹

¹Quaternary Geology Group, Institute for Geology and Mineralogy, University of Cologne, Germany

²Organic Geochemistry Unit, School of Chemistry, University of Bristol, UK

Palynological data with a millennial temporal resolution from the Lake Ohrid DEEP record corresponding to the Early Pleistocene (Marine Isotope Stages 43 to 35) confirm that the Ohrid catchment fostered numerous subtropical species during this interval. Tree species such as *Cedrus*, *Tsuga*, *Carya*, *Pterocarya*, *Cathaya*, *Parrotia*, *Liquidambar*, *Taxodium* and *Eucommia* formed important constituents of the Early Pleistocene flora of the Ohrid catchment (such as *Cedrus* and *Tsuga* with up to 40% and 20% respectively). Pollen percentages of relict tree species (i.e. absent in modern flora of the region) indicate continuous presence in the catchment during interglacials, which are characterized by a remarkable species diversity. These findings are in good agreement with pollen records from Southern Italy and point to the refugial characteristics of the Italian and Balkan peninsulas. Ongoing palynological analyses of the Ohrid DEEP core suggest receding populations of these trees within the catchment throughout the Mid-Pleistocene Transition (MPT) and they become extinct gradually during post-MPT high amplitude climatic cycles (Chalk et al., 2017). There is an increase of conifer tree percentages observed over the study interval with pines dominating pollen spectra during the MIS 38 and MIS 36. Pollen and biomarker data suggest a rather forested landscape with relatively limited erosion activity during interglacial and glacial intervals of the Early Pleistocene.

Maxima in tree pollen and fern spore concentrations in MIS 41 and MIS 35 suggest high terrestrial productivity within the catchment that led to the accumulation of significant plant biomass and to an increased fire frequency within these intervals. Aquatic vascular plant concentrations also show maxima in MIS 41 and MIS 35, but green algae (comprising *Pediastrum* and *Botryococcus* species) values indicating lake productivity are higher within the older half of the study interval (i.e. MIS 43

and MIS 41). Maxima of aquatic vascular plant, herb (mostly grasses including reeds) and green algae concentrations indicate changes in the littoral zone and a higher lake productivity most likely linked to changes in nutrient availability and lake-level fluctuations.

These findings support the working hypothesis presented in the original proposal, namely that a shallower Lake Ohrid is most likely characterized by an extensive littoral zone and more eutrophic conditions in comparison to the deeper oligotrophic lake described in the Late Pleistocene (Sadori et al., 2016, Wagner et al., 2017). Pollen and biomarker findings suggest that Lake Ohrid during the early stages of its existence was an entirely different ecosystem resembling the one found in the Prespa catchment: shallow, with more extended littoral zones, including wetlands, and significantly more productive (Panagiotopoulos et al., 2014; Cvetkovska et al., 2015). Increasing pollen sample resolution (centennial) and concluding biomarker analyses over the entire study interval will significantly improve our understanding of drivers of terrestrial and aquatic ecosystem change in the early stage of the existence of Lake Ohrid.

References:

- Chalk, Thomas, B., Capron, E., Drew, M., Panagiotopoulos, K. (2017): *Interglacials of the 41 ka-world and the Mid-Pleistocene Transition*, QUIGS Workshop report, Past Global Changes Magazine, vol. 25(3), 155. DOI: <https://doi.org/10.22498/pages.25.3.155>.
- Cvetkovska, A., Levkov, Z., Reed, J., Wagner, B., Panagiotopoulos, K., Leng, M. J., Lacey, J. (2015): *Quaternary climate change and Heinrich Events in the southern Balkans: Lake Prespa diatom palaeolimnology from the last interglacial to present*, *Journal of Paleolimnology*. DOI: <http://dx.doi.org/10.1007/s10933-014-9821-3>.
- Panagiotopoulos, K., Böhm, A., Schäbitz, F. & Wagner, B. (2014): *Climate variability over the last 92 ka in SW Balkans from analysis of sediments from Lake Prespa*, *Climate of the Past*, 10, 643-660. DOI: <http://dx.doi.org/10.5194/cp-10-643-2014>.
- Sadori, L., Koutsodendris, A., Panagiotopoulos, K., Masi, A., Bertini, A., Combourieu-Nebout, N., Francke, A., Kouli, K., Joannin, S., Mercuri, A. M., Peyron, O., Torri, P., Wagner, B., Zanchetta, G., Sinopoli, G., Donders, T. H. (2016): *Pollen-based paleoenvironmental and paleoclimatic change at Lake Ohrid (south-eastern Europe) during the past 500 ka*, *Biogeosciences*, 13, 1423-1437. DOI: [10.5194/bg-13-1423-2016](https://doi.org/10.5194/bg-13-1423-2016).
- Wagner B., Wilke T., Francke A., Albrecht A., Baumgarten H., Bertini A., Combourieu-Nebout N., Cvetkoska A., D'Addabbo M., Donders T. H., Föllner K., Giaccio B., Grazhdani A., Hauffe T., Holtvoeth J., Joannin S., Jovanovska E., Just J., Kouli K., Koutsodendris A., Krastel S., Lacey J. H., Leicher N., Leng M. J., Levkov Z., Lindhorst K., Masi A., Mercuri A. M., Nomade S., Nowaczyk N., Panagiotopoulos K., Peyron O., Reed J. M., Regattieri E., Sadori L., Sagnotti L., Stelbrink B., Sulpizio R., Tofilovska S., Torri T., Vogel H., Wagner T., Wagner-Cremer F., Wolff G. A., Wonik T., Zanchetta G., Zhang X. (2016): *The environmental and evolutionary history of Lake Ohrid (FYROM/Albania): Interim results from the SCOPSCO deep drilling project*, *Biogeosciences Discuss.*, <http://www.biogeosciences-discuss.net/bg-2016-475/>.

IODP

Heat exchange through the Indonesian Throughflow during the Middle Pleistocene Transition

B. F. PETRICK¹, G. AUER², A. MARTINEZ-GARCIA¹, D. DE VLEESCHOUWER³, B. A. CHRISTENSEN⁴, C. STOLFI⁴, L. REUNING⁵, T. BUCKLEY⁵, S. J. GALLAGHER⁵, C. S. FULTHORPE⁶, K. BOGUS⁷, G. HAUG¹

¹Max-Planck-Institut für Chemie, Mainz

²Department of Biogeochemistry, JAMSTEC

³MARUM - Center for Marine Environmental Science

⁴School of Earth Sciences, University of Melbourne

⁵Geological Institute, WTH Aachen University

⁶Institute for Geophysics, University of Texas at Austin

⁷Ocean Discovery Program, Texas A&M University

The Mid-Pleistocene Transition (MPT; ~1.4 – 0.4 Ma) represents a climatic shift from obliquity forced climate vari-

ability towards the quasi-100-kyr cyclicity of the Pleistocene ice ages. While high-resolution data covering the MPT from is available from globally distributed archives, there is only sparse evidence on changes in heat exchange between the Pacific and Indian Oceans, which represents a crucial part of the global thermohaline circulation. Deciphering the influence of this heat exchange via the Indonesian Throughflow (ITF) is an important step in understanding the causes of the MPT.

The Leeuwin Current off Western Australia is directly influenced by the ITF and can therefore be used as a tracer of ITF variability during the MPT. We present the first continuous reconstruction of changes in the Leeuwin Current during the MPT using data from IODP Expedition 356 Site U1460, located at 29°S in the path of the Leeuwin current. We reconstruct paleoenvironmental variability by combining XRF, organic geochemistry, ICP-MS and XRD data to reconstruct Leeuwin Current and ITF variability. High sedimentation rates (~30 cm/ka) at Site U1460 provide the opportunity for high-resolution reconstruction of the MPT.

Initial results show clear indications that upwelling off Western Australia intensified during the MPT, indicated by increased primary productivity related to increased nutrient levels, from 900-600 ka. However instead of changes in the Leeuwin Current these changes seem to be more related to strengthening of the West Australian current (WAC) bringing more nutrients to the site. This intensification of the WAC may have had major implications for the global Thermohaline Circulation increasing the amount of cold water input into the Indian Ocean leading to a possible Indian Ocean cooling around 900 ka. This seems to be coupled with an intensification of the Leeuwin current bringing more rainfall to western Australia. There seems to be an indication that the modern ocean circulation at this site was not established until after 600 ka. Therefore it suggests that a combination of changes in the ITF and the WAC both had major impact on Indian Ocean and Global Thermohaline Circulation.

ICDP

Linking downhole logging data and clay mineralogy analysis in the ICDP Lake Junin drilling Project, Peru

S. PIERDOMINICI¹, A. M. SCHLEICHER¹, J. KÜCK¹, D. T. RODBELL²,
 M. B. ABBOTT³ AND THE ICDP LAKE JUNIN WORKING GROUP

¹Helmholtz-Zentrum Potsdam Deutsches GeoForschungsZentrum GFZ, Germany

²Union College, Schenectady, NY 12308, USA

³Dep. Of Geology and Planetary Science, University of Pittsburg, PA 15260-3332, USA

The Lake Junin drilling project, co-funded by the International Continental Scientific Drilling Program (ICDP), was performed during the summer season 2015. This drilling project aims to obtain high-resolution paleoclimate records from lacustrine sediments to reconstruct the history of the continental records covering the glacial-interglacial cycles. Lake Junin is located at 4000 m a.s.l. (what does this stand for?) in the tropical Andes of Peru, and is characterized by a thick (> 125 m) sediment package deposited at a high rate (0.2 to 1.0 mm yr⁻¹). It is one of the few lakes in the tropical Andes that predates the maximum extent of glaciation and is in a geomorphic position to record the waxing and waning of glaciers in the nearby Cordillera, hence making the lake a key site for investigating the Quaternary climate evolution in the inner-tropics of the Southern Hemisphere (Rodbell et al., 2012). Several boreholes

were drilled with the goal to obtain both high-resolution paleoclimate records from lacustrine sediments and to reconstruct the history of the continental records covering the glacial-interglacial cycles. The boreholes reached a maximum depth of 110.08 m and continuous coring was performed at three sites with 11 boreholes. An extensive geophysical downhole logging campaign was performed on five boreholes (1A, 1C, 1D, 2A and 3B) by the Operational Support Group of ICDP and comprise total and spectrum gamma ray, magnetic susceptibility, borehole geometry, temperature, and sonic p-wave velocity. Downhole logging data reveal information about the lithology and lithological changes along the boreholes mostly due to changes in element compositions (K, Th, U). In particular Th and K values are used as a proxy for a first estimate and characterization of clay content in the lake sediments, which are present as montmorillonite, smectite, illite, and kaolinite in different amounts. A more detailed mineralogical and geochemical characterization of the rocks can only be done when analyzing the rock itself. We have personally selected core material from boreholes 3B (103 m) and 1D (110 m) at the LacCore repository in Minneapolis (USA) that showed changes in element distribution first determined in logging data. The samples are selected based on the content and type of silt (massive, medium bedded, mottled, thinly bedded silt). Subsequently X-ray diffraction (XRD) analysis at GFZ laboratory is performed to investigate in detail the bulk mineralogy as well as the clay mineralogy at depth. Linking the clay minerals in core samples with the downhole logging data will allow assessing the geological history of the lake and the relationship to climate change processes.

Reference:

Rodbell, D.T., Abbott, M.B. and the 2011 ICDP Lake Junin Working Group (2012). Workshop on Drilling of Lake Junin, Peru: Potential for Development of a Continuous Tropical Climate Record. *Scientific Drilling*, 13, 58-60.

IODP

Origin of the deepest NW Atlantic water masses during the Last Glacial Maximum and deglaciation

F. PÖPPELMEIER¹, M. GUTJAHN², P. BLASER¹, L. D. KEIGWIN³, J. LIPPOLD¹

¹Institute of Earth Sciences, Heidelberg University, 69120 Heidelberg, Germany (frerk.poepfelmeier@geow.uni-heidelberg.de)

²GEOMAR Helmholtz Centre for Ocean Research Kiel, 24148 Kiel, Germany

³Department of Geology and Geophysics, Woods Hole Oceanographic Institution, Woods Hole, MA 02543, USA

The notion of a shallow northern-sourced intermediate water mass is a well evidenced and widely accepted feature of the Atlantic circulation scheme during the Last Glacial Maximum (LGM; e.g. [1,2]). However, recent observations from stable carbon isotopes ($\delta^{13}\text{C}$) at the Corner Rise in the deep North West Atlantic suggested a significant contribution of a Northern Component Water mass to the abyssal (> 5000 m water depth) North West Atlantic basin that has not been described before [3]. Here we test the hypothesis of this northern-sourced water mass underlying the southern-sourced Antarctic Bottom Water by measuring the neodymium (Nd) isotopic composition from the identical sediment material, IODP Site U1313 and ODP Sites 1059-1061 from Blake Ridge. Neodymium isotopes act as a water mass tag capable of distinguishing between Northern and Southern Component Waters at the North West Atlantic (e.g. [4]).

Our new Nd isotopic record resolves various water mass changes from the LGM to the early Holocene in concert with existing Nd based reconstructions from all over the West Atlantic Ocean. Especially pronounced are the changes during the Younger Dryas and Bølling-Allerød with amplitudes never reported before. For the LGM we found evidence for a northern-sourced water mass contributing to abyssal depth, thus being in agreement with the previous $\delta^{13}\text{C}$ data. Overall, however, the deep North West Atlantic was still dominated by southern-sourced water, excluding the possibility of a distinct northern-sourced water mass. Furthermore, this new record indicates that carbon and Nd isotopes are partly decoupled, hinting to non-conservative behavior of one or more likely of both water mass proxies during the LGM.

References:

- [1] Sarnthein et al. (1994), *Paleoceanography* 9, 209-267
 [2] Curry and Oppo (2005), *Paleoceanography* 20 (1)
 [3] Keigwin and Swift (2017), *PNAS* 114 (11), 1-5
 [4] Roberts et al. (2010), *Science* 327, 75-78

IODP

Evidence for mantle plume origin of the Shatsky Rise from systematics of chalcophile and siderophile elements in volcanic glasses

M. PORTNYAGIN¹, R. ALMEEV², D. GARBE-SCHÖNBERG³

¹ GEOMAR Helmholtz Center for Ocean Research Kiel

² Leibniz Universität Hannover, Institut für Mineralogie

³ Christian-Albrecht University Kiel

Shatsky Rise is a large igneous plateau in Central Pacific, which was formed at a triple-ridge junction in the Early Cretaceous. The compositions of the Shatsky Rise magmas are similar to those of mid-oceanic ridge basalts (MORB) but the magma supply rate during the plateau formation exceeded significantly a typical rate of crust accretion at mid-ocean ridges and implies specific conditions and/or magma source characteristics. In 2009, Integrated Ocean Drilling Program Expedition 324 has cored the Shatsky Rise oceanic plateau to test its plume vs. non-plume origin (Expedition 324 Scientists, 2010). Post-cruise petrological and geochemical studies including isotope determinations of Sr, Nd, Hf and He in the rocks testified that the majority of the Shatsky Rise magmas originated from a slightly enriched MORB-type source and underwent MORB-like crystal fractionation. However the data provided in previous studies, have no conclusive evidence for the Shatsky Rise formation by either deep-sourced mantle plume melting or by melting of a shallow upper mantle enhanced by tectonic processes and/or its fertile composition (e.g., Sano et al., 2012; Husen et al., 2013; Heydolph et al., 2014).

DFG project AL1189/9-1 is aimed to reconcile the origin of the Shatsky Rise using systematics of chalcophile (Cu, Ag, Au, Se) and siderophile (Pt, Ir) elements in volcanic glasses. In the first year of the project, we obtained such data for 48 volcanic glass samples from three IODP sites on Shatsky Rise (U1346, U1347A, and U1350A). The glasses were analysed by LA-ICP-MS using specially designed analytical protocol, which included a number of improvements to precision and sensitivity compared to a conventional analysis and allowed us to quantify low abundance chalcophile elements in natural samples with detection limit as low as 0.2 ppb at spatial resolution of 160 μm . Pressed nanoparticulate powder pellets (Garbe-Schönberg, Müller, 2014) made of 14 international reference rock samples (BHVO-2, BIR-1, JA-2, TDB-1 etc.) were used for calibration

and testify our ability to measure concentrations of rare metals with accuracy of 20% at 1 ppb concentration level. In addition to the aforementioned elements, 50 other trace elements were analysed in the same laser spots, providing consistent and the most comprehensive geochemical data set of Shatsky Rise volcanic glass compositions to date.

The data show that all Shatsky Rise glasses are enriched in Cu (112-375 ppm), Ag (0.04-0.08 ppm), Au (0.6-9.5 ppb) and Pt (0.5-22 ppb) compared to typical MORB. Low-MgO glasses from the oldest Tamu Massif (U1347A site) are extremely enriched in chalcophile and highly siderophile elements (>10x MORB), whereas primitive glasses from Ori (U1350A) and Shirshov (U1346) massifs are less enriched but still plot outside the typical MORB range (e.g. Jenner and O'Neill, 2012). The most primitive (MgO~8.2 wt%) glasses from Ori Massif have Cu and Au contents similar to some Reykjanes Ridge glasses (Atlantic), which are strongly influenced by the Icelandic mantle plume (Webber et al., 2013).

We conclude from the first data that Shatsky Rise magmas were formed by mantle plume melting, which is responsible for the elevated concentrations of chalcophile and highly siderophile elements due to deeper depths and higher degrees of melting compared to MORB. Our future efforts will focus on quantification of the Shatsky magma origin and understanding distinctive enrichments observed for different volcanic massifs comprising the plateau.

References:

- Expedition 324 Scientists (2010). IODP Prel. Rept, 324.
 Jenner, F.E. & O'Neill, H.S.C. (2012). *Geochemistry Geophysics Geosystems* 13, Q02005.
 Garbe-Schönberg, D., Müller S. (2014). *JAAS* 29(6): 990-1000
 Heydolph et al. (2014). *Lithos*, 200–201: 49–63
 Husen, A. et al. (2014). *Geochemistry Geophysics Geosystems* 14, doi:10.1002/ggge.20231.
 Sano, T. et al. (2012). *Geochemistry Geophysics Geosystems* 13, Q08010.
 Webber, A.P. et al. (2013). *Geology* 41 (1), 87-90.

IODP

Floristic and climatic characterization of the New Jersey hinterland during the Oligocene-Miocene transition in relation to major glaciation events

S. PRADER^{1,2}, U. KOTTHOFF^{1,2}, F. M. G. MCCARTHY³, G. SCHMIEDL^{2,4}, T. H. DONDEERS⁵, D. R. GREENWOOD⁶

¹Center for Natural History, Hamburg University, Bundesstraße 55, 20146 Hamburg, Germany

²Institute of Geology, University of Hamburg, Bundesstrasse 55, 20146 Hamburg, Germany

³Department of Earth Sciences, Brock University, 1812 Sir Isaac Brock Way, St. Catharines, Ontario, L2S 3A1, Canada

⁴Center for Earth System Research and Sustainability, Hamburg University, Bundesstraße 55, 20146 Hamburg, Germany

⁵Palaeoecology, Department of Physical Geography, Heidelberglaan 2 3584 CS Utrecht, The Netherlands

⁶Department of Biology, Brandon University, 270 18th Street, Brandon, Manitoba, R7A 6A9, Canada

Mid-Oligocene to Early Miocene sediments from the New Jersey hinterland (eastern North America: IODP-Expedition 313) were analysed for their terrestrial palynomorphs assemblages. Using light microscopy and scanning electron microscopy, altitudinal spatial and long-term temporal vegetation migration in context of global climate change was inferred. The mesophytic forest was the most widespread vegetation type in the hinterland, with *Quercus* (Group *Quercus*, *Quercus*/ *Lobatae* and aff. Group *Protobalanus*) being the dominant taxon.

Pollen grains of the extinct genus *Eotriconobalanus* (Fagaceae) were also documented, as well as *Diospyros*, *Reevesia* or *Gordonia*.

In order to assess topographic palaeovegetation movements during the selected time interval, terrestrial palynomorphs were assigned to six vegetation units. Their relative abundances show only weak temporal and spatial fluctuations, with the units comprising bisaccate pollen grains showing the most pronounced variations and of different intensions.

Periodic changes in vegetation units imply that movements of the plant cover responded to orbital-scale glacial-interglacial changes. Relative abundances of several taxa (e.g. *Carya*) did not change significantly during the Oligocene, but alterations are recognizable when compared with an already published late Middle Miocene record (Prader et al., 2017) from the same area, this probably indicates biotic responses to environmental change. A pollen-based bioclimatic analysis with four standard parameters (mean annual temperature, mean temperatures of the coldest and warmest month, mean annual precipitation) was performed to reconstruct palaeoclimatic changes indicating weak fluctuations in temperature and precipitation.

References:

Prader, S., Kotthoff, U., McCarthy, F.M.G., Schmiedl, G., Donders, T.H., Greenwood, D.R., 2017. Vegetation and climate development of the New Jersey hinterland during the late Middle Miocene (IODP Expedition 313 Site M0027). *Palaeogeography, Palaeoclimatology, Palaeoecology* 485, 854-868.

IODP

Orbital-driven paleovegetation changes in the New Jersey hinterland during a short time interval (300.000 yrs) of the Burdigalian

S. PRADER^{1,2}, U. KOTTHOFF^{1,2}, D. BUNZEL^{2,3}, Y. MILKER^{2,3},
 F. M. G. MCCARTHY⁴, G. SCHMIEDL^{2,3}, D. R. GREENWOOD⁵

¹Center for Natural History, Hamburg University, Bundesstraße 55, 20146 Hamburg, Germany

²Institute of Geology, University of Hamburg, Bundesstrasse 55, 20146 Hamburg, Germany

³Center for Earth System Research and Sustainability, Hamburg University, Bundesstraße 55, 20146 Hamburg, Germany

⁴Department of Earth Sciences, Brock University, 1812 Sir Isaac Brock Way, St. Catharines, Ontario, L2S 3A1, Canada

⁵Department of Biology, Brandon University, 270 18th Street, Brandon, Manitoba, R7A 6A9, Canada

Core sediments from IODP-Expedition 313 to the New Jersey Shallow Shelf (NJSS) bear a diverse and very well preserved marine and terrestrial fossil assemblages, including palynomorphs (e.g. Prader et al., 2017; Prader et al., 2018), allowing the reconstruction of Cenozoic palaeoenvironments. The chronostratigraphic control performed by Browning et al. (2013) permits studying of long-term vegetation dynamics and climate history of eastern North America during the Cenozoic, particularly the Miocene and estimating the relation to global climatic evolution. The Miocene is divide into to two general phases of climatic conditions, a warm time-period during the Early to Middle Miocene (18-14 Ma) and a subsequent cooling and glaciation period (14-5 Ma; Mudelsee et al., 2014).

The orbital configuration, which determined the Miocene climatic conditions and the formation of Antarctic ice sheets were coupled to long-term (400 k.y.) and short-term (100 k.y.) eccentricity cycles minima (Zachos et al, 2001, Abels et al., 2005; Pälike et al., 2006; Holbourn et al., 2007; Liebrand et al., 2011)

Information about episodic vegetation responds during the Miocene related to specific orbital configuration, indicate for

example a coupling of obliquity-triggered spreading of thermophilous elements and a contemporaneous retreat of mesothermic-riparian elements in Spain (Jiménez-Moreno et al., 2007). The observed downward directed movement of a conifer forest of the mid latitudes of Europe however, were most likely dominated by short-term eccentricity minima (Jiménez-Moreno et al., 2009). The most pronounced Miocene glacial phases, like the Mi-1 event (23.03 Ma), the Mi-3a (14.2 Ma) or the Mi-2b (13.8 Ma) have comparable orbital configurations, in which eccentricity cycles minima coincidence with maxima of long-term (1.2 Myr) obliquity modulations (Zachos et al, 2001b, Abels et al., 2005; Pälike et al., 2006; Holbourn et al., 2007; Liebrand et al., 2011). Obliquity highly influenced the seasonality in high latitudes resulting in significant reduction of insulation and low seasonality during obliquity maxima, which pushed the waxing of Antarctic ice sheets (Zachos et al., 2001).

In the light of the above, we have analysed sediment cores from Site M0027 (IODP Exp. 313) in a relative high-temporal resolution to identify orbitally influenced palaeovegetation variability in the hinterland of the NJSS during the Burdigalian (18.0 Ma to 17.7 Ma). Sixty-five samples of the Burdigalian Sequence m5.45 were analyzed for marine and terrestrial palynomorphs. Identified terrestrial palynomorphs were grouped according to Prader et al. (2017) into 7 palaeovegetation units (PVUs). Additionally, mean annual temperature (MAT), mean annual of the coldest month (CMMT) and warmest month (WMMT), mean annual precipitation (MAP) were calculated using the bioclimatic analysis after Greenwood et al. (2005) and Prebble et al. (2017) in order to describe the palaeoenvironmental conditions. To detect periodicities (orbital cycles) within the pollen dataset, Blackman-Tukey spectral analyses were performed using AnalySeries 2.0 (Paillard et al., 1996). Relative abundances of PVU's (1-5) were previously plotted against interpolated ages. A Gaussian broad-band filter (Paillard et al., 1996) was assessed to each PVU to clarify the orbital oscillation signal.

The Blackman-Tukey spectral analyses of Burdigalian PVUs show clear cyclic orbital forced changes, with different responding signals. The spectral analysis suggest an obliquity-triggered responds of PVU-5 (mesophytic forest growing on moist/wet soils) and an eccentricity-triggered forcing of relative abundances of PVU-1 and PVU-2 (high-altitude conifer forest/mid-altitude conifer forest). Our results indicate that eccentricity and obliquity operated in different altitudes and most likely modified specific threshold values, which regulated regional plant productivity and their competition. According to this, the small but significant continental palaeovegetation changes documented during a relatively warm time period with only modest amplitude of climatic variability (Liebrand et al., 2017), emphasises that the palaeovegetation of the New Jersey hinterland was not stable, in opposite to what various climate models indicate (von der Heydt and Dijkstra, 2006; Herold et al., 2011; 2012).

References:

Abels, H.A., Hilgen, F.J., Krijgsman, W., Kruk, R.W., Raffi, I., Turco, E., Zachariasse, W.J., 2005. Long-period orbital control on middle Miocene global cooling: Integrated stratigraphy and astronomical tuning of the Blue Clay Formation on Malta. *Paleoceanography* 20, PA4012, doi:10.1029/2004PA001129.

Browning, J.V., Miller, K.G., Sugarman, P.J., Barron, J., McCarthy, F.M.G., Kulhanek, D.K., Katz, M.E., Feigenson, M.D., 2013. Chronology of Eocene-Miocene sequences on the New Jersey shallow shelf: Implications for regional, interregional, and global correlations. *Geosphere* 9, 1434-1456.

Greenwood, D.R., Archibald, S.B., Mathewes, R.W., Moss, P.T., 2005. Fossil biotas from the Okanagan Highlands, southern British Columbia and northeastern Washington State: climates and ecosystems across an Eocene landscape. *Canadian Journal of Earth Sciences* 42, 167-185.

Herold, N., Huber, M., Müller, R.D., 2011. Modeling the Miocene Climatic Optimum: Part 1 Land and Atmosphere, *Journal of Climate* 24, 6353-6372.

- Herold, N., Huber, M., Müller, R.D., Seton, M., 2012. Modeling the Miocene Climatic Optimum: Ocean circulation, *Paleoceanography* 27, PA1209, doi:10.1029/2010PA002041.
- Holbourn, A., Kuhnt, W., Schulz, M., Flores, J.-A., Andersen, N., 2007. Orbitally-paced climate evolution during the middle Miocene "Monterey" carbon-isotope excursion. *Earth and Planetary Science Letters* 261, 534-550.
- Liebrand, D., Lourens, L.J., Hodell, D.A., de Boer, B., van de Wal, R.S.W., Pälike, H., 2011. Antarctic ice sheet and oceanographic response to eccentricity forcing during the early Miocene. *Climate of the Past* 7, 869-880.
- Liebrand, D., de Bakker, A.T.M., Beddow, H.M., Wilson, P.A., Bohaty, S.M., Ruessink, G., Pälike, H., Batenburg, S.J., Hilgen, F.J., Hodell, D.A., Huck, C.E., Kroon, D., Raffi, I., Saes, M.J.M., van Dijk, A.E., Lourens, L.J., 2017. Evolution of the early Antarctic ice ages. *Proceedings of the National Academy of Sciences* 114, 3867-3872.
- Mudelsee, M., Bickert, T., Lear, C.H., Lohmann, G., 2014. Cenozoic climate changes: A review based on time series analysis of marine benthic $\delta^{18}\text{O}$ records. *Reviews of Geophysics* 52, 333-374.
- Paillard, D., Labeyrie, L., and Yiou, P., 1996. Macintosh program performs time-series analysis, *Eos Transactions of the American Geophysical Union* 77, 379-379.
- Pälike, H., Norris, R.D., Herrle, J.O., Wilson, P.A., Coxall, H.K., Lear, C.H., Shackleton, N.J., Tripathi, A.K., Wade, B.S., 2006. The heartbeat of the Oligocene climate system. *Science* 314, 1894-1898.
- Prader, S., Kotthoff, U., McCarthy, F.M.G., Schmiel, G., Donders, T.H., Greenwood, D.R., 2017. Vegetation and climate development of the New Jersey hinterland during the late Middle Miocene (IODP Expedition 313 Site M0027). *Palaeogeography, Palaeoclimatology, Palaeoecology* 485, 854-868.
- Prader, S., Kotthoff, U., McCarthy, F.M.G., Schmiel, G., Donders, T.H., Greenwood, D.R., 2018. Plants in movement - Floristic and climatic characterization of the New Jersey hinterland during the Palaeogene-Neogene transition in relation to major glaciation events. *Biogeosciences Discussions*. doi.org/10.5194/bg-2017-511.
- von der Heydt, A., Dijkstra, H.A., 2006. Effect of ocean gateways on the global ocean circulation in the late Oligocene and early Miocene. *Paleoceanography* 21, PA1011, doi:10.1029/2005PA001149.
- Zachos, J.C., Shackleton, N.J., Revenaugh, J.S., Pälike, H.B., Flower, B.P., 2001b. Climate response to orbital forcing across the Oligocene-Miocene boundary. *Science* 292, 274-278.

ICDP

North American Plio-Pleistocene sedimentary record from the extinct paleo-lake Idaho, USA – a progress report

A. PROKOPENKO

University of Cologne, Institute for Geology and Mineralogy,
50674 Cologne

A progress report is presented on the current project exploring the potential of a new Plio-Pleistocene sedimentary record recovered in a drill core from the extinct large rift paleo-Lake Idaho, Western USA. This project is a spin-off of the ICDP "Project HOTSPOT", a.k.a "The Snake River Scientific Drilling Project" (2010-2012), as this lake drill core became a 'bonus' of drilling for under- and overlying volcanic sequences of the Snake River Plain. After the Lake Baikal and Lake Elgygytyn Drilling Projects, the paleo-Lake Idaho sediment sequence is in fact the third ICDP-funded lake drill core record to have recovered the warm Pliocene period, the Plio-Pleistocene transition and the initiation of the Northern Hemisphere glaciations at ca. 2.7 Ma, all in one sequence. It is the first record of this kind in continental North America.

Of the ca. 800-meter lake sediment sequence recovered by MHAFB11 drill cores, the Pliocene portion potentially of interest to the paleoclimate studies comprises ca. 320 m and consists primarily of fine calcareous hemipelagic mud. Whole-core magnetic susceptibility record indicates large-scale cycles in sediment deposition. Split-core images and initial description reveal finer variations on centimeter and mm scale, apparent from lamination and variable silt content. The extinction of deep paleo-lake at the study site is marked by the onset of deposition of medium to coarse sand capped by series of thin (8 to 32 cm) basalt flows with hot basal contacts and cold top

contacts with embedding lake sediments. Fine sequence of lake mud pre-dates 2 Ma. It was previously believed that the lake drained because of headwater erosion at its outlet. The new data in the current project suggest, however, that even during the deep-water phase the lake experienced series of repeated significant lowstands which may have been driven by changes in the regional hydrologic balance. The full potential of this new Pliocene sediment archive as a regional paleoclimate record will become better understood with the progress of age model construction based on magnetostratigraphic measurements and with proxy development based on the initial geochemical studies.

IODP

Evidence for selective tungsten enrichment in altered oceanic crust

R. REIFENRÖTHER¹, C. MÜNKER¹, B. SCHEIBNER¹

¹Institut für Geologie und Mineralogie, Universität zu Köln,
Zülpicher Straße 49b, 50674 Köln

A better understanding of the global W cycle between the Earth's different geochemical reservoirs is of great importance for numerous petrological and geochemical models, e.g., for the correct interpretation of the ^{182}Hf - ^{182}W age of core formation. So far, the geochemical behaviour of W in different tectonic settings, such as in fresh oceanic basalts or subduction zones has already been studied [1]. However, it remains uncertain, whether all processes that potentially affect the geochemical cycle of W, i.e. by fractionating W from Th, U and Ta in different geochemical reservoirs have already been fully identified. Due to similar incompatibility of the elements involved, ratios of W/Th and W/U have long been regarded as being constant in most silicate reservoirs and were taken to mass-balance the W cycle.

In contrast to this long-standing view, W enrichments relative to Th and Ta in many arc lavas have recently been found and were explained by fluid-controlled W enrichment in the subarc mantle wedge [2]. However, very little is known, as to whether hydrothermal alteration of the oceanic crust on its path to the subduction factory could already trigger W redistribution and enrichment of W in distinct portions of the oceanic crust. This can be tested by measuring W together with similarly incompatible elements like U, Th or Ta in different sections of the oceanic crust.

Here, we present high-precision W-Th-U-Ta data obtained by isotope dilution for samples from altered oceanic crust. Measurements were performed using mixed U-Th and W-Ta-Zr-Hf-Lu tracers using the Thermo Neptune MC-ICPMS at Cologne. Our sample suite covers well characterised samples from IODP Hole 1256D, covering all major alteration styles within the upper as well as the uppermost part of the lower oceanic crust at a high depth resolution (7-20 m steps). The segment of oceanic crust sampled in IODP Hole 1256D formed at the Cocos-Pacific plate boundary between 19 and 12 Ma ago during an interval of superfast (< 220mm/a) spreading rates. It is the first in-situ borehole comprising a complete section of upper oceanic crust down to the gabbros [3].

Our results demonstrate that systematic fractionation of W from Th, U and Ta within the altered oceanic crust is clearly resolvable, pointing towards a progressive enrichment of W in the Lava and Sheeted Dike Complex sections of Hole 1256D. Additionally, elemental ratios of W/Th, Ta/W and W/U show now overlap with pristine MORB ratios and indicate even larger W

enrichment than reported for arc lavas worldwide that were analysed in previous studies [4].

References:

- [1] Arevalo et al. (2008) *Earth and Planetary Science Letters* 272, 656-665
- [1] König et al. (2008) *Earth and Planetary Science Letters*, 274(1-2), 82 – 92
- [2] Wilson et al. (2006) *Science*, 312, 1016 – 1020
- [3] König et al. (2011) *Geochimica et Cosmochimica Acta*, 75 2119 - 2136

IODP

Sedimentology and geochemistry of peritidal sediments from the Northwest Shelf of Australia and Abu Dhabi

L. REUNING¹, K. SPARWASSER¹

¹EMR – Geological Institute, RWTH Aachen University

Site U1464 drilling during IODP Expedition 356 and located in the Roebuck Basin on the Northwest Shelf of Australia contains a well dated Miocene sequence containing three distinct black layers in close association with evaporites and dolomites (Groeneveld et al., 2017). A similar association of organic matter rich layers in carbonate and evaporite dominated sediments can be found in the coastal sabkha of Abu Dhabi. A modern analogue study including petrographic and geochemical analysis was conducted to show if the Miocene carbonate-evaporite deposits at Site U1464 were deposited in a sabkha environment and will explain the related processes of dolomitisation. The lowermost black layer was deposited during an overall rise in sea-level, whereas the upper two were deposited following a sea-level fall. The carbonates interbedded with these upper two black layers host sulphate minerals (celestite, gypsum, bassanite, anhydrite) and halite also typical for the coastal sabkha of Abu Dhabi. Bright luminescent dolomite at Site U1464 with a lighter oxygen isotope signature likely formed from normal marine Miocene seawater. Dull luminescent dolomite with a heavier oxygen isotope signature likely formed by reflux dolomitisation from circulating brines. In summary, sediments at Site U1464 are more similar to the hyperarid coastal sabkha of Abu Dhabi than to the modern more humid sabkha sediments of Australia.

References:

- Groeneveld, J; Henderiks, J; Renema, W; McHugh, CM; De Vleeschouwer, D; Christensen, BA; Fulthorpe, CS; Reuning, L; Gallagher, SJ; Bogus, K; Auer, G; Ishiwa, T, Australian shelf sediments reveal shifts in Miocene Southern Hemisphere westerlies. *Sci Adv.* 2017 May 10;3(5):e1602567. doi: 10.1126/sciadv.1602567.

ICDP

Long term tectonic and paleoclimatic history of Lake Issyk-Kul, Kyrgyzstan

A. REUSCH¹, V. SPIESS¹, H. KEIL¹, C. GEBHARDT², K. ABDRAKHMATOV³

¹University of Bremen, Faculty of Geosciences, Klagenfurter Straße, 28359 Bremen, Germany

²Alfred-Wegener Institut für Polar- und Meeresforschung, 27568 Bremerhaven, Germany

³Institute of Seismology, NAS KR, Bishkek, Kyrgyzstan

Lake Issyk-Kul in Kyrgyzstan became a potential target for ICDP drilling through a group of scientists who organized an ICDP workshop in 2011 in Baet/Kyrgyzstan (Oberhänsli and Molnar, 2012). Lake Issyk-Kul, located in the Kyrgyz Republic, is one of the deepest and largest lakes in the world. The lake floor is between 600 and 700 m deep. It occupies a deep basin

within the Tien Shan mountain range in Central Asia, which is presently one of the Earth's tectonically most active intra-continental mountain belts. Up to 3500 m of terrestrial sediments have been deposited in the basin, including glacial, fluvio-glacial, fluvial and lacustrine formations (Fortuna, 1993), of which the oldest are believed to date back to Oligocene – Miocene times (Abdrakhmatov et al., 1993; Chedia, 1986).

Lake sediments can act as important “recorders” of the regional processes active during and after their deposition. Lake Issyk-Kul's sediments comprise a promising record of tectonic events and past climate changes in the region, potentially ranging back to Miocene times. In order to gain a better understanding of the deeper lake basin, a multichannel airgun seismic survey was organized, jointly funded by the Museum für Naturkunde Berlin, the University of Bremen, the AWI Bremerhaven, Centre of Seismology, Bishkek, Research Group Marine Technology/Environmental Research, Geosciences, Bremen and the ICDP coordination in May 2013. With these multichannel seismic data, it is possible to investigate the lake history further back in time, including reconstruction of the tectonic evolution, paleoseismic activity as well as climatic indications such as water level fluctuations. Preliminary results indicate seismic penetration down to 500ms TWT in shelf areas (~350 m) and down to the first multiple (~1.8 s) ~675 m below lake-floor, probably deeper, in the deeper basin. Furthermore, anticline structures may be used for ICDP drilling of the complete lake sequence, and an gradually increasing tilt may indicate asymmetric subsidence. Further processing and interpretation work is needed to identify deeper sediment packages. However, due to logistical limitations regarding the equipment during the 2013 campaign, seismic penetration could not reach the target depth of 2 km, and horizontal resolution suffered from a short streamer and low shot rates. Also, due to operational and time limitations, the overall coverage of the large lake was very limited. Since drilling targets had not yet been defined, dedicated site survey was not carried out. Therefore, a new proposal was submitted in August 2017 to DFG for a further seismoacoustic survey campaign as part of parallel proposals for a complementary coring and seismoacoustic survey campaign and to cooperate on preparing an ICDP drilling proposal in the near future. We propose to collect a high quality multichannel seismic dataset and carry out more dedicated survey grids across potential drill sites, e.g. in the vicinity of the anticline ridge. Also, we propose to collect narrow beam sediment echosounder data in order to support a coring campaign and map in detail sedimentary features in the deep basin. The joint research strategy has a focus on drilling the deep lake basin, in the contrary to the 2011 plans where shelf and land drilling had been proposed.

References:

- Abdrakhmatov, K. E., Turdukulov, A. T., and Khristov, E. B., 1993, Detailed seismic zoning of the Issyk-Kul basin.: Ilim Publications. Frunze.
- Chedia, O. K., 1986, Morphology and neotectonics of the Tien Shan: Ilim Publications. Frunze, p. 313.
- Fortuna, A. B., 1993, Detailed seismic profiling of the Issyk-Kul depression.: Ilim Publications.
- Oberhänsli, H., and Molnar, P., 2012, Climate Evolution in Central Asia during the Past Few Million Years: A Case Study from Issyk Kul: *Sci. Drill.*, v. 13, p. 51-57.

IODP

Target-rock fluidization during peak-ring formation of the Chicxulub impact crater inferred from Expedition 364 drill core

U. RILLER¹, F. SCHULTE¹, M. POELCHAU², A. S. P. RAE³, R. A. F. GRIEVE⁴, J. LOFF⁵, J. MORGAN³, N. MCCALL⁶, S. P. C. GULICK⁶.

¹ Institut für Geologie, Universität Hamburg, Bundesstrasse 55, 20146 Hamburg, Germany

² Universität Freiburg, Geologie, Albertstr. 23b, 79104 Freiburg, Germany

³ Department of Earth Science and Engineering, Imperial College London, UK

⁴ Earth Sciences Sector, Natural Resources Canada, Ottawa, Ontario, Canada, K14 0E4

⁵ Géosciences Montpellier, Université de Montpellier, France

⁶ Institute for Geophysics, University of Texas, Austin, TX, USA

The floors of large impact structures are largely flat and contain one or more morphological rings. The formation of the innermost topographic ring, the so-called peak ring, and the causes of target rock weakening leading to observed flat crater floors are not well understood. Constraining these mechanisms is the prime structural geological objective of Expedition 364 “Drilling the K-Pg Impact Crater”, using the Chicxulub impact structure, Mexico, as a terrestrial analogue for the formation of planetary impact basins. A total of 829 meters of core was recovered from borehole M0077A drilled into the peak ring of the Chicxulub crater. From bottom to top, the core is crudely composed of: (1) pervasively shocked granitoid target rock hosting meter- to decameter-thick impact melt rock and suevite dike-like bodies, (2) a 130 m thick impact melt rock and suevite unit overlying the target rocks, and (3) a 112 m thick section of post-impact pelagic carbonate rocks. Based on visual appraisal of the drill core, we determined prominent impact-induced deformation structures in target rock pertaining to rock fluidization during cratering.

In addition to microscopic planar structures formed by shock metamorphism, the target rocks are replete with impact-induced, mesoscopic planar deformation structures. These structures include: (1) cataclastic deformation zones, (2) striated shear faults, (3) crenulated mineral foliations, and (4) ductile shear band structures. Structural overprinting criteria point to a relative age for these structures. Zones of cataclasite are consistently displaced or utilized by shear faults. Cataclasite bands in target rock fragments included in suevite are cut by the latter and a striated target rock fragment was found in impact melt rock. Suevite and impact melt were emplaced in zones of dilation, often localized by shear faults. Collectively, these observations suggest that cataclastic deformation was followed by shear faulting, followed in turn by emplacement of suevite and melt into dilation zones. This succession of deformation mechanisms is corroborated by the observation that suevite and impact melt bodies are devoid of cataclasite and shear faults. These lithologies were still viscous when they were deformed by ductile band structures. Thus, the shear band structures formed after the shear faults. Based on the structural overprinting relationships, we relate the mesoscopic planar structures to cratering stages known from impact mechanics.

IODP

South China Sea tephra and sedimentary basement provenance

J.C. SCHINDLBECK¹

¹Institute of Earth Sciences, University of Heidelberg, 69120 Heidelberg, Germany

The South China Sea (SCS) is a large, relatively young (Mid- to Late Cenozoic) basin in eastern Asia and located in a tectonically complex area at the junction of the Eurasian, Australian, Indian, and Pacific plates. The marine sediment record of the SCS basins record terrestrial input from diverse source regions (e.g., South China, Indochina, Borneo, Sumatra, Taiwan, Philippines) including volcanic input from active volcanic regions, especially from the Philippine and Sumatra volcanic arcs (e.g., Ku et al., 2008, 2009). Longterm explosive eruption records for most of the adjacent volcanoes are not available on land because of erosion or overlying younger sediments or lavas. The marine tephra record therefore provides the opportunity to study the evolution of the explosive volcanism on a longer timescale.

The SCS has been the target area of ODP Expedition 184 in 1999 (Prell, Wang, Blum et al., 1999), IODP Expedition 349 in 2014 (Li, Lin, Expedition 349 Scientists, 2015) and the recent Expeditions 367/368 in 2017 (Stock, Sun, Klaus and the Expedition 367 Scientists, in press; Jian, Larsen, Alvarez Zarikian and the Expedition 368 Scientists, in press) that aimed to study the tectonic and sedimentary history of the different basins.

Within this project I will analyze ash, sediment mixed with ash and sandstone samples from all three expeditions for correlation and provenance studies (collaboration with K. Dadd, Sydney University, C. Liu, Louisiana State University and S. Kutterolf, GEOMAR Kiel). Volcanic ashes found in the sediment sections provide constraints on the activity of the volcanic arcs of the region whereas the sandstones recovered as basement lithology may provide a window in the early basin history.

In detail, I have the following scientific objectives.

- (1) Establish a tephrostratigraphy for the South China Sea, which includes provenance studies as well as correlations between the different sites.
- (2) Determine temporal variations and cyclicities in the volcanic productivity and input of the adjacent area.
- (3) Investigate the provenance and depositional environment of the sedimentary basement to derive the source areas of the clastic components and track their origin temporally with respect to the early basin history and their relation to transport pathways.

References:

- Jian Z, Larsen HC, Alvarez Zarikian C, and the Expedition 368 Scientists (in press) Expedition 368 Preliminary Report: South China Sea Rifted Margin. International Ocean Discovery Program. <https://doi.org/10.14379/iodp.pr.368.2017>
- Ku Y-P, Chen C-H, Newhall CG, Song S-R, Yang TF, Iizuka Y, McGeethin J (2008) Determining an age for the Inararo Tuff eruption of Mt. Pinatubo, based on correlation with a distal ash layer in core MD97-2142, South China Sea. *Quaternary International* 178(1):138-145
- Ku Y-P, Chen C-H, Song S-R, Iizuka Y, Shen JJS (2009) A 2 Ma record of explosive volcanism in southwestern Luzon: Implications for the timing of subducted slab steepening. *Geochemistry, Geophysics, Geosystems* 10(6)
- Li C-F, Lin J, Expedition 349 Scientists (2015) Proceedings of the International Ocean Discovery Program, 349: South China Sea Tectonics: College Station, TX (International Ocean Discovery Program). <http://dx.doi.org/10.14379/iodp.proc.349.2015>
- Prell WL, Wang P, Blum P (1999) Ocean drilling program leg 184 preliminary report: South China Sea. Texas A&M University, College Station, TX
- Stock J, Sun Z, Klaus A, and the Expedition 367 Scientists (in press) Expedition 367 Preliminary Report: South China Sea Rifted Margin. International Ocean Discovery Program. <https://doi.org/10.14379/iodp.pr.367.2017>

IODP

Fault core deformation mechanisms deduced from microstructures, mineralogy and geochemistry of the Alpine Fault, New Zealand

 B. SCHUCK¹, C. JANSSEN¹, A. M. SCHLEICHER², V. G. TOY³, G. DRESEN^{1,4}
¹Helmholtz-Zentrum Potsdam, GFZ, Section 4.2: Geomechanics and Rheology, Telegrafenberg 14473 Potsdam, Germany

²Helmholtz-Zentrum Potsdam, GFZ, Section 3.1: Inorganic and Isotope Geochemistry, Telegrafenberg 14473 Potsdam, Germany

³Department of Geology, University of Otago, P.O. Box 56, Dunedin 9054, New Zealand

⁴Institut für Erd- und Umweltwissenschaften, Universität Potsdam

The transpressive Alpine Fault is the main structure forming the Australian and the Pacific Plate boundary through New Zealand's South Island. It exposes rocks from 35 km depth with a long-term exhumation rate of 6 – 9 mm a⁻¹ (Little et al., 2005). The Alpine Fault is currently locked and it has been demonstrated that it is capable of generating large (i.e. $M_w > 8$) earthquakes with an assumed recurrence interval of 250 years (Nicol, 2016).

The Alpine Schist forms the hanging wall. Over a distance of about 1 km to the fault's principal slip zone (PSZ) it is progressively deformed into an ultramylonite. Fractured ultramylonites and cataclasites comprising the fault's damage zone outcrop within 50 m of the PSZ. The fault core is characterized by a 2 to 30 cm thick package of cataclasites and fault gouge (Toy et al., 2015). The footwall comprises Quaternary fluvio-glacial sediments, overlying metasediments intruded by Paleozoic to Cretaceous granitoids.

The seismogenic zone and the underlying brittle-ductile transition are located at very shallow depths (likely < 8 km) due to the fast uplift rates. This provided motivation to drill the Alpine Fault to investigate seismogenic and brittle-ductile transition processes (Townend et al., 2009). In 2011, two shallow boreholes penetrated the Alpine Fault at 91 m and 128 m depth, respectively, during the first phase of the Deep Fault Drilling Project (DFDP-1) (Sutherland et al., 2012).

We are currently investigating outcrop samples and the DFDP-1 cores to describe and understand strain localization in the fault's PSZ. In this contribution we compare microstructural, mineralogical and geochemical analyses obtained from a transect across the fault core at the Waikukupa Slip location. At this exposure the PSZ is identified as a thin (<5 cm) and continuous band, which is formed by a complex structure consisting of several, clearly distinguishable layers ranging in size from < 1 to 2 cm. X-ray diffraction analysis indicates the mineralogy is mostly quartz, plagioclase, calcite, chlorite, illite and mica. Qualitatively, the mineralogical composition does not vary significantly from the hanging- to the footwall, but there are marked changes in the amount of individual mineral phases. High-resolution scanning and transmission electron microscopy demonstrates characteristic microstructural variations along the investigated transect. Grain sizes in the hanging-wall decrease towards the PSZ, within which pulverized rigid particles range down to 100 nm in size. The PSZ comprises distinct domains, each displaying different microstructures. These characteristically include fragments of mylonite as well as reworked gouge clasts (up to 1.5 and 0.5 cm, respectively) and chemically altered feldspars in a fine-grained matrix that includes newly grown phyllosilicates (mostly illite). Within distinct domains of the PSZ, calcite veins generated during multiple crack-seal events form a dense and anastomosing network with various cross-cutting relationships. These microstructures point to a va-

riety of different deformation mechanisms such as grain scale fracturing, twinning, pressure solution and sealing.

The results presented imply that the PSZ served as pathway for large volumes of Ca-rich fluids circulating within the fault gouge. Additionally, fluid pulses resulted in the precipitation of several vein generations, which represent episodes of dilatant fracturing and sealing of the PSZ. This is notable, because the PSZ acts as an impermeable hydraulic seal in the current interseismic period (Menzies et al., 2016).

References:

- Little, T. A., Cox, S., Vry, J. K. & Batt, G. E. (2005): Variations in exhumation level and uplift rate along the oblique-slip Alpine Fault, central Southern Alps, New Zealand. – *Geological Society of America Bulletin* **117**: pp. 707 – 723.
- Menzies, C. D., Teagle, D., Niedermann, S., Cox, S. C., Craw, D., Zimmer, M., Cooper, M. J., Erzinger, J. (2016): The fluid budget of a continental plate boundary fault: Quantification from the Alpine Fault New Zealand. – *Earth and Planetary Science Letters* **445**: pp. 125 – 135.
- Nicol, A. (2016): Alpine Fault Paleoseismic Record and Seismic Hazard analysis. – *Proceedings of the Annual Conference of the Geoscience Society of New Zealand*, Nov 28 – Dec 1, 2016.
- Sutherland, R., Toy, V. G., Townend, J., Cox, S. C., Eccles, J. D., Faulkner, D. R., Prior, D. J., Norris, R. J., Mariani, E., Boulton, C., Carpenter, B. M., Menzies, C. D., Little, T. A., Hasting, M., De Pascale, G. P., Langridge, R. M., Scott, H. R., Reid Lindroos, Z., Fleming, B., Kopf, A. J. (2012): Drilling reveals fluid control on architecture and rupture of the Alpine fault, New Zealand. – *Geology* **40**: 1143 – 1146.
- Townend, J., Sutherland, R., and Toy, V. G. (2009): Deep Fault Drilling Project. – *Scientific Drilling* **8**: p. 75 – 82.
- Toy, V. G., Boulton, C., Sutherland, R., Townend, J., Norris, R. J., Little, T. A., Prior, D. J., Mariani, E., Faulkner, D. R., Menzies, C. D., Scott, H., Carpenter, B. M. (2015): Fault rock lithologies and architecture of the central Alpine Fault, New Zealand, revealed by DFDP-1 drilling. – *Lithosphere* **7**: pp. 155 – 173.

IODP

Impact melt dynamics during peak-ring formation of the Chicxulub crater, Mexico

 F. M. SCHULTE¹, S. JUNG², U. RILLER¹
¹Institut für Geologie, Universität Hamburg, Bundesstrasse 55, 20146 Hamburg, Germany

²Mineralogisch-Petrographisches Institute, Universität Hamburg, Grindelallee 48, 20146 Hamburg, Germany

Drill core of IODP/ICDP Expedition 364 consists from bottom to top of: (1) 587 m shocked granitoid target basement rock, (2) 36 m of impact melt rock, (3) 95,5 m of suevite, and (4) 112 m of post-impact platform carbonate rocks. Furthermore, a 96 m thick zone of impact melt rock and polymict breccia occurs in granitoid basement rock at the bottom of the drill core. Based on visual inspection of line scans, microstructural and electron microprobe analyses, we compare the structural and chemical characteristics of the two melt rock zones to better understand respective processes during emplacement and solidification of melt.

The upper impact melt rock zone is layered and can be divide into four subunits. From bottom to top these are: i) A 9 m thick basal subunit consists of two black, silicate melt rock phases evident by the plagioclase composition and rock texture. This subunit contains fragments that are derived predominantly from the underlying granitoid basement rocks. The glassy and mottled texture of the melt rock phases points to quenching and auto-brecciation of a solidifying melt. ii) A 16 m thick subunit is characterized by two interlayered melt rock phases. One phase consist of pitch-black silicate, the other phase is bright green and derived from carbonate rock. Both phases display convoluted, centimetre-scale folds. Cusp-and-lobe geometry of the melt rock phases indicates that the silicate phase was more viscous than the carbonate phase during folding and solidification. iii) A

6 m thick melt breccia unit consists of the same melt rock phases as the previous ones. Flow-textured, carbonate melt rock envelopes angular to sub-rounded silicate melt rock fragments displaying an enhanced contrast in mechanical competency. iv) Finally, a 5 m thick unit is composed mostly of quenched fragments set in a brown calcareous matrix. Collectively, the structural and chemical characteristics of the upper melt rock zone point to incomplete separation of a silicate and a carbonate melt during solidification and less severe deformation.

Melt rock of the lower zone is composed of silicates mixed with polymict breccia showing evidence for viscous flow. The breccia consists of highly diverse basement rock and melt rock fragments, but is devoid of carbonate fragments. The structural characteristics of the lower portion of the melt rock point to juxtaposition of brecciated basement rocks, thereby entraining impact melt between basement rock slivers. This process can be explained by overthrusting of surficial impact melt by granitoid basement rock during peak-ring formation.

ICDP

The tectonic system at Lake Nam Co, Tibetan Plateau – Results from high-resolution 2D seismic data

N. SCHULZE¹, V. SPIESS¹, J. VAN DER WOERD², G. DAUT³,
T. HABERZETTL^{3,4}, J. WANG⁵, L. ZHU⁵

¹ University of Bremen, Department of Geosciences, MTU, Klagenfurter Straße, 28359 Bremen, Germany

² Institut de Physique du Globe de Strasbourg, UMR CNRS/UdS 7516, 5, Rue Descartes, 67084 Strasbourg, France

³ Friedrich-Schiller-University Jena, Institute of Geography, Physical Geography, Loebdergraben 32, 07743 Jena, Germany

⁴ University of Greifswald, Institute of Geography and Geology, Physical Geography, Friedrich-Ludwig-Jahn Str. 16, 17489 Greifswald, Germany

⁵ Chinese Academy of Sciences, Institute of Tibetan Plateau Research, 16 Lin Cui Road, Chaoyang District, Beijing 100101, P.R. China

Nam Co is a 100 m deep and hydrologically closed lake located on the central Tibetan Plateau (TP) at the intersection of westerly and monsoonal air masses. As the influence of the Tibetan Plateau on the Indian monsoon system is of particular importance for the atmospheric circulation and for the global water cycle, Nam Co's high-resolution sedimentary paleoclimate archive will help to decipher the timing and the influences of past climate changes.

In the context of the ICDP project 'Seismic Pre-Site Survey for ICDP Drilling Locations at Lake Nam Co' multichannel seismic surveys have been jointly conducted by the Institute of Tibetan Plateau Research and the Universities of Jena and Bremen in 2014 and 2016. The surveys confirmed the existence of several hundred meters of mostly undisturbed sedimentary deposits.

Intense mapping and interpretation of the high-resolution 2D seismic data allow us a detailed understanding of the tectonic evolution in the lake area. The comprehension of the tectonic evolution is the basis for assessing the sedimentation history of the basin and, therefore, the sedimentary paleoclimate archive, especially as we assume syn-sedimentary faulting during the last 100,000 yrs.

It is mostly accepted that north-south crustal shortening and thickening, in a state of isostatic equilibrium, has built the Tibetan Plateau (e.g., Tapponnier et al., 2001) and that a major change in its development occurred long after collision, when roughly north-south trending graben structures developed ac-

ross southern Tibet (e.g., Armijo et al., 1986). The onset of normal faulting on the TP is locally different (e.g., Blisniuk et al., 2001). For southern Tibet, an initiation between 4 Ma (Mahéo et al., 2007) and 2.5 Ma (Armijo et al., 1986) was determined.

The Nam Co basin is located in the Karakorum-Jiali-Fault Zone, which separates the southern TP zone of predominant rifting from the northern TP zone where normal faulting is subordinate to minor strike-slip faulting (Armijo et al., 1986). The basin was most likely created as a pull apart basin. Nowadays, the basin extents are limited by a chain of hills and a dextral NW-SE strike-slip fault towards the north, to the east by a mountain range and the proximal extensional N-S Gulu graben, which connects to the sinistral SW-NE strike-slip and normal fault system of the Nyainqentanglha Mountain Range in the south (Fig. 1).

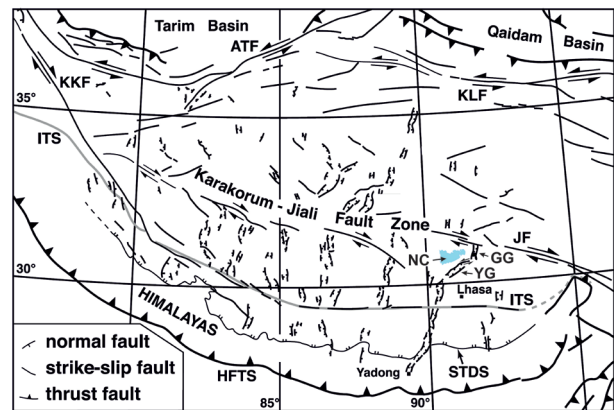


Fig. 1: Overview map of the Tibetan Plateau and adjacent regions. Major faults with demonstrated Cenozoic displacement are highlighted. Abbreviations: ATF, Altyn Tagh fault; HFTS, Himalayan Frontal Thrust System; ITS, Indus-Tsangpo suture; KKF, Karakorum fault; KLF, Kunlun fault; STDS, South Tibetan Detachment System; YG, Yangbajian graben; GG, Gulu graben; NC, Nam Co (after Blisniuk and Sharp [2003]).

With the high resolution seismic data, we were able to reveal a narrowly spaced pattern of normal faults within Lake Nam Co. The fault planes strike mainly N-S, following a trend of striking NNE-SSW in the western part to striking NNW-SSE in the eastern part of the basin.

By measuring the vertical offset (throw) of hanging and foot wall of the normal faults, two clusters of major faults became visible. The clusters describe two major graben structures within the center of the lake, with fault offsets of up to 40 m. These grabens acted as depocenters for sediments. According to our interpretation of the seismic data the sedimentation rate of deposits younger than Marine Isotope Stage (MIS 5) age inside the grabens is 1.5 mm a⁻¹ in contrast to the sedimentation rate outside the graben structure of 1.1 mm a⁻¹.

By plotting cumulative fault throw versus stratigraphic horizons in T-H-plots, as introduced by Hongxing and Anderson (2007), we were able to assess styles, timing, and kinematic history of the normal faults. The initiation of the tectonic activity started between MIS 7 and MIS 5, approximately 200-100 ka ago. Older sedimentary deposits show post-depositional faulting, while from MIS 5 until Holocene times, active syn-sedimentary faulting takes place. Holocene sediments bury the majority of the faults, indicating the modern inactive tectonic phase.

Calculated cumulative vertical displacement rates of maximum 0.3 mm a⁻¹ fit the slip-rate measurements of Blisniuk and Sharp (2003) on normal faults in the central Tibetan Shuang Hu

graben. However, they are distinctly lower than the slip rate of 1.9 ± 0.6 mm a⁻¹ inferred for normal faults bounding the Gulu graben system by Armijo et al. (1986). In an ongoing study, we compare the tectonic setting of the Nam Co normal faults to the Gulu graben in the east to identify whether the same stress field is present in the two settings and whether the Nam Co faults are a parallel extension of the Gulu graben. These results will support the ICDP workshop ‘Nam Co’, 22nd to 24th of May 2018 in Beijing.

References:

- Armijo, R., P. Tapponnier, J. Mercier, and T.-L. Han, 1986, Quaternary extension in southern Tibet: Field observations and tectonic implications: *Journal of Geophysical Research: Solid Earth*, v. 91, no. B14, p. 13803–13872.
- Blisniuk, P. M., B. R. Hacker, J. Glodny, L. Ratschbacher, S. Bi, Z. Wu, M. O. McWilliams, and A. Calvert, 2001, Normal faulting in central Tibet since at least 13.5 Myr ago: *Nature*, v. 412, no. 6847, p. 628–632.
- Blisniuk, P. M., and W. D. Sharp, 2003, Rates of late Quaternary normal faulting in central Tibet from U-series dating of pedogenic carbonate in displaced fluvial gravel deposits: *Earth and Planetary Science Letters*, v. 215, no. 1, p. 169–186.
- Hongxing, G., and J. K. Anderson, 2007, Fault throw profile and kinematics of Normal fault: conceptual models and geologic examples: *Geol. J. China Univ.*, v. 13, no. 75, p. e88.
- Mahéo, G., P.-H. Leloup, F. Valli, R. Lacassin, N. Arnaud, J.-L. Paquette, A. Fernandez, L. Haibing, K. Farley, and P. Tapponnier, 2007, Post 4 Ma initiation of normal faulting in southern Tibet. Constraints from the Kung Co half graben: *Earth and Planetary Science Letters*, v. 256, no. 1, p. 233–243.
- Tapponnier, P., X. Zhiqin, F. Roger, B. Meyer, N. Arnaud, G. Wittlinger, and Y. Jingsui, 2001, Oblique stepwise rise and growth of the Tibet Plateau: *Science*, v. 294, no. 5547, p. 1671–1677.

ICDP

Hipercorig – A modular Direct Push Coring Rig for extended reach in unconsolidated sediments on- and offshore and its operation

A. SCHWALB¹, V. WITTIG², R. BRACKE², U. HARMS³

¹ Institute of Geosystems und Bioindication, Technische Universität Braunschweig, Langer Kamp 19c, 38106 Braunschweig, Germany

² International Geothermal Centre, Hochschule Bochum, Lennerhofstraße 140, 44801 Bochum, Germany

³ Helmholtz Centre Potsdam, GFZ German Research Centre for Geosciences, Telegrafenberg, 14473 Potsdam, Germany

A new and efficient compact rig to recover continuous sediment cores from up to 100 m depth in water depths of up to 300 m is currently being released for use by the scientific community. The very mobile device will close the gap between simple, man-powered piston corers that may only reach sediment depths a few meters and large, heavy-duty drill rigs capable of reaching depths well beyond 1.000 m while also requiring a professional drill crew and intense, expensive logistics with limited access capabilities.

A crucial issue with today’s piston coring is the loss of power along the drill string due to dampening effects as forces are being applied uphole. This can be eliminated by deploying a down-the-hole hydraulic hammer directly above the piston with the drill string. This makes for the novel central design of Hipercorig, thus integrating advanced, inexpensive piston coring with field-proven, hydraulic hammer techniques powered by a high-pressure pump in a modular, mobile system. This includes a modular barge platform, the complete coring system, iron roughneck, winches, service boat and other auxiliary equipment all transportable in four 20-foot standard containers.

Areas of operation do not only include lakes, estuaries and shallow marine areas, but also land-based utilization in bogs, environmental sites etc. are possible. Barge deployment can be achieved manually without docks and heavy cranes due to

the modular, limited weight design. Cost of operations depend mainly on mobilization, i.e. shipping of the 20-foot containers, wear parts and consumables. A minimum of one or two coring experts plus at least two helpers will be needed to operate the rig and instrument efficiently and safe.

The acquisition and initial test are funded by the Deutsche Forschungsgemeinschaft, DFG. Central equipment like the hydraulic hammer-coring device had been already successfully tested on Lake Mondsee, Austria in November 2016. Meanwhile, in winter 2017/2018 the complete barge and drill rig system including its auxiliary parts have been assembled and the hydraulic DTH hammer, rod handling, casing setting system as well as anchor winches are being finally tested. Final decommissioning will include sampling runs and borehole measurements on the Lakes Mondsee and Constance in March and April 2018. Interested parties can apply to visit the test sites.

Hipercorig will be available for scientific projects for merely the maintenance fees and upkeep, guaranteeing to sustain the rig functionality including repairs, spare parts and improvements. The device will be provided primarily to science teams with funded drilling projects. Additional costs to be covered are an operations and mobilization crew of at least four and transportation for four 20’ sea containers with complete equipment including service boats. In addition to scientific coring projects, Hipercorig will also be used for demonstration and training purposes, e.g. GESEP School or other trainings courses and limited industrial use if availability allows.

IODP

A new stratigraphy of the middle Bengal Fan – results from correlation of seismic data with Site U1444, Expedition 353

T. SCHWENK¹, V. JUNGE¹, V. SPIESS¹ AND EXPEDITION 353 SCIENTISTS

¹Marine Technology/Environmental Research, Department of Geoscience, University of Bremen, Klagenfurter Str. 2-4, 28359 Bremen, Germany

The Bengal Fan covers the floor of the whole Bay of Bengal from the continental margins of India and Bangladesh to the sediment-filled Sunda Trench off Myanmar and the Andaman Islands, and along the west side of the Ninetyeast Ridge. Its southern end is located at about 7°S. The length of at least 2800 km, a maximum width of 1430 km, the area of 3x10⁶ km² and the volume of 12.5x10⁶ km³ make the Bengal Fan the largest submarine fan on Earth (Curry et al., 2003). The Bengal Fan is fed by the Ganges-Brahmaputra river system which drains approximately ¼ of the Himalayan mountain range and recently delivers more than 1 Gt/yr of terrigenous sediment. One third of these sediments is transported to the deep sea fan via a deeply incised shelf canyon by turbidity currents. This makes the Bengal Fan to the most complete recorder to study interactions among the growth of the Himalaya and Tibet, the development of the Asian monsoon, and processes affecting the carbon cycle and global climate. Because sedimentation in the Bengal Fan responds to both, climate and tectonic processes, its terrigenous sediment records the past evolution of both the Himalaya and regional climate.

IODP Site U1444 was drilled in 2015 in the north-western part of the Middle Bengal Fan in 3133 mbsl at 14°N, 84°49.74’E. In total, four distinct units over a core length of 331 m could be identified (Clemens et al., 2016):

1) Unit I is a 95 m (0 - 95 mbsf) thick layer which mainly comprises turbidites (2.54/m) with lithologies extending from silty sand to silty clay.

2) Unit II ranges von 95 - 169 mbsf, covering a thickness of 74 m, and is a mostly hemipelagic interval of nannofossil-rich clay and clay with nannofossils with silty clay.

3) Unit III is about 87 m thick and ranges from 169 - 256 mbsf. The main lithology consists of silty sand comprising intervals of silty clay. The recovery of only 11% of the sediment indicates that the missing intervals are likely composed of unconsolidated sand brought by turbidity currents.

4) Unit IV ranges from 256 - 324 mbsf and covers a thickness of 68 m. It is a largely hemipelagic unit, turbidites occur more frequent (2.39/m) compared to Unit II, but they are thinner than in Unit I.

The multichannel seismic Profile GeoB97-041 crosses IODP Site U1444 at its westernmost part, just on top of the so-called 85° Ridge. East of the 85° Ridge, a basin developed, which is again bordered to the east by a ridge, namely the Ninetyeast Ridge. Tracing of the mainly hemipelagic Unit II into the basin reveal, that this unit splits into three layer, which are separated by turbiditic sediments including channel-levee systems. The top of these layers appear as angular unconformities in the seismic data and correspond to the already identified unconformities described by Schwenk & Spiess (2009). This pattern shows in general, that before and/or during deposition of Unit II at Site U1444 an uplift of the 85° Ridge must have occurred. As a result, no turbidite was deposited on top of the 85° Ridge, but turbidity currents were guided into the basin between the both ridges. Dating of drilled sediments suggests, that this uplift must have started in the late Pliocene and stopped latest in middle Pleistocene.

A main focus of this study was the stacking pattern of channel-levee systems in Unit I. Overall, 64 channel-levee systems were identified within Profile GeoB97-041 over a distance of 520 km. Since the uppermost hemipelagic sediments of Unit II were deposited 0.4 Myrs ago, an average lifetime of 6.25 kyrs per systems can be assumed. However, tracing of bases of individual channel-levee systems to continuous horizons makes it possible to separate Unit I into four subunits, and it turned out that the lifetimes of individual lifetimes must have varied between 2.77 kyrs and 11.11 kyrs. This irregular pattern suggests, that levee breaks and channel avulsion further upfan is an autocyclic process, and not controlled by any cyclic events like sea-level changes etc.. A comparison shows, that the average lifetime of channel-levee systems at 14°N is much less as further south at 8°N, where channel-levee systems were drilled during IODP Expedition 354 (France-Lanord et al., 2016; see presentation of Bergmann et al.). Since channel-levee systems drilled at 8°N had developed during a different timeframe (0.8 - 0.3 Ma) as the channel-levee systems at 14°N (0.4 Ma - recent), this result suggests that the Bengal Fan is build-up by different subfans with significant different dynamics.

References:

- Clemens, S.C., Kuhnt, W., LeVay, L.J., and the Expedition 353 Scientists, Indian Monsoon Rainfall. Proceedings of the International Ocean Discovery Program, vol 353. College Station, TX (International Ocean Discovery Program). doi:10.14379/iodp.proc.353.104.2016
- France-Lanord, C., Spiess, V., Klaus, A., Schwenk, T., and the Expedition 354 Scientists, 2016. Bengal Fan. Proceedings of the International Ocean Discovery Program, 354: College Station, TX (International Ocean Discovery Program). <http://dx.doi.org/10.14379/iodp.proc.354.2016>
- Curry, J.R. et al., 2003, The Bengal Fan: morphology, geometry, stratigraphy, history and processes: *Mar. and Petr. Geol.*, 19, 1191-1223
- Schwenk, T. & Spiess, V., 2009, Architecture and stratigraphy of the Bengal Fan as response to tectonic and climate revealed from high resolution seismic data. In Kneller, B., Martinsen, O.J., and McCaffrey, B., *SEPM Spec. Pub.* 92, 107-131

ICDP

Pre-stack depth migration in an anisotropic crystalline environment at the COSC-1 borehole, central Sweden

H. SIMON¹, F. KRAUSS², S. BUSKE¹, R. GIESE², P. HEDIN³, C. JUHLIN³

¹Institute of Geophysics and Geoinformatics, TU Bergakademie Freiberg

²Centre for Scientific Drilling, Helmholtz Centre Potsdam GFZ German Research Centre for Geosciences

³Department of Earth Sciences, Uppsala University

The Scandinavian Caledonides, a part of the North Atlantic Caledonides, represent a well preserved deeply eroded inactive Palaeozoic orogen. Today, after four hundred million years of erosion along with uplift and extension during the opening of the North Atlantic Ocean, the geological structure of central western Sweden consists of allochthons, underlying autochthonous units, and a shallow west-dipping décollement that separates the two (see Fig. 1). This surface is closely associated with a thin layer of Cambrian black shales. The structure of the basement underneath the décollement is highly reflective and apparently dominated by mafic sheets intruded into either late Paleoproterozoic granites or Mesoproterozoic volcanic rocks and sandstones. The ICDP project COSC (Collisional Orogeny in the Scandinavian Caledonides) focuses on the Caledonide Orogen in order to better understand orogenic processes from the past and in recently active mountain belts, like the Himalayas (Gee et al., 2010). Therefore, the structure and physical conditions of the orogen units, in particular the Seve Nappe Complex (as part of the Middle Allochthons), the Lower Allochthon and the underlying basement will be investigated with two approximately 2.5 km deep fully cored scientific boreholes in central Sweden. Thus, a continuous 5 km tectonostratigraphic profile through the Caledonian nappes into Baltica's basement will be recovered.

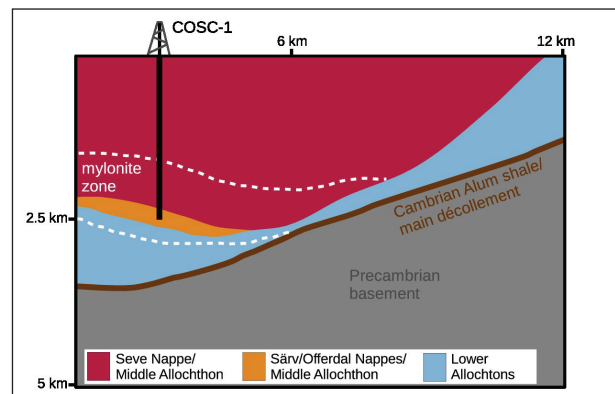


Fig. 1: Simplified geological sketch section showing the main structural units in relation to the borehole COSC-1 (after Juhlin et al., 2016).

The first borehole COSC-1 was successfully drilled to 2.5 km depth in 2014 (Lorenz et al., 2015) near the town of Åre (ICDP drill site 5054-1-A). Thus, a continuous cored section through the seismically highly reflective Lower Seve Nappe and the underlying mylonite zone was obtained. The Seve Nappe Complex, mainly consisting of felsic (gneisses) and mafic (amphibolites) rocks, has been deformed ductilely and emplaced hot onto the Lower Allochthons during the collisional orogeny that formed the Scandinavian Caledonides.

In order to allow the extrapolation of results from core analysis and downhole logging to the structures around the bore-

hole, several surface and borehole based seismic experiments were conducted right after drilling completed. These included: 1) a high-resolution zero-offset Vertical Seismic Profile (VSP) (Krauß et al., 2018), 2) a spatially limited 3D seismic survey (Hedin et al., 2016) and 3) a multi-azimuthal walkaway VSP in combination with three up to 10 km long surface profiles centred around the borehole (Simon et al., 2017).

In this study the data from the walkaway VSP and the long offset lines were used to image the structures in the vicinity of the borehole. In a first step a detailed P-wave velocity model around the COSC-1 borehole was derived by a tomographic approach (Simon et al., 2017). Clear differences in vertical and horizontal velocities, observed by comparing velocities from the tomography results (mainly horizontally traveling rays) with a 1D velocity function calculated from zero-offset VSP first arrivals (mainly vertically traveling rays), made it necessary to also account for anisotropy during velocity model building. The resulting anisotropic VTI (transversely isotropic with vertical axis of symmetry) model consists of the 1D vertical P-wave velocity function from zero-offset VSP and homogeneous Thomsen parameters of $\delta = 0.3$ and $\epsilon = 0.03$. The latter were derived from lab measurements (Wenning et al., 2016) and the seismic walkaway VSP data. This anisotropic model explains first arrivals for both, surface and borehole data, very well and provides the basis for the subsequent application of seismic imaging approaches, like Kirchhoff-based pre-stack depth migration, including calculation of Green's functions using an anisotropic eikonal solver (Riedel, 2016). The resulting images were compared to the corresponding migration results based on an isotropic velocity model. Both images are dominated by strong and clear reflections. However, they appear more continuous and better focused in the anisotropic result. Most of the reflections originate below the bottom of the borehole and therefore are probably situated within the Precambrian basement or at the transition zones between Middle and Lower Allochthons and the basement (Fig. 2). The deeper reflections might also represent dolerite intrusions or deformation zones of Caledonian or pre-Caledonian age. Their origin remains enigmatic and might only be revealed by drilling the proposed borehole COSC-2, which is supposed to penetrate some of these reflectors.

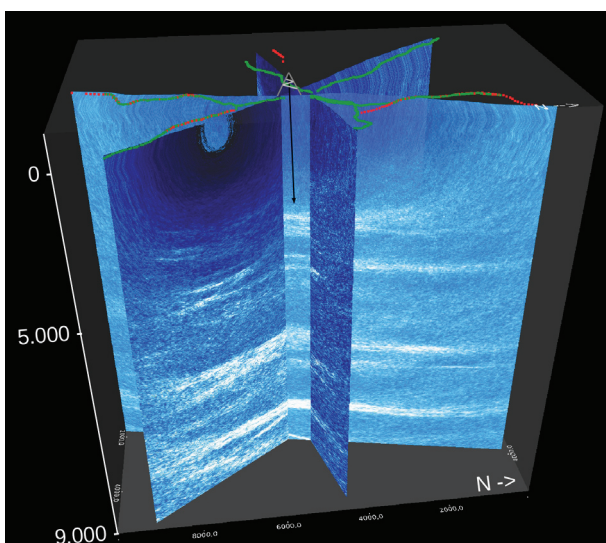


Fig. 2: 3D view of anisotropic pre-stack depth migration results of the three independently processed surface profiles, showing dominant reflections below the borehole COSC-1 down to a depth of 9 km. The used shot and receiver positions are marked in red and green, respectively.

References:

- Gee, D. G., Juhlin, C., Pascal, C., & Robinson, P. (2010). Collisional Orogeny in the Scandinavian Caledonides (COSC). *GFF*, 132(1), 29–44.
- Hedin, P., Almqvist, B., Berthet, T., Juhlin, C., Buske, S., Simon, H., Giese, R., Krauß, F., Rosberg, J. E., Alm, P. G. (2016). 3D reflection seismic imaging at the 2.5 km deep COSC-1 scientific borehole, central Scandinavian Caledonides. *Tectonophysics*, 689, 40–55.
- Juhlin, C., Hedin, P., Gee, D. G., Lorenz, H., Kalscheuer, T., Yan, P., (2016). Seismic imaging in the eastern Scandinavian Caledonides: Siting the 2.5 km deep COSC-2 borehole, central Sweden. *Solid Earth*, 7, 769–787.
- Krauß, F., (2018). Combination of Borehole Seismic and Downhole Logging to Investigate the Vicinity of the COSC-1 Borehole in Western Scandinavia. PhD Thesis, TU Bergakademie Freiberg (submitted).
- Lorenz, H., Rosberg, J.-E., Juhlin, C., Bjelm, L., Almqvist, B. S. G., Berthet, T., Conze, R., Gee, D. G., Klonowska, I., Pedersen, K., Roberts, N. M. W., Tsang, C.-F. (2015). COSC-1 – drilling of a subduction-related allochthon in the Palaeozoic Caledonide orogen of Scandinavia. *Scientific Drilling*, 19, 1–11.
- Riedel, M., (2016). Efficient computation of seismic traveltimes in anisotropic media and the application in pre-stack seismic migration. PhD Thesis, TU Bergakademie Freiberg.
- Simon, H., Buske, S., Krauß, F., Giese, R., Hedin, P., Juhlin, C. (2016). The derivation of an anisotropic velocity model from a combined surface and borehole seismic survey in crystalline environment at the COSC-1 borehole, central Sweden. *Geophysical Journal International*, 210, 1332–1346.
- Wenning, Q., Almqvist, B. S. G., Hedin, P., Zappone, A. (2016). Seismic anisotropy in mid to lower orogenic crust: Insights from laboratory measurements of V_p and V_s in drill core from central Scandinavian Caledonides. *Tectonophysics*, 692, 14–28.

ICDP

High-resolution seismic survey at a planned PIER-ICDP fluid-monitoring site in the Eger Rift zone, Czech Republic

H. SIMON¹, S. BUSKE¹, T. FISCHER²

¹Institute of Geophysics and Geoinformatics, TU Bergakademie Freiberg

²Faculty of Sciences, Charles University Prague

The Eger Rift zone (Czech Republic) is an intra-continental non-volcanic region and is characterized by outstanding geodynamic activities, which result in periodically occurring earthquake swarms and significant CO₂ emanations (e.g. Fischer et al., 2010; Weinlich et al., 1998). Because fluid flow and fluid-induced stress can trigger earthquake swarms, both natural phenomena are probably related to each other (e.g. Heinicke et al., 2018; Heinicke et al., 2009; Horálek and Fischer, 2008; Kämpf et al., 1989). The epicentres of the earthquake swarms cluster at the northern edge of the Cheb Basin near the village Nový Kostel (Fischer and Michálek, 2008). Although the location of the cluster coincides with the major Mariánské-Lázně Fault Zone (MLFZ) the strike of the focal plane indicates another fault zone, the N-S trending Počátky-Plesná Fault Zone (PPFZ) (Bankwitz et al., 2003). Isotopic analysis of the CO₂-rich fluids revealed a significant portion of upper mantle derived components, hence a magmatic fluid source in the upper mantle was postulated (Weinlich et al., 1999).

Because of these phenomena, the Eger Rift area is a unique site for interdisciplinary drilling programs to study the fluid-earthquake interaction. The ICDP project PIER (Drilling the Eger Rift: Magmatic fluids driving the earthquake swarms and the deep biosphere) will set up an observatory, consisting of five shallow monitoring boreholes (Dahm et al., 2013).

The main geological structures in the survey area are the Cheb Basin, the crustal-scale MLFZ and the potentially seismically active PPFZ. The Cheb Basin is a small intra-continental basin which covers the northwestern part of the Bohemian massif. It is situated in the western part of the Eger Rift at the intersection of the SW-NE striking Eger Graben and the MLFZ. It covers mainly granites and Lower Paleozoic series. The basin

is deepening towards the east where it is limited by the MLFZ. The thickness of the Neogene sediments of the Cheb Basin is at its maximum less than 300 m and they are underlain by Paleozoic metamorphics and granites. So far, only shallow geophysical imaging studies have recovered subsurface structures in the Cheb basin (e.g. Flechsig et al., 2010; Fischer et al. 2012). Several deep seismic profiles in the West Bohemia/Vogtland area were acquired and recently re-processed, e.g. 9HR (Mullick et al., 2015) and MVE (Bleibinhaus et al., 2003). They revealed structures throughout the entire crust but the extent of the fault zones MLFZ and PPFZ could not be imaged at all.

In preparation for the drilling, the goal of this study is the characterization of the projected fluid-monitoring drill site at the CO₂ degassing mofette field near the village Hartoušov. Therefore, a 6 km long reflection/refraction profile with dense source and receive spacing was acquired in October 2017. The W-E trending profile crosses the proposed drill site and the surface traces of the MLFZ and the PPFZ (see Fig. 1). Up to 1200 Vibroseis shots were recorded with 312 single-component geophones deployed in two spreads along the profile, resulting in maximum offsets of 4 km. The Vibroseis truck (32 tons, 250 kN peak force), owned by the Institute of Geophysics and Geoinformatics, TU Bergakademie Freiberg was used as the seismic source and generated 3-5 sweeps at each source position with a length of 16 s and a frequency bandwidth of 10-120 Hz. The data quality is generally good, although bad coupling of the geophones (due to soft ground) and strong noise from traffic and a nearby factory had a strong impact on the data acquisition. Nevertheless, in most cases the first breaks can be identified for the entire offset and some near surface reflections are visible even in the raw data (Fig. 2). Processing of these recently acquired new data is now ongoing and includes first arrival tomography and the application of focusing pre-stack depth migration methods, like Fresnel Volume Migration.

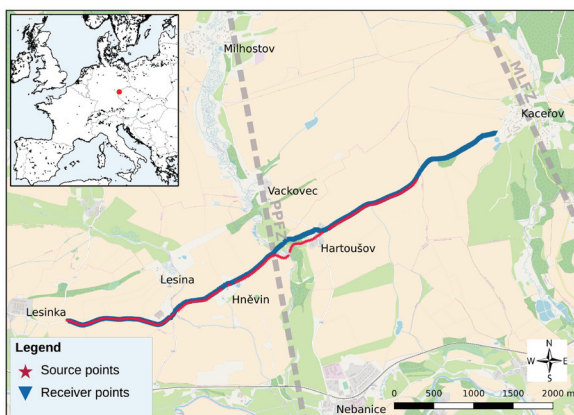


Fig. 1: Map of the new seismic reflection/refraction survey showing the source and receiver point distribution along the profile. The approximate surface traces of the Mariánské-Lázně Fault Zone (MLFZ) and the Počátky-Plesná Fault Zone (PPFZ) are marked in grey.

The outcome of this work will be a detailed near-surface velocity model, high-resolution structural images of potential reflectors (within the Cheb Basin and related to the fault systems of MLFZ and PPFZ) and will provide crucial constraints on the petrophysical properties of the prevailing rock formations. During interpretation of the seismic data, a resistivity model derived from a geoelectrical survey acquired along the same profile line will provide important constraints, especially with respect to the suspected fluid pathways related to the earthquake swarms and the CO₂ emanations.

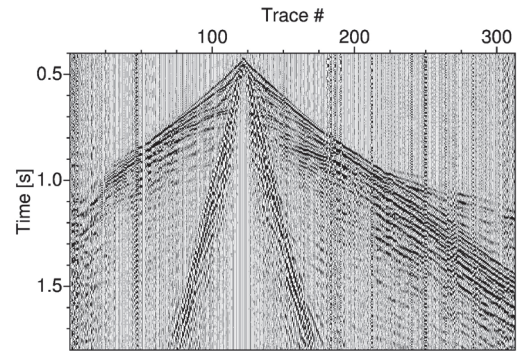


Fig. 2: The first 1.8 seconds of an exemplary shot gather. So far processing only included bandpass filtering (30-80 Hz) and automatic gain control. First breaks are visible for almost the entire shot gather and near surface reflections can be clearly identified.

References:

- Bankwitz, P., G. Schneider, H. Kämpf, and E. Bankwitz (2003), Structural characteristics of epicentral areas in Central Europe: study case Cheb Basin (Czech Republic), *J Geodyn* 35(1-2), 5-32.
- Bleibinhaus F., Stich D., Simon M. and Gebrande H., (2003), New results from amplitude preserving prestack depth migration of the Münchberg/Vogtland segment of the MVE deep seismic survey. *J. Geodyn.*, 35, 33-43.
- Dahm, T., Hrubcova, P., Fischer T., Horálek, J., Korn, M., Buske, S., and D. Wagner (2013), Eger Rift ICDP: An observatory for the study of non-volcanic, midcrustal earthquake swarms and accompanying phenomena, *Scientific drilling* 16, 93-99.
- Fischer, T. and Michálek, J. (2008), Post 2000-swarm microearthquake activity in the principal focal zone of West Bohemia/ Vogtland: space-time distribution and waveform similarity analysis, *Stud. Geophys. Geod.*, 52, 493-511.
- Fischer, T., Horálek, J., Michálek, J. and A. Bouskova (2010), The 2008 West Bohemia earthquake swarm in the light of the WEBNET network, *J. Seismol.*, 14(4), 665-682.
- Fischer T., Štěpančíková P., Karousová M., Tábořík P., Flechsig C. and Gaballah M., (2012), Imaging the Mariánské Lázně Fault (Czech Republic) by 3-D ground penetrating radar and electric resistivity tomography. *Stud. Geophys. Geod.*, 56, 1019-1036.
- Flechsig, C., Fabig, T., Rücker, C., Schütze, C., (2010); Geoelectrical investigations in the Cheb basin/W-Bohemia: An approach to evaluate the near-surface conductivity structure. *Stud. Geophys. Geod.* 54, 417-437.
- Heinicke, J., Fischer, T., Gaupp, R., Götze, J., Koch, U., Konietzky, H., Stanek, K.-P. (2009) Hydrothermal alteration as a trigger mechanism for earthquake swarms: the Vogtland/NW Bohemia region as a case study. *Geophys. J. Int*, 178, 1-13.
- Heinicke, J., Woith, C., Alexandrakos, C., Buske, S., Telesco, L., (2018), Can hydroseismicity explain recurring earthquake swarms in NW-Bohemia? *Geophys. J. Int*, 212, 211-228.
- Horálek, J. and Fischer T. (2008) Role of crustal fluids in triggering the West Bohemia/Vogtland earthquake swarms: just what we know (a review). *Stud. Geophys. Geod.*, 52, 455-478.
- Kämpf, H., G. Strauch, P. Vogler, and W. Michler (1989), Hydrogeologic changes associated with the December 1985/January 1986 earthquake swarm activity in the Vogtland/NW Bohemia seismic area, *Z. Geol. Wiss.*, 17, 685-689.
- Mullick, N., Buske, S., Hrubcova, P., Ruzek, B., Shapiro, S., Wigger, P., Fischer, T., 2015. Seismic imaging of the geodynamic activity at the western Eger rift in central Europe. *Tectonophysics* 647-648, 105-111.
- Weinlich, F. H., J. Tesar, S. M. Weise, K. Bräuer, and H. Kämpf (1998), Gas flux distribution in mineral springs and tectonic structure in the western Egger Rift, *J. Czech. Geol. Soc.*, 43, 91-110.
- Weinlich, F. H., K. Bräuer, H. Kämpf, G. Strauch, J. Tesar, and S. M. Weise (1999), An active subcontinental mantle volatile system in the western Eger Rift, central Europe: Gas flux, isotopic (He, C, and N) and compositional fingerprints, *Geochim. Cosmochim. Acta*, 63, 3653-3671.

IODP

Frictional behavior of Juan de Fuca sediments approaching the Cascadia subduction zone

 K. STANISLAWSKI¹, M. J. IKARI¹
¹MARUM – Center for Marine Environmental Sciences, University of Bremen, Leobener Str. 8, 28359 Bremen, Germany

Geological evidence, for instance turbidite deposits, of past megathrust earthquakes on the Cascadia subduction zone is a valid reason to assume that another event will occur in the future. Consequences of such an earthquake pose an enormous hazard for the population in the coastal areas of western North America. The nucleation of earthquakes and also various types of slow slip are controlled by the frictional fault slip behavior of geologic material in the subduction system. Laboratory friction experiments on natural material from the system deliver essential information on fault slip and the processes controlling it. However, there are very few friction studies for the Cascadia subduction zone.

Here, we performed friction experiments on natural material from the Juan de Fuca plate being input to the Cascadia subduction zone. The material was obtained from cores recovered during IODP Expedition 301. In total, four samples of hemipelagic clay, silt turbidites, and sand turbidites from depths of 65 to 259 mbsf were tested. Using a direct shear device, the samples were sheared under in-situ effective normal stress conditions, at room temperature, and saturated with simulated seawater. In our experiments, we measure the steady-state frictional strength and cohesion, and also conducted velocity step tests ranging from plate convergence rates of 0.0017 $\mu\text{m/s}$ (5 cm/yr) up to 30 $\mu\text{m/s}$. We observed a significant decrease in the coefficient of sliding friction from 0.65 to 0.2 with increasing depth, bulk phyllosilicate content, and calcite content. For all our tested samples, the rate-dependent friction parameter $a-b$ predominantly shows velocity-weakening frictional behavior, a key requirement for unstable fault slip and earthquake nucleation. These results demonstrate that even the frictionally weak strata on the Juan de Fuca plate have the potential for earthquake nucleation when being subducted.

IODP

Early Cretaceous South Atlantic opening - modelling the effects of geography, bathymetry and radiative forcing

 S. STEINIG¹, W. DUMMANN², S. FLÖGEL¹, W. PARK¹, T. WAGNER³,
 J. O. HERRLE^{4,5}, P. HOFMANN²
¹GEOMAR Helmholtz Centre for Ocean Research Kiel,
 Wischhofstr. 1-3, 24148 Kiel, Germany

²Institute of Geology and Mineralogy, University of Cologne,
 Zùlpicher Str. 49a, 50674 Cologne, Germany

³Sir Charles Lyell Centre, School of Energy, Geoscience, Infra-
 structure and Society, Heriot-Watt University, Edinburgh,
 EH14 4AS, UK

⁴Institute of Geosciences, Goethe-University Frankfurt,
 Altenhøferallee 1, 60438 Frankfurt am Main, Germany

⁵Biodiversity and Climate Research Centre (BIK-F),
 Senckenberganlage 25, 60325 Frankfurt am Main, Germany

Paleoceanographic data indicate large-scale perturbations of the Early Cretaceous (i.e. Aptian-Albian) global climate system associated with severe changes of the marine carbon cycle (Jenkyns, 2010). At the same time, the ongoing break-up of Gondwana and the related opening of the South Atlantic and

Southern Ocean led to the emergence of young ocean basins, characterised by vast shelf areas and limited circulation (Pérez-Díaz and Eagles, 2017). Several studies relate these evolving basins and their restricted environments to periods of increased black shale formation and carbon burial (Trabucho-Alexandre et al., 2012) with a particular importance of the developing South Atlantic (McAnena et al., 2013).

Within this project, we target the question whether increased carbon burial in the early Cretaceous South Atlantic influenced or even triggered global climate perturbations. We further test the hypothesis that the development and destruction of regional marine carbon sinks in the South Atlantic are primarily controlled by the progressive opening of several key oceanic gateways. For this purpose we tightly combine a new stratigraphical framework for several sites across the South Atlantic and the Southern Ocean (see abstract of Dumann et al.) with a joint physical and biogeochemical modelling approach. The model simulations are designed to test hypotheses generated from sea water-derived neodymium (Nd) isotope signatures and to assess possible influences of regional circulation changes on the marine carbon cycle.

In a first step we employ a global atmosphere-ocean general circulation model, the Kiel Climate Model (KCM), under Early Aptian (120 Ma) boundary conditions and evaluate the simulated large-scale dynamics and mean climatic conditions of the reference simulation. Land topography and ocean bathymetry are based on reconstructions from Müller et al. (2008) and Blakey (2008). Surface freshwater routing strictly follows the model topography (Hagemann and Dümenil, 1998). We apply a zonal mean, climatic zone dependent surface vegetation with no continental ice and glaciers (Ando et al., 2009). The solar constant is reduced by 1% and three different atmospheric $p\text{CO}_2$ concentrations of 300, 600 and 1200ppm are used to reflect the large range of available reconstructions (Jing and Bainian, 2017). Additional experiments with different ocean bathymetries representing key stages of the South Atlantic opening are used to assess the sensitivity of the regional oceanic circulation to changes in geography and bathymetry. Varying levels of atmospheric $p\text{CO}_2$ are applied to distinguish between signals caused by local tectonic or global radiative processes.

Simulated sea surface temperatures at $p\text{CO}_2$ levels of 1200ppm show highest agreement with available proxy data. Corresponding steady state global mean surface air temperatures in the control simulation are elevated by nearly 10°C compared to pre-industrial and reach 23.5°C. The surface warming is mainly radiatively driven by the higher atmospheric $p\text{CO}_2$ levels (~70% of the warming) and a surface albedo reduction (~30% of the warming). High-latitude surface albedo changes reduce the global meridional surface temperature gradient (MTG) by 15°C. Cloud feedbacks partly compensate the polar amplification and strengthen the MTG by up to 4°C compared to a pre-industrial reference simulation.

High atmospheric $p\text{CO}_2$ levels lead to an enhanced hydrological cycle with amplified evaporation over the coastal shelf areas and a subsequent halokinetic circulation with warm and saline intermediate and bottom waters in the South Atlantic. We find a high sensitivity of the South Atlantic and Southern Ocean circulation and water mass stratification to the local basin geometry and gateway depths. A sufficient northward extension of the young South Atlantic strengthens the evaporatively driven intermediate water production and therefore also the basin wide meridional overturning circulation. Higher rates of rainfall and river runoff in the northern Angola Basin potentially suppress the local formation of intermediate water at lower $p\text{CO}_2$ levels and reverse the sign of the meridional circulation. The opening

of the Georgia Basin gateway leads to a net export of the dense, saline bottom waters produced in the South Atlantic into the Southern Ocean. These scenarios can be matched to distinctively different paleoenvironments found in the proxy data. Ongoing geochemical modelling aims to transfer these circulation changes into responses of key biogeochemical cycles and carbon burial variations.

References:

- Ando, A., Huber, B. T., MacLeod, K. G., Ohta, T., & Khim, B. K. (2009). Blake Nose stable isotopic evidence against the mid-Cenomanian glaciation hypothesis. *Geology*, 37(5), 451–454
- Blakey, R.C. (2008). Gondwana paleogeography from assembly to breakup - A 500 m.y. odyssey, Resolving the late Paleozoic ice age in time and space. *Geological Society of America Special Paper*, 441, 1-28
- Hagemann, S., & Dümenil, L. (1998). A parametrization of the lateral waterflow for the global scale. *Climate Dynamics*, 14(1), 17–31
- Jenkyns, H. C. (2010). Geochemistry of oceanic anoxic events. *Geochemistry, Geophysics, Geosystems*, 11(3), 1–30
- Jing, D., & Bainian, S. (2017). Early Cretaceous atmospheric CO₂ estimates based on stomatal index of *Pseudofrenelopsis papillosa* (Cheirolepidiaceae) from southeast China. *Cretaceous Research*, in press
- McAnena, A., Flögel, S., Hofmann, P., Herrle, J. O., Griesand, A., Pross, J., Talbot, H.M., Rethemeyer, J., Wallmann, K. & Wagner, T. (2013). Atlantic cooling associated with a marine biotic crisis during the mid-Cretaceous period. *Nature Geoscience*, 6(7), 558–561
- Müller, R. D., Sdrolias, M., Gaina, C., Steinberger, B., & Heine, C. (2008). Long-term sea-level fluctuations driven by ocean basin dynamics. *Science*, 319(5868), 1357–1362
- Pérez-Díaz, L., & Eagles, G. (2017). South Atlantic paleobathymetry since early Cretaceous. *Scientific Reports*, 7(1), 11819
- Trabucho-Alexandre, J., Hay, W. W., & De Boer, P. L. (2012). Phanerozoic environments of black shale deposition and the Wilson Cycle. *Solid Earth*, 3(1), 29–42

ICDP

3D deep seismic imaging of the magmatic-hydrothermal system and architecture of the Campi Flegrei caldera to complement an amphibian ICDP/IODP drilling effort

L. STEINMANN¹, V. SPIESS¹, M. SACCHI²

¹ Faculty of Geosciences, University of Bremen, Klagenfurter Strasse, 28359 Bremen, Germany

² Institute for Coastal Marine Environment (IAMC), Italian Research Council (CNR), Calata Porta di Massa, Porto di Napoli, 80133 - Napoli, Italy

The Campi Flegrei caldera (CFc) – situated in southern Italy at the border of the densely populated city of Naples – represents one of the world’s highest volcanic risk areas as proven by its history of catastrophic eruptions, caldera resurgence, as well as volcanic unrest. The caldera complex was formed in the course of two large-scale eruption, being the Campanian Ignimbrite (CI, 39 ka) and Neapolitan Yellow Tuff (NYT, 15 ka) eruptions. In fact, the larger of the two (CI) has even been invoked as trigger for the decline of the Neanderthals, thereby considerably influencing human evolution. Also in the post-collapse phase, volcanic activity continued with at least 60 eruption of which the most recent one occurred in AD 1538. In particular, the causes of the ongoing unrest remain strongly debated and may either be attributed to hydrothermalism, magmatism or a combination of both, in each case with different implications for the hazard and risk assessment. As a future eruption of the CFc poses an imminent threat to millions of people living in its vicinity with potential impacts also on a global scale (e.g. air traffic, climate), understanding the unrest’s mechanisms and their role in the generation of eruptions is of paramount importance. Therefore, the CFc has become subject to an amphibious ICDP-IODP approach with the overarching scientific objective

of understanding the most explosive and dangerous volcanism on Earth related to large collapse calderas.

Here, we present a 3D low-frequency multichannel reflection seismic dataset (25 m line spacing; 20-200 Hz) from the submerged portion of the CFc, providing an outstanding signal penetration in the range of the ICDP-IODP target depth of ~2-3 km. This deep-penetrating dataset complements a preceding 3D high-frequency multichannel seismic study (up to 1000 Hz, 100-150 m line spacing), allowing for a detailed investigation of the interconnection between shallow hydrothermal and magmatic features and their deep-seated roots. In fact, these datasets are unprecedented, thereby holding the potential to revolutionise our understanding of the hydrothermal/magmatic features within an active caldera setting.

In detail, the main scientific aims of the present study are to (1) investigate the deep-seated caldera architecture (e.g. fault zones, magma ascent pathways, maximum thickness of caldera fill), (2) shed light on the mechanisms of large-scale caldera-forming eruption as well as estimating volume and distribution of volcanic zones, and (3) examine the manifestation of hydrothermalism (e.g. fluid escape pathways, hydrothermal reservoirs) and magmatism (e.g. feeder dykes, sills) at depth and their connection to previously identified shallow features (e.g. shallow trapped fluids, submarine vents). Such information is fundamental to fully understand eruption kinematics of large-scale caldera-forming eruptions as well as magmatic-hydrothermal processes. Ultimately, the study’s outcomes will provide the ideal foundation for the final adjustment of the marine drilling locations and for the spatial extrapolation and linkage of ICDP-IODP drilling results.

So far, our seismic analysis has shown clear evidence for the existence of a deep fracture zone (vertical low-amplitude to reflection-free zone) along the southern caldera margin. Following the idea of a so-called *leaky caldera fault*, as established during a 2017 Campi Flegrei Drilling Magellan Workshop, it is likely that this fracture zone represents an eruption site of the CI. The quick ejection and emplacement of the CI deposits could for instance explain the acoustic transparency. This fractured area is associated with the presence of intrusions and submarine vents and, thus, may be regarded as a weak, permeable caldera segment, favouring magma ascent. In the same area, local low-frequency seismoacoustic indications (incoherent, high-amplitude patches) for the presence of a hydrothermal reservoir were found at ~1.5 s TWT (~1.3 km). Also, the high-frequency data revealed shallow (<40 m) anomalous patches (high-amplitude, reversed phase reflection) along the fault zone interpreted as fluids. Therefore, we hypothesize that these fluids originate from a hydrothermal reservoir at ~1.3 km depths, migrating along the highly permeable fault zone to shallower levels. Hence, this fault zone seemingly has a strong control on the ascent of both fluids and magma, thereby depicting a key location for the interconnectivity between the surface and the deep magmatic-hydrothermal system. Thus, they may also play an important role during the recent unrest episodes, for instance by acting as pressure release conduits. Moreover, the shallow fluids cover an area four times larger than the main onshore degassing site around the Solfatara crater, indicating that the marine portion of the CFc plays a substantial role for hydrothermal activity and for the overall degassing budget.

Overall, our findings update the hypothesis of an extension of the hydrothermal system into the offshore sector of the CFc. Furthermore, the fracture zone is seemingly prone to the rise of magma and, thus, may represent a favourable site for future eruptions, which in return has crucial implications for the hazard and risk assessment. Moreover, this study demonstrat-

ed the effectiveness of 3D seismic data in providing reliable constraints on the structural framework and magmatic-hydrothermal processes in (partly) submerged volcanic settings. In summary, our work clearly showed that the submerged portion must be considered to be able to fully understand magmatic, hydrothermal, and volcanic processes at partly marine or lacustrine calderas.

ICDP

Microbially mediated alteration and Fe mobilization from basaltic rocks of the HSDP2 drill core, Hilo, Hawaii

M. STRANGHOENER¹, A. SCHIPPERS², S. DULTZ³, H. BEHRENS¹

¹Institute of Mineralogy, Leibniz Universität Hannover, Hanover, Germany

²Geomicrobiology, Federal Institute for Geosciences and Natural Resources, Hanover, Germany

³Institute of Soil Science, Leibniz Universität Hannover, Hanover, Germany

Weathering of volcanic rocks is a key factor for the transport and the geochemical cycle of elements between lithosphere and hydrosphere. Young volcanic islands comprising both, relatively fresh as well as altered chemical reactive rocks are a potential source for increased Fe supply to ocean surface waters. The supply of the micronutrient Fe to ocean surface waters plays a critical role since it controls phytoplankton growth and hereby affect the global carbon cycle (Tagliabue et al. 2014). Dissolved Fe in the Pacific surface waters was found to increase near the Hawaiian Islands from 0.1 nM to 0.6 nM with a maximum of 1.56 nM close to the Kauai Coast (Brown et al. 2005). The majority of the chemical weathering products of volcanic islands is transported via submarine ground- and seawater discharge to the oceans (Rad et al. 2007, Schopka & Derry 2012). However, the contribution of microorganisms to the release of elements and especially mobilization of Fe from basaltic rocks is still not completely understood.

To better understand the role of microbial activity on alteration and Fe mobilization, we investigated the interaction of a single bacterial model species (*Burkholderia fungorum*) with basaltic rocks from the HSDP2 drill core and synthetic basaltic glasses in batch experiments. The microorganism was found in basaltic aquifers of Snake River Plain as well as Hawaiian volcanic deposits (Sebat et al. 2003, Dunfield & King 2005) and is known to weather rocks for nutrient acquisition (Wu et al. 2007, Mailloux et al. 2009). Two types of experiments were performed: (I) incubation experiments with core samples (pillow basalts, hyaloclastites, basaltic flows) at different temperatures (8 °C and 30 °C) for 41 days in the dark and (II) colonization experiments with synthetic basaltic glasses of different Fe redox states and strain at 30 °C for 42 days in the dark. A nutrient depleted medium was used which entirely lacks most base cations (Wu et al. 2007). Concentrations of dissolved major elements, pH, bacterial growth and glucose consumption were measured over time (I) or at the end of the experiment (II).

In abiotic experiments with core samples and synthetic glasses, pH changes were negligible compared to biotic experiments where strong pH variations were observed between samples with different specific surface areas (SSA) and Fe redox states. The influence of *B. fungorum* in incubation experiments on elements released to solution strongly depends on the SSA. For core rocks with a high SSA (> 20 m²/g), we observed less release of Fe and other major elements (e.g. Si, Al, Mg) to

solution in presence of *B. fungorum* compared to their abiotic analogues. In contrast, core rocks with low SSA (< 4 m²/g) showed higher concentrations of dissolved major elements in presence of bacteria. We assume that for rocks with high SSA abiotic alteration alone released sufficient nutrients to solution for growth of *B. fungorum*, thus the bacterium is not forced to actively scavenge nutrients from the rock. Results from a sequential extraction on HSDP2 core rocks, where high amounts of oxalate soluble Fe (amorphous secondary Fe oxides) were observed for samples with high SSA, confirm this assumption. However, using solely the concentrations of dissolved elements as a measure of alteration excludes the possibility that the bacterial cells and the biofilm can be a sink for released elements as well. From observations of biotic colonization experiments with synthetic basaltic glasses, it was deduced that the release of major elements to solution increased with increasing strain and Fe(II) content. SEM analysis revealed that cells in incubation experiments with HSDP2 core samples are concentrated on glassy surfaces as well as in cracks and holes and are nearly absent on smooth mineral surfaces. In contrast, in colonization experiments with synthetic basaltic glasses with high strain and high Fe(II) surfaces are intensely covered with cells and biofilm whereas glasses with low Fe(II) or low strain are sparsely colonized only.

We therefore conclude that structurally bound Fe(II) is most probably used by *B. fungorum* as a nutrient. Furthermore, we assume that microbial activity increases rock dissolution and Fe mobilization as soon as the microorganisms are forced to acquire micronutrients from the rock itself. Our results from experiments with synthetic basaltic glasses indicate that besides surface morphology also physicochemical factors such as redox state and strain are important parameters controlling microbial behavior and therefore alteration of basaltic rocks and glasses

References:

- Tagliabue, A., Aumont, O., Bopp, L. (2014): The impact of different external sources of iron on the global carbon cycle. *Geophysical Research Letters* 41, 920-926.
- Brown, M.T., Landing, W.M., Measures, C.I. (2005): Dissolved and particulate Fe in the western and central North Pacific: Results from the 2002 IOC cruise. *Geochemistry, Geophysics, Geosystems* 6, 1-20.
- Rad, S.D., Allègre, C.J., Louvat, P. (2007): Hidden erosion on volcanic islands. *Earth and Planetary Science Letters* 262, 109-124.
- Schopka, H.H., Derry, L.A. (2012): Chemical weathering fluxes from volcanic islands and the importance of groundwater: The Hawaiian example. *Earth and Planetary Science Letters* 339-340, 67-78.
- Sebat, J.L., Colwell, F.S., Crawford, R.L. (2003): Metagenomic Profiling: Microarray Analysis of an Environmental Genomic Library. *Applied and Environmental Microbiology* 69, 4927-4934.
- Dunfield, K.E., King, G.M. (2005): Analysis of the distribution and diversity in recent Hawaiian volcanic deposits of a putative carbon monoxide dehydrogenase large subunit gene. *Environmental Microbiology* 7, 1405-1412.
- Wu, L., Jacobson, A.D., Chen, H.C., Hausner, M. (2007): Characterization of elemental release during microbe-basalt interactions at T = 28 °C. *Geochimica et Cosmochimica Acta* 71, 2224-2239.
- Mailloux, B.J., Alexandrova, E., Keimowitz, A.R., Wovkulich, K., Freyer, G.A., Herron, M., Stolz, J.F., Kenna, T.C., Pichler, T., Polizzotto, M.L., Dong, H., Bishop, M., Knappett, P.S.K. (2009): Microbial mineral weathering for nutrient acquisition releases arsenic. *Applied and environmental microbiology*, 75(8), 2558-2565.

IODP

Changes of the Atlantic meridional overturning circulation of the past 30 ka recorded in a depth transect at the Blake Outer Ridge

F. SÜFKE¹, F. PÖPPELMEIER¹, P. BLASER¹, M. GÜTJAHRT², T. GOEPFERT²,
J. GRÜTZNER³, B. ANTZ⁴, J. LIPPOLD¹

¹Institute of Earth Sciences, Heidelberg University, Im Neuenheimer Feld 234, Heidelberg, Germany
(finn.suefke@geow.uni-heidelberg.de)

²GEOMAR Helmholtz Centre for Ocean Research, Kiel, Germany

³AWI Helmholtz Centre for Polar and Marine Research, Bremerhaven, Germany

⁴Institute of Environmental Physics, Heidelberg University, Heidelberg, Germany

Oceans and climate are a tightly coupled system interacting with each other in various ways such as storage of carbon dioxide in the deep ocean. Within the global conveyor belt the Atlantic Meridional Overturning Circulation (AMOC) holds a key function, transporting warm salty surface waters from the tropical to the northern Atlantic where deep water formation takes place. Following the continental rise of North America this newly formed deep water propagates southward as Western Boundary Undercurrent (WBUC) ventilating the deep Atlantic. In the past (e.g. the last glacial cycle) strength and geometry of the AMOC have changed significantly [1]. This study aims to provide a better understanding of the temporal and spatial (also depth dependent) evolution of the AMOC in the western Atlantic sector since the last glacial (~30 ka). We have investigated four sediment cores of the Blake Outer Ridge (30°N, 74°W; ODP 1059 to 1062) in a depth transect from 3000 to 4700 m water depth in the main flow path of the WBUC. We measured four down-core profiles of neodymium (ϵNd) and $^{231}\text{Pa}/^{230}\text{Th}$ isotopes for the reconstruction of water mass provenance and circulation strength of the last ~30 ka. In contrast to published Nd isotope [2] and $^{231}\text{Pa}/^{230}\text{Th}$ [3] records from the Blake Ridge area our records are of unprecedented resolution, resolving climate key features of the North Atlantic region: Heinrich Stadials (HS) 1 and 2, the Last Glacial Maximum (LGM), the Bølling-Allerød and Younger Dryas (YD). Radiogenic Nd isotope signatures during the LGM reveal AABW to be the prevalent water mass in the deep western North Atlantic. The trend to more unradiogenic signatures during the deglaciation point to an increased formation of NADW which was again replaced by AABW during YD. The Holocene shows the most unradiogenic signatures and therefore established NADW. The circulation strength-proxy $^{231}\text{Pa}/^{230}\text{Th}$ indicates reduced LGM deep circulation, a pronounced slowdown during HS1 and a strong and deep circulation during the Holocene. Compared to isotopic records from the Bermuda Rise (ODP 1063; [4]) we found depth dependent geometry changes of the WBUC which have occurred through the last glacial. Here, we focus on how deep northern sourced water has reached during phases of reduced circulation (indicated by increased $^{231}\text{Pa}/^{230}\text{Th}$ ratios) and the timing of this southward progradation of lower NADW.

References:

- [1] Lynch-Stieglitz, J. et al. (2007), *Science* 316 (66-69);
[2] Gutjahr, M. et al. (2008), *EPSL* 266 (61-77);
[3] Lippold, J. et al. (2016), *EPSL* 445 (68-78);
[4] Böhm, E. et al. (2015), *Nature* 517 (73-76).

IODP

Coccolithophore productivity and carbonate budget at the Indian-Atlantic Ocean Gateway since the Miocene

D. TANGUNAN

Department of Geoscience, University of Bremen, 28359 Bremen, Germany

Frontal zones are crucial players in marine ecosystem of the subpolar regions because of their ability to absorb large quantities of carbon dioxide, which impacts the biological carbonate pump and the global carbon cycle (Read et al., 2000). It is thought that the efficiency of carbon export through the biological pump is controlled by surface water biogeochemistry and abundances of different phytoplankton groups in the photic layer (e.g., Arrigo et al., 1999; Toggweiler et al., 2003; Matsumoto and Sarmiento, 2008). Thus, these regions are key locations to explore the link between nutrient availability and the climatic factors that drive changes in phytoplankton distribution and production, and its consequent impact on the global biogeochemical cycle. One of these frontal regions is located in the southern Indian Ocean, where meridional shifts in the Southern Ocean subtropical front (STF) were suggested to have occurred over the last 800 kyr. Using sediment material recovered from International Ocean Discovery Site U1475 on the Agulhas Plateau (41°25.61'S; 25°15.64'E, 2669 m water depth), where surface water hydrography is influenced by the STF and associated water masses, this proposal is set to answer the following key questions: 1) Did coccolithophore calcification alter the carbonate system and impact regional and global climates since the Miocene?; 2) Can coccolithophore morphological characteristics be used to infer local carbonate chemistry changes in the water column?; and 3) How did the individual coccolithophore taxon respond to changes in water column characteristics driven by changing STF hydrodynamics (e.g., frontal migration, stratification)? These questions will be addressed by morphological characterization of different species belonging to the coccolithophore genus *Scyphosphaera* and quantification of its carbonate contribution over the past 7 Myr (~25 kyr). A contemporaneous high-resolution (~1.5 kyr) productivity reconstruction of the upper 500 kyr will also be generated based on coccolithophore assemblage, accumulation rate, and alkenone concentration. Results from this research will therefore shed light on the dynamics of coccolithophore communities in the Indian-Atlantic Ocean Gateway and resolve the long standing puzzle of the potential of these organisms to alter the carbonate system and impact regional and global climates.

References:

- Arrigo, K. R., Robinson, D. H., Worthen, D. L., Dunbar, R. B., DiTullio, G. R., VanWoert, M., & Lizotte, M. P. (1999). Phytoplankton community structure and the drawdown of nutrients and CO₂ in the Southern Ocean. *Science*, 283(5400), 365-367.
Matsumoto, K., Sarmiento, J. L., & Brzezinski, M. A. (2002). Silicic acid leakage from the Southern Ocean: A possible explanation for glacial atmospheric pCO₂. *Global Biogeochemical Cycles*, 16(3).
Read, J. F., M. I. Lucas, S. E. Holley, and R. T. Pollard. "Phytoplankton, nutrients and hydrography in the frontal zone between the Southwest Indian Subtropical gyre and the Southern Ocean." *Deep Sea Research Part I: Oceanographic Research Papers* 47, no. 12 (2000): 2341-2367.
Toggweiler, J. R., Dixon, K., & Broecker, W. S. (1991). The Peru upwelling and the ventilation of the South Pacific thermocline. *Journal of Geophysical Research: Oceans*, 96(C11), 20467-20497.

IODP

Facies derived compaction trends integrated into a New Jersey shelf hydrogeological model

 A. THOMAS¹, S. REICHE¹, M. RIEDEL², S. BUSKE²
¹Institute for Applied Geophysics and Geothermal Energy, RWTH Aachen University, Mathieustrasse 10, 52074 Aachen, Germany.

²Institute of Geophysics and Geoinformatics, Technische Universität Bergakademie Freiberg, Gustav-Zeuner-Straße 12, 09596 Freiberg, Germany

The existence of offshore fresh groundwater has been observed in several regions around the world. The New Jersey passive margin represents one of the best documented occurrences of this phenomenon, with the first discovery of fresh groundwater dating back to the U.S Geological Survey Atlantic Margin Coring Project, 1976 (Hathaway et al., 1979). Subsequent drilling during ODP Expedition legs 150, 174A and IODP Expedition leg 313 revealed fresh water reservoirs that occur down to 400 m below the sea floor. This study is part of a project ultimately aiming to understand the mechanisms responsible for fresh groundwater emplacement offshore New Jersey based on numerical simulations. A detailed hydrogeological model, which accounts for the highly heterogeneous shelf environment as well as porosity compaction trends, is key to the validity of this numerical analysis. In this study, we use newly re-processed, depth-migrated seismic data tied to IODP 313 wells to perform a detailed seismostratigraphic interpretation along a 2D line extending from the New Jersey coast to the shelf break. A facies distribution model was generated using this structural framework and facies probability trend derived from well data.

The distribution of facies in the shelf environment is the first order control on grain size and shape which are key determinants of porosity. We thus used the facies model as a basis for populating our model domain with petrophysical properties. In order to obtain model porosities, we used IODP 313 core data and extracted porosities according to our facies classifications of sand, silt and shale. This approach allowed for the capture of different compaction trends exhibited by different grain sizes. An exponential regression trend was fitted to data in each facies group for all wells associated with IODP Expedition 313. Mean compaction trends were applied to the entire model domain. The porosity model therefore integrates two key aspects influencing regional groundwater flow: the reduction of porosity with depth due to overburden as well as the contribution of facies heterogeneity to the specific compaction rate at any given part of the shelf. Considering the limited permeability data available from IODP 313 wells measured by Lofi et al. (2013), the hydrogeological model has been assigned permeability values consistent with facies classifications. Sand, silt and shale correspond to high, medium and low permeability, respectively.

Initial numerical simulations performed with this model give key insights into the mechanisms related to preservation of fresh water deposits in the shelf environment. We simulated a period of 15000 years using the simplified assumption that fresh groundwater saturated the upper shelf by the end of the last glacial period. Simulation results indicate that saline groundwater permeates more rapidly into coarser grain sediment packages, while fresh water in fine grained, low permeability sediments survived for longer periods. These results suggest that fresh water reservoirs can survive until present day, with their distribution being primarily controlled by permeability variations. Finally, our simulation results are consistent with observations made by pore water analysis of Expedition 313 wells, where

fresh water was encountered mainly in fine grained sediment intervals.

References:

- Hathaway, J. C., Poag, C. W., Valentine, P. C., Miller, R. E., Schultz, D. M., Manhe, F. T., Kohout, F. A., Bothner, M. H., and Sangi, D. A. (1979). US geological survey core drilling on the Atlantic Shelf. *Science*, Vol. 206: pp. 515-527.
- Lofi, J., Inwood, J., Proust, J.-N., Monteverde, D. H., Loggia, D., Basile, C., Otsuka, H., Hayashi, T., Stadler, S., Mottl, M. J. (2013). Fresh-water and salt-water distribution in passive margin sediments: Insights from integrated ocean drilling program expedition 313 on the new jersey margin. *Geosphere*, 9(4):1009–1024.

ICDP

Holocene Paleohydrology and Extreme Floods in the Dead Sea Region

 R. TJALLIGNI¹, M.J. SCHWAB¹, M. AHLBORN¹, Y. BEN DOR², M. ARMON², Y. ENZEL², J. HASAN SHOQEIR³, A. BRAUER¹ AND PALEX SCIENTIFIC TEAM

¹GFZ German Research Centre for Geosciences, Section 5.2 – Climate Dynamics and Landscape Evolution, Potsdam, Germany

²The Hebrew University of Jerusalem (HUJ), Institute of Earth Sciences, Edmond Safra Campus, Givat Ram, Israel

³Al Quds University, Department of Earth and Environmental Sciences, Abu-Dies, Jerusalem – Palestinian Authority

The strong precipitation gradient and extreme environment of the Levante region is exceptionally sensitive to shifts of atmospheric circulation pattern and related hydrological conditions of mid-latitude climatic zones (Kushnir and Stein, 2010; Neugebauer et al., 2016; Torfstein et al., 2015). Investigate origin and mechanisms driving hydrological and environmental changes are emerging challenges for the population in this region. The PALEX ('Paleohydrology and Extreme Floods from the Dead Sea ICDP sediment core') project addresses all aspects of extreme hydro-meteorological events in this region through a joint effort of scientist from Israel, Palestine and Germany. PALEX has been designed as a project within the DFG Trilateral program with the aim of fostering scientific cooperation in the Near East (grant no. BR2208/13-1/-2).

The long sediment cores obtained by the ICDP ('International Continental Scientific Drilling Program') drilling from the deep basin of the Dead Sea (DSDDP) provide a unique archive to reconstruct the natural hydro-climatic variability for the last 220 kyrs. Our novel approach of combining the observation of recent flash floods using cutting-edge technologies with advanced reconstructions of long flood time-series over several thousand years from the Dead Sea sediment record at high temporal resolution. This approach provided new evidence of an increased frequency of localized torrential rainstorms during a multi-century late Holocene drought in the eastern Mediterranean associated with changes in the synoptic atmospheric circulation pattern (Neugebauer et al., 2015). Our latest results reveal that only local rainstorms exceeding a threshold of 30 mm h⁻¹ for at least one hour can trigger the debris flows at the central western Dead Sea margin (Ein Gedi), which are an exceptional feature Active Red Sea Trough synoptic atmospheric circulation patterns (Ahlborn et al. in press).

Local rainstorm events detected in sediment records of the western Dead Sea margin mark extreme events but local precipitation events and direct linking of these events with the sediment records of ICDP site 5017-1 is still ambiguous. Exact chronological markers and spatial distribution of event layers can improve our interpretation of event layers recorded in core 5017-1. Newly found tephra glass particles of the early Holocene S1 tephra (Neugebauer et al., 2017) allows detailed chronological correlation of event layers between the western

Dead Sea margin and ICDP site 5017-1. Additionally, new exposure of early Holocene lacustrine sediments at the north-western Dead Sea margin (Ein Feshkha) that provide additional sediment sequence complementary to the existing profiles at the south (Ze'elim) and central (Ein Gedi) Dead Sea margin. The second phase of the PALEX program (2018-2020) will focus on the chronological correlation of these three sites using tephra-chronology to provide new details on the distribution of local rainstorms along the western Dead Sea margin. This chronology in combination with chemical characterization of detrital event layers using XRF core scanning data in combination with Nd and Sr isotopes, will be used to determine the origin, frequency and sedimentology of event layers observed sediment record of ICDP site 5017-1.

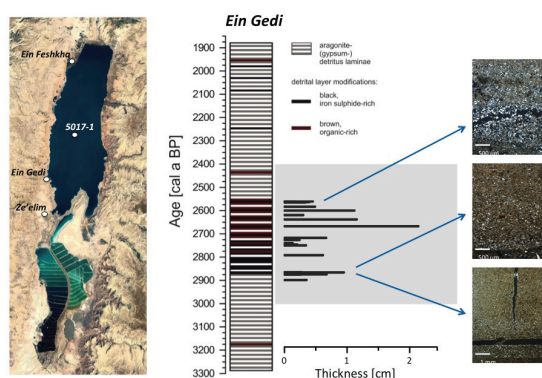


Fig. 1: Coring locations of the Dead Sea basin and sediment profile of Ein Gedi after Neugebauer et al. (2015) and Ahlborn et al. (in press). The increase frequency of grades layers found in the Ein Gedi sediment profile indicate debris flow deposits triggered by local rain storms that require intense rainfall (>30 mm/hr) directly at the slope of the western margin.

References:

- Ahlborn, M., Armon M., Ben Dor, Y., Neugebauer, I., Schwab, M.J., Tjallingii, R., Shoqair, J.H., Morin, E., Enzel, Y., Brauer, A., *in press*. Increased frequency of torrential rainstorms during a regional late Holocene eastern Mediterranean drought. *Quaternary International*.
- Kushnir, Y., Stein, M., 2010. North Atlantic influence on 19th-20th century rainfall in the Dead Sea watershed, teleconnections with the Sahel, and implication for Holocene climate fluctuations. *Quat. Sci. Rev.* 29, 3843–3860. doi:10.1016/j.quascirev.2010.09.004
- Neugebauer, I., Brauer, A., Schwab, M.J., Dulski, P., Frank, U., Hadzhiivanova, E., Kitagawa, H., Litt, T., Schiebel, V., Taha, N., Waldmann, N.D., 2015. Evidences for centennial dry periods at 3300 and 2800 cal. yr BP from micro-facies analyses of the Dead Sea sediments. *The Holocene*. doi:10.1177/0959683615584208
- Neugebauer, I., Schwab, M.J., Waldmann, N.D., Tjallingii, R., Frank, U., Hadzhiivanova, E., Naumann, R., Taha, N., Agnon, A., Enzel, Y., Brauer, A., 2016. Hydroclimatic variability in the Levant during the early last glacial (~117–75 ka) derived from micro-facies analyses of deep Dead Sea sediments. *Clim. Past* 12, 75–90. doi:10.5194/cp-12-75-2016
- Neugebauer, I., Wulf, S., Schwab, M.J., Serb, J., Plessen, B., Appelt, O., Brauer, A., 2017. Implications of S1 tephra findings in Dead Sea and Tayma palaeolake sediments for marine reservoir age estimation and palaeoclimate synchronisation. *Quat. Sci. Rev.* 170, 269–275. doi:10.1016/j.quascirev.2017.06.020
- Torfstein, A., Goldstein, S.L., Kushnir, Y., Enzel, Y., Haug, G., Stein, M., 2015. Dead Sea drawdown and monsoonal impacts in the Levant during the last interglacial. *Earth Planet. Sci. Lett.* 412, 235–244. doi:10.1016/j.epsl.2014.12.013

ICDP

Classifying past climate variation in the Chew Bahir basin, southern Ethiopia, using recurrence quantification analysis

M. H. TRAUTH^{*1}, A. ASRAT², W. DUESING¹, V. FOERSTER³, H. KRAEMER^{1,5}, H. LAMB⁴, N. MARWAN⁵, M. A. MASLIN⁶, F. SCHAEBITZ³ AND THE HSPDP SCIENCE TEAM

¹University of Potsdam, Institute of Earth and Environmental Science, Potsdam, Germany

²Addis Ababa University, School of Earth Sciences, Addis Ababa, Ethiopia

³University of Cologne, Institute of Geography Education, Cologne, Germany

⁴University of Aberystwyth, Department of Geography and Earth Sciences, UK

⁵Potsdam Institute for Climate Impact Research, Potsdam, Germany

⁶Department of Geography, University College London, London, UK

The Chew Bahir Drilling Project (CBDP) aims to test hypothesized linkages between climate and mammalian (including hominin) evolution in tropical-subtropical eastern Africa by the acquisition and analysis of long (~280 m) sediment cores that have recorded environmental change in the Chew Bahir basin. In our statistical project, we describe the Chew Bahir paleolake as a dynamical system composed of interacting components, such as the water body, the sediment below the bottom of the (paleo-)lake, and the organisms living in the lake and its surroundings. A common feature of dynamical systems is the property of recurrence, where patterns of recurring states reflect typical system characteristics whose description contribute significantly to understanding its dynamics. In our example it could be a recurrence of changes in the state variables precipitation, evaporation and wind speed, which lead to similar (but not identical) conditions in the lake (e.g., depth and size of the lake, alkalinity and salinity of the lake water, species assemblage in the water body, diagenesis in the sediment). A recurrence plot (RP), first introduced by J.P. Eckmann in 1987, is a graphical display of such recurring states of the system, calculated from the distance (e.g. Euclidean) between all pairs of observations $x(t)$, within a cutoff limit. To complement the visual inspection of recurrence plots, measures of complexity were introduced for their quantitative description to perform the recurrence quantification analysis (RQA). Here we present and discuss preliminary results of a RQA of the ~550 kyr long environmental record from the Chew Bahir basin.

ICDP

Subsurface Observatory at Surtsey, SUSTAIN Drilling Project

A. TÜRKE¹, W-A. KAHL¹, W. BACH¹

¹Universität Bremen, Klagenfurter Str 2, 28357 Bremen

Surtsey is a 50-year-old volcanic island in the southern offshore extension of the SE Icelandic rift zone and provides a uniquely well-documented record of the explosive eruption of basalt into seawater and the rapid alteration of basaltic glass and crystals in an active hydrothermal system. The ICDP SUSTAIN drilling project, builds on prior results from a 181-m-deep cored drill hole achieved in 1979 (SE-1) which provided highly precise time-lapse observations of the hydrothermal system at 15°C to 141°C, the mineralogical, geochemical, geomagnetic and microbiological processes.

Drilling in 2017 in the Surtsey Natural Reserve and UNESCO World Heritage site re-occupied the 1979 drill site and produced nearly 700 m of core, of which samples will be available after the sampling party (anticipated for summer 2018). We deployed a Subsurface Observatory, a 187 m deep, 47.6 mm diameter (NQ) chamber with T 6061 anodized aluminum casing and five perforated sections at 38, 63, 106, 136, and 161 mbs. These flow-through chambers contain miniature temperature loggers and perforated PEEK (polyetheretherketone) incubators, hung on Vectran rope. A two-year incubation experiment using basaltic glass granules melted from Surtsey lava was installed.

We investigate pore space evolution in the hydrothermally altered tephra and its effect on the Surtsey microbial biosphere. We present details on the in situ incubation experiments and laboratory based supporting flow through cell experiments that will be carried out in the following months.

IODP

Prydz Bay sediment drifts: Archives of modifications in East Antarctic climatic and oceanographic conditions

G. UENZELMANN-NEBEN¹

¹Alfred-Wegener-Institut Helmholtz-Zentrum für Polar- und Meeresforschung, Am Alten Hafen 26, 27568 Bremerhaven

The detailed onset of the Antarctic glaciation during the Eocene/Oligocene and the later ice sheet dynamic in response to warm phases during the Miocene and Pliocene is still under discussion. Attempts to solve the open questions by scientific drilling have been limited by the fact that early Oligocene to early Miocene sediments, which bear witness to the onset of glaciation and early dynamics of the ice sheet, have been eroded from the continental shelf or are buried below thick Neogene sequences and could thus not be sampled during ODP Legs 119 and 188. Several hypotheses place the onset of bottom water formation as the result of down welling due to strong cooling into the Miocene, the late Oligocene, or the late Eocene, which shows the range of uncertainty in dating this event. The dynamical response, e.g., of the Lambert Glacier-Amery Ice Shelf drainage system to climate variability is recorded in the sediments of Prydz Bay and the adjacent slope and rise of the Cooperation Sea. Thus a study of sedimentary features and structures and the prevailing sediment transport patterns can help to understand the development of this system and its sensitivity to climate change.

The analysis of seismic reflection data allows to reconstruct sediment input and sediment transport patterns. This represents an important tool, even if an indirect one, to infer past changes in climate and oceanography in the absence of direct information from drilled geological samples. A large dataset of high-quality seismic lines has been acquired along the Prydz Bay margin, is available via the SCAR seismic data library system and will be analysed with respect to documents of down-slope, i.e., the result of material input via advancing the ice sheet, and along-slope, i.e., features resulting from the shaping of bottom and deep water, to infer past changes in climate and oceanography in combination with results from ODP Leg 119 and 188. This way we also intend to close the gap, which could not be sampled by drilling (the early Oligocene to early Miocene).

ICDP

Paleoenvironmental indications and cyclostratigraphic studies of sediments from tropical Lake Towuti obtained from downhole logging

A. ULFERS¹, K. HESSE¹, T. WONIK¹

¹Leibniz Institute for Applied Geophysics, Stilleweg 2, 30655 Hanover, Germany

Lake Towuti is a tectonic lake in the Mailili lake system in central Sulawesi, Indonesia. Its location (2.75°S, 121.5°E) within the Indo-Pacific-Warm-Pool (IPWP) points out its uniqueness for the reconstruction of terrestrial paleoclimate in this globally important environment which delivers the highest amounts of heat and moisture into atmospheric convection. (Lehmusluoto et al., 1995; Visser et al., 2003)

Pre-site surveys using seismic applications and piston corers showed the potential of the lake to investigate its age and the climate history. (Russell & Bijaksana, 2012; Russell et al., 2014)

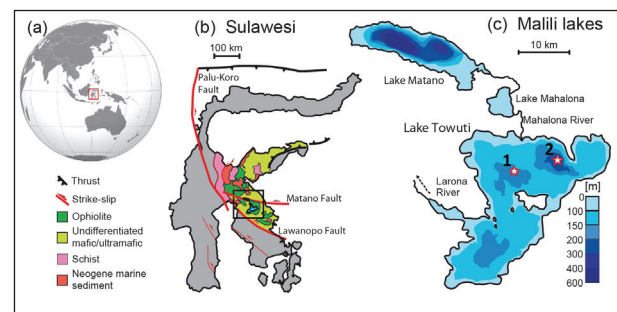


Fig. 1: Overview map of the study area (a) the location of Sulawesi in the Indo-Pacific region, (b) the regional geology of Sulawesi (modified after Kadarusman et al., 2004), and (c) the configuration of the Mailili lake system with the logged drill sites 1 & 2 indicated by red stars. (modified after Russell et al., 2016)

During the drilling campaign in May/June 2015, a set of logging tools (e.g. spectral gamma ray, magnetic susceptibility, resistivity, sonic velocity, dipmeter, ultrasonic image of the borehole wall) was applied in two drill sites to obtain physical and chemical properties of the sediment. Site 1 is characterised by a lacustrine facies in the upper ~103 meters below lake floor (mblf) followed by a pre-lake facies until ~162 mblf and bedrock below 162 mblf. In site 2 drilling was executed down to the border of the lacustrine to pre-lake facies at ~133 mblf. (Russell et al., 2016)

These datasets will be used to reconstruct the paleoenvironmental history of the lake, to construct a continuous lithological log and to link with data gained by seismic surveys. Global climate cycles will be investigated by using cyclostratigraphic methods. This enables the estimation of an age-depth relationship, the sedimentation rates and their changes over time, respectively.

References:

- Lehmusluoto, P., Machbub, B., Terangna, N., Ruspituro, S., Achmad, F., Boer, L., Brahmana, S.S., Priadi, B., Setiadji, B., Sayuman, O. & Margana, A. (1995): National inventory of the major lakes and reservoirs in Indonesia. General limnology. - FAO-FINNIDA.
- Kadarusman, A., Miyashita, S., Maruyama, S., Parkinson, C. D., and Ishikawa, A. (2004): Petrology, geochemistry, and paleogeographic reconstruction of the East Sulawesi ophiolite, Indonesia, *Tectonophysics*, 392, 55–83.
- Russell, J. & Bijaksana, S. (2012): The Towuti Drilling Project: Paleoenvironments, biological evolution, and geomicrobiology of a tropical Pacific lake. – *Scientific Drilling*, 14: 68-71.

- Russell, J., Vogel, H., Konecky, B.L., Bijaksana, S., Hunag, Y., Melles, M., Wattrus, N., Costa, K. & King, J.W. (2014): Glacial forcing of central Indonesian hydroclimate since 60,000 y B.P. – PNAS Early edition; 6p.
- Russell, J. M., Bijaksana, S., Vogel, H., Melles, M., Kallmeyer, J., Ariztegui, D., Crowe, S., Fajar, S., Hafidz, A., Haffner, D., Hasberg, A., Ivory, S., Kelly, C., King, J., Kirana, K., Morlock, M., Noren, A., O'Grady, R., Ordóñez, L., Stevenson, J., von Rintelen, T., Vuillemin, A., Watkinson, I., Wattrus, N., Wicaksono, S., Wonik, T., Bauer, K., Deino, A., Friese, A., Henny, C., Imran, Marwoto, R., Ngkoimani, L. O., Nomosatryo, S., Safiuddin, L. O., Simister, R., and Tamuntuan, G. (2016) : The Towuti Drilling Project: paleoenvironments, biological evolution, and geomicrobiology of a tropical Pacific lake, *Scientific Drilling*, 21: 29-40.
- Visser, K., Thunell, R. & Stott, L. (2003): Magnitude and timing of temperature change in the Indo-Pacific warm pool during deglaciation. - *Nature*, 421: 152-155.

ICDP

Imaging fluid channels using ambient seismic noise (Hartoušov Mofette Field (CZ))

J. UMLAUFT¹, H. FLORES-ESTRELLA¹, M. KORN¹

¹Universität Leipzig, Institut für Geophysik und Geologie, Talstraße 35, 04103 Leipzig

Presently ongoing geodynamic processes within the intracontinental lithospheric mantle give rise to different natural phenomena in the NW Bohemia/Vogtland region (CZ), among others: earthquake swarms, mineral springs and degassing zones of mantle-derived fluids (mofettes). Their interaction mechanisms and relations are not yet fully understood, therefore they are intensively studied using geophysical, geological and biological approaches.

The PIER-ICDP project focuses on the location and investigation of near-surface channels that conduct mantle-originating fluids as well as CO₂. It is aimed to detect and image the fluid channel structure, to determine their depth of origin as well as to characterize the degassing activity at the surface in terms of temporal and spatial variations.

The Hartoušov Mofette Field within the Cheb Basin (NW Bohemia/Vogtland region) is a key site to study fluid flow as it is characterized by strong and constant surface degassing of CO₂. On this field, we installed a dense instrumental array of 95 seismic sensors (45 Data Cubes + 50 Summit XOne Channels) within 1.0 x 0.5 km² extent and measured ambient seismic noise continuously during 3 days in November 2016.

To locate mofette structures on that field as well as adjacent fluid channels into the depth, we applied Matched Field Processing (Vandemeulebrouck et al. 2010, Flores-Estrella et al. 2016), considering the signals generated by surface degassing and subsurface fluid flow as seismic noise sources. Time-lapse analysis of several hours of data shows two stable source areas, that can be followed into the depth and which can be linked to CO₂ degassing zones. However, we also observed small-scale spatio-temporal changes of the source shape and activity. We compared that to continuous wellhead pressure and gas flux data from a gauging well situated within the array at the test site. The MFP outputs and the well-log-data show similar intensity trends over the time.

Hence, it can be shown, that the CO₂ flow acts as an ambient seismic noise source and that we are able to detect degassing areas, small-scale changes of mofette activity in space and time as well as fluid channels into the depth using Matched Field Processing.

IODP

First basaltic melts and early hydrothermal processes at continental breakup - IODP Expeditions 367/368: South China Sea Rifted Margin

F. M. VAN DER ZWAN^{1,2} AND S. PETERSEN

¹GEOMAR Helmholtz Centre for Ocean Research Kiel, 24148 Kiel, Germany

²Institute of Geosciences, Christian-Albrechts-University, 24118 Kiel, Germany

Continental breakup and ocean basin formation has occurred for at least half of Earth's history. However, details on the initial break-up processes, the petrological and geochemical characteristics of the first oceanic crust and its associated hydrothermal systems remain unknown. To study these breakup processes IODP Expedition 367 and 368 (Spring 2017) drilled multiple sites on a transect across the transition zone between continental and oceanic crust in the rifted margin of the South China Sea (SCS). The SCS breakup is unrelated to magmatic plume activity and shows seismic characteristics of a 'hyper-extended margin' (Sun et al., 2016). To determine if the SCS exhibits the exposure of sub-continental lithospheric mantle, similar as e.g. the Iberia margin the expeditions cored the continent-ocean transition (COT) zone by Holes U1499, U1500 and U1502 into the acoustic basement to determine its nature, as well as the outer margin high (OMH), interpreted as continental crust, and the more mature oceanic crust (Sun et al., in press; Jian et al., in press; Fig. 1).

One of the main questions of the South China Sea Rifted Margin Expeditions is the timing of the first magmatic activity related to ocean crust formation. Also the characteristics of these first basaltic melts and their mantle source as well as processes driving melting rifted margins have poorly been studied. Investigating the characteristics of the sources (e.g. chemistry, depth, temperature) the reasons for melting can be determined, which is the key for understanding the breakup mechanisms of the SCS. Magma reservoir contamination processes give insights into the nature of the deeper crust as well as into the extent of the magmatic system. Complimentary to the magmatic system, hydrothermal (cooling) processes are highly important for the formation of the oceanic crust, but the first hydrothermal systems at ocean formation are hardly investigated because they are usually covered by sediments or lava and therefore out of reach. Studying minerals formed by hydrothermal alteration can give information on the temperatures, depths, activity and resource potential of young volcanic-hydrothermal systems.

Here we present our proposed post-cruise research plan to investigate the deep magmatic and the hydrothermal systems of the SCS rifted margin by a combination of different geochemical techniques. The deep magmatic system and its mantle source as well as the melting characteristics will be examined by the study of major, trace and volatile elements of melt inclusions in minerals of igneous rocks. The chemistry of the melt

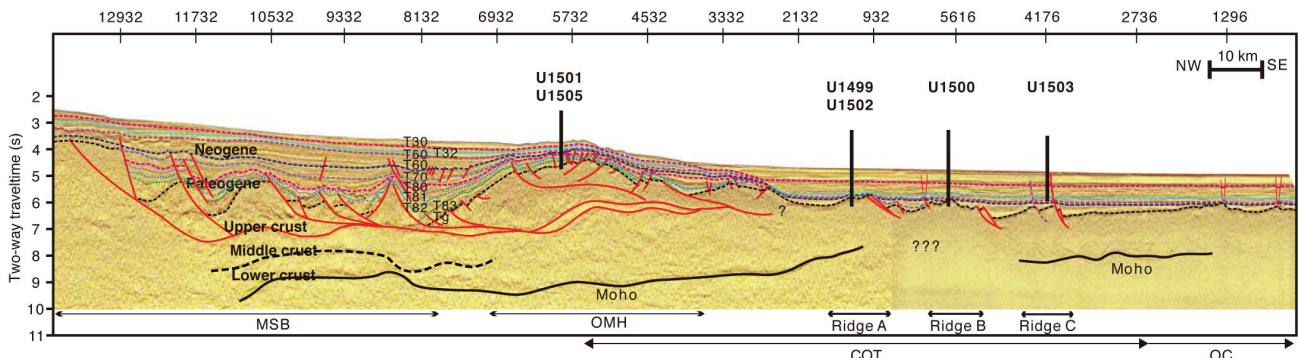


Fig. 1: Deep crustal time-migrated seismic reflection data on a transect across the South China Sea Rifted Margin with interpretation. COT= Continent-ocean boundary; OMH= Outer margin high. The major seismic unconformities are shown in purple and blue. The location of the drill holes U1499 to U1505 of Expeditions 367/368 are indicated on the seismic transect. Seismic data is from Line 04ec1555-08ec1555 (courtesy of the Chinese National Offshore Oil Corporation [CNOOC]) and the figure is after Sun et al., 2016).

inclusions also gives information on assimilation processes in the deep crust and on the nature of this crust. The physicochemical characteristics of the hydrothermal system will be evaluated by a direct study of the major and trace elements, S-isotopes and fluid inclusions of hydrothermal minerals. The deep hydrothermal system will be assessed by chlorine markers in magmatic rocks and their melt inclusions as chlorine is a sensitive tracer for hydrothermal circulation (e.g. van der Zwan et al., 2017). The study of the complementary heating (magma) and cooling (hydrothermal) aspects of continental plate rupture and oceanic crust formation will help in forming a model for the initial breakup mechanisms at the SCS and gives a better global understanding of continental breakup and the formation of oceanic lithosphere.

References:

- Sun Z., Stock J., Jian Z., McIntosh K., Alvarez-Zarikian C., Klaus A. (2016) Expedition 367/368 scientific prospectus: South China Sea rifted margin. International Ocean Discovery Program. doi:10.14379/iodp.sp.367368.2016
- Sun Z., Stock J., Klaus A. and the Expedition 367 Scientists, in press. Expedition 367 Preliminary Report: South China Sea Rifted Margin. International Ocean Discovery Program. doi:https://doi.org/10.14379/iodp.pr.367.2017
- Jian, Z., Larsen, H.C., Alvarez Zarikian, C., and the Expedition 368 Scientists, in press. Expedition 368 Preliminary Report: South China Sea Rifted Margin. International Ocean Discovery Program. https://doi.org/10.14379/iodp.pr.368.2017
- van der Zwan F.M., Devey C.W., Hansteen T.H., Almeev R.R., Augustin N., Frische M., Haase K.M., Basaham A., Snow J.E. (2017) Lower crustal hydrothermal circulation at slow-spreading ridges: evidence from chlorine in Arctic and South Atlantic basalt glasses and melt inclusions. Contributions to Mineralogy and Petrology 172(11-12):97

IODP

The Plio-Pleistocene ACEX (Leg 302) record revisited – A high resolution mineralogical record

C. Vogt¹

¹Crystallography, Geosciences & MARUM, University of Bremen, Klagenfurter Str. 2-4, 28359 Bremen, Germany

Full pattern quantitative phase analysis from X-ray diffraction (QXRD) was performed on approx. 700 samples of the upper 60 composite depth meter of the Arctic Coring Expedition (IODP Leg302) to provide for the coverage of abrupt sedimentation events in the Central Arctic Ocean. This sequence records the approx. last 3.5 Ma of the dominantly terrestrial, glacial and sea-ice dominated sedimentation at the Lomonosov Ridge, Central Arctic Ocean. During that time multiple changes

in the glaciation of the northern hemisphere, the reorganisation of the Arctic Oceanography, the sea-ice producing areas and

sea-level changes influence the transport of terrestrial materials towards the coring sites. Based on former work on short sediment cores, some particular mineral assemblages delineate transport events like deglacial events of the surrounding large ice sheets.

Based on a detailed cyclostratigraphy of the upper 60 m sediment at the Lomonosov Ridge (O'Regan et al., 2010), Central Arctic Ocean, this presentation illustrates the paleoceanography of the Arctic Ocean during the step-wise glaciation of the Northern Hemisphere. The Lomonosov Ridge is situated in the confluence of the Transpolar Drift which today transports sea-ice (sediment) from the Eurasian Siberian shelves towards the Fram Strait between Greenland and Svalbard and the Beaufort Gyre which is known to transport sea-ice and icebergs of Canadian/Alaskan origin towards the centre of the Arctic Ocean. Knies et al. (2009) have pointed out the stepwise glaciation (3 phases: 3.5-2.4, 2.4-1.0 and after 1.0 Ma) of the Barents/Svalbard region while the initiation of the Laurentian Ice Sheet (Canada/Alaska) and/or Ice Shelf Ice Sheets in the Amerasian Siberian Arctic are not as well constrained.

Former work of the author and others has illustrated that input from the Canadian Arctic can be traced by the content of detrital carbonate minerals related to ice rafted debris (IRD) in the Lomonosov sediments. According to our new data the initiation of that transport occurred around approx. 0.7 Ma just during the Mid-Pleistocene Transition.

A mineral assemblage tracing the input of Laptev and Kara Sea derived materials (see Vogt & Knies, 2008) shows enhanced input from about 1.8 to 2 Ma onwards in the ACEX cores. The amplitudes and frequencies of the contents of these minerals are strongly increased. One can assume frequent changes of the Transpolar Drift / Beaufort Gyre system trickered by deglaciation events of the surrounding ice sheets including flooding and aerial exposure of big parts of the shallow Eurasians shelves of Siberia.

These terrestrial input signals are partly masked by authigenic diagenetic processes exemplified by several occurrences of Mn-carbonates and siderite below 20 m core depth. The later in combination with pyrite.

Only QXRD allows for the detrending of the different influences on the mineral assemblage in unprecedented resolution at the ACEX site.

References:

- Knies, J. et al., 2009. The Plio-Pleistocene glaciation of the Barents Sea-Svalbard region: a new model based on revised chronostratigraphy. *Quaternary Science Reviews*, 28(9-10): 812-829, doi:10.1016/j.quascirev.2008.12.002.
- O'Regan, M. et al., 2010. Plio-Pleistocene trends in ice rafted debris on the Lomonosov Ridge. *Quaternary International*, 219(1): 168-176, <https://doi.org/10.1016/j.quaint.2009.08.010>.
- Vogt, C. and Knies, J., 2008. Sediment dynamics in the Eurasian Arctic Ocean during the last deglaciation -- The clay mineral group smectite perspective. *Marine Geology*, 250(3-4): 211-222, doi:10.1016/j.margeo.2008.01.006

IODP

Clumped isotope thermometry and $\delta^{18}\text{O}$ seawater composition of key climate events during the Oligocene

J. VOIGT¹

¹MARUM – Center for Marine Environmental Sciences,
Leobener Str. 8, 28359 Bremen, Germany
(correspondence: jvoigt@marum.de)

The Oligocene is a climate epoch of interest as it marks the establishment of the icehouse world following the warm greenhouse climate of the Palaeocene and Eocene. The first permanent, large continental ice sheets formed on Antarctica at the onset of the Oligocene at ~34 million years ago (Ma) (e.g., Miller et al. 1991; Zachos et al. 2001a). Benthic foraminiferal $\delta^{18}\text{O}$ records show a >1‰ increase during the Eocene-Oligocene transition (EOT), consisting of two distinct steps that are interpreted as an initial cooling step, followed by a step of combined cooling and ice growth (e.g., Coxall et al. 2005; DeConto et al. 2008; Lear et al. 2008). The high $\delta^{18}\text{O}$ values (\geq ~2.5‰) after the EOT indicate permanent ice sheets on Antarctica and cold bottom water temperatures of ~4°C, in contrast to warm Eocene bottom water temperatures (up to ~12°C) (Zachos et al. 2001b). This currently accepted interpretation of the stepwise increase in foraminiferal $\delta^{18}\text{O}$ values was long debated because conventional temperature proxies, such as Mg/Ca ratios of benthic foraminifera, did not show a decrease across the transition (e.g., Lear et al. 2004). The lack of bottom water temperature decrease was caused by changes in the carbonate saturation state resulting in biased benthic foraminiferal Mg/Ca values (e.g., carbonate ion effect) (Coxall et al. 2005). Therefore, estimates of absolute bottom water temperatures across the EOT are still controversial because of the uncertainties derived from traditional temperature proxies (e.g., Coxall et al. 2005). Thus, estimates of the ice extent during the EOT are compromised and very variable (~40-130% of the modern Antarctic ice volume; Zachos et al. 2001b; Coxall et al. 2005; Lear et al. 2008; Liu et al. 2009).

Carbonate clumped isotope (Δ_{47}) thermometry is thermodynamically based and therefore provides temperature estimates independent of the isotopic composition of the source water, in contrast to other carbonate temperature proxies ($\delta^{18}\text{O}$ and Mg/Ca ratios) (e.g., Ghosh et al. 2006). Thus, Δ_{47} allows the calculation of the $\delta^{18}\text{O}$ composition of the water, from which the carbonates precipitated, and estimation of global ice volume changes. Furthermore, Δ_{47} is independent of biological processes and pH (e.g., Ghosh et al. 2006; Kele et al. 2015) which causes large uncertainties in reconstructions of seawater temperatures based on traditional temperature proxies. Using clumped isotope analyses, Δ_{47} , $\delta^{18}\text{O}$ and $\delta^{13}\text{C}$ values of the same aliquot can be determined, thereby enabling a direct comparison of the values. Recent technical advances of the measurement of clumped isotopes allow measurements of small samples (e.g., Schmid and Bernasconi 2010; Meckler et al. 2014). This is important as in palaeoclimate research sample size is

often limited. This method provides data with an analytical error comparable to other temperature proxies and as small as ± 1 -2°C depending on the number of replicate measurements (e.g., Grauel et al. 2013; Thornalley et al. 2015; Fernandez et al. 2017). Another recently developed approach is the paired measurement of clumped isotopes and Mg/Ca ratios on the same foraminiferal tests providing independent temperature estimates and eliminating differences in depth habitat or seasonality when different archives are used (e.g., temperatures derived from biomarkers and foraminiferal tests) (Breitenbach et al., submitted).

Petersen and Schrag (2015) focussed on the Eocene-Oligocene transition at Southern Ocean Site 689 (64°S) using clumped isotopes showing no evident temperature change across the transition. This result is unexpected because a high-resolution $\delta^{18}\text{O}$ record of this site clearly shows a steep increase, which is supported by temperatures derived from biomarkers at a nearby site, showing a temperature change across this interval (Liu et al. 2009). This lack of temperature change could arise from uncertainties in the Δ_{47} -T calibration at low temperatures. Therefore, the aim of the proposed study is to 1) establish a Δ_{47} -T calibration of surface-, thermocline-dwelling and benthic foraminifera of high latitude Southern Ocean sites to better constrain published clumped isotope calibration equations on the low-temperature end, and 2) reconstruct reliable temperatures for bottom and surface seawater at different sites using paired measurements of foraminiferal Δ_{47} and Mg/Ca ratios of specific time intervals of the Oligocene (such as the EOT, Oi-2b, Mi-1 glaciations) to evaluate the seawater temperatures, seawater $\delta^{18}\text{O}$ composition and global ice volume changes.

References:

- Coxall H. K., Wilson P. A., Palike H., Lear C. H., and Backman J. (2005) Rapid stepwise onset of Antarctic glaciation and deeper calcite compensation in the Pacific Ocean. *Nature* **433**, 53-57.
- DeConto R. M., Pollard D., Wilson P. A., Palike H., Lear C. H., et al. (2008) Thresholds for Cenozoic bipolar glaciation. *Nature* **455**, 652-656.
- Breitenbach S. F. M., Mleneck-Vautravers M. J., Grauel A.-L.; Lo L., Bernasconi S. M., et al., Coupled Mg/Ca and clumped isotope analyses of foraminifera provide consistent water temperatures. *submitted to Geochim. Cosmochim. Acta*.
- Fernandez A., Müller I. A., Rodriguez-Sanz L., van Dijk J., Looser N., et al. (2017). A reassessment of the precision of carbonate clumped isotope measurements: Implications for calibrations and paleoclimate reconstructions. *Geochim. Geophys. Geosyst.* **18**, 4375-4386.
- Ghosh P., Adkins J., Affek H. P., Balta B., Guo W., et al. (2006) ^{13}C - ^{18}O bonds in carbonate minerals: A new kind of paleothermometer. *Geochim. Cosmochim. Acta* **70**, 1439-1456.
- Grauel A.-L., Schmid T. W., Hu B., Bergami C., Capotondi L., et al. (2013) Calibration and application of the 'clumped isotope' thermometer to foraminifera for high-resolution climate reconstructions. *Geochim. Cosmochim. Acta* **108**, 125-140.
- Kele S., Breitenbach S. F. M., Capezuoli E., Nele Meckler A., Ziegler M., et al. (2015) Temperature dependence of oxygen- and clumped isotope fractionation in carbonates: a study of travertines and tufas in the 6-95°C temperature range. *Geochim. Cosmochim. Acta* **168**, 172-192.
- Lear C. H., Rosenthal Y., Coxall H. K., and Wilson P. A. (2004) Late Eocene to early Miocene ice sheet dynamics and the global carbon cycle. *Paleoceanography* **19**, PA4015.
- Lear C. H., Bailey T. R., Pearson P. N., Coxall H. K., and Rosenthal Y. (2008) Cooling and ice growth across the Eocene-Oligocene transition. *Geology* **36**, 251-254.
- Liu Z., Pagani M., Zinniker D., DeConto R., Huber M., et al. (2009) Global cooling during the Eocene-Oligocene climate transition. *Science* **323**, 1187-1190.
- Meckler A. N., Ziegler M., Millan M. I., Breitenbach S. F. M., and Bernasconi S. M. (2014) Long-term performance of the Kiel carbonate device with a new correction scheme for clumped isotope measurement. *Rapid Commun. Mass Spectrom.* **28**, 1705-1715.
- Miller K. G., Wright J. D., and Fairbanks R. G. (1991) Unlocking the ice house: Oligocene-Miocene oxygen isotopes, eustasy, and margin erosion. *J. Geophys. Res.* **96**, 6829-6848.
- Petersen S. V. and Schrag D. P. (2015) Antarctic ice growth before and after the Eocene-Oligocene transition: New estimates from clumped isotope paleothermometry. *Paleoceanography* **30**, 1305-1317.
- Schmid T. W. and Bernasconi S. M. (2010) An automated method for 'clumped-isotope' measurements on small carbonate samples. *Rapid Commun. Mass Spectrom.* **24**, 1955-1963.

- Thornalley D. J. R., Bauch H. A., Gebbie G., Guo W., Ziegler M., *et al.* (2015) A warm and poorly ventilated deep Arctic Mediterranean during the last glacial period. *Science* **349**, 706-710.
- Zachos J. C., Shackleton N. J., Revenaugh J. S., Palike H., and Flower B. P. (2001a) Climate response to orbital forcing across the Oligocene-Miocene boundary. *Science* **292**, 274-278.
- Zachos J., Pagani M., Sloan L., Thomas E., and Billups K. (2001b) Trends, rhythms, and aberrations in global climate 65 Ma to present. *Science* **292**, 686-693.

ICDP

Diagenetic siderites and vivianites in ferruginous sediment from Lake Towuti, Indonesia

A. VUILLEMIN^{1,2}, R. WIRTH¹, H. KEMNITZ¹, J. A. SCHUESSLER¹,

L. G. BENNING^{1,3}, A. FRIESE¹, A. LUECKE⁴, C. MAYR⁵, C. HENNY⁶,

K. BAUER⁷, J. M. RUSSELL⁸, S. BIJAKSANA⁹, H. VOGEL¹⁰, S. A. CROWE^{7,11},

J. KALLMEYER¹ AND THE ICDP TOWUTI DRILLING PROJECT SCIENCE TEAM

¹GFZ German Research Centre for Geosciences, Helmholtz Centre Potsdam, 14473 Potsdam, Germany

²Department of Earth & Environmental Sciences, Paleontology and Geobiology, Ludwig-Maximilians-Universität München, 80333 Munich, Germany

³Department of Earth Sciences, Free University of Berlin, 14195 Berlin, Germany

⁴Research Center Juelich, Institute of Bio- & Geosciences 3: Agrosphere, 52425 Juelich, Germany

⁵Institute of Geography, University of Erlangen-Nürnberg, 91054 Erlangen, Germany

⁶Research Center for Limnology, Indonesian Institute of Sciences (LIPI), Cibinong-Bogor, Indonesia

⁷Department of Earth, Ocean, and Atmospheric Sciences, University of British Columbia, Vancouver, Canada

⁸Department of Earth, Environmental, and Planetary Sciences, Brown University, 13 Providence, RI, 02912, USA

⁹Faculty of Mining and Petroleum Engineering, Institut Teknologi Bandung, 15 Bandung, 50132, Indonesia

¹⁰Institute of Geological Sciences & Oeschger Centre for Climate Change Research, University of Bern, 3012 Bern, Switzerland

¹¹Department of Microbiology and Immunology, University of British Columbia, Vancouver, Canada

Lake Towuti is a deep tectonic basin surrounded by ultramafic rocks and lateritic soils. Its geographic position in central Indonesia and relatively great age (estimated >500 ky) makes the lake a prime location to record paleoclimatic changes in the tropical Western Pacific warm pool in its sedimentary sequence (Russell *et al.*, 2016). It was therefore chosen as a drilling target by the International Continental Drilling Program (ICDP). Ultramafic rocks and lateritic soils eroded from the catchment supply Lake Towuti with little sulfate but considerable amounts of iron oxyhydroxides/oxides (Vuillemin *et al.*, 2016, 2017). In the monimolimnion, bottom water anoxia allows for microbially-mediated iron reduction. The extreme scarcity of sulfate and nitrate/nitrite in Lake Towuti's anoxic bottom water represents conditions analogous to those of the Archean Ocean. Nevertheless, Lake Towuti may mix on occasion, resulting in transient oxygenation of its bottom water, which could profoundly change paleoclimatic and microbiological proxies (Costa *et al.*, 2015). These geochemical conditions, which are relatively rare on the modern Earth, make Lake Towuti an ideal site to study Fe mineral formation and diagenesis under conditions relevant to the early Earth.

In May to July 2015, the ICDP Towuti Drilling Project recovered a total >1000 m of sediment cores from three sites, including a 114 m long core dedicated to geomicrobiological studies (Friese *et al.*, 2017). Siderite (FeCO₃) was recovered from 50 distinct layers and investigated to assess authigenesis. Vivianite (Fe₂[PO₄]₂·8H₂O) was found in 5 different horizons

and the crystals handpicked. SEM and TEM imaging showed that siderites exist as both micritic phases and mosaic monocrystals, developing strong twinings and aggregation in deeper samples. Elemental mapping revealed Mn/Fe zonations with Mn enrichment in the center of the minerals, implying mineral formation and growth under variable pore water chemistry. Green rust (Fe₆[OH]₁₂×[CO₃×2H₂O]) and magnetite (Fe₃O₄) were observed in association within individual siderite specimens, suggesting multiple and variable diagenetic pathways and potential oxidative overprinting. The presence/absence of siderite and vivianite may reflect dynamics at the paleo water-sediment interface, and ensuing variability in the relative burial of ferric iron, phosphorus, and organic matter and subsequent diagenetic processes in the sediment. Notably, we observe siderite-rich intervals that are entirely devoid of vivianite. These siderites display heavy d¹³C but light δ⁵⁶Fe compositions. In contrast, siderites, which are less abundant in vivianite-containing intervals, display persistent light d¹³C and δ⁵⁶Fe compositions.

References:

- Costa, K.M., Russell, J.M., Vogel, H., and Bijaksana, S. (2015) Hydrological connectivity and mixing of Lake Towuti, Indonesia, in response to paleoclimatic changes over the last 60,000 years. *Palaeogeogr. Palaeoclimatol.* **417**: 467-475.
- Friese, A., Kallmeyer, J., Kitte, J.A., Montañó Martínez, I., Bijaksana, S., and Wagner, D. (2017) A simple and inexpensive technique for assessing contamination during drilling operations. *Limnol. Oceanogr. -Meth.* **15**: 200-211.
- Russell, J.M., Bijaksana, S., Vogel, H., Melles, M., Kallmeyer, J., Ariztegui, D., *et al.* (2016) The Towuti Drilling Project: Paleoenvironments, biological evolution, and geomicrobiology of a tropical Pacific lake. *Sci. Dri.* **21**: 29-40.
- Vuillemin, A., Friese, A., Alawi, M., Henny, C., Nomosatryo, S., Wagner, D., Crowe, S.A., and Kallmeyer, J. (2016) Geomicrobiological features of ferruginous sediments from Lake Towuti, Indonesia. *Front. Microbiol.* **7**: e1007.
- Vuillemin, A., Horn, F., Alawi, M., Henny, C., Wagner, D., Crowe, S., and Kallmeyer, J. (2017) Preservation and significance of extracellular DNA in ferruginous sediments from Lake Towuti, Indonesia. *Front. Microbiol.* **8**: e1440.

ICDP

Tephrochronology of a 415 ka sediment record from the Fucino Basin, Central Italy

B. WAGNER¹, B. GIACCIO², N. LEICHER², G. MANNELLA³, S. NOMADE⁴, E. REGATTIERI³, T. WONIK⁵, G. ZANCHETTA³

¹University of Cologne, Cologne, Germany

²Istituto di Geologia Ambientale e Geoingegneria, CNR, Roma, Italy

³Dipartimento di Scienze della Terra, University of Pisa, Pisa, Italy

⁴Laboratoire des sciences du climat et de l'environnement, CEA/CNRS/UVSQ, Gif-Sur-Yvette, France

⁵Leibniz Institute for Applied Geophysics, Hannover, Germany

The Fucino Basin is located at ~650 m a.s.l. in the Central Apennine, Italy. Its formation started during the Plio-Pleistocene and was driven by the currently active Fucino Fault System (e.g., Galli *et al.* 2008). During glacial periods, the basin was not glaciated, but glaciers covered the surrounding mountains and reduced the hydrological budget (e.g., Giraudi & Giaccio 2015). Until historical time the Fucino Basin hosted the Lake *Fucinus*, which covered a surface area of 150 km². The lake was partly drained during the 1st-2nd century AD and drainage was completed at the end of the 19th century. Thus, the Fucino Basin is likely the only Central Apennine basin that documents continuously the sedimentary history since the Early Pleistocene and up to the historical times (Giaccio *et al.* 2015).

Its good range of distance downwind of the peri-Tyrrhenian volcanic centres (< 150 km) makes the Fucino Basin the best candidate available in the central Mediterranean that allows the assemblage of a long and continuous tephrochronological record independently dated by the ⁴⁰Ar/³⁹Ar method. The chronology can be directly anchored to a comprehensive time series of proxies from the lacustrine sediments, which are highly

sensitive to climate variations (Giaccio et al. 2015). Transferring chronological and stratigraphic information and long- and short-term climate variability derived from the Fucino record to the network of long terrestrial Mediterranean records further to the East (e.g. Dead Sea, Lake Van, Lake Ohrid and Tenaghi Philippon) and to the West, i.e. North Atlantic climate records, sets the framework for a better understanding of the spatio-temporal variability, the magnitude, and the different expressions of Quaternary orbital and millennial-scale paleoclimatic changes.

The sediment architecture of the Fucino Basin is relatively well defined by several seismic lines (Cavinato et al. 2002, Patacca et al. 2008), which depict a semi-graben geometry in the basin with increasing thickness of the sedimentary infilling from the West to the East and from the north-western and south-western tips to its central part. Based on the seismic information available, a ~82 m-long sediment succession (F1-F3) was recovered from the eastern-central area of the Fucino Basin in June 2015. The lithology of the sediments is rather homogeneous and is dominated by fine-grained lacustrine sediments composed of grey calcareous marl with variable proportions of clay and organic matter. 23 tephra layers, five of which were newly dated using the $^{40}\text{Ar}/^{39}\text{Ar}$ method, constrain the chronology of the core continuously back to 190 ka (Giaccio et al. 2017). The tephra layers originate from different Italian volcanoes, and comprise key Mediterranean marker tephra layers, such as the Neapolitan Yellow Tuff, Y-7, C-22, X-5, and X-6. The tephrochronological information is the basis for the establishment of an age model for the F1-F3 core and to correlate geochemical and bio-geochemical data from the F1-F3 record to climate variability.

Based on the promising results from the F1-F3 core, an international consortium of scientists formed and raised funding from different institutions, including IGAG-CNR (Italy), IGG-CNR (Italy), INGV (Italy), LIAG (Germany), and the Universities of Pisa (Italy), Rome (Italy), Cologne (Germany), Geneva (Switzerland), and Nottingham (UK), for a new coring campaign and borehole logging. A new site (F4-F5) was selected, where seismic and pollen data from a previous drilling indicated a lower sedimentation rate compared to the F1-F3 site. In June 2017, two ca. 86 m long cores were recovered at the new site and borehole logging was carried out in hole F4 down to ca. 80 m. First core analyses comprise multi-sensor core logging (MSCL, GEOTEK Co.), line scan imaging, and XRF scanning (ITRAX, COX Ltd). Based on these data and on optical information after core opening, the individual, overlapping 1.5 m long sediment sequences are correlated to a core composite. Subsampling of discrete sediment samples and tephra horizons for paleomagnetic, geochemical, sedimentological, and tephrostratigraphical studies started in autumn 2017 and we already found more than 130 tephra or cryptotephra horizons back to ca. 415 ka (MIS 11).

For the establishment of a deep drilling campaign within the scope of ICDP, the main objective is to assemble a high-precision $^{40}\text{Ar}/^{39}\text{Ar}$ dated tephrochronological record anchored to a detailed paleoclimate record that may be regionally to globally spread via tephrostratigraphic synchronizations and paleoclimatic alignments. Arising aims of this main objective are (i) to determine the sequence, the timing, the duration and the dynamics of past climate events of terrestrial and marine records and related biodiversity changes, (ii) to improve the knowledge on volcanology, petrology and geodynamics, and (iii) to improve the knowledge on the age, dynamics and tempo of paleomagnetic excursions.

The new project here applied for will use the F4-F5 (and also the F1-F3) record (i) to establish a master record for Mediterranean tephrostratigraphy by detailed geochemical characterisation and direct $^{40}\text{Ar}/^{39}\text{Ar}$ dating, (ii) to prove undisturbed and continuous sedimentation in the basin after the Mid-Brunhes event, (iii) to provide detailed chronological information on the timing and duration of climatic and paleomagnetic events, (iv) to improve the knowledge of the eruptive activity, the recurrence, and geodynamic evolution of the main volcanic districts of southern and particularly of central Italy during the last 415 ka, and (v) to allow investigation of the lower limits of crystal size requirements for $^{40}\text{Ar}/^{39}\text{Ar}$ dating by a methodological approach.

The project will be carried out in close collaboration with national and international partners. Major and minor geochemical elements will be measured in cooperation with B. Giaccio (IGAG-CNR, Rome, Italy), who is the leading expert for the tephrostratigraphic work in the project. Analysis of trace elements of tephra layers will be carried out in cooperation with R. Fonseca from the University of Bonn, Germany. Isotope analysis (Sr-Nd) on tephra will be conducted within the geochemistry working group of C. Münker at the University of Cologne, Germany. $^{40}\text{Ar}/^{39}\text{Ar}$ will be carried out in cooperation with S. Nomade (CEA-CNRS-UVSQ, Gif-sur-Yvette, France). Multi-proxy sedimentological and geochemical analyses and joint paleoclimatic interpretation of the proxies will be carried out in cooperation with G. Zanchetta, E. Regattieri, and G. Manella (Università di Pisa, Italy). Paleomagnetic analyses on the F1-F3 and on the new F4-F5 sequence will be carried out in cooperation with Fabio Florindo (INGV, Roma, Italy). Palynological studies on the F1-F3 and on the new F4-F5 sequence will be coordinated by Laura Sadori (University of Roma "La Sapienza", Italy).

References:

- Cavinato GP, Carusi C, Dall'Asta M, Miccadei E & Piacentini T. 2002. Sedimentary and tectonic evolution of Plio-Pleistocene alluvial and lacustrine deposits of Fucino Basin (central Italy). *Sedimentary Geology*, 148, 29–59.
- Galli P, Galadini F & Pantosti D. 2008. Twenty years of paleoseismology in Italy. *Earth-Science Reviews*, 88, 89–117.
- Giaccio B, Niespolo EM, Pereira A, Nomade S, Renne PR, Albert PG, Arienzo I, Regattieri E, Wagner B, Zanchetta G, Gaeta M, Galli P, Mannella G, Peronace E, Sottili G, Florindo F, Leicher N, Marra F & Tomlinson EL. 2017. First integrated tephrochronological record for the last ~190 kyr from the Fucino Quaternary lacustrine succession, central Italy. *Quaternary Science Reviews*, 158, 211–234.
- Giaccio B, Regattieri E, Zanchetta G, Wagner B, Galli P, Mannella G, Niespolo E, Peronace E, Renne PR, Nomade S, Cavinato GP, Messina P, Sposato A, Boschi C, Florindo F, Marra F & Sadori L. 2015. A key continental archive for the last 2 Ma of climatic history in central Mediterranean area: a preliminary report on the Fucino deep-drilling project, central Italy. *Scientific Drilling*, 20, 13–19.
- Giraudi C & Giaccio B. 2015. The Middle Pleistocene glaciations on the Apennines (Italy): New chronological data and considerations about the preservation of the glacial deposits. *Geological Society, London, Special Publications*, 433 (5), doi:10.1144/SP433.1.
- Patacca E, Scandone P, Di Luzio E, Cavinato G & Parotto M. 2008. Structural architecture of the central Apennines: interpretation of the CROP 11 seismic profile from the Adriatic coast to the orographic divide. *Tectonics*, 27, TC3006.

IODP

Petrogenesis of Snake River Plain basalts from the Kimama core: an experimental study on ferrobasalts

 M. WANG¹, O. NAMUR², R. ALMEEV¹, B. CHARLIER³, F. HOLTZ¹
¹Leibniz Universität Hannover, Institute of Mineralogy, Germany

²Department of Earth and Environmental Sciences, KU Leuven, Belgium

³Department of Geology, University of Liege, Belgium

The Snake River Plain-Yellowstone (SRPY) province is among the most voluminous expressions of magmatic activity at the Earth's surface and also represents one of the best examples of bimodal basalt-rhyolite volcanism (Bonnichsen et al., 2008; Ellis et al., 2013). Drilling by the ICDP HOTSPOT project at Kimama was performed between September 2010 and January 2011 and reached a final depth of 1912 m. The Kimama drill hole is dominated by basalt, with thin intercalations of sediment in the upper 200 m and lower 300 m. Detailed lithologic and geophysical logging have documented ~557 basalt flows, comprising at least 30 flow groups (13 to 170 m thick) representing distinct time periods, and magma batches, with the oldest lavas being dated at ~6 Ma (Bradshaw et al., 2012; Champion and Duncan, 2012; Potter et al., 2012). In this study, we conducted a detailed petrological study of the rocks from the Kimama drill core that we combined with crystallization experiments. The aims are to understand the mechanisms of basaltic differentiation in the crust, the magma storage conditions and the petrological link between basalts and rhyolites.

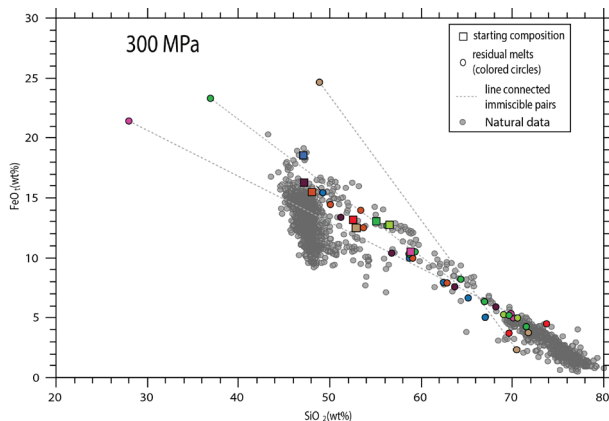


Fig. 1: FeO_T vs SiO₂ binary diagram in 300MPa showing the liquids experimentally produced in this study compared to the range of bulk-rock compositions of natural samples observed in the SRPY province. Colored squares represent different starting compositions and colored circles represent different residual melts. Grey circles represent all the compositions of the natural samples from Kimama drill cores. The 600MPa experiments are not shown but two run products show immiscibility features.

Hundred and ninety core samples were studied carefully for petrography. Out of them, 105 samples were measured for major and trace elements analyses and 25 representative samples were chosen for detailed microprobe analyses. Kimama rocks range from highly-phyric to crystal-poor lavas with less than 10% of phenocrysts. The typical mineral assemblage of phenocrysts contains olivine (some with Cr-spinel inclusions) and plagioclase. Clinopyroxene is abundant in the groundmass along with plagioclase, olivine, magnetite, ilmenite and apatite. Whole rock compositions plotted on Harker diagrams and along stratigraphic column demonstrate that fractionation is evident across different flow groups, showing a gradual change

from more primitive basalts at depth to evolved basalts in the upper section. The major and trace element variations are consistent with the fractionation of the observed mineral assemblage (Ol + Plg ± Cpx). The most evolved Fe-Ti-rich basalts with 17-19 wt% total Fe₂O₃ and 3.2 - 4.8 wt% TiO₂ occur in two stratigraphic intervals (1045-1047 m and 1731-1797 m). These rocks have a very fine-grained groundmass with abundant Fe-Ti oxide mineral.

Plagioclase phenocrysts core and rim compositions were obtained for 115 crystals. Core compositions of plagioclase phenocrysts can be classified into four groups by calcium contents, i.e., ~An₈₀, ~An₇₅ ~An₆₅, and ~An₅₅. Pyroxenes are represented by augite and pigeonite. Analyses of 290 crystals show that clinopyroxene compositions vary from Mg# 82 to Mg# 32, with a prominent peak at ~Mg# 70. Olivine compositions vary from Fo₈₂ to Fo₃₂. Detailed microprobe profiles (with intervals of ~4-6 μm) of major (Si, Fe, Mg, Mn) and minor (Ca, Ni) elements were measured in a total of 100 olivine crystals from various samples. Based on the range of Fo values and the shape of zoning patterns observed in all our analyses we distinguished four types of olivine zoning. Olivine crystals are characterized by zoning patterns ranging from 1) 'normal' (decreasing Fo towards the rim) to 2) 'reverse' (lower Fo core with higher rim), or more complex zoning, with reversely zoned interiors and normally zoned rims (3&4). Different zoning types in olivine crystals and the quantitative interpretation of the compositional profiles will be helpful to resolve the timescales of magmatic processes during magma storage (e.g., time between different replenishment events).

In order to better understand the pre-eruption storage conditions, we conducted diffusion modeling, which is useful to obtain time-scale information. The diffusion profiles correspond to Fe-Mg exchange between the core and rim of the crystal. To increase the accuracy and precision of timescales, we also determined crystallographic axis orientations of the minerals by electron backscatter diffraction (EBSD, Prior et al., 1999). The electron backscatter patterns (EBSP) were obtained using Stereo32 software developed to calculate the angles between measured electron microprobe traverses and crystallographic axes in olivine (Costa and Chakraborty, 2004). This allowed us to correct the strongly anisotropic diffusion of Fe and Mg in olivine, where diffusion along the [001] crystallographic orientation is around six times faster than along [100] or [010] (Dohmen and Chakraborty, 2007). The residence timescales range from ~3 to 420 days, reflecting the diversity of crystal histories within magma chambers in depth. A possible interpretation is that olivines stored in deeper chamber(s) are subsequently introduced into a different magmatic environment. These results are of importance to interpret seismic and geodetic data in term of pre-eruptive magma storage and transport of magmas in the crust.

The petrological link between basalts and rhyolites was investigated by high pressure phase equilibria experiments conducted with different starting materials. We initially selected four mafic representative compositions that were used as starting compositions for high-temperature (>1,020°C) experiments. The four selected evolved ferrobasaltic compositions as starting materials for high temperature experiments include three compositions represent the most evolved basaltic lavas from the Kimama core (S1, S2, C4-1), and one composition S3 with 55 wt% SiO₂ represents ferrobasalt from the Crater of the Moon (Leeman et al., 1976). To simulate and characterize the liquid lines of descent, especially at conditions where high crystal contents were observed, we synthesized new starting compositions based on the microprobe data of the glass

compositions obtained from the experimental products of mafic starting materials. To achieve this goal, six new compositions have been synthesized (SiO₂ contents in the range 51 to 58 wt% SiO₂).

The six evolved compositions were selected along the liquid lines of descent for relatively low temperature experiments (<1,020°C), which are required to produce SiO₂-rich compositions similar to those of natural SRP rhyolites.

Accordingly, 54 individual experiments have been conducted using all these ten compositions. All starting materials are synthetic glass analogues matching natural compositions and prepared using high purity reagent grade oxides, silicates and carbonates. All experiments have been conducted at 300 and 600 MPa, under nominally dry conditions (the water content of the melt is estimated to be less than 0.4 wt% H₂O; Husen et al., 2016). The intrinsic redox conditions correspond to ca. FMQ buffer at nominally dry conditions. Different experimental procedures were applied. For some experiments, the sample was held above the liquidus temperature for ca. 24 h before dropping to the target temperature and equilibrating for 2-4 days. Other experiments were performed with a cooling rate of 1.2 °C/h between liquidus and target temperature and then equilibrated at the final temperature for 1-2 additional days. To increase the size of the mineral phases so that accurate analyses are possible, we applied a temperature cycling in some experiments following the method (Erdmann and Koepke, 2016).

Experimental liquid lines of descent of the studied ferrobasalts and their evolved products are summarized in Fig.1. We obtained measurable glass pools up to the level of 82% of crystallization. The solid phase of the samples was always represented by Cpx + Pl ± Mt ± Ilm ± Ap mineral assemblage. Olivine was not observed in our experimental products, indicating that it was not stable at such high crystallization degrees. Experimental residual liquids contained up to 73.8 wt% SiO₂ (Fig.1), thus fully approaching the compositions of less evolved natural rhyolite (>72% SiO₂). Clinopyroxenes [augite (Aug) and pigeonite (Pig)] are stable phases in all experiments. Plagioclase (Pl) is only absent occasionally in two 600 MPa runs at higher temperature (1080°C). The crystallization order of S1 composition is Aug + Mt à Ap à Pl → Pig. The crystalline phases of S2 composition is Pl + Aug + Mt at 300 MPa and 600 MPa. At 300 MPa Ap, Pig and Ilm are observed at lower temperatures. The composition S3 is unique compared to other three compositions, as its crystallization products always resulted in formation of two residual immiscible liquids at the two investigated pressures. It is emphasized that the formation of immiscible Si-rich and Fe-rich liquids has been experimentally demonstrated at high pressure (600 MPa) for the first time (Fig.2). Except for one experiment (1,060°C /600 MPa), all the immiscible pairs are comparable with those obtained in tholeiitic system in previous experiments. Figure 2 shows that with cooling, immiscible melt pairs become increasingly contrasted in composition. Felsic end members with very high Silica contents were observed (73.8 wt.% SiO₂; 4.6 wt.% FeOtot; 11.9 wt.% Al₂O₃).

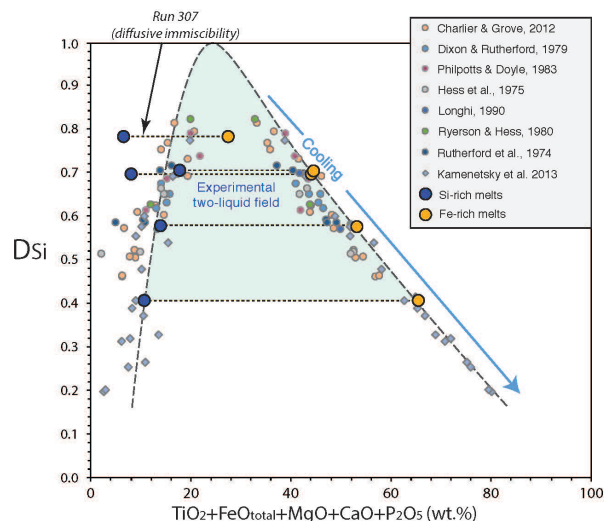


Fig. 2: Compositions of conjugate immiscible melts in this study compared to previous experimental melt pairs in tholeiitic systems and native iron-hosted melt inclusions in lavas of the Siberian Traps (Kamenetsky et al., 2013). D_{Si} , the partitioning of SiO₂ between the Fe-rich and Si-rich melts, expresses the compositional gap between the two melts, plotted as a function of elements partitioned into the Fe-rich melts.

The crystallization experiments are pertinent to test the potential development of silicate liquid immiscibility along basalt to rhyolite differentiation in Snake River Plain. Particularly, the range of alkali (Na₂O+K₂O) and P₂O₅ contents of the selected compositions is a critical parameter for the development of a two-liquid field (e.g. Charlier and Grove, 2012). It is also remarkable that the Si-rich immiscible liquids obtained both at 600 MPa and 300MPa also approaches natural SRPY rhyolite compositions, providing new evidences for the importance of liquid immiscibility in magma genesis of rhyolites from the SRPY and other bimodal volcanic provinces.

References:

- Bradshaw, R.W., Christiansen, E.H., Dorais, M.J., Shervais, J.W., Potter, K.E., 2012. *Eos Trans. AGU*: V13B-2840
- Bonnichsen, B., Leeman, W., Honjo, N., McIntosh, W., Godchaux, M., 2008. *Bulletin of Volcanology* 70(3): 315-342
- Champion, D., Duncan, R.A., 2012. *Eos Trans. AGU*: V13B-2842.
- Charlier, B., Grove, T., 2012. *Contrib. Miner. Petrol.* 164(1): 27-44.
- Dohmen, R. and Chakraborty, S., 2007. *Physics and Chemistry of Minerals* 34(6): 409-430.
- Dixon, S., Rutherford, M. J., 1979. *Earth and planetary science letters* 45, 45-60.
- Ellis, B.S., Wolff, J.A., Boroughs, S., Mark, D.F., Starkel, W.A., Bonnichsen, B., 2013. *Bulletin of Volcanology* 75(8): 1-19.
- Erdmann, M., J. Koepke., 2016. *American Mineralogist* 101(4): 960-969.
- Leeman, W.P., Vitaliano, C.J., Prinz, M., 1976. *Contributions to Mineralogy and Petrology* 56(1): 35-60.
- Longhi, J., 1990. *Proc. Lunar Planet. Sci. Conf.* 20. 13-24.
- Hess, P. C., Rutherford, M. J., Guillemette, R. N., Ryerson, F. J., Tuchfeld, H. A., 1975. *Lunar Planet. Sci. Conf.* 6. 895-909.
- Husen, A., Almeev RR, Holtz, F., 2016. *Journal of Petrology* 57(2): 1-35.
- Kamenetsky, V.S., Charlier, B., Zhitova, L., Sharygin, V., Davidson, P., Feig, S., 2013. *Geology* 41, 1091-1094.
- Philpotts, A. R., Doyle, C. D., 1983. *American Journal of Science* 283, 967-986.
- Prior, D.J., 1999. *Journal of Microscopy*, 195(3): 217-225.
- Potter, K.E., Shervais, J.W., Champion, D., Duncan, R.A., Christiansen, E.H., 2012. *Eos Trans. AGU*: V13B-2839.
- Rutherford, M. J., Hess, P. C., Daniel, G. H., 1974. *Proc. Lunar Planet. Sci. Conf.* 5. 569-583.
- Ryerson, F. J., Hess, P. C., 1980. *Geochim. Cosmochim. Acta* 42, 921-932.

IODP

IODP Expedition 382 – Iceberg Alley Paleoceanography & South Falkland Slope Drift

M.E. WEBER¹, M. RAYMO², Y.M. MARTOS³, C. ALLEN⁴, S. BELT⁵,
 P.U. CLARK⁶, M. GARCIA⁷, M. GUTJAH⁸, I. HALL⁹, G. KUHN¹⁰,
 F. BOHOYO¹¹, G. LOHMANN¹⁰, N. MCCAVE¹², J.X. MITROVICA¹³,
 R. SCHNEIDER¹⁴, D. SPRENK¹⁵, J. STONER⁶, A. TIMMERMANN¹⁶,
 T. WILLIAMS¹⁷, N.R. GOLLEDGE¹⁸, R. DECONTO¹⁹, R. GLADSTONE²⁰,
 A. HEIN²¹, K. HENDRY²², A. LEVERMANN²³, J. PIKE²⁴, D. POLLARD²⁵,
 V. PECK⁴

- ¹ Steinmann Institute, University of Bonn, Bonn, Germany
² Lamont-Doherty Earth Observatory of Columbia University, Palisades, NY, USA
³ NASA Goddard Space Flight Center, Greenbelt, USA
⁴ British Antarctic Survey, Cambridge, UK
⁵ School of Geography, Earth and Environmental Sciences, University of Plymouth, Plymouth, U.K.
⁶ College of Earth, Ocean, and Atmospheric Sciences, Oregon State University, USA,
⁷ Instituto Andaluz de Ciencias de la Tierra (IACT), Granada, Spain
⁸ GEOMAR Helmholtz Centre for Ocean Research, Kiel, Germany
⁹ School of Earth and Ocean Sciences, Cardiff University, UK
¹⁰ Alfred-Wegener-Inst. Helmholtz Center for Polar and Marine Research (AWI), Bremerhaven, Germany
¹¹ Instituto Geológico y Minero de España (IGME), Madrid, Spain
¹² Department of Earth Sciences, University of Cambridge, UK
¹³ Department of Earth And Planetary Sci., Harvard University, Cambridge, MA, USA
¹⁴ Research Group Paleoceanography and climate, Institute of Geology, University of Kiel, Germany
¹⁵ University of Cologne, Institute of Geology and Mineralogy, Germany
¹⁶ Center for Climate Physics, Pusan University, Busan, Republic of Korea
¹⁷ International Ocean Discovery Program, Texas A&M University, USA
¹⁸ Antarctic Research Centre, Victoria University of Wellington, New Zealand
¹⁹ Department of Geosciences, University of Massachusetts, Amherst, USA
²⁰ Arctic Centre, University of Lapland, Rovaniemi, Finnland
²¹ School of Geosciences, University of Edinburgh, UK
²² School of Earth Sciences, University of Bristol, UK
²³ Sustainable Solutions, Potsdam Institute for Climate Impact Research, Germany
²⁴ School of Earth and Ocean Sciences, Cardiff University, UK
²⁵ College of Earth and Mineral Sciences Pennsylvania State University, State College, USA

Several decades of research on the paleoceanography and paleoclimatology of the Scotia Sea using short cores and remote-sensing data have revealed a wealth of information on Late-Pleistocene ice sheet-ocean-climate interactions, but deep drilling is required for understanding the evolution of these interactions and their sensitivity to different boundary conditions over longer timescales. Drilling deep sites in Pirie Basin and in Dove Basin shall decipher the geological history back to the Miocene and to test competing hypotheses in this important yet undersampled region.

International Ocean Discovery Program (IODP) Expedition 382 is scheduled to start in Punta Arenas, Chile, on 20 March 2019 and to end in Punta Arenas, Chile, on 20 May 2019. Expedition objectives shall be achieved through the first deep drilling in the Scotia Sea. Six sites should recover up to 600 m long Late Neogene sequences to reconstruct past variability in Antarctic Ice Sheet (AIS) mass loss, oceanic and atmospheric circulation.

We will deliver the first spatially integrated record of variability in iceberg flux from Iceberg Alley, where a substantial

number of Antarctic icebergs exit into the warmer Antarctic Circumpolar Current (ACC). In particular, we will characterize the iceberg flux during key times of AIS evolution: Middle Miocene glacial intensification of the East Antarctic Ice Sheet, mid-Pliocene warm interval, Late Pliocene glacial intensification of the West Antarctic Ice Sheet, mid-Pleistocene transition, warm interglacials of the last 800 kyr, and glacial terminations. We will use the geochemical provenance of detrital material to determine regional sources of AIS mass loss, address inter-hemispheric phasing of ice-sheet and climate events, and the relation of AIS variability to sea level.

We will also provide critical information on changes in Drake Passage throughflow, meridional overturning in the Southern Ocean, water-mass changes, CO₂ transfer via wind-induced upwelling, sea-ice variability, bottom water outflow from the Weddell Sea, Antarctic weathering inputs, and changes in oceanic and atmospheric fronts in the vicinity of the ACC by comparing N-S variations across the Scotia Sea.

Comparing changes in dust proxy records between the Scotia Sea and Antarctic ice cores will provide a detailed reconstruction of changes in the Southern Hemisphere westerlies on millennial and orbital time scales for the last 800 kyr. Extending this comparison beyond 800 kyr will help evaluating climate-dust couplings since the Pliocene, its potential role in iron fertilization and atmospheric CO₂ drawdown during glacials, and whether dust and changes in Antarctic ice volume played a role in the mid-Pleistocene transition.

Post-cruise analytical work will include: magneto-, bio-, and tephrostratigraphy, combined with dust tuning, stable isotopes, and relative paleointensity to establish the chronology; production of seawater-derived radiogenic isotope records, iceberg-rafted debris, physical properties, XRF scanning, and provenance studies to constrain ice dynamics; geochemistry, sortable silt, stable isotopes, biomarkers, and diatom assemblages to reconstruct ocean temperature, current strength, productivity, and sea-ice extent. Models will help investigating possible physical mechanisms causing changes in ice-sheet dynamics, ocean-atmosphere interactions, and sea-level changes.

IODP

Transport, Removal and Accumulation of sediments Numerically Simulated for Paleo-Oceans and Reconstructed from cores of The Eirik Drift (TRANSPORTED)

T. WEBER¹, C. DRINKORN, J. SAYNISCH¹, G. UENZELMANN-NEBEN²,
 M. THOMAS^{1,3}

¹ GFZ German Research Centre for Geosciences, Telegrafenberg, 14473 Potsdam, Germany

² Alfred-Wegener-Institut Helmholtz-Zentrum für Polar- und Meeresforschung, Am Handelshafen 12, 27570 Bremerhaven, Germany

³ Freie Universität Berlin, Carl-Heinrich-Becker Weg 6-10, 12165 Berlin, Germany

The Eirik Drift south of Greenland records the changes in sediment transport by the deep ocean currents of the North Atlantic. The most influential bottom current is the Western Boundary Undercurrent (WBUC) which plays a major role in the global meridional overturning circulation and is driven by deep water formation in the Greenland, Labrador, Norwegian and Iceland Seas. Tectonic events and changing climate conditions have altered the pathway and strength of the WBUC over the last millions of years (Uenzelmann-Neben et al. (2016)). These changes are recorded in the sediments of Eirik Drift. By

means of seismic profiles (e.g., Müller-Michaels and Uenzelmann-Neben (2014, 2015)) and drill cores (Expedition 303 Scientists (2006), Shipboard Scientific Party (1987)), sedimentation rate and grain sizes can be determined since the late Miocene and the Pliocene. Both time slices have attracted interest of the climatological community due to their resemblance to possible future anthropogenically modified climate states (Salzmann et al. (2009)). Several numerical climate and ocean studies have linked local temperature and precipitation proxies to global climate changes during the late Miocene and the Pliocene. In the project TRANSPORTED we will link tectonic events and climate change to alterations of the strength and flowpaths of the WBUC and, hence, to sedimentation rates and grain sizes recorded in the cores from Sites 646 and U1305-1307 in the Eirik Drift.

The numerical simulations will be carried out with the Regional Ocean Modeling System (ROMS, Shchepetkin and McWilliams (2005)). A regionalization to the North Atlantic enables us to simulate the areas of deep water formation in the North Atlantic and the Nordic Seas at unusually high spatial resolution and to resolve sediment transport by the WBUC in time and space. ROMS is a modern and highly modular ocean model code that uses terrain following sigma coordinates. The resulting higher resolution of oceanic bottom layers and the state of the art sediment and sea ice modules make ROMS a suitable choice for the proposed sensitivity simulations (cf., Li (2012)). This will lead to quantitative comparisons between simulated and reconstructed sediment transports at the Eirik Drift for the first time. Variations in sedimentation rate, sediment transport and grain sizes can be linked to climatic and tectonic events.

References:

- Expedition 303 Scientists, 2006, Expedition 303 summary, in Channell, J. E. T., Kanamatsu, T., et al, eds., Proc. IODP, Volume 303/306: College Station, Integrated Ocean Drilling Program Management International, p. 30.
- Li, X., 2012. Numerical Simulation of Sediment Transport at the Agulhas Drift on the South African Gateway in relation to its Geodynamic Development. (PhD thesis, University of Bremen).
- Müller-Michaelis, A., and Uenzelmann-Neben, G., 2014, Development of the Western Boundary Undercurrent at Eirik Drift related to changing climate since the early Miocene: Deep Sea Research Part I: Oceanographic Research Papers, v. 93, p. 21-34.
- Müller-Michaelis, A. & Uenzelmann-Neben, G., 2015. Using seismic reflection data to reveal high-resolution structure and pathway of the upper Western Boundary Undercurrent at Eirik Drift. *Mar. Geophys. Res.* 36, 343–353.
- Salzmann, U., Haywood, A. M. & Lunt, D. J., 2009. The past is a guide to the future? Comparing Middle Pliocene vegetation with predicted biome distributions for the twenty-first century. *Philos. Trans. A. Math. Phys. Eng. Sci.* 367, 189–204.
- Shchepetkin, A. F., McWilliams, J. C., 2005. The regional oceanic modeling system (ROMS): a split-explicit, free-surface, topography-following-coordinate oceanic model. *Ocean Model.* 9(4), 347–404.
- Shipboard Scientific Party, 1987a, Site 646, in Srivastava, S. P., Arthur, M., Clement, B., and et al., eds., *Repts. Volume 105: College Station, Ocean Drilling Program*, p. 419-674.
- Uenzelmann-Neben, G., Weber, T., Thomas, M., and Gruetzner, J., 2017, Transition from the Cretaceous ocean to Cenozoic circulation in the western South Atlantic - a twofold reconstruction: *Tectonophysics*, doi: 10.1016/j.tecto.2016.05.036.

ICDP

Regional two-dimensional magnetotelluric profile in West Bohemia/Vogtland reveals deep conductive channel into the earthquake swarm region

U. WECKMANN^{1,2}, G. MUÑOZ¹, J. PEK³, S. KOVÁČIKOVÁ³, R. KLANICA^{3,4}

¹ GFZ German Research Centre for Geosciences, Potsdam, Germany

² Institute of Earth- and Environmental Science, University of Potsdam, Germany

³ Institute of Geophysics of the Czech Academy of Sciences, Prague, Czech Republic

⁴ Faculty of Sciences, Charles University, Prague, Czech Republic

The West Bohemia/Vogtland region, characterized by the intersection of the Eger (Ohře) Rift and the Mariánské Lázně fault, is a geodynamically active area exhibiting repeated occurrence of earthquake swarms, massive CO₂ emanations and mid Pleistocene volcanism. The Eger Rift is the only known intra-continental region in Europe where such deep seated, active lithospheric processes currently take place. We present an image of electrical resistivity obtained from two-dimensional inversion of magnetotelluric (MT) data acquired along a regional profile crossing the Eger Rift (Muñoz et al., 2018). At the near surface, the Cheb basin and the aquifer feeding the mofette fields of Bublák and Hartoušov have been imaged as part of a region of very low resistivity. The most striking resistivity feature, however, is a deep reaching conductive channel which extends from the surface into the lower crust spatially correlated with the hypocentres of the seismic events of the Nový Kostel Focal Zone. This channel has been interpreted as imaging a pathway from a possible mid-crustal fluid reservoir to the surface. The resistivity model reinforces the relation between the fluid circulation along deep-reaching faults and the generation of the earthquakes. Additionally, a further conductive channel has been revealed to the south of the profile. This other feature could be associated to fossil hydrothermal alteration related to Mýtina and/or Neualbenreuth Maar structures or alternatively could be the signature of a structure associated to the suture between the Saxo-Thuringian and Teplá-Barrandian zones, whose surface expression is located only a few kilometres away.

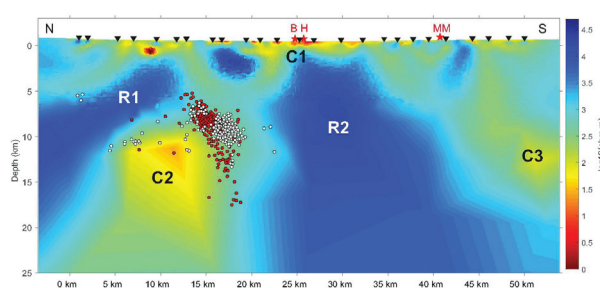


Fig. 1: Electrical resistivity model obtained from 2D inversion. Red stars show the locations of Bublák (B) and Hartoušov (H) mofettes and Mýtina Maar Volcano (MM). White and red dots correspond to the projected locations of earthquake swarm events in the Nový Kostel focal zone. Overall high resistivity (> 1000 Wm; R1 and R2) relates to the old crystalline basement. Near surface shallow conductive anomalies are found beneath the Cheb Basin (C1) and the Hartoušov and Bublák mofettes. A deep reaching conductive channel extends from C1 at the surface down to a conductive feature (C2). To the south, another deep reaching conductive feature (C3) is spatially correlated with the surface expression of Mýtina Maar.

Since we planned to obtain a full image from mid-crustal to drillable (<100 m) depth, we conducted different MT experiments. Near-surface pathways of mineral fluids containing CO₂ can be imaged in detail with the Radio-Magnetotelluric (RMT) method (Rulff, 2018). Two- and three-dimensional models indicate that the subsurface below wet degassing sites such as the Hartoušov mofette is characterised by an increase in electrical conductivity in form of a electrically conductive channels connecting deeper aquifers. Gaseous CO₂ is more resistive and consequently inversion result of the northern measurement area seems to correlate with a dry mofette structure. These models can be compared with electrical resistivity tomography (ERT) profiles (Flechsich et al., 2008; Nickschick et al., 2015) and logging data from the nearby Hartoušov borehole (Bussert et al., 2017).

References:

- Bussert, R., Kämpf, H., Flechsich, C., Hesse, K., Nickschick, T., Liu, Q., Umlauf, J., Vylita, T., Wagner, D., Wonik, T., Flores, H. & Alawi, M. (2017) Drilling into an active mofette- pilot-hole study of the impact of CO₂-rich mantle-derived fluids on the geo-bio-interaction in the western Eger-Rift (Czech Republic). *Scientific Drilling* 23, pp. 13-27.
- Flechsich, C., Bussert, R. & Rechner, J. (2008) The Hartoušov Mofette Field in the Cheb Basin, Western Eger Rift (Czech Republic): a Comparative Geoelectric, Sedimentologic and Soil Gas Study of a Magmatic Diffuse CO₂-Degassing Structure. *Zeitschrift für Geologische Wissenschaften* 36.3, pp. 177-193
- Muñoz, G., Weckmann, U., Pek, J., Kováčiková, S. & Klanica, R. (2018) Regional two-dimensional magnetotelluric profile in West Bohemia/Vogtland reveals deep conductive channel into the earthquake swarm region, Tectonophysics, <https://doi.org/10.1016/j.tecto.2018.01.012>.
- Nickschick, T., Kämpf, H., Flechsich, C., Mrlina, J. & Heinicke, J. (2015) CO₂ degassing in the Hartoušov mofette area, western Eger Rift, imaged by CO₂ mapping and geoelectrical and gravity surveys. *International Journal of Earth Science (Geologische Rundschau)* 104, pp. 2107-2129.
- Rulff, P. (2018) Radiomagnetotellurics for imaging mofette structures in the Eger Rift System, Czech Republic - a comparative study, MSC Thesis, Institute for Earth and Environmental Sciences, University of Potsdam, Germany

IODP

A new high-resolution Maastrichtian to Late Campanian cyclostratigraphic record from equatorial Atlantic ODP Sites 1258 and 1259

T. WESTERHOLD¹, U. RÖHL¹, R. H. WILKENS²

¹MARUM – Center for Marine Environmental Sciences, University of Bremen, Leobener Straße, 28359 Bremen, Germany

²Institute of Geophysics and Planetology, University of Hawaii, Honolulu, HI 96822, USA

The latest Cretaceous is characterized by much higher concentrations of greenhouse gases and warmer mean global temperatures than today. The latest Campanian to Maastrichtian (75-66 Ma) interval is of particular interest, because Earth's overall warm climate cooled to an extent that possibly allowed ephemeral glaciations of the poles (Friedrich et al. 2012). Mainly bulk stable isotope records from deep-sea and land sections have been used to compile a Campanian-Maastrichtian carbon-isotope stratigraphy (Voigt et al., 2012). Very detailed astronomical age models for the Maastrichtian and Late Campanian have also been developed recently using classic outcrops in Bidart, Hendaia, Sopelana, Zumaia (all Bask Country; Spain/France) and deep-sea records (DSDP 525A, ODP 762C, 1258A, 1267) utilizing cyclic variations in lithology, color and magnetic susceptibility (Batenburg et al. 2012, 2014; Hussone et al. 2011, 2014; Dinares-Turell et al. 2013). Bulk δ¹³C data are commonly used to correlate between different sections because of uncertainties in biostratigraphic events (e.g. Voigt et al. 2012). Although the overall results are more or less convincing, most stable isotope data originate from incomplete, single holes (DSDP 525A, ODP 762C, 1210B). Recently, late Maastrichtian

bulk carbon isotope data from North Atlantic (Newfoundland Margin) IODP Site 342-U1403 exhibit that the bulk carbon-isotope stratigraphy in its details is much more complex. At the moment no high-resolution bulk carbon isotope record is available from the equatorial Atlantic.

Here, we present new data from the latest Campanian to Maastrichtian equatorial Atlantic ODP Sites 1258 and 1259 (Leg 207, Demerara Rise) section. X-ray fluorescence (XRF) core scanning data and core images were utilized for correlation to fill recovery gaps and to revise the composite records of both sites. Scanning XRF Fe records from both sites are dominated by eccentricity modulated precession cycles, similar to the observations made at the Zumaia section (Batenburg et al. 2012, 2014; Dinares-Turell et al. 2013). We also XRF scanned latest Campanian to Maastrichtian cores from Hole 516F (Rio Grande Rise, DSDP Leg 72), as well as from Sites 525, 527, and 528 (Walvis Ridge, DSDP Leg 74), which also exhibit eccentricity modulated precession cycles throughout the investigated interval. In combination with published records from ODP Sites 1262 and 1267 (Westerhold et al. 2008) we were able to compile a Maastrichtian Equatorial to South Atlantic framework that allows validating of the available bio- and magnetostratigraphy. Subsequently a cyclostratigraphic age model based upon the stable 405-kyr eccentricity cycle was developed, similar to the approaches of Westerhold et al. (2008), Hussone et al. (2011), Dinares-Turell et al. (2013), and Batenburg et al. (2014).

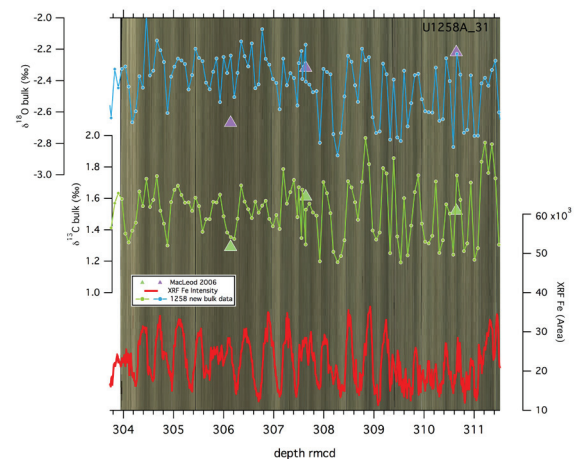


Fig. 1. New ODP Site 1258 bulk stable isotope and X-ray fluorescence data from 304 to 311.5 mrcd of Core 1258A-31R. Also shown are low-resolution bulk isotope data (MacLeod 2006). Please note the overall strong correlation between color of the core image, Fe intensities and bulk stable isotope data. Our record clearly shows that sampling at resolutions lower than 10 cm will result in serious aliasing of the true signal.

We analyzed a total number of 1865 bulk stable isotope samples (1569 from Site 1258; 296 from Site 1259) resulting in an almost 95-m long bulk carbon isotope record at 5 cm resolution. This record is crucial for validating the existing Campanian-Maastrichtian carbon-isotope stratigraphy (Voigt et al. 2012, Wendler 2013). Sample positions were selected based on XRF core scanning data in order to avoid aliasing. Our new data clearly show that Sites 1258 and 1259 can be correlated in detail and that the material is suitable for stable isotope analysis. A previous study at Sites 1258 and 1259 (MacLeod 2006) severely aliased the high-frequency precession signal due to the coarse sample resolution and thus could not establish a correlation. Our new bulk isotope data exhibit spectacular, unprecedented cyclicity. Carbon isotopes values range from 1.2 to

2.0 ‰ in the late Maastricht during magnetic polarity chron C30n to C31n. After an overall 0.35 ‰ shift towards lighter values, the data vary between 0.9 and 1.6 ‰ close to the Campanian/Maastricht boundary. During the late Campanian the bulk carbon isotope data show a much larger amplitude of 0.1 to 1.8 ‰. Most interestingly the precessional bulk carbon and oxygen isotope cycles co-vary with the XRF Fe intensity variation (Fig. 1). The observed shifts are in line with globally distributed bulk isotope records and thus reinforces the application of bulk stable isotopes, at least looking at the general pattern, for global correlations. But our study also demonstrates that most of the other bulk stable isotopes records spanning the latest Campanian to Maastrichtian very likely have not been sampled in high enough resolution to resolve the individual precession cycle, which led to severe aliasing of the signal and thus making global correlation difficult. On an individual cycle scale at 1258/1259 heavier, more positive bulk isotopes values correspond to higher Fe intensities and darker intervals in the core images – see from 308 to 309 rmdc in Figure 1. This phase relationship is opposite to other records (e.g., Zumaia) and is currently explored in more detail. The next step in our project will be to compare the Sites 1258/1259 data to the new bulk stable isotope record from the North Atlantic Site U1403 (IODP Exp. 342 Newfoundland, Batenburg et al. 2017).

References

- Batenburg, S. J., Sprovieri, M., Gale, A. S., Hilgen, F. J., Hüsing, S., Laskar, J., Liebrand, D., Lirer, F., Orue-Etxebarria, X., Pelosi, N., and Smit, J.: Cyclostratigraphy and astronomical tuning of the Late Maastrichtian at Zumaia (Basque country, Northern Spain), *Earth and Planetary Science Letters*, 359–360, 264–278, <http://dx.doi.org/10.1016/j.epsl.2012.09.054>, 2012.
- Batenburg, S. J., Gale, A. S., Sprovieri, M., Hilgen, F. J., Thibault, N., Boussaha, M., and Orue-Etxebarria, X.: An astronomical time scale for the Maastrichtian based on the Zumaia and Sopelana sections (Basque country, northern Spain), *Journal of the Geological Society*, 10.1144/jgs2013-015, 2014.
- Batenburg, S. J., Friedrich, O., Moriya, K., Voigt, S., Cournède, C., Moebius, I., Blum, P., Bornemann, A., Fiebig, J., Hasegawa, T., Hull, P. M., Norris, R. D., Röhl, U., Sexton, P. F., Westerhold, T., Wilson, P. A., and the IODP Expedition 342 Scientists: Late Maastrichtian carbon isotope stratigraphy and cyclostratigraphy of the Newfoundland Margin (Site U1403, IODP Leg 342), *Newsletters on Stratigraphy*, 10.1127/nos/2017/0398, 2017.
- Dinarès-Turell, J., Pujalte, V., Stoykova, K., and Elorza, J.: Detailed correlation and astronomical forcing within the Upper Maastrichtian succession in the Basque Basin, *Boletín Geológico y Minero*, 124, 253–282, 2013.
- Husson, D., Galbrun, B., Laskar, J., Hinnov, L. A., Thibault, N., Gardin, S., and Locklair, R. E.: Astronomical calibration of the Maastrichtian (Late Cretaceous), *Earth and Planetary Science Letters*, 305, 328–340, 10.1016/j.epsl.2011.03.008, 2011.
- Husson, D., Thibault, N., Galbrun, B., Gardin, S., Minoletti, F., Sageman, B., and Huret, E.: Lower Maastrichtian cyclostratigraphy of the Bidart section (Basque Country, SW France): A remarkable record of precessional forcing, *Palaeogeography, Palaeoclimatology, Palaeoecology*, 395, 176–197, <http://dx.doi.org/10.1016/j.palaeo.2013.12.008>, 2014.
- Voigt, S., Gale, A. S., Jung, C., and Jenkyns, H. C.: Global correlation of Upper Campanian-Maastrichtian successions using carbon-isotope stratigraphy: development of a new Maastrichtian timescale, *Newsletters on Stratigraphy*, 45, 25–53, 10.1127/0078-0421/2012/0016, 2012.
- Wendler, I.: A critical evaluation of carbon isotope stratigraphy and biostratigraphic implications for Late Cretaceous global correlation, *Earth-Science Reviews*, 126, 116–146, <http://dx.doi.org/10.1016/j.earscirev.2013.08.003>, 2013.
- Westerhold, T., Röhl, U., Raffi, I., Fornaciari, E., Monechi, S., Reale, V., Bowles, J., and Evans, H. F.: Astronomical calibration of the Paleocene time, *Palaeogeography, Palaeoclimatology, Palaeoecology*, 257, 377–403, 10.1016/j.palaeo.2007.09.016, 2008.

IODP

Fluid migration in the Nankai Trough Kumano forearc basin

T. WIERSBERG¹, S. HAMMERSCHMIDT², T. TOKI³, A. KOPF², J. ERZINGER¹

¹GFZ German Research Centre for Geosciences

²Center for Marine Environmental Sciences (MARUM)

³University of the Ryukyus, Department of Chemistry, Biology and Marine Science

Noble gas abundance and isotope data from drilling mud gas samples obtained during IODP Expedition 338 between October 2012 and January 2013 and Expedition 348 between September 2013 and January 2014 provide new insights on the origin and migration of fluids in the southern rim of the Kumano forearc basin offshore SE Japan. Drilling mud gas was sampled from three adjoining boreholes (C0002F, C0002N and C0002P) and depths between 950 and 3050 meter below sea floor (mbsf), samples are composed of air with variable contribution of mantle-derived and crustal fluids.

The air-corrected ³He/⁴He ratios of samples from Exp. 338 are highly variable and fall between 0.44±0.24 Ra and 3.26±0.28 Ra. Samples #1400 and #1800 (sample number denotes depth in mbsf) are strongly dominated by crustal helium, while the air-free helium isotope composition of #950 is the highest observed in our study and in good agreement with the estimated helium isotope value (3.4 Ra) of the subducting Philippine Sea Plate (PSP) in southwest Japan (Umeda et al., 2012). In contrast, samples collected during Exp. 348 in the depth interval 1700–3050 mbsf show only binary mixing between air and a mantle-derived component with a ³He/⁴He ratio of 2.4 Ra and no significant depth variation.

Helium isotope and radon data from Exp 338 indicate channelized and active fluid flow through permeable strata from the subducting PSP for #950, while active fluid flow from another source enriched in crustal helium accounts for the helium isotopic composition in #1400 and #1800. We interpret the findings from Exp 338 as a short-term episodic fluid flow event, maybe caused by reactivation of buried trust faults.

Elevated ²²²Radon activities observed during Exp 338 were not found during drilling one year later (Exp 348), which suggest pervasive migration of fluids through pore space along mineral grain boundaries with little input of in-situ produced crustal helium for Exp 348. Application of the fluid-flow model from Kennedy et al. (1997) results in flow rates of ~7cm per year in the accretionary prism of the Kumano Basin. These values agree well with calculated average diffusion lengths for helium in marine sediments.

References:

- Kennedy BM, Kharaka YK, Evans WC, Ellwood A, DePaolo DJ, Thordsen J, Ambats G, Mariner RH (1997) Mantle Fluids in the San Andreas Fault System, California. *Science* 278:1278 – 1281. doi: 10.1126/science.278.5341.1278
- Umeda K, Kusano T, Asamori K, McCrann GF (2012) Relationship between ³He/⁴He ratios and subduction of the Philippine Sea plate beneath southwest Japan. *J Geophys Res Solid Earth* 117:B10204. doi: 10.1029/2012JB009409.

IODP

Ca isotope geochemistry in marine deep sea sediments of the Eastern Pacific

 A. WITTKÉ¹, N. GUSSONE¹, D. DERIGS², M. SCHÄLLING¹, C. MÄRZ³,
 B. M. A. TEICHERT⁴
¹Institut für Mineralogie, Westfälische-Wilhelms-Universität Münster, Germany

²Physikalisches Institut, Universität zu Köln, Germany

³School of Earth and Environment, University of Leeds, United Kingdom

⁴Institut für Geologie und Paläontologie, Westfälische-Wilhelms-Universität Münster, Germany

Changes in marine pore water chemical composition are important indicators of early diagenetic processes and fluid fluxes. The Ca isotope ratio ($\delta^{44/40}\text{Ca}$) is a powerful tool to investigate diagenetic reactions in marine sedimentary porewater systems, as it is sensitive to processes such as carbonate dissolution, precipitation and recrystallization, due to the isotopic difference between dissolved Ca and solid carbonate minerals, and is also affected by ion exchange as well as deep fluid sources (e.g. Teichert et al. 2009; Ockert et al. 2013). Thus, it is part of the CO_2 cycle and directly linked to climate changes. In the past decade, the Ca isotope system has been applied as proxy for diagenetic reactions such as CaCO_3 dissolution, CaCO_3 precipitation, ion exchange and recrystallization. To extract the pore water from a sediment core, the so-called whole round (WR) method has been successfully used for decades. The WR method has some limitations: It is usually applied at relatively low depth resolution because it disturbs the sediment record (Dickens et al., 2007) and the press has to be cleaned between every sampling to avoid contamination. Further, the pressure exerted in the hydraulic press to extract the pore fluid (250-300 MPa) destroys microbial cells and was suggested to cause carbonate contamination due to release of cytoplasm and carbonate dissolution (Schrum et al., 2012) since the pressure is much higher than any water pressure in the deep ocean sediments (Miller et al., 2014). A more recent method to retrieve pore water is the so-called Rhizon sampling technique, first applied to marine sediment cores by Seeberg-Elverfeldt et al. (2005) and Dickens et al. (2007). Applying a gentle vacuum, the pore water is sucked out of the sediment without major disturbance of the sediment record. In addition, achieving a higher sampling resolution is more feasible using the Rhizon sampling techniques. There are only a few studies that evaluate the comparability of both sampling techniques, especially for isotope ratios. Initial results indicate possible differences between whole round and Rhizon sampling techniques, e.g. for alkalinity, Cl^- concentration, oxygen and hydrogen isotope ratios and dissolved inorganic carbon (DIC) (Schrum et al., 2012; Miller et al., 2014). In this study, we systematically compare Rhizon and WR sampling techniques in terms of their effect on stable calcium isotope ratios in the extracted pore waters. The WR and Rhizon sampling methods have been applied during IODP Exp. 320/321 at Site U1332 at the parallel Holes A and C (Pälike et al., 2010). The parallel sediment cores were selected for Ca isotope analyses because they show a difference in the pore water concentrations of Ba^{2+} , Ca^{2+} , Li^+ and Mg^{2+} (Pälike et al., 2010). We recognized a systematic offset in $\delta^{44/40}\text{Ca}$ between both sampling techniques with higher values for the Rhizon sampling technique. Rayleigh fractionation and mixing calculation models indicate that the whole round sampling technique is most likely more representative for the pristine pore water than Rhizon sampling. Further, we conducted a press test to determine, if different time or pressure during WR sampling may have an

effect on the Ca isotope composition of the porewater sample. The outcome of this experiment demonstrates that different time or pressure during WR sampling do not have an effect on the Ca isotopy of the extracted porewater sample. Although the offset between WR and corresponding Rhizons is systematic, the deviation is generally within analytical uncertainties, but may become more important with increasing analytical precision or other sediment composition.

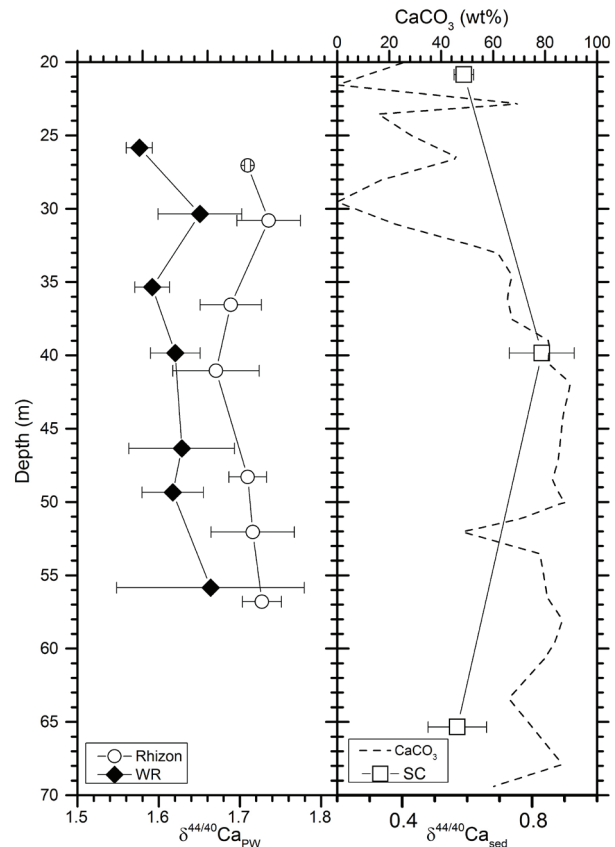


Fig. 1: Comparison of $\delta^{44/40}\text{Ca}$ of pore water (PW) retrieved by WR (Hole U1332A) and Rhizon (Hole U1332C) sampling (this work), corresponding CaCO_3 concentration (Pälike et al., 2010) and three $\delta^{44/40}\text{Ca}$ values (this work) of the sediment (SC; Hole U1332A). Ca isotope measurements of WR and Rhizon samples show the same overall pattern, but Rhizon samples have slightly higher $\delta^{44/40}\text{Ca}$ values. The CaCO_3 content ranges mostly between 20 and 90 wt% (Pälike et al., 2010).

Further, we studied diagenetic reactions in deep sea sediments from the Equatorial Eastern Pacific by analysing Ca isotope ratios of porewater and sediment on eight sediment cores from IODP Exp. 320/321. Two sediment cores show Ca isotope profiles that start at the sediment/water interface with seawater-like values, then decrease to sediment-like values due to recrystallization and then increase in the bottom part again to seawater-like values. The other studied cores show different degrees of flattening of this middle bulge. We interpret this systematic flattening either as an effect of sediment thickness, decreasing recrystallization rates and/or fluid advection at the respective sampling sites. Element concentration profiles and Sr-isotope variations on some of these sediment cores show a similar behavior, supporting our findings (Pälike et al. 2010; Voigt et al. 2015). The seawater-like values at the bottom of the sediment pile are supposed to be caused by fluids migrating through the oceanic basement, fed by seawater influx at (inactive) seamounts (e.g. Villinger et al. 2017). There are two hypotheses for such a fluid

flow: a) two seamounts or bathymetric pits are connected, with a recharge and a discharge site (Bekins et al., 2007), or b) up-taken fluids could be released through the surrounding seafloor as well due to diffusive exchange with the underlying oceanic crust (e.g. Mewes et al., 2016). Our Ca isotope results combined with a transport reaction model approach support the latter hypothesis, since the recrystallization rate and fluid velocity rate depends on the sediment composition and length, thus it is not a time depending series.

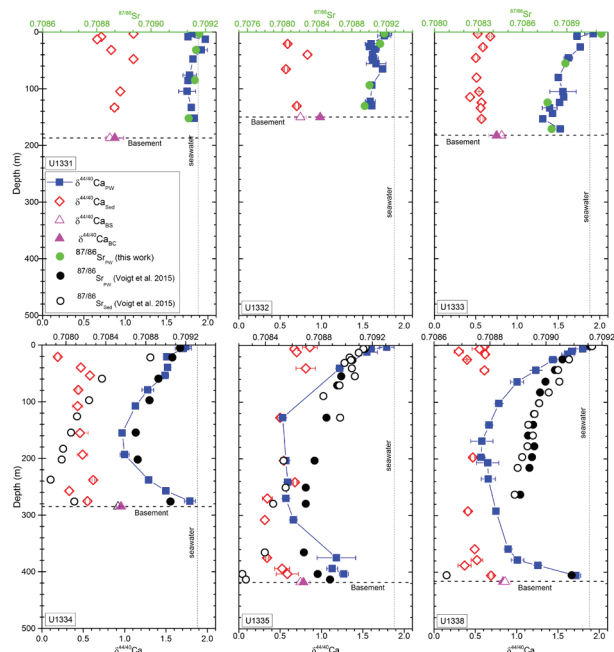


Fig. 2: $\delta^{44/40}\text{Ca}$ of the pore water, sediment and basalt (both carbonate and silicate phases) compared to $^{87}\text{Sr}/^{86}\text{Sr}$ of the pore water of all sites (this work; Voigt et al., 2015) and the sediment of site U1334-U1338 (Voigt et al., 2015).

References:

- Bekins B. A., Spivack A. J., Davis E. E. and Mayer L. A. (2007) Dissolution of biogenic ooze over basement edifices in the equatorial Pacific with implications for hydrothermal ventilation of the oceanic crust. *Geol* 35, 679.
- Dickens, G.R., Koelling, M., Smith, D.C., Schindlers, L., 2007. Rhizon Sampling of Pore Waters on Scientific Drilling Expeditions: An Example from the IODP Expedition 302, Arctic Coring Expedition (ACEX), in: Backman, J., Moran, K., McInroy, D.B., Mayer, L.A. (Eds.), *Proceedings of the IODP, 302*, vol. 302. Integrated Ocean Drilling Program, pp. 22–25.
- Mewes K., Mogollón J. M., Picard A., Rühlemann C., Eisenhauer A., Kuhn T., Ziebis W. and Kasten S. (2016) Diffusive transfer of oxygen from seamount basaltic crust into overlying sediments. *Earth and Planetary Science Letters* 433, 215–225.
- Miller, M.D., Adkins, J.F., Hodell, D.A., 2014. Rhizon sampler alteration of deep ocean sediment interstitial water samples, as indicated by chloride concentration and oxygen and hydrogen isotopes. *Geochem. Geophys. Geosyst.* 15 (6), 2401–2413.
- Ockert C., Gussone N., Kaufhold S. and Teichert B. (2013) Isotope fractionation during Ca exchange on clay minerals in a marine environment. *Geochimica et Cosmochimica Acta* 112, 374–388.
- Pälike H., Lyle M., Nishi H., Raffi I., Gamage K. and Klaus A. (eds.) (2010) *Proceedings of the IODP, 320/321*. Integrated Ocean Drilling Program.
- Schrum, H.N., Murray, R.W., Gribsholt, B., 2012. Comparison of Rhizon Sampling and Whole Round Squeezing for Marine Sediment Porewater. *Scientific Drilling* (13, April 2012).
- Seeberg-Elverfeldt, J., Schlüter, M., Feseker, T., Kölling, M., 2005. Rhizon sampling of porewaters near the sediment-water interface of aquatic systems. *Limnol. Oceanogr. Methods* 3 (8), 361–371.
- Teichert B. M., Gussone N. and Torres M. E. (2009) Controls on calcium isotope fractionation in sedimentary porewaters. *Earth and Planetary Science Letters* 279, 373–382.
- Villinger H. W., Pichler T., Kaul N., Stephan S., Pälike H. and Stephan F. (2017) Formation of hydrothermal pits and the role of seamounts in the Guatemala Basin (Equatorial East Pacific) from heat flow, seismic, and core studies. *Geochem. Geophys. Geosyst.* 18, 369–383.
- Voigt J., Hathorne E. C., Frank M., Vollstaedt H. and Eisenhauer A. (2015) Variability of carbonate diagenesis in equatorial Pacific sediments deduced from radiogenic and stable Sr isotopes. *Geochimica et Cosmochimica Acta* 148, 360–377.

ICDP

Thermal Expansivity Between 150 and 800°C of Hydrothermally Altered Conduit Dyke Samples from USDP-4 Drill Core (Mt Unzen, Shimabara, Japan)

T. I. YILMAZ¹, K.-U. HESS¹, J. VASSEUR¹, F. B. WADSWORTH¹, H. A. GILG², S. NAKADA³, D. B. DINGWELL¹

¹Department of Earth and Environmental Sciences, Ludwig-Maximilians-Universität München (LMU), Theresienstrasse 41/III, 80333 Munich, Germany

²Lehrstuhl für Ingenieurgeologie, Technische Universität München (TUM), Arcisstr. 21, 80333 Munich, Germany

³Earthquake Research Institute (ERI), University of Tokyo, 1-1-1 Yayoi, Bunkyo, 113-0032, Japan

When hot magma intrudes the crust, the surrounding rocks expand. Similarly, the cooling magma contracts. The expansion and contraction of these multiphase materials is not simple and often requires empirical constraint. Therefore, we constrained the thermal expansivity of Unzen dome and conduit samples using a NETZSCH® DIL 402C. Following experiments, those samples were scanned using a Phoenix v|tome|x m to observe the cracks that may have developed during the heating and cooling. The dome samples do not show petrological or chemical signs of alteration. However, the alteration of the conduit dykes is represented by the occurrence of the main secondary phases such as chlorite, sulfides, carbonates, R1 (Reichweite parameter) illite-smectite, and kaolinite. These alteration products indicate an (I) early weak to moderate argillic magmatic alteration, and a (II) second stage weak to moderate propylitic hydrothermal alteration.

The linear thermal expansion coefficient α_L of the dome material is $\sim 5 \cdot 10^{-6} \text{ K}^{-1}$ between 150°C and 800°C and shows a sharp peak of up to $\sim 2.5 \cdot 10^{-5} \text{ K}^{-1}$ around the alpha-beta-quartz-transition ($\sim 573^\circ\text{C}$). In contrast, α_L of the hydrothermally altered conduit samples starts to increase around 180°C and reaches $\sim 1.5 \cdot 10^{-5} \text{ K}^{-1}$ at $\sim 400^\circ\text{C}$ (Fig 1). We interpret this effect as being due to the water content of the kaolinite and the R1 illite-smectite, which induces larger expansions per degree temperature change. Furthermore, the altered conduit samples show a more pronounced increases of α_L between 500°C and 600°C of up to peaks at $\sim 1.3 \cdot 10^{-4} \text{ K}^{-1}$ (Fig. 2), which is generated by the breakdown of chlorite, iron-rich dolomite solid solutions, calcite, and pyrite.

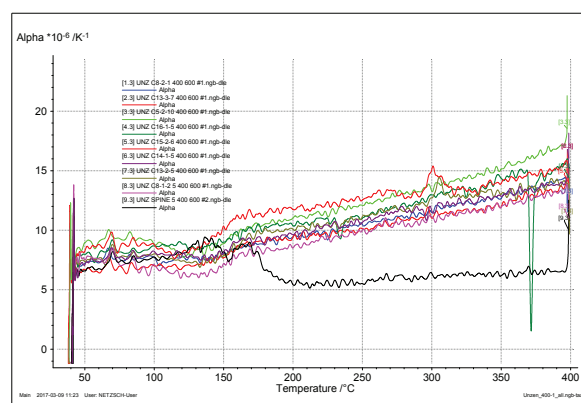


Fig. 1: Temperature vs. linear thermal expansion coefficient α_L plot of heating cycle 1 between 0°C and 400°C.

We use a 1D conductive model of heat transfer to explore how the country rock around the Unzen conduit zone would heat up after intrusion. In turn, we convert these temperature profiles to thermal stress profiles, assuming the edifice is largely undeformable. We show that these high linear thermal expansion coefficients of the hydrothermally altered conduit rocks may large induce thermal stresses in the surrounding host rock and therefore promotes cracking, which may in turn lead to edifice instability.

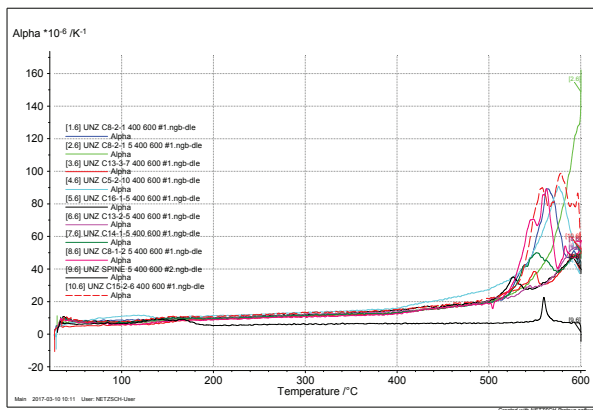


Fig. 2: Temperature vs. linear thermal expansion coefficient α_L plot of heating cycle 2 between 0°C and 600°C.

IODP

Melt-peridotite interaction at crust-mantle boundary: An experimental perspective

C. ZHANG¹, J. KOEPKE¹, O. NAMUR², S. FEIG³

¹Institut für Mineralogie, Leibniz Universität Hannover, 30167 Hannover, Germany

²Department of Earth and Environmental Sciences, University of Leuven, Belgium

³Central Science Laboratory, University of Tasmania, Australia

The coherent cores of layered gabbros drilled by IODP (International Ocean Discovery Program) Expedition 345 at Site 1415 at the Hess Deep Rift validates the use of Penrose model based on ophiolites for interpreting the structure of fast-spreading oceanic crust. One remarkable finding is the occurrence of orthopyroxene as an abundant phase in these deep-level cumulate rocks, which is however unexplainable by crystallization experiments from primary MORB melts. The current model (Coogan et al. 2002) invokes interaction between MORB melt and mantle rocks and subsequent crystallization of modified MORB melt in an isolated environment. In this experimental study, we performed (and will perform more) melt-peridotite interaction experiments and consequent crystallization of modified melts, aiming to shed light on the origin of the orthopyroxene-rich layered gabbros in the lower oceanic crust as well as the formation of dunite at the base of oceanic crust.

To simulate melt-peridotite interaction experiments, we mixed a starting glass that has a primitive MORB composition estimated based on bulk crust of Hess Deep (Gillis et al. 2014), and a natural lherzolite. Three types of experiment were designed. The 1st type experiments were run at a constant temperature, which serve as a pointer for investigating phase stabilities at the melt-peridotite mixed environment. The 2nd type

experiments were run starting from a high temperature (near liquidus) and to finish at a lower temperature, in between with slow cooling rate, similar to the approach of Saper and Liang (2014). Melt-peridotite interaction is supposed to be most active near the liquidus, whereas it should be negligible at the lower temperature. The 3rd type experiments contain two independent steps, with the first step at near-liquidus temperature for efficient melt-peridotite interaction, and second step at a lower temperature for crystallization using a synthesized starting glass composition identical to the modified melt from the first step experiment. The experiments were performed in the Internally Heated Pressure Vessels (IHPV) at dry and reduced conditions with a constant pressure of 2 kbar (corresponding to the depth of the base of the oceanic crust). Melt-peridotite interaction experiments were in all cases performed simultaneously with equilibrium crystallization experiments using pure a primitive MORB glass, which allows easy assessment of the effect of melt-peridotite interaction. Up to now, the 1st and 2nd type experiments are completed, and the 3rd type experiments are still under work.

Our experiments show that interaction between MORB melt and peridotite can effectively increase SiO₂ content without changing MgO largely in modified melts (Fig. 1a), evolving towards compositions that favor orthopyroxene saturation. In one melt-peridotite interaction experiment at 1180 °C, magmatic orthopyroxene is observed coexisting with magmatic olivine and plagioclase and a large proportion of melt (Fig. 1b), clearly demonstrating that orthopyroxene can crystallize at an early-to-middle magmatic stage from the modified melt. Therefore, our experiments provide strong evidence for melt-peridotite interaction as an important mechanism for dissolving orthopyroxene in the peridotite at crust-mantle boundary and consequently generating melts close to opx-saturation which migrate to lower crust resulting in opx-rich gabbros.

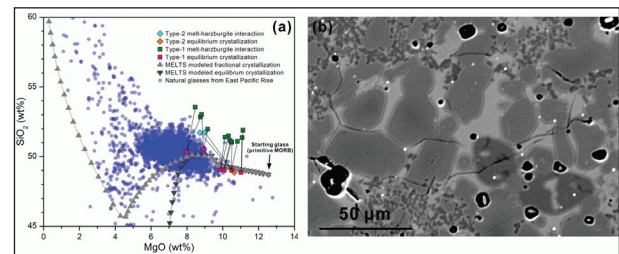


Fig. 1: (a) Experimental melts in comparison with MELTS modeled melts and natural glasses from East Pacific Rise. Melt-peridotite interaction-modified melts show strong increase in SiO₂ content. (b) Magmatic assemblage of olivine + orthopyroxene + plagioclase together with a large proportion of melt.

References:

- Coogan LA, Gillis KM, MacLeod CJ, Thompson GM, Hékinian R (2002) Petrology and geochemistry of the lower ocean crust formed at the East Pacific Rise and exposed at Hess Deep: A synthesis and new results. *Geochemistry, Geophysics, Geosystems* 3(11):8604
- Gillis KM, Snow JE, Klaus A, Abe N, Adrião ÁB, Akizawa N, Ceuleneer G, Cheadle MJ, Faak K, Falloon TJ, Friedman SA, Godard M, Guerin G, Harigane Y, Horst AJ, Hoshida T, Ildefonse B, Jean MM, John BE, Koepke J, Machi S, Maeda J, Marks NE, McCaig AM, Meyer R, Morris A, Nozaka T, Python M, Saha A, Wintsch RP (2014) Primitive layered gabbros from fast-spreading lower oceanic crust. *Nature* 505:204-207
- Saper L, Liang Y (2014) Formation of plagioclase-bearing peridotite and plagioclase-bearing wehrlite and gabbro suite through reactive crystallization: an experimental study. *Contrib Mineral Petrol* 167(3):1-16

Nachgereichte Abstracts:

ICDP

How near source region double difference attenuation in North-West Bohemia can benefit from ICDP borehole seismometry

M. KRIEGEROWSKI¹, S. CESCA², M. OHRNBERGER¹, F. KRÜGER¹

¹University of Potsdam, Institute for Earth and Environmental Science
²Helmholtz Centre Potsdam, GFZ German Research Centre for Geoscience

We developed a differential attenuation (1/Q) tomography technique exploiting amplitude spectral ratios to gain insight into the rock properties of the North-West Bohemian earthquake swarms.

Attenuation of this seismically active region has been tackled in previous studies on regional scales using methods that focus on frequencies below the corner frequency. However, these applied approaches are not suited to resolve attenuation within the source region on scales down to few tens of meters which can be easily assessed from Fresnel volumes. Our proposed method uses higher frequencies, above the corner frequency of S and P phases. This allows to draw conclusions on properties in between couples of sources sharing a common ray path from the source region to a receiver.

The method and analysis approach is validated using simulated realistic seismograms with additive noise recorded by the WEBNET seismological network. Furthermore, we discuss the effect of source directivity, rupture dimensions and magnitudes on our tomographic approach based on synthetic tests and conclude that either rupture directivities need to either closely resemble each other or require random distribution.

From our analysis we estimate that P and S phase attenuation (1/Q) within the source region are significantly reduced in comparison to background attenuation. We observe significant scatter of solutions which is dominated by high frequency noise and limited bandwidth. As an attempt to further enhance resolution and investigate high frequency limits of different event magnitudes, the University of Potsdam installed short period seismometers sampling at 1000 Hz in Saxony, Germany close to the Czech border in October, 2017. We discuss the benefit of the increased bandwidth by means of several case study events which were recorded during the installation period. It becomes evident that events with magnitudes down to M10.0 have exploitable frequency content (signal-to-noise ratio > 3) at 200 Hz and above, expressing the need for increased sampling rates and supporting the ICDP plans of borehole seismometry in that region.

IODP

Geomorphology of the Belize Barrier Reef margin: a survey for IODP drilling

E. GISCHLER¹, F. S. ANSELMETTI²

¹Institut für Geowissenschaften, Goethe-Universität, Altenhöferallee 1, 60438 Frankfurt am Main, Germany
²Institut für Geologie, Universität Bern, Baltzerstrasse 1+3, 3012 Bern, Switzerland

As precondition for IODP drilling along the Belize Barrier Reef, a systematic bathymetric study along selected sections of the forereef area between ca. 20-150 m water depth of this major reef margin using multibeam bathymetric and shallow seismic techniques is planned. To date, no detailed and GPS-controlled bathymetry and continuous high-resolution seismic data of this barrier reef margin exists. Based on the data to be acquired, we intend to select suitable sites for IODP drilling. We aim at locating fore-reef sites, which will be suitable to recover postglacial (20-10 kyr BP) and underlying older Pleistocene deposits along a series of core traverses. Furthermore, an international workshop is planned to bring together interested scientists to explore the possibilities of developing a drilling proposal for the IODP.

Based on a successful pre-site survey and workshop, an IODP proposal would have four potential objectives including (1) the reconstruction of postglacial sea-level rise, (2) to analyze and quantify postglacial reef composition and architecture as response to sea-level and climate change, and (3) to obtain environmental data on temperature and carbonate saturation during that time window. In addition, (4) aspects of Pleistocene reef initiation and paleoecology may be investigated, depending on recovery of older Pleistocene successions. In the light of the modelled 21st century increases in sea-level rise, especially postglacial drowned reef sequences along the Belize margin can potentially be used for future sea-level projections.

In contrast to the Indo-Pacific region where several highly resolved and scientifically robust reef-based postglacial sea-level records have been acquired (Huon Peninsula, Tahiti, Great Barrier Reef), there is only one such record in the tropical western Atlantic (Barbados, eastern Caribbean). As valuable as the Barbados sea-level record is, it remains controversial because the sea-level data from Tahiti (IODP leg 310) and the Great Barrier Reef (IODP leg 325) only recorded meltwater pulse (MWP) 1A whereas MWP 1B is missing. In addition, abundant postglacial microbialite facies as found in Tahiti and the Great Barrier Reef and many other early Holocene reefs is apparently absent in Barbados for hitherto unknown reasons. This asks for the investigation of additional and independent sites. Because microbialite facies in postglacial reefs were formed by simple organisms (bacteria), they may provide key proxy data (thickness, volume) that are largely environmentally controlled and presumably easier to interpret as proxy data (growth and calcification rates, $\delta^{18}\text{O}$, Sr/Ca) from enzymatically controlled reef-builders such as corals. In summary, a second postglacial reefal archive from Belize would certainly help to answer these open and debated questions and to constrain the nature of postglacial sea-level rise in the western Atlantic / Caribbean realm.